The use of AAV vectors for transgene expression in primary afferent neurons in vitro and in vivo, and their utility in investigation of primary afferent anatomy and physiology

Khovanov, Nikita

Awarding institution:
King's College London

The use of AAV vectors for transgene expression in primary afferent neurons *in vitro* and *in vivo*, and their utility in investigation of primary afferent anatomy and physiology

Nikita Khovanov

PhD Neuroscience

King's College London

Abstract

The aim of this project is to express various transgenic tools in adult mouse primary afferent neurons in vivo and use them to study various aspects of physiology and anatomy of primary afferent neurons. In order to achieve expression, we used non-pathogenic adeno-associated virus serotype 9 (AAV9). Our first aim was to establish an AAV delivery method that achieves high transduction in vivo in adult mouse primary afferents. We used AAV9 containing eGFP transgene in order to identify and characterise transduced neurons. We designed a new intrathecal delivery method that produces reliable and reproducible transduction in the majority of the L4 DRG neurons. After that, we investigated the impact various experimental parameters, such as viral titre and time post injection, have on the transduction pattern.

After a successful delivery method was established, our next aim was to deliver functional transgenes to primary afferent neurons, such as GCaMP6s, in order to study activity of these neurons *in vivo* and *in vitro*. We assessed the performance of GCaMP6s in primary afferent cultures and attempted to establish an *in vitro* sensitisation model for calcium imaging that uses electrical stimulation as an activity trigger. Finally, we explored the use of our method of transgene delivery to express other transgenic tools *in vivo*, including Cre recombinase for the control of gene expression and an engineered glutamate-gated chloride channel for neuronal silencing.

Acknowledgements

I couldn't have finished this project without the help of a group of wonderful people, and I would like to give my thanks before getting into the thesis.

First and foremost, I would like to thank my supervisors Prof McMahon and Prof Bennett for letting me work with them, and for their continuous help and support. I would also like to thank Vivian Cheah, Caroline Abel and John Grist for their incredible support for the whole research group.

In addition, it would be impossible to make any progress without the friendly atmosphere within the research group and Wolfson CARD, so I say thank you to all members of the McMahon group and people working in Wolfson CARD. In particular, I would like to thank Dr Jayne Kelleher, Dr Katalin Bartus, Dr Fran Denk, Dr Nickolai Vysokov, Dr Maggie Crow, Dr Federica La Russa, Dr Sara Jager, Dr Athansios Didangelos, Dr Michelle Edye, Kez Hammet, Elin Vinsland and Joseph Lloyd for sharing the office with me and making me feel at home here. However, their contribution stretches far beyond merely creating a good office atmosphere. Each of these wonderful people helped me out significantly with parts of my project, for which I would love to give my sincere thanks. I would also like to give special thanks to Drs Kim Chisholm, Douglas Lopes, Maggie Crow and Gregory Weir for letting me collaborate with them, which resulted in three publications. Finally, I give my thanks to Drs Jayne Kelleher, Barbara Hänzi and Fran Denk for offering help in checking and correcting the draft version of this thesis.

Contents

List of abbreviations

AAV – adeno-associated virus

AAVR – adeno-associated viral receptor

AMPA – α-Amino-3-Hydroxy-5-Methyl-4-Isoxazolepropionic Acid

ASIC – acid-sensing ion channel

ATP – adenosine triphosphate

AV – adenovirus

BBB – blood-brain barrier

BDA – biotinylated dextran

BK – bradykinin

CBA – chicken β-actin

CFA – complete Freund's adjuvant

CGRP – calcitonin gene-related peptide

CM – cisterna magna

CMV – cytomegalovirus

CNS – central nervous system

cpEGFP – circular permutated enhanced green fluorescent protein

crRNA – CRISPR-associated RNA

CSF – cerebrospinal fluid

DAPI - 4',6-diamidino-2-phenylindole

DPBS – Dulbecco's phosphate-buffered saline

DREADD – designer receptor exclusively activated by designer drugs

DRG – dorsal root ganglia

eGFP – enhanced green fluorescent protein

ER – endoplasmic reticulum

FACS – fluorescence activated cell sorting

FBS – foetal bovine serum

FRET – fluorescence resonance energy transfer

FSC – forward scatter

FSK – forskolin

GDNF – glial cell-derived neurotrophic factor

GECI – genetically-encoded calcium indicator

GFP – green fluorescent protein

GFAP – glial fibrillary acidic protein

gRNA – guide RNA

HCN – hyperpolarization-activated cyclic nucleotide-gated

HDAC4 – histone deacetylase 4

HIV-I – human immunodeficiency virus type 1

HSV – herpes simplex virus

HVA – high voltage activated

IASP – International Association for the Study of Pain

IB4 – isolectin B4

ICC – immunocytochemistry

ICV – intracecrebroventricular

IHC – immunohistochemistry

IS – inflammatory soup

IT – intrathecal

ITR – inverted terminal repeat

IV – intravenous

IVM – ivermectin

LamR – laminin receptor

LGCC – ligand-gated chloride channel

LGIC – ligand-gated ion channel

LP – lumbar puncture

LTP – long-term potentiation

LV – lentivirus

LVA – low voltage activated

MACS – magnetic-assisted cell sorting

MAG – myelin associated glycoprotein

MCU – mitochondrial calcium uniporter

mGluR – metabotropic glutamate receptor

MRGPRD – Mas-related gene product receptor D

Nabs – neutralising antibodies

nAchR – nicotininc acetylcholine receptor

NCX – Na^{+}/Ca^{2+} exchanger

NeuN – neuronal nuclear protein

NF200 – neurofilament 200

NGF – nerve growth factor

NMDA – N-Methyl-D-Aspartate

NMDAR – N-methyl-D-aspartate receptor

NS – nervous system

OD – outer diameter

PBS – phosphate-buffered saline

PCR – polymerase chain reaction

PFA – paraformaldehyde

PGE2 – prostaglandin E2

PKA – protein kinase A

PKC – protein kinase C

PLC – phospholipase C

PLL – poly-L-lysine

PMCA – Plasma Membrane Ca^{2+} ATPase

PNS – peripheral nervous system

PTEN – phosphatase and tensin homolog

PTFE – polytetrafluoroethylene

RFP – red fluorescent protein

RPM – rounds per minute

scAAV – self-complimentary AAV

SEM – standard error of mean

SERCA – sarco/endoplasmic reticulum calcium ATPase

SSC – side scatter

STAT3 – signal transducers and transcription activator 3

TG – trigeminal ganglia

TH – tyrosine hydroxylase

tracrRNA – *trans*-activating CRISPR RNA

TRPA1 - transient receptor potential ankyrin 1

TRPV1 – transient receptor potential vanilloid 1

UV – ultraviolet

VAMP2 – vesicle-associated membrane protein 2

VGCC – voltage dated calcium channels

YC – Yellow Cameleon

ZFN – zinc finger nucleases

List of Figures and tables

Chapter 1: General Introduction

1.1 The nervous system and pain

The nervous system (NS) is one of the most complex parts of an organism, comprising of billions of neurons and glial cells and significantly more numerous connections between them (Andrade-Moraes *et al.*, 2013; von Bartheld, Bahney and Herculano-Houzel, 2016). One of the main functions of the NS is to gather and process information about the changing external and internal organismal environment (Ringkamp *et al.*, 2013). This environment is continuously monitored by the sensory division of the peripheral nervous system (PNS) (Frings, 2012). Primary afferent neurons are the PNS neurons responsible for detecting various stimuli, such as thermal (skin warming in the sun) and mechanical stimuli (gentle touch or muscle stretch) (Ringkamp *et al.*, 2013). The cell bodies of these primary afferent neurons are located in the dorsal root ganglia (DRG) and trigeminal ganglia (TG) (Purves *et al.*, 2018). Their axons bifurcate, with one branch innervating a target, such as skin or muscle, and the other projecting into the central nervous system (CNS) (Todd and Koerber, 2013). When a stimulus is detected by the sensory afferent in the periphery, it is converted into an electrical signal and passed along the axon into the CNS. There, it is integrated and processed, leading to generation of a sensation that reflects the nature of the stimulus (Purves *et al.*, 2018).

One of the most important sensations is pain. Pain is defined by the International Association for the Study of Pain as “an unpleasant sensory and emotional experience associated with actual or potential tissue damage, or described in terms of such damage“ (IASP Task Force on Taxonomy, 1994). Pain serves a protective role, as it signals the threat of injury or its occurrence, and promotes protective behaviour that facilitates healing (Woolf, 2004). Pain sensation can be elicited following detection of a noxious (injurious or potentially injurious) stimulus by the PNS and its processing in the CNS (Ringkamp *et al.*, 2013). Neural encoding of a noxious stimulus is known as nociception (IASP Task Force on Taxonomy, 1994; Baliki and Apkarian, 2015). Several distinct parts of the neural circuitry contribute to nociception and

pain. First, primary nociceptive neurons are activated in the periphery by a noxious mechanical, thermal or chemical stimulus (Kelleher, Tewari and McMahon, 2017). These neurons project to the dorsal horn of the spinal cord, where they pass on the signal to second-order neurons (Schaible, 2006). This signal then undergoes partial processing in interneuron circuits before being passed onto ascending projection neurons that carry the signal to the targets in the brainstem and thalamus (Todd, 2010). From there, the information is passed to many cortical areas and the sensation of pain is elicited (Apkarian *et al.*, 2005; Basbaum *et al.*, 2009) . In addition, there are descending pathways, mostly originating from nucleus raphe magnus and locus coeruleus, that project to the dorsal horn of the spinal cord and are capable of modulating nociceptive input (Todd, 2010; West *et al.*, 2015).

1.2 Primary afferents and nociception

Primary afferent neurons that detect only high-intensity noxious stimuli are classified as nociceptors (Basbaum and Jessell, 2000). These neurons are a crucial part of the pain circuitry, as they are responsible for sensing damage or the threat of damage and triggering the cascade leading to pain sensation. Nociceptors can be divided into two broad categories, A-fibre and C-fibre nociceptors (Basbaum *et al.*, 2009). A-fibre nociceptors include medium diameter thinly myelinated afferent (Aδ fibres). These neurons have superior conduction velocities compared to C-fibre afferents and are mostly responsible for evoking acute, sharp, fast pain upon injury (Slugg, Meyer and Campbell, 2000; Basbaum *et al.*, 2009; Ringkamp *et al.*, 2013). They can be further sub-divided into two types: type I and type II. Most of the type I A-fibre nociceptors are polymodal, capable of detecting noxious thermal, mechanical and chemical stimuli, and have a high heat response threshold and a relatively slow response to intense heat (Treede *et al.*, 1998; Ringkamp *et al.*, 2013). Type II A-fibre nociceptors have a much faster response to intense heat and a lower threshold of activation with thermal stimuli, but have a very high mechanical threshold (Treede *et al.*, 1998; Basbaum *et al.*, 2009). In contrast, C-fibre nociceptors are small diameter, unmyelinated fibres with slower conduction speeds compared

to A-fibres (Ringkamp *et al.*, 2013). Most of these fibres are also polymodal, responding robustly to mechanical and heat stimuli, and to a smaller extent, chemical stimuli (Davis, Meyer and Campbell, 1993; Schmidt *et al.*, 1995). In addition, some of C-fibre nociceptors are mechanically-insensitive, but can develop mechanosensitivity after exposure to chemicals released upon tissue injury (Schmidt *et al.*, 1995; Basbaum *et al.*, 2009).

Peripheral projections of nociceptors do not innervate any specialised structures, and instead terminate in the target area as free nerve endings (Caterina, Gold and Meyer, 2005). These nerve endings contain all the machinery required for the transduction of a noxious chemical, thermal and mechanical stimuli into electrical signals (Gold, 2013). Noxious stimuli, detected by their respective specialised receptors in the free nerve endings, trigger generator potentials, which in turn give rise to action potentials and propagation of a signal (Gold, 2013). A large number of proteins have been shown to play a role in detecting noxious stimuli, including transient receptor potential vanilloid 1 (TRPV1) receptor for noxious heat (Caterina *et al.*, 1997; Tominaga *et al.*, 1998), transient receptor potential ankyrin 1 (TRPA1) for noxious cold and several noxious chemicals like mustard oil and formalin (Story *et al.*, 2003; Jordt *et al.*, 2004; Karashima *et al.*, 2007, 2009; McNamara *et al.*, 2007), acid-sensing ion channels (ASICs) for protons and low pH (Lingueglia, 2007), and Piezo2 for noxious mechanical stimuli, although the role of this channel is still under investigation (Coste *et al.*, 2010).

Central projections of the DRG neurons terminate in the dorsal horn of the spinal cord. Most projections from nociceptive A- and C-fibres terminate in the lamina I and lamina II of the dorsal horn (Todd, 2010). Here, they synapse onto excitatory and inhibitory interneurons, as well as projection neurons (Todd, 2010). The interneuron circuitry is complex and plays a crucial role in modulating the signal carried by the primary nociceptive neurons before passing it on to projection neurons (Todd and Koerber, 2013; West *et al.*, 2015). However, some nociceptors can synapse directly onto the projection neurons, for example peptidergic C-fibre

nociceptors can synapse onto neurokinin 1 receptor-expressing projection neurons in lamina I (Todd *et al.*, 2002).

One of the core features of nociceptors is that they can exhibit the phenomenon of hyperalgesia (Ringkamp *et al.*, 2013). Nociceptors that exhibit hyperalgesia show greatly augmented responses to stimuli that would normally trigger only moderate activity. For instance, responses of A- and C-fibre rat nociceptors to suprathreshold mechanical stimuli were much more intense after the induction of hyperalgesia by Complete Freund's Adjuvant (CFA)-induced inflammation (Andrew and Greenspan, 1999). A similar increase in neuronal discharge is evident in human A-fibres responses to a suprathreshold heat stimulus after a burn injury (Meyer and Campbell, 1981). This potentiation of nociceptor responses is caused by the action of various inflammatory mediators that are released after injury (Basbaum *et al.*, 2009). Binding of inflammatory mediators to their respective receptors on the nociceptor's peripheral terminals can initiate a secondary-messenger cascade that triggers modification of the receptors responsible for detecting noxious stimuli (Dawes *et al.*, 2013). For instance, activation of bradykinin B1 or B2 receptors by bradykinin leads to a secondary messenger cascade involving phospholipase C (PLC) and protein kinase C (PKC), which results in phosphorylation of TRPV1 and potentiation of neuronal responses to heat and capsaicin (Chuang *et al.*, 2001; Vellani *et al.*, 2001; Bhave *et al.*, 2003; Vellani, Zachrisson and McNaughton, 2004). In addition to sensitising nociceptors to noxious stimuli, inflammatory mediators have been shown to lower the threshold of activation for the nociceptors to such a degree that non-noxious stimuli are capable of activating nociceptors and eliciting pain behaviour (Martin *et al.*, 1987; Ahlgren, Wang and Levine, 1996; Bishop *et al.*, 2010; Lennertz *et al.*, 2012; Weinkauf *et al.*, 2013). This process of peripheral sensitisation serves to promote protective behaviour, forcing the individual to take care not to damage the injury site further and to promote rest and healing (Ringkamp *et al.*, 2013).

1.3 Pain disorders and nociceptors

The importance of correct functioning of the nociceptive circuitry is best highlighted by its disorders. For instance, genetic conditions, such as congenital insensitivity to pain, can result in the inability to feel pain. This leads to a severely reduced life expectancy and quality of life (Goldberg *et al.*, 2007), since patients experience serious or life threatening injuries without noticing them. They do not realise when a bone is fractured and cannot protect the affected limb, preventing it from healing (Schon, Parker and Woods, 2018). On the other end of the pain disorders spectrum are individuals that have a gain-of-function mutation, e.g. in the *SCN9A* gene which encodes the voltage-gated sodium channel $Na_v1.7$ (Yang *et al.*, 2004; Dib-Hajj *et al.*, 2005). These mutations cause patients to experience extreme pain in the absence of noxious stimuli, which dramatically reduces quality of life (Fischer and Waxman, 2010; Bennett and Woods, 2014).

These genetic disorders, although severe, are not common in the general population (Bennett and Woods, 2014). Conversely, chronic pain generally affects approximately 20% of the population, and has severe socio-economic and quality of life implications (Breivik *et al.*, 2006; Treede *et al.*, 2015). Chronic pain is defined as a persistent or recurrent pain lasting longer than 3 months, and can be divided into different types based on the cause (Treede *et al.*, 2015). These include chronic inflammatory pain after prolonged inflammation, and neuropathic pain following a nerve injury (Treede *et al.*, 2015). Often, the sensation of pain is disproportionate to the severity of the initial injury and this extends beyond the time of injury resolution and is associated with functional disability and emotional distress (Van Hecke, Torrance and Smith, 2013; Treede *et al.*, 2015). Critically, our capability of managing chronic pain disorders is limited, with many individuals responding poorly to the current available treatments (Garland, 2014; Rajapakse, Liossi and Howard, 2014).

Several core mechanisms that underlie this disorder have been uncovered, one of which is dysfunction of primary afferent nociceptors (Basbaum *et al.*, 2009).For instance, persistent

inflammation, such as that seen in arthritis, causes permanent changes in peripheral nociceptors (Schaible, 2012; Nassini *et al.*, 2014). These include a change in the expression of certain ion channels. The overexpression of the hyperpolarization-activated cyclic nucleotide-gated (HCN) channel 2 in chronic inflammatory pain causes an increased I_h current, which leads to membrane depolarisation toward the action potential threshold (Weng *et al.*, 2012). Changes in membrane receptors also take place, for example upregulation of TRPA1 causes increased activity of nociceptors (Obata *et al.*, 2005; Nassini *et al.*, 2014). Similar changes are also seen in neuropathic pain, with reports of altered expression of sodium and potassium ion channels, as well as membrane receptors (Persson *et al.*, 2009; Hammer *et al.*, 2010; Devor, 2013). Their upregulation causes increased activity of nociceptors that is independent of the initial injury, for example nerve injury can cause ectopic firing in primary afferents, leading to the sensation of pain (Woolf, 2004; Devor, 2013). In chronic inflammatory pain, a persistent state of sensitisation primes nociceptors to respond to noxious stimuli with a greatly exaggerated activity, rendering even mild noxious as well as non-noxious stimuli painful (Fornasari, 2012; Lolignier, Eijkelkamp and Wood, 2014). In addition, the central terminals of the nociceptors can also exhibit physiological alterations, such as loss of inhibition and sensitisation of glutamate receptors (Basbaum *et al.*, 2009). Finally, therapies that target primary afferent neurons, such as lidocaine-induced silencing, have been shown to be successful in alleviating chronic pain (Gammaitoni, Alvarez and Galer, 2003; Argoff *et al.*, 2004). This highlights the importance of continuing to study all aspects of primary afferent neurons, from their anatomy to their physiology and activity patterns, to better understand the pathology associated with chronic pain, and to identify new targets that can be used to develop better therapies.

1.4 Approaches to study DRG neurons

There are a large number of experimental approaches and techniques that can be used to study DRG neurons, both in in the healthy state and under pathological conditions, such as

chronic pain. These approaches can be roughly split into two different types. The first focuses on monitoring aspects of the physiology of primary afferents, for example electrophysiological recordings of neuronal activity (Wickenden, 2014). The second approach is to actively interfere with cellular processes in primary afferents using methods such as overexpression or knock out of genes of interest to study the effect this has on both neuronal physiology as well as on the whole animal, for example the knockout of the TRPV1 gene (Caterina *et al.*, 2000). However, these techniques are rarely used in isolation, and studies often utilise techniques that combine both observational and modulational approaches. Below I provide an overview of a few of these approaches, as well as examples of the tools and techniques used.

As previously described, the pain circuit is an incredibly complex network of various types of neurons with a precise pattern of neuronal connections. Therefore, understanding the way that different parts of the pain circuit wire together is pivotal to gaining insight into their functions. The most common method for studying the morphology and anatomy of neurons is through the use of neuronal tracers (Vercelli *et al.*, 2000; Basbaum and Bráz, 2010). Tracers have been used to study neuronal anatomy since the late 20th century, and there are numerous types of dyes available for a range of applications (Köbbert *et al.*, 2000). For instance, a chemical fluorescent retrograde tracer Fluoro-gold (Ju, Han and Fan, 1989) has been used to study the nociceptor population that innervates the knee joint (Ivanavicius *et al.*, 2004), wrist joint (Kuniyoshi *et al.*, 2007) and the mandibular incisor (Mosconi, Snider and Jacquin, 2001), as well as the central circuitry involved in nociception (Ding *et al.*, 1995; Taguchi *et al.*, 2007). Anterograde tracers, such as biotinylated dextran (BDA), have been used to study the projection targets of neurons in the pain circuit, for example primary nociceptor projections to the bladder (Spencer *et al.*, 2018), and projections from the dorsal reticular nucleus in the medulla, which are involved in the descending modulation of the nociceptive circuitry (Leite-Almeida, Valle-Fernandes and Almeida, 2006). Furthermore, a combined approach of tracer application and immunohistochemical analysis of tissue has been used to interrogate both the anatomical projections and the identity of the synaptic targets of neurons

involved in nociception, for example to study spinal cord targets of non-peptidergic VGluT2 positive mouse primary afferents (Clarke *et al.*, 2011).

Tracer studies have contributed immensely to our understanding of the pain circuitry; however, the use of tracers also has some drawbacks. Dye injection into the tissue will result in all cells in the injection site taking up the dye, including those that are not the focus of the study. For example, injection into the dorsal horn will label interneurons as well as projection neurons (Basbaum and Bráz, 2010). This can be circumvented by tracer delivery via an intracellular injection, but this is a complex procedure and only labels one neuron per injection (Mason, Larkman and Eldridge, 1988). Alternatively, transgenic mouse lines expressing fluorescent proteins controlled by a specific promoter of interest can be used to visualise neurons of a particular population. For instance, this approach can be used when studying various classes of dorsal horn interneurons (Boyle *et al.*, 2017; Gutierrez-Mecinas *et al.*, 2018) or non-peptidergic Mas-related gene product receptor D (MRGPRD) - positive nociceptors (Olson *et al.*, 2017). Transgenic mice have been developed that express the trans-synaptic neuronal tracer wheat germ agglutinin under a specific promoter or Cre-recombinase control (Yoshihara *et al.*, 1999; Braz, Rico and Basbaum, 2002). However, most of the transgenic lines available are limited to mice, and the correct transgenic line for a particular neuronal population may not be available.

Neuroanatomy is only one aspect of the physiology of neurons involved in the pain circuit. It is equally important to understand the way in which these neurons communicate with each other, what kind of stimuli they respond to, and what their activity patterns are. The main technique for studying neuronal activity in nociceptors is electrophysiology (Carter and Shieh, 2015). There is a multitude of different electrophysiological techniques that makes it possible to extensively study many aspects of the activity patterns in nociceptors and related circuitry (Vertes and Stackman, 2011). It is beyond the scope of this thesis to compare them all, so only a few examples of their use for studying nociceptors are listed below. Intracellular and patch-clamp recording of neuronal activity allows analysis of a single cell activity with unmatched

temporal precision (Carter and Shieh, 2015; Rubaiy, 2017). Both intracellular and patch-clamp techniques have been used to study various aspects of nociceptor physiology (Koerber, Druzinsky and Mendell, 1988; Traub and Mendell, 1988; Ritter and Mendell, 1992; Gee *et al.*, 1999), and their responses to various stimuli such as heat or capsaicin (Koplas, Rosenberg and Oxford, 1997; Davis *et al.*, 2000; Woodbury *et al.*, 2004). It is also possible to record the activity of a single neuron using a teased-nerve preparation. This technique does not require access to cell soma and leaves the circuitry predominantly intact, making it possible to record responses following application of stimuli to the innervation target of the neuron (Fleischer, Handwerker and Joukhadar, 1983; Lewin and McMahon, 1991; Kress *et al.*, 1992; Koltzenburg, Stucky and Lewin, 1997). Furthermore, using a teased-nerve technique *in vitro* in conjunction with the nerve innervation target, such as skin, allows tight control over experimental variables such as the effective concentrations of applied compounds and their precise pattern of spread in the tissue (Reeh, 1986; Kress *et al.*, 1992). This approach has been used to investigate nociceptor responses to stimuli such as heat and inflammatory mediators applied to the skin (Liang, Haake and Reeh, 2004; Derow *et al.*, 2007).

In summary, electrophysiological techniques are a powerful tool for studying neuronal activity, providing unmatched temporal resolution and sensitivity (Carter and Shieh, 2015). However, they also have some disadvantages, such as the necessity for physical contact with the tissue and the challenges associated with recording activity in more than a handful of neurons at the same time (Anderson, Zheng and Dong, 2018). Another technique for recording neuronal activity that circumvents these drawbacks is calcium imaging. This technique uses calcium-sensitive dyes that change their visual properties based on the level of intracellular calcium (Paredes *et al.*, 2008). In neurons, a sharp rise in intracellular calcium is observed during an action potential (Clapham, 2007). Calcium dyes provide the visual read-out for this increase, which in turn is used as a proxy for neuronal activity (Anderson, Zheng and Dong, 2018). Traditionally, chemical dyes such as Fura-2 AM have been extensively used to study responses of DRG neurons to various stimuli such as heat, capsaicin and inflammatory mediators (Kano *et*

al., 1994; Paredes *et al.*, 2008; Wooten *et al.*, 2014), however genetically-encoded calcium indicators (GECI) such as GCaMP are becoming more and more popular. GECI can be used to visualise activity in a specific subset of neurons using cell-specific promoters, in addition to circumventing some of the difficulties associated with loading of traditional chemical dyes (Tian, Hires and Looger, 2012; Pérez Koldenkova and Nagai, 2013; Lin and Schnitzer, 2016). A much more detailed description of the calcium imaging technique and its variations, is provided in the introduction to chapter 3.

One final approach to studying nociceptors that I would like to mention in this overview is using tools that allow manipulation of cellular gene expression profiles. Neurons express thousands of genes throughout their lifetime, and this plays an important part in defining their physiology (F. C. Yang *et al.*, 2013; Smith *et al.*, 2013; Usoskin *et al.*, 2015). The pattern of gene expression can change in response to changes in their environment, for instance nociceptors have been shown to alter their gene expression pattern in pathological conditions such as neuropathic pain (Smith *et al.*, 2015; Cobos *et al.*, 2018). By studying changes in genes expression in neurons within the pain circuit it may be possible to find ways to reverse, or at least attenuate, the pathology of these conditions (Mogil, Max and Belfer, 2013). This can be done using transgenic mouse lines. For example, deletion of the TRPV1 gene in a transgenic mouse line helped to elucidate the importance of TRPV1 for nociception (Caterina *et al.*, 2000). Alternatively, several transgenic tools, such as Cre recombinase, CRISPR and zinc finger nucleases (ZFN) can be used to alter gene expression (Lewandoski, 2001; Gavériaux-Ruff and Kieffer, 2007; Urnov *et al.*, 2010; Sander and Joung, 2014). These tools can be used to selectively knock out genes of interest and can be controlled both spatially (e.g. by using cell-specific promoters for their expression, such as the $Na_v1.8$ promoter for nociceptors (Stirling *et al.*, 2005)) and temporally (e.g. an inducible Cre recombinase fused with a mutated oestrogen receptor T2 (Feil *et al.*, 1996; Indra *et al.*, 1999; Feil, Valtcheva and Feil, 2009)). A more extensive discussion of the use of Cre recombinase for modulation of gene expression is provided in chapter 4.

Listed above are just a few examples of different experimental approaches used to study the neurons involved in nociception and pain sensation. Importantly, they all have something in common: all these approaches can take advantage of transgenic tools. There is a multitude of transgenic tools available for almost every experimental approach to studying nociceptors, from visualising parts of a neuron with targeted fluorescent proteins (e.g. visualising presynaptic terminal by using GFP fused to Vesicle-associated membrane protein 2 (VAMP2) (D'Acunzo *et al.*, 2014)) to controlling neuronal activity with optogenetics (Zhou, Pan and Lin, 2015). However, all these tools have to be expressed by the cells of interest in order to be utilised, which is often achieved by using transgenic mouse lines that may not always be available. An alternative way of delivering transgenic tools to cells of interest that is quicker and does not require transgenic animals is the use of viral vectors.

1.5 Viral vectors for transgene delivery

Viral vectors are modified viral particles that can be used to deliver various genetic sequences into cells (Kantor *et al.*, 2014). All viral vectors are derived from wild-type viruses. However, they are rendered incapable of replication within the host cell by removing most of the wild-type viral genome and replacing it with the gene of interest (Lentz, Gray and Samulski, 2012). Usually, the part of the viral genome removed encodes proteins necessary for the correct assembly of the viral capsid and/or envelope, so it has to be supplied externally during viral vector production (Kantor *et al.*, 2014). Most commonly, viral vectors are produced by transfecting an immortalised mammalian cell line, like HEK-293, with the plasmid that contains the gene of interest (expression cassette) and the plasmids that encode the viral machinery needed for vector production, as well as those encoding proteins for capsid and/or envelope assembly (packaging cassette) (Aponte-Ubillus *et al.*, 2018; Penaud-Budloo *et al.*, 2018; Sharon and Kamen, 2018).

Many types of viral vectors exist, each with their own unique properties. They can be used for a large number of applications for studying the nervous system, including the delivery of gene

sequences to correct pathology and delivery of transgenic tools such as GECI, channelrhodopsin and Cre recombinase (Lentz, Gray and Samulski, 2012; Woodward and Pava, 2012; Shimano *et al.*, 2013; Gierut, Jacks and Haigis, 2014; Sengupta *et al.*, 2017; Le Duigou *et al.*, 2018). Below, I will describe some of the most popular viral vectors used for transgene delivery in the nervous system. These include lentiviral (LV) vectors, herpes simplex viral (HSV) vectors, adenoviral (AV) vectors and adeno-associated viral (AAV) vectors (Lentz, Gray and Samulski, 2012).

1.5.1 Lentiviral vectors

One of the most widely used viral vectors in the nervous system are lentiviral (LV) vectors. These vectors are based on the human immunodeficiency virus type I (HIV-I) (Naldini et al. 1996). LV vectors have a single-stranded RNA genome and their cloning capacity is around 8 kb (Jakobsson and Lundberg, 2006). They were first used to transduce adult neurons in the rat brain in the 1996 (Naldini, Blomer, *et al.*, 1996). Since then, LVs have undergone a number of rounds of optimisation and modification, and have been used extensively for gene delivery in the nervous system (Parr-Brownlie *et al.*, 2015).

Initially, only two plasmids were used for LV vector production, one encoding the gene of interest and another encoding all the required viral genes: *gag* (viral matrix and capsid), *pol* (enzymes necessary for viral genome processing), and *env* (envelope glycoprotein), as well as regulatory genes *rev* and *tat* and accessory genes (*nef, vif, vpr*, and *vpu*) (Naldini, Blomer, *et al.*, 1996; Coffin, Hughes and Varmus, 1997). However, the use of only two plasmids for LV vector production often yielded LVs that were replication-competent, making them cytotoxic. Therefore, the packaging cassette was soon altered to delete the unnecessary accessory proteins and split into two separate plasmids (Zufferey *et al.*, 1997; Dull *et al.*, 1998). These alterations reduced the chances of generating replication-competent viruses without lowering the yield or the transduction efficiency (Kantor *et al.*, 2014).

Another example of LV vector modification is pseudotyping. LV vectors have the ability to incorporate envelope proteins from different viruses (Kantor *et al.*, 2014). The envelope of the virus is crucial in determining its tropism, so by introducing specific proteins (often from other viruses) into the viral envelope (pseudotyping) it is possible to restrict the cell types that can be transduced with the LV vector (Bischof and Cornetta, 2010). There are a number of different envelopes available for pseudotyping, including those with broad transduction patterns like Vesicular stomatitis virus G-protein, and those with tropism for neurons like Rabies-G envelope (Schlegel *et al.*, 1983; Reiser *et al.*, 1996; Cronin, Zhang and Reiser, 2005; Rahim *et al.*, 2009).

LV vectors are powerful tools that can effectively transduce a large variety of cells and result in strong and stable transgene expression (Parr-Brownlie *et al.*, 2015). However, there are some disadvantages to using LV vectors. The stability of transgene expression observed with LV vectors is due to integration of the vector genome into the host DNA (Escors and Breckpot, 2010). This can be problematic, as the integration of the LV genome can disrupt the host's genome and cause tumorigenesis (Themis *et al.*, 2005). Several methods of overcoming this drawback have been designed, mostly focusing on the generation of non-integrating LV vectors, whose genomes exist in the nucleus as episomes within the transduced cell. This can be done by introducing a mutation into the *Int* gene that encodes the integrase, so that it is rendered non-functional (Bayer *et al.*, 2008; Kantor *et al.*, 2009). Alternatively, it is possible to mutate the integrase attachment sites on the viral DNA so that the integrase cannot interact with it (Apolonia *et al.*, 2007). These non-integrating LV have been shown to have a very low incidence of integration into the host genome, however the transgene expression levels are lower than those of an integrating LV vector (Bayer *et al.*, 2008; Kantor *et al.*, 2014). Also, LV vectors are relatively large particles (~100 nm), which limits the spread of the LV vectors in the extracellular space, leading to the transduction only in cells close to the injection epicentre *in vivo* (Parr-Brownlie *et al.*, 2015). This may be a disadvantage if extensive transduction is desired.

1.5.2 Herpes simplex viral vectors

Vectors derived from Herpes Simplex virus (HSV) are large particles (~186 nm), and can have a packaging capacity of up to ~150 kb (Lentz, Gray and Samulski, 2012). These vectors consist of a nucleocapsid harbouring double-stranded DNA genome, and a viral envelope with specific glycoproteins that are required for cell transduction (Lentz, Gray and Samulski, 2012). Between the nucleocapsid and the envelope is the tegument containing structural proteins and enzymes that are important for DNA replication and cell infection (Lentz, Gray and Samulski, 2012; Kantor *et al.*, 2014). Upon infection, the wild-type HSV genome persists as an episome in the nucleus and is capable of remaining latent with little detrimental effect on the host for a long period of time. However, the wild-type HSV genome can also initiate a lytic pathway by the sequential expression of immediate-early proteins encoding transcription regulatory proteins, early proteins encoding the viral DNA polymerase and late proteins that mostly encode structural proteins (Lachmann, 2004; Kantor *et al.*, 2014). There are three kinds of viral vectors that have been derived from HSV: replication-competent, replication-defective and amplicon vectors (Marconi *et al.*, 2009). These vectors are suitable for use in the nervous system since the HSV is capable of retrograde transport and its envelope exhibits neuronal tropism (Lentz, Gray and Samulski, 2012).

Replication-competent HSV vectors have an incomplete viral genome, lacking certain genes like thymidine kinase and ICP34.5 that are responsible for virulence and pathogenicity of the HSV (Todo, 2008). These mutations make it impossible for these vectors to initiate a lytic pathway in non-dividing cells. However, a lytic infection is still triggered in dividing cells present in tumours, as these vectors can take advantage of the physiological changes in tumour cells, that allow them to replicate and lyse these cells (Todo, 2008). Although not suitable for transgene delivery to healthy cells, replication-competent HSV vectors have been used for cancer therapy (Post *et al.*, 2004).

Replication-deficient HSV vectors were created by deleting the genes encoding the proteins necessary for triggering the lytic pathway (Wu *et al.*, 1996; Samaniego, Neiderhiser and DeLuca, 1998). This significantly reduces their toxicity, making them suitable for transgene delivery to cells of interest (Kaplitt and Makimura, 1997; Krisky *et al.*, 1998). These vectors have been used to deliver a wide variety of transgenes to neurons, for example pathology-correcting hexosaminidase in a model of Tay-Sachs disease (Martino *et al.*, 2005), and short hairpin RNA to inhibit accumulation of amyloid-β in a mouse model of Alzheimer's disease (Hong *et al.*, 2006). They have also been used in the field of pain research, for instance to investigate the protective role of NGF and neurotophin-3 in sensory neuropathy (Goss *et al.*, 2002; Chattopadhyay *et al.*, 2005), or the antinociceptive effect of enkephalin expression in the DRG neurons (Braz *et al.*, 2001; Goss *et al.*, 2001).

Finally, amplicon vectors consist of a bacterial plasmid carrying an HSV origin of replication site and packaging signal, but no other viral genes (Spaete and Frenkel, 1982). Co-transfection with the helper HSV plasmid during production creates vectors that are identical to HSV, except for replacement of viral DNA with a bacterial plasmid (Epstein, 2005). This dramatically reduces toxicity of these vectors, as well as allowing more space for the insertion of the desired DNA sequence (up to 150 kb) (Epstein, 2009). It has been used in various studies of the nervous system, including those investigating the effect of NGF and NMDA receptors on learning and memory (Brooks *et al.*, 2000; Adrover *et al.*, 2003).

HSV vectors are well-suited for gene delivery in the nervous system, as they possess an innate ability to target neurons and are capable of retrograde transport. In addition, they have a large packaging capacity. However, production of HSV vectors is not trivial, and sometimes results in production of cytotoxic replication-competent vectors alongside the desired viral vectors (Lentz, Gray and Samulski, 2012; Kantor *et al.*, 2014).

1.5.3 Adenoviral vectors

Adenoviral (AV) vectors are derived from adenoviruses, non-enveloped icosahedral viruses containing ~26-40 kb double stranded DNA (Campos and Barry, 2008). Initial research into the use of adenoviruses as viral vectors resulted in first-generation AV vectors derived from AV serotypes 2 and 5 that lacked the genes necessary for triggering DNA synthesis and viral replication (Graham *et al.*, 1977). Upon infection, viral DNA did not integrate within the host's DNA and was maintained as a nuclear episome (Lentz, Gray and Samulski, 2012). However, these first-generation AV vectors still elicited low-level expression of viral antigens in the host cell membrane, which lead to detection and elimination of the transduced cells by the host immune system, resulting in only transient expression of the transgene *in vivo* (McConnell and Imperiale, 2004). Further development of AV vectors resulted in generation of helper-dependent "gutless" AV vectors, in which most of the viral genes have been removed and only the elements required for genome replication and encapsidation remain, increasing the packaging capacity to around 35 kb and reducing the host immune response (Palmer and Ng, 2005). However, a significant degree of immune response still persists that can cause serious side-effects (Lehrman, 1999; Bessis, GarciaCozar and Boissier, 2004; Muruve, 2004).

AV vectors have been used extensively for gene delivery in a large number of research fields, including pain. For example, AV vectors have been used to study the physiology of endogenous analgesia via expression of a potassium channel on descending noradrenergic neurons, thus inhibiting their activity and causing hyperalgesia in rats (Howorth *et al.*, 2009). AV vectors have also been used to express GDNF in DRG neurons after chronic constriction injury, which resulted in an improved myelination profile and attenuation of nocifensive behaviour (Shi *et al.*, 2011).

The large packaging capacity and retrograde transport capabilities, as well as neuronal tropism, have made AV vectors popular tools for studying the nervous system (Kantor *et al.*, 2014). However, AV vectors have some disadvantages, the major one being the high probability of

eliciting an immune response to the vector particles, and therefore only transient expression *in vivo* due to cell clearance by the immune cells (Lentz, Gray and Samulski, 2012).

1.5.4 Adeno-associated viral vectors

Adeno-associated viral (AAV) vectors are derived from adeno-associated viruses, which are a type of dependoviruses. AAV viral particles are only ~20 nm in diameter and do not have a viral envelope. Their genome is ~4.7 kb of singe-stranded DNA that has two Inverted Terminal Repeat (ITR) sequences, and encodes four replication proteins (*rep*) and three structural proteins (*cap*) (Kantor *et al.*, 2014). Upon infection, the viral genome can stably integrate into the host's DNA or persist as an episome (Samulski *et al.*, 1991; Duan *et al.*, 1998). As the wild-type AAV genome does not encode all the proteins needed for replication, co-infection with a helper virus, such as an adenovirus, is required for AAVs to replicate (Murlidharan, Samulski and Asokan, 2014).

In AAV vectors, only the ITR sequences are retained, while the rest of the genome is replaced with the transgene and an appropriate promoter (Xiao *et al.*, 1997). This results in the packaging capacity very close to that of the wild-type vector, ~4.7 kb (Dong, Fan and Frizzell, 1996). For manufacturing, the *rep* and *cap* genes are expressed using a separate packaging AAV plasmid, while the essential non-AAV genes are expressed using a helper plasmid (Xiao, Li and Samulski, 1998). This plasmid separation prevents the formation of wild-type AAV, therefore dramatically reducing the frequency of integration into the host DNA (Lentz, Gray and Samulski, 2012; Kantor *et al.*, 2014). In addition, AAV vectors have been shown to induce little to no innate immune response (Zaiss *et al.*, 2002; Bessis, GarciaCozar and Boissier, 2004).

There are many AAV serotypes, each with a different capsid composition, primary receptor for infection and tropism (Wu, Asokan and Samulski, 2006). The desired expression plasmid can be packaged into any of them, and the serotype selection will influence the AAV vector's cell specificity, which is highly beneficial for targeting transduction to a particular cell type (Rabinowitz *et al.*, 2002). For instance, IV injection of AAV vector serotypes 1 - 9 encoding the

same *luciferase* has been shown to result in different transduction patterns and cell specificity for every serotype (Zincarelli *et al.*, 2008). Furthermore, artificial modification of capsid can be achieved through rational design, directed and unbiased mutagenesis and peptide insertion (Kantor *et al.*, 2014). Rational design aims to enhance or alter the properties of the AAV based on the current knowledge of capsid protein structure and interactions, for example using amino acid sequences from two or more serotypes to enhance targeting (Bowles *et al.*, 2012). On the other hand, development of new capsids through unbiased mutagenesis involves randomly mutating and shuffling *cap* sequences from several serotypes before screening the products for the desired properties (Schaffer and Maheshri, 2004; Maheshri *et al.*, 2006), for example the ability to cross a seizure-compromised blood-brain barrier (BBB) (Gray *et al.*, 2010). Finally, it is also possible to insert non-viral peptides into the capsid to alter its selectivity, for example insertion of NMDAR agonist-derived peptide and a dynein motif into the capsid greatly enhanced transduction and retrograde transport of AAV2 in the CNS (Xu *et al.*, 2005).

Another significant breakthrough in the AAV vector field was the development of self-complimentary AAV (scAAV) vectors. The single stranded DNA of these vectors has two complimentary copies of the desired transgene separated by a mutated resolution sequence. This allows spontaneous re-annealing of the DNA, therefore eliminating the need for second strand synthesis in the infected cell (McCarty, Monahan and Samulski, 2001). This makes the onset of expression of the transgene much faster, and also increases transduction efficiency 10- to 100-fold (McCarty, Monahan and Samulski, 2001; Kantor *et al.*, 2014). However, by introducing a second copy of the transgene, the packaging capacity of scAAV vectors is reduced to ~2.2 kb (Kantor *et al.*, 2014).

Ease of production, low immunogenicity, high transduction efficiency, long-lasting transgene expression, availability of a large number of serotypes and advancements in vector design have made AAV vectors one of the most popular viral vectors for experimental and gene therapy

applications in the nervous system (Gray, Woodard and Samulski, 2010; Lentz, Gray and Samulski, 2012; Gray, 2013). AAV vectors have been used to deliver pathology-correcting transgenes in a variety of disease modes, including spinal muscular atrophy (Foust *et al.*, 2010), glycogen storage disease type I (Koeberl *et al.*, 2008), Krabbe's disease (Marshall *et al.*, 2018) and stroke (Yu *et al.*, 2013). In the context of pain research, AAV vectors have been used to target many parts of the pain circuitry (Guedon *et al.*, 2015; Zheng *et al.*, 2018), including primary afferent neurons (Fischer *et al.*, 2014; Chen *et al.*, 2018), and the spinal cord circuitry (Gutierrez-Mecinas *et al.*, 2018). However, it is important to note that despite low immunogenicity, some inflammatory responses may still be present after injection of the AAV (Ciesielska *et al.*, 2013; Chew *et al.*, 2016; Yang *et al.*, 2016; Colella, Ronzitti and Mingozzi, 2018). Interestingly, the responses are often caused by the vector product and not the AAV vector itself (Ciesielska *et al.*, 2013; Chew *et al.*, 2016). Therefore, it is important to control for these side-effects when using AAV vectors.

Overall, AAV vectors seem to be well suited for studying primary afferent neurons, and have several advantages over other available vectors, including low immunogenicity, neuronal tropism, efficient transduction and low cell toxicity (Lentz, Gray and Samulski, 2012; Kantor *et al.*, 2014). Therefore, in this study we decided to use AAV vectors as delivery tools to interrogate various aspects of the anatomy and physiology of primary afferent nociceptors.

1.6 Project hypothesis and aim

This project's hypothesis is as follows:

"AAV vectors, in particular AAV9, can be used to achieve high transduction in the primary afferent neurons following intrathecal and other delivery methods, and this approach can be used to to deliver functional transgenic tools that are then used to interrogate various aspects of neuronal physiology, including neuronal activity and gene expression."

The aim of this project is to express various transgenic tools in adult mouse primary afferent neurons *in vivo* and use them to study the various aspects of physiology and anatomy of

primary afferent neurons. In order to achieve expression of transgenes, we use non-pathogenic adeno-associated virus serotype 9 (AAV9). Our first aim is to establish an AAV delivery method that achieves high transduction *in vivo* in adult mouse primary afferents. We use an AAV9 expressing an eGFP transgene to identify and characterise the transduction pattern in DRG neurons. Secondly, we aim to deliver functional transgenes to primary afferent neurons, such as GCaMP6s, to study activity of these neurons *in vitro* and *in vivo*. Before transitioning into *in vivo* GCaMP6s applications, we first assess the performance of GCaMP6s in primary afferents *in vitro*. To do that, we aim to establish an *in vitro* sensitisation model for calcium imaging that uses electrical stimulation as an activity trigger, and then use it in conjunction with virally-delivered GECI GCaMP6s to image neuronal activity. Finally, we explore the use of our intrathecal AAV9 delivery method to assess the functionality of other transgenic tools *in vivo*, including GCaMP6s for neuronal activity visualisation, Cre recombinase for the control of gene expression, and chemogenetic neuronal silencing using engineered glutamate-gated chloride channel.

Chapter 2: Transduction of DRG neurons following intrathecal delivery of AAV9

2.1 Introduction

As discussed in the previous chapter, transgenic tools are invaluable assets to studying pain physiology and pathology. One of the most popular methods for gene expression is to transduce cells with viral vectors. AAV vectors are one of the most widely used types of vectors due to their low pathogenicity (Lentz, Gray and Samulski, 2012). There are also a large number of AAV serotypes available, each with its own specific transduction properties (Zheng *et al.*, 2018). Furthermore, administration of the same AAV via different delivery routes can produce transduction patterns that are drastically different. Therefore, it important that the correct combination of serotype and delivery route is used to effectively target the specific cell type/structure that is being studied. Given our interest in pain physiology, with a particular focus on the primary afferent neurons, we sought to find a way of transducing large numbers of DRG neurons with AAV vectors in adult mice.

2.1.1 Factors influencing AAV transduction

AAV transduction efficiency can be influenced by a number of factors, including serotype tropism, receptor availability, and delivery route. Since the initial discovery of AAV2 in 1965 by Atchison et al, many AAV serotypes have been isolated (Atchison, Casto and Hammon, 1965). Transduction capabilities of these serotypes are affected by the expression of specific AAV receptors by the target cells. The presence of some receptors, such as the recently identified AAV receptor (AAVR), are a common requirement among many AAV serotypes, where knock-out of its gene renders the cell lines or whole animals resistant to AAV infection with all serotypes (Pillay *et al.*, 2016). Several serotypes require an additional receptor to be present to achieve successful transfection, for instance AAV9 requires a specific surface glycan, *N*-linked galactose, for successful transduction (Shen *et al.*, 2011). Sialic acid linkages that obscure *N*-

terminal galactose can be removed with neuraminidase, which in turn can facilitate transduction in cells that are normally resistant to AAV9, such as airway epithelial cells (Bell *et al.*, 2011). Some receptors are shared between several AAV serotypes, like the laminin receptor for AAV 2,3,8 and 9 or sialic acid for AAV1,4,5 and 6 (Kaludov *et al.*, 2001; Wu *et al.*, 2006). Overexpression of laminin receptor (LamR) can boost transduction, while administration of an anti-LamR antibody reduces transduction efficiency in mice *in vivo* (Akache *et al.*, 2006). Furthermore, pathology that alters the availability of the AAV receptor, such as masking it with sialic acid in lysosomal storage disease, can impair transduction with any AAV serotype that uses that receptor (Y. H. Chen *et al.*, 2012). These studies show that receptor availability in the target cell type is one of the main factors that determines transduction efficiency. However, it is important to note that most cell types express multiple AAV receptors, so receptor availability alone may not be sufficient to determine a suitable AAV serotype (Srivastava, 2016).

There are numerous AAV serotypes that have been isolated from living organisms, as well as those of synthetic origin (Lentz, Gray and Samulski, 2012). All these AAV serotypes differ not only in their respective receptors required for transduction, but also in their tissue tropism and transduction efficiency (Murlidharan, Samulski and Asokan, 2014; Srivastava, 2016). Therefore, it is important to examine these properties together in order to choose the correct serotype for a specific study.

Moreover, it is important to note that the delivery route also has a major impact on transduction properties of AAV serotypes. There is a large body of literature that details the use of AAV vectors to study almost all aspects of the nervous system, using a broad range of serotypes and delivery routes. As the main aim of this project is to use AAVs to study primary sensory neurons involved in nociception and related pain circuitry, it is important to choose a serotype and delivery route that results in high transduction efficiency in the DRGs (where the cell bodies are located) and/or dorsal spinal cord (where their projections terminate). Below,

possible delivery routes for transduction of the nervous system in conjunction with transduction efficiency for various serotypes are described, together their advantages and disadvantages.

2.1.2 AAV delivery routes to the nervous system

2.1.2.1 Direct injection into the parenchyma of the brain or spinal cord

Direct administration of AAVs into the brain or spinal cord parenchyma is one of the more popular routes of delivery to the central nervous system in pre-clinical studies, first used in mammals in 1994 (Kaplitt *et al.*, 1994). Typically, direct brain injection of AAV results in a high level of transduction at the injection epicentre, and therefore can be used to target specific regions of the brain (Murlidharan, Samulski and Asokan, 2014). Burger et al tested how well injection of AAV1, 2 or 5 transduced different parts of the adult rat CNS, including the hippocampus, striatum, cortex and spinal cord. They found that all three vectors almost exclusively target neurons. AAV1 and 5 performed much better than AAV2, having greater spread, evidence of retrograde labelling and higher transgene expression in all parts of the CNS (Burger *et al.*, 2004). Similar results were seen in the mouse brain, where AAV serotype 2 performed worse than AAV serotypes 1,5,7 and 8 (Davidson, 2000; Taymans *et al.*, 2007).

In other studies, AAV serotypes 9 and rh10 were found to produce superior labelling when compared to most other serotypes (AAV1-8), with AAV9 also showing retrograde transport capabilities (Cearley and Wolfe, 2006; Klein *et al.*, 2008; Aschauer, Kreuz and Rumpel, 2013; Vincent, Gao and Jacobson, 2014). However, most robust retrograde transport in the CNS has been found for the AAV2.retro serotype, specifically designed for maximum retrograde capabilities (Tervo *et al.*, 2016; Haenraets *et al.*, 2017).

Although direct brain injections of AAVs mostly target neurons, several studies report that several AAV serotypes, including 8, 9 and rh10, also transduce astrocytes and oligodendrocytes both in the brain and in spinal cord (Aschauer, Kreuz and Rumpel, 2013; Ciesielska *et al.*, 2013; Löw, Aebischer and Schneider, 2013; Haenraets *et al.*, 2017).

Interestingly, driving transgene expression with a cytomegalovirus (CMV) promoter was found to be less efficient than chicken β-actin (CBA) in the CNS (Klein *et al.*, 2008). However, after injection into the spinal cord AAV9 under the CBA promoter showed poor labelling of motor neurons, while the CMV promoter achieved higher levels of transgene expression in motor neurons (Snyder *et al.*, 2011).

To summarise, direct parenchyma injection has the advantage of avoiding the blood-brain barrier, which would otherwise severely limit viral access to the CNS. However, each injection only targets a small area of the CNS, so multiple injections are required for targeting larger regions. Overall, this delivery route would be applicable in our project to study CNS nociceptive pathways, but it does not enable labelling of primary sensory neurons.

2.1.2.2 Direct injection into DRGs

AAV injections of a small volume into the DRG can be used to target primary sensory neurons. Mason et al compared AAV serotypes 1-6 and 8 to assess the efficiency of DRG transduction after intraganglionic injection. They found that AAV serotype 5 performed best, with ~48% neurons transduced per DRG after 2 weeks, and ~75% after 4 weeks. Out of these neurons, a large proportion were small diameter, with 33% calcitonin gene-related peptide (CGRP)-positive, and 48% isolectin B4 (IB4)-positive neurons (Mason *et al.*, 2010). A different study showed that intraganglionic injection of AAV9 results in transduction in ~40% of L4 DRG neurons (Haenraets *et al.*, 2017).

However, AAV targeting of neuronal sub-populations has been shown to differ depending on the serotype and promoter used. AAV8, for example, has been shown to prefer large-diameter neurons following intrganglionic injection (Jacques *et al.*, 2012). On the other hand, intraganglionic injection of AAV9 with transgene under the control of the human synapsin promoter resulted in low transduction of IB4 positive neurons (Haenraets *et al.*, 2017).

Although direct DRG injection of AAV typically produces good levels of transduction among the primary sensory neurons, it is a difficult and invasive procedure that can have some

undesirable side effects on the animal. Rats injected with AAV8 into the L4 and L5 DRGs showed transient mechanical allodynia and thermal hyperalgesia, as well as declining rotarod motor performance (Fischer *et al.*, 2011). DRG injection is an even more technically challenging procedure in mice, with a potential for greater side-effects due to the small size of the DRG itself. An alternative to using direct injections into the DRG or CNS parenchyma is to infuse the AAV into the cerebrospinal fluid (CSF) via cerebral ventricles, cisterna magna or lumbar puncture.

2.1.2.3 Infusion of AAV into CSF via cerebral ventricles

CSF is vital for the correct functioning of the brain, spinal cord and DRGs, as it provides nutrients and clears solutes from the brain and spinal cord (Sakka, Coll and Chazal, 2011). Most of the CSF is produced by the choroid plexus in the cerebral ventricles (Sakka, Coll and Chazal, 2011). Since the CSF is in close contact with the brain, spinal cord and DRGs, it can serve as a medium for delivery of AAVs to a large proportion of the nervous system. One of the methods used to infuse the vectors into the CSF is by injection into cerebral ventricles. Interestingly, Intracecrebroventricular (ICV) administration of AAV2,4 or 5 in adult mice results in almost exclusive transduction of ependymal cells, with limited neuronal transduction (Davidson, 2000). AAV9, on the other hand, has shown promising results by producing extensive neuronal labelling in the brain and spinal cord 6 weeks after ICV delivery, but it was only tested in a single rat (Jackson *et al.*, 2016).

The transduction profile in neonates is drastically different from that in adults. ICV delivery of AAV straight after birth (P1) results in widespread transduction throughout brain parenchyma (Passini and Wolfe, 2001; Spampanato *et al.*, 2011; Glascock *et al.*, 2012). This has been observed with several serotypes, including AAV1, 2, 5, 7, 8 and 9, however, serotypes 8 and 9 achieved best transduction (Chakrabarty *et al.*, 2013; J.-Y. Kim *et al.*, 2014; Hammond *et al.*, 2017). Interestingly, transduction throughout the brain was greatly diminished when viral

injection was done at P2 or P3, suggesting that the timing of injection is crucial. (Chakrabarty *et al.*, 2013)

Overall, ICV injection is effective in transducing a large proportion of brain parenchyma, but only if the AAV is delivered at P1. There is evidence that AAV9 is capable of transducing spinal cord neurons in adults, but it is too unspecific for studying pain circuitry and there is no evidence of DRG transduction (Donsante *et al.*, 2016). However, delivery into the CSF at lower spinal regions may produce a different transduction profile.

2.1.2.4 Infusion into CSF via the Cisterna Magna

An alternative way of accessing the CSF is via infusion into the cisterna magna (CM) through the atlanto-occipital membrane. While ICV CSF delivery requires a craniotomy and the needle to be advanced through the brain parenchyma in order to target the ventricles, infusion into the CM is less invasive. It requires only the removal of muscle overlaying the atlanto-occipital membranes.

CM Delivery of scAAV2 has been shown to transduce the adult brain and spinal cord all the way to the lumbar level (Fu *et al.*, 2003). Furthermore, intravenous (IV) infusion of mannitol prior to CM delivery further increased the transduction efficiency (Fu *et al.*, 2003). CM injection of AAVrh10 results in extensive transduction throughout the whole of the spinal cord, including interneurons, ascending projections and motor neurons (Hordeaux *et al.*, 2015). In addition, DRG transduction was present in both adults and neonates (Hordeaux *et al.*, 2015). In neonates, CM delivery of AAV8 and 9 results in efficient transduction in the brain and spinal cord parenchyma (Ayers *et al.*, 2015). Moreover, AAV9 has been shown to transduce the spinal cord and brain after CM delivery both in neonates and adults (Lukashchuk *et al.*, 2016; Sinnett *et al.*, 2017).

Although CM delivery transduces spinal cord neurons and DRGs, transduction diminishes with increasing distance from the injection point. This is a disadvantage for the pain research, since it often focuses on the lower limbs and their associated pathways. Therefore, achieving high

transduction in the lumbar DRGs and spinal cord is essential. By shifting the point of injection to the lower regions using methods such as lumbar puncture it might be possible to target these regions preferentially.

2.1.2.5 Infusion into CSF via Lumbar Puncture

Lumbar puncture (LP) delivery to CSF is a simpler procedure compared to CM delivery and may produce higher transduction in the lumbar regions. Adult mice injected with AAV6 via LP show the highest level of transduction in the L4 DRG neurons, with >50% of neurons transduced after a single injection. Moreover, labelling of the lumbar spinal cord was confined to laminae I and II possibly indicating preference for labelling nociceptive pathways (Towne *et al.*, 2009). Similar results were seen with AAV5 and AAV8, although DRG labelling was not as extensive (Vulchanova *et al.*, 2010). Interestingly, transgene levels in the spinal cord were significantly diminished in injected animals after dorsal rhizotomy. This suggests that most of the transgene expression observed in the spinal cord is located in primary afferent projections (Vulchanova *et al.*, 2010). In a study by Homs et al intrathecal injection of AAV2 or 8 produced sparse labelling. AAVrh10, on the other hand, labelled the majority of L4 DRG neurons, 60% of which were CGRP or IB4 positive, suggesting a preference for nociceptors (Homs *et al.*, 2014). Intrathecal delivery of AAVrh10 also produced extensive labelling in the spinal cord (Guo *et al.*, 2016). Greatest DRG transduction, however, was achieved with intrathecal administration of AAV9, with transgene expression in over 70% of L4 DRG neurons, around 60% of which were small-diameter (Schuster *et al.*, 2014). Transgene labelling in the spinal cord was also extensive, both in the dorsal and ventral horns (Schuster et al. 2014; Bey et al. 2017).

Of note, the possible labelling of the deep spinal cord may be dependent on the injection technique. In mice, injections of AAV9 under pia mater produced extensive labelling throughout spinal cord, however in animals receiving intrathecal injection of AAV9, without damaging the pia, labelling was confined to the dorsal horn and dorsal funiculus (Miyanohara et al. 2016).

Overall, intrathecal injection via LP is an efficient method for transduction in the lumbar DRGs and dorsal spinal cord. However, it is important to consider other delivery methods, like peripheral injections and intravenous delivery.

2.1.2.6 Peripheral and intravenous injections

Labelling of specific sensory neurons innervating peripheral anatomical structures of interest may be possible by injecting AAV directly into these structures. AAV can then be taken up by the peripheral terminals of sensory neurons and transported retrogradely to the DRG. The sensory neurons labelled by peripheral injection will be confined to DRG levels that send projections to that structure.

For instance, delivery of AAV6 by direct injection into the sciatic nerve labels DRG neurons in L4 (Towne *et al.*, 2009). However, subcutaneous and intramuscular delivery did not label any neurons, which may be due to limited AAV6 retrograde transport capabilities. In another study, Pleticha et al showed that direct administration of AAVrh20 into the sciatic nerve produces labelling in L4 and L5 DRGs (Pleticha *et al.*, 2014).

Another peripheral delivery method to transduce sensory neurons and the CNS is intravenous infusion (IV). This delivery method is minimally invasive, and can potentially achieve good spread with a single injection (Murlidharan, Samulski and Asokan, 2014). However, intravenous delivery has a greater chance for off-target transduction, especially in tissues that all AAVs have tropism for, such as liver and heart (Zincarelli *et al.*, 2008). The greatest drawback, however, is that many AAV serotypes have difficulties crossing the blood-brain barrier (BBB), making it difficult for IV injections to transduce the spinal cord and possibly DRG neurons (Towne *et al.*, 2008; Foust *et al.*, 2009). Indeed, AAV9 IV injection in adult mice results in limited neuronal transduction, but widespread transduction in the astrocytes, whose endfeet surround capillary endothelial cells (Foust *et al.*, 2009). However, there is evidence that some AAV serotypes can cross the adult BBB. For instance, IV delivery of scAAV9 resulted in extensive transduction in the spinal cord and brain (Duque *et al.*, 2009; Foust *et al.*, 2009;

Gray, Foti, *et al.*, 2011; Yang *et al.*, 2014). Interestingly, extensive neuronal transduction was not observed with ssAAV9 (Foust *et al.*, 2009; Schuster *et al.*, 2014). Futhermore, when Yang et al compared transduction in the mouse adult brain and the spinal cord after IV injection of several AAV serotype, they found that AAV8, AAV9 and AAV.rh10 result in extensive transduction in the CNS neurons, while other serotypes did not produce such as strong expression, suggesting that these serotypes are more efficient at crossing an adult BBB (Yang *et al.*, 2014).

Another way of circumventing the problem of crossing the BBB is pre-treatment with mannitol, that can temporarily disrupt the BBB (Pan, Liu and Liu, 2000). Mannitol pre-treatment has enabled scAAV2 to transduce neurons and glia in the brain after IV injection (Fu *et al.*, 2003). Widespread brain transduction after mannitol treatment has also been seen with AAVrh.10 (Foley *et al.*, 2014). Of note, precise timing of mannitol administration is crucial, with the best AAV2 transduction in the CNS achieved when virus was administered 8 minutes after the mannitol treatment (McCarty *et al.*, 2009).

The more popular way of achieving high CNS transduction with IV-delivered AAVs is to administer them shortly after birth, when the BBB is not yet mature (Engelhardt and Liebner, 2014). Many serotypes that do not efficiently transduce adult CNS after IV delivery show increased efficiency when administered in P1 (Zhang *et al.*, 2011). IV delivery of AAV9 to neonatal rats and mice resulted in extensive transduction in the brain and spinal cord (Foust *et al.*, 2009, 2010; Wang *et al.*, 2010)..

Although IV administration produces widespread labelling, it does not transduce DRG neurons and spinal cord transduction is too widespread to be of use to this project. Additionally, all cited studies reported off-target transduction in liver or heart. Overall, IV injection is useful when widespread CNS transduction is desired, but it is not very suitable for studying nociceptive pathways.

2.1.3 Preferred serotype and administration route to transduce DRG neurons and chapter aim

Serotype	*Direct Parenchymal*	*Direct DRG*	*Cerebro-ventricular*	*Cisterna Magna*	*Lumbar Puncture*	*Intravenous*
AAV1	+	+	++	-	++	+
AAV2	+	+	+	+	-	+
AAV4	-	+	-	NA	NA	-
AAV5	++	++	+	-	+	-
AAV6	+	++	+	NA	++	+
AAV7	+	NA	+	NA	NA	++
AAV8	++	+	++	+	+	+
AAV9	+++	++	+++	++	+++	++
AAVrh10	++	NA	NA	+++	++	++
AAV2.retro	++	NA	NA	NA	NA	NA

Table 2.1 *–* ***Comparison of transduction for different AAV serotypes and different delivery methods****. Relative performance of different AAV serotypes in different delivery scenarios in mouse neurons. The arbitrary scale form minus to three plusses represents "little to no transduction" to "strong and extensive transduction". Table compiled with data from* (Davidson, 2000; Passini and Wolfe, 2001; Fu *et al.*, 2003; Burger *et al.*, 2004; Cearley and Wolfe, 2006; Taymans *et al.*, 2007; Klein *et al.*, 2008; Iwamoto *et al.*, 2009; McCarty *et al.*, 2009; Towne *et al.*, 2009; Mason *et al.*, 2010; Vulchanova *et al.*, 2010; Gray, Matagne, *et al.*, 2011; Spampanato *et al.*, 2011; Zhang *et al.*, 2011; Glascock *et al.*, 2012; Aschauer, Kreuz and Rumpel, 2013; Chakrabarty *et al.*, 2013; Homs *et al.*, 2014; Schuster *et al.*, 2014; Vincent, Gao and Jacobson, 2014; Yang *et al.*, 2014; Dirren *et al.*, 2014; Ayers *et al.*, 2015; Hordeaux *et al.*, 2015; Jackson *et al.*, 2016; Lukashchuk *et al.*, 2016; Tervo *et al.*, 2016; Bey *et al.*, 2017; Sinnett *et al.*, 2017).

After reviewing the available AAV serotypes and delivery methods (**Table 2.1**), we decided to use serotype 9, as it showed the greatest neuronal transduction when delivered via various routes, including direct parenchymal injection (Cearley and Wolfe, 2006), direct DRG injection

(Yu, Fischer and Hogan, 2016), ICV infusion (Chakrabarty *et al.*, 2013), intrathecal infusion (Schuster *et al.*, 2014), and peripheral injections (Foust *et al.*, 2009). Additionally, to achieve greatest DRG transduction possible, we decided to use the lumbar puncture method to deliver AAV9 into the CSF. This method produced the highest level of transduction in the DRG neurons of all the review methods (Schuster *et al.*, 2014). Furthermore, intrathecal delivery of AAV via the lumbar puncture is a relatively quick and simple procedure that is not very invasive, compared to intraparenchymal, ICV and intraganglionic injections.

The aim of this chapter is to determine the transduction pattern that lumbar puncture delivery of AAV9 produces in DRG neurons and the spinal cord. Further, we will investigate the effect on transduction pattern and efficiency of factors like time post injection and virus titre. Finally, we will use peripheral injections into anatomical structures to achieve retrograde labelling in the DRG of sensory neurons innervating these structures.

2.2 Methods:

2.2.1 Animals

All procedures were in accordance with the UK Home Office guidelines and Animals (Scientific Procedures) Act 1986. C57Bl/6J mice were obtained from Charles River. Both males and females 3-6 months of age were used for intrathecal and peripheral vector delivery experiments. For *in vitro* experiments, 2-3 month old males and females were used.

2.2.2 Viral Vectors

All adeno-associated virus (AAV) vectors were obtained from UPENN Vector Core and were store d at -80 °C. Construct information and titres can be found in **Table 2.2**

Vector Name	***In-text name***	***Serotype***	***Transgene***	***Titer (GC/ml)***
AAV9.CB7.CI.eGFP.WPRE.rBG	AAV9-eGFP	AAV9	eGFP	$6.39x10^{12}$ - $2.52x10^{13}$
AAV9.CB7.CI.mCherry.WPRE.rBG	AAV9-mCherry	AAV9	mCherry	$1.49x10^{13}$
AAV9.CAG.GCaMP6s.WPRE.SV40	AAV9-GCaMP6s	AAV9	GCaMP6s	$1.69x10^{13}$
AAV9.CMV.PI.Cre.rBG	AAV9-Cre	AAV9	Cre	$3.29x10^{13}$
AAV8.CB7.CI.eGFP.WPRE.rBG	AAV8-eGFP	AAV8	eGFP	$1.78x10^{13}$
AAV9 - GluClβ	AAV9-GluClβ	AAV9	GluClβ	$2.4x10^{13}$
AAV9 - GluClα	AAV9-GluCl	AAV9	GluClα	$1.5x10^{13}$

Table 2.2 – Viral vectors used in this project

2.2.3 Lumbar puncture AAV injections

The procedure was executed by Clive Gentry. Mice were restrained in a cardboard tube. Vertebrae L3 and L4 were identified percutaneously. A gauge 26 needle attached to a Hamilton syringe was then carefully inserted at an angle between these two vertebrae, and 5 µl of virus was injected. The needle was then left in place for 10 seconds before its removal. Animal weight was monitored after the procedure for up to 7 days.

2.2.4 Catheter mediated intrathecal injections

First, the catheters were prepared by inserting 1.5cm of small diameter tubing (0.2 mm OD, Braintree Scientific, SUBL 080) into 15-20 cm of large diameter tubing (0.64 mm OD, VWR, 60-

011-01) and secured using Epoxy glue, to form a long catheter with a short thin end. Glue was left to dry overnight, and the catheters were sterilised using UV light.

On the day of the surgery, one catheter was attached to a 300 µl insulin syringe that was linked to a syringe pump. The syringe and large tubing was filled with sterile saline, then the virus was loaded after an air bubble was created to separate the virus from the saline. This was done to minimise pressure fluctuations and to ensure steady infusion of the virus. A mark was made on the large tubing at 6.6 cm from the junction with the small cannula to denote 5 µl volume of the large tubing. This length of the catheter has the volume of 5 µl, and the mark was used as a guide for virus loading.

The mouse was then anaesthetised in the induction chamber with 5% Isofluorane (Henry Schein, 900-8931), and kept at 2-2.5% Isofluorane throughout the procedure. The mouse was given 50 µl 0.5% v/v carprieve (Norbrook) diluted in saline and 100 µl sterile saline subcutaneously before being shaved and the incision area disinfected with iodine.

The animal was then transferred to the surgery area equipped with a heat mat, covered with a sterile drape containing a surgery window, and Viscotears were applied to the eyes to prevent their drying. Before proceeding, the absence of hindpaw pinch withdrawal reflexes were checked to ensure surgical anaesthesia depth, and were monitored throughout the procedure

After that a 2cm skin incision was made on top of the vertebral column at the lumbar level. Region between vertebrae T12 and T13 was located and muscle between these vertebrae carefully removed using fine Rongeurs (Item 16221-14, Fins Scientific Tools). The vertebral column was stabilised using a “third hand” tool, and the mouse was slightly rotated towards the surgeon for easier access. Leftover muscle was cleaned up with no.5 forceps to expose the intervertebral ligament, which was then removed using no.5 forceps to expose the dura. Solution of 0.1% w/v Methylene Blue (Sigma, 66719) in sterile saline was applied on top of dura to visualise it, and then removed using a cotton bud. Dura was carefully lifted using fine

forceps (Item 11413-11, Fine Scientific tools), and a small hole was made with a gauge 30 needle.

Using fine forceps, dura was lifted caudally to the hole to allow easier intrathecal access. The thin end of the cannula was then inserted 1.2 cm into the caudal direction, to allow virus delivery at the L4 DRG level. After the cannula was fully inserted, 5 µl of virus was infused at a rate of around 1.2 µl per minute.

After the infusion, cannula was left in place for 2 minutes to minimise backflow caused by cannula retraction. After cannula removal, mouse was unclamped, the incision washed with sterile saline and skin was closed using metal clips. Animal was then allowed to recover in the incubator at 32°C and monitored for any impairments. Weight was monitored until it returned to the pre-surgery value and clips were removed 7-10 days after surgery.

2.2.5 Peripheral injections

Intraneural injections

Mice were anaesthetised using 5% isofluorane, they received 50 µl 0.5% v/v carprieve subcutaneously and their left hind limb was shaved. Mice were then placed on a heat mat, eyes covered with Viscotears and covered with a sterile drape. Anaesthesia was maintained with 2-2.5% isofluorane. Before proceeding, the absence of hindpaw pinch withdrawal reflexes were checked to ensure surgical anaesthesia depth and were monitored throughout the procedure. A skin incision was made to expose the sciatic nerve. The nerve was stabilised with no.5 forceps and 1 µl of virus was injected into the nerve at a rate of 0.25 µl/min using a microinjector. After injection, the glass needle was left in place for 2 minutes to minimise backflow. The needle was retracted, and skin closed using metal clips. Mice were left to recover in the incubator at 32°C and monitored for weight loss and impairments. Clips were removed 7-10 days after surgery.

Intraplantar injections

Mice were anaesthetised using 5% isofluorane and given 50 µl 0.5% v/v carprive subcutaneously. Mice were placed on a heatmat, eyes covered with Viscotears and sterile drape put over the mouse. Hindpaw was extended and 5 µl of virus was injected into the plantar surface of the paw using an insulin syringe. Needle was left in place to minimise backflow. Mice were left to recover in the incubator at 32°C and monitored for weight loss and impairments.

Intraarticular injection

Injection technique adapted from (Salo and Tatton, 1993). Mice were anaesthetised using 5% isofluorane and given 50ul 0.5% v/v carprive subcutaneously. Mice were placed on a heatmat, eyes covered with Viscotears and sterile drape put over the mouse. Anaesthesia was maintained with 2-2.5% isofluorane. Before proceeding, the absence of hindpaw pinch withdrawal reflexes were checked to ensure surgical anaesthesia depth and were monitored throughout the procedure. An incision was made on the knee to expose the patella tendon. Glass needle was inserted through the tendon into the knee joint using micromanipulator and 0.5 µl of virus was injected at a rate of 0.25 µl/min. The needle was left in place for 2 minutes to prevent backflow and skin was closed using a metal clip. Mice were monitored for weight loss and impairments. Clips were removed 7-10 days after surgery.

2.2.6 Dissection and immunohistochemistry

Mice were injected with 100 µl of Euthatal intraperitoneally. Reflexes were checked and once terminal anaesthesia was achieved mice were perfused transcardially using a handheld syringe first with 30 ml of phosphate-buffered saline (PBS) and then with 30 ml of 4% paraformaldehyde (PFA) for immunohistochemistry (IHC). After perfusion, 3 cervical and 3 thoracic DRGs from both sides were dissected, as well as L4 DRGs and the lumbar spinal cord. They were placed in 4% PFA for 2 hours (DRGs) or overnight (spinal cords). Tissue was then washed in PBS and placed into 30% sucrose in PBS with 0.01% sodium azide overnight.

2.2.7 Tissue preparation and image acquisition

Tissue was embedded in OCT (VWR 361603E), frozen on dry ice with Isopentane (Sigma, M32631), and stored at -80 °C. Blocks of tissue were cut using Bright Instruments Cryostat. The thickness of slices was 10 µm for DRGs and 20 µm for spinal cords. Sections were collected onto Superfrost slides (Thermo Fisher, J1800AMNZ) in series, ensuring that slices from all levels of thetissue are present and evenly distributed among the slide series. Slides were then stored at -20 °C.

Type	*Fluorophore*	*Antigen*	*Species*	*Dilution*	*Provider*	*ID*
Primary	n/a	β-III-Tubulin	Rabbit	1:1000	Abcam	ab18207
	n/a	β-III-Tubulin	Mouse	1:1000	Promega	G7121
	n/a	GFP	Chicken	1:1000	Abcam	ab13970
	n/a	GFP	Rabbit	1:1000	Abcam	ab290
	n/a	CGRP	Rabbit	1:500	Enzo Life Sciences	BML-CA1134
	n/a	NF200	Mouse	1:500	Sigma	N0142
	n/a	NF200	Chicken	1:500	Millipore	AB5539
	n/a	NeuN	Rabbit	1:500	New England Biolabs	12943
	n/a	RFP	Rabbit	1:1000	Abcam	ab62341
Secondary	Alexa Fluor 568	Rabbit IgG	Donkey	1:1000	Thermo Fisher	A10042
	Alexa Fluor 488	Chicken IgG	Goat	1:1000	Thermo Fisher	A11039
	Alexa Fluor 546	Mouse IgG	Donkey	1:1000	Thermo Fisher	A10036
	Alexa Fluor 488	Rabbit IgG	Donkey	1:1000	Thermo Fisher	A21206
Special	Alexa Fluor 647	IB4, biotin-conjugated	n/a	1:250	Thermo Fisher	L32450

Table 2.3 – Antibodies used for ICC and IHC

For IHC, slides were taken out of the freezer and left at room temperature for 30 minutes. Hydrophobic Pappen was applied to restrict the spread of the antibody solution. Sections were rehydrated with PBS and then incubated in blocking medium (1xPBS with 10% normal donkey serum (Sigma, S30-M) and 0.01% sodium azide) for 1 hour in humidifier chamber to prevent

non-specific binding. Blocking solution was then removed and 300 µl of primary antibody diluted in PBS with 0.1% Triton X and 0.01% sodium azide was applied to the slides and left overnight at room temperature. Slides were then washed 3 times with PBS and secondary antibody diluted in PBS with 0.1% triton X and 0.01% sodium azide was applied for 2 hours at room temperature. After 3 PBS washes slides were coveslipped using Fluoromount-G with 4',6-diamidino-2-phenylindole (DAPI) (Thermo Fisher, 00-4959-52) and left to dry overnight. Antibodies used are shown in **Table 2.3**. Images were taken on the Carl Zeiss microscope with 10x and 20x objectives, using AxioVision software. At least 3 sections were imaged per DRG, giving preference to section with the largest number of neurons. As the minimum distance between two consecutive sections on the same slide is 60 µm (due to collecting tissue on the cryostat in series), we assumed that we would not be sampling the same cell twice.

After acquisition, images were processed using Fiji, an ImageJ package available online (Schindelin *et al.*, 2012; Rueden *et al.*, 2017). To determine the percentage of positive eGFP neurons in DRG, all cells positive for β-III-tubulin were selected and the selection was used as a mask to measure the intensities of the corresponding ROIs in the eGFP channel. To determine the cut-off for eGFP-positive cells, intensity of the 5 visually least positive cells was taken, and threshold was set as the mean of these cells + 1 SEM. Cells with a higher intensity than the cut-off were deemed positive. The proportion of eGFP-positive neurons to all neurons was calculated for each image. The results from the same DRG were then averaged to give the final proportion of neurons transduced for that DRG. Same principle was applied for neuronal marker quantification, however in the absence of β-III-tubulin innate neuronal autofluorescence coupled with the presence of a neuronal-like DAPI nucleus was used to create a mask.

2.2.8 Von Frey test

All testing was done between 9:00am and noon. An up-down Von Frey method has been used (Chaplan *et al.*, 1994). Mice were baselined 1 week before the surgeries. They were left to

acclimatise in the Von Frey cages for 45 minutes. Von Frey filaments of varying strength were used to assess the hindpaw mechanical threshold. The first filament used on either paw was 0.6g, and if there was no response, a stronger filament was used next. Conversely, if the response was elicited, a weaker filament was used next. There were 10 testing rounds in total, alternating between paws, with 5 rounds per paw. The mechanical threshold for each paw was calculated based on the pattern of filament responses (Bonin, Bories and De Koninck, 2014).

2.2.9 Mixed DRG tissue cultures

Coverslips in 4 well plates were pre-coated with 10% poly-L-lysine (PLL) (Sigma, P4707) for at least 2 hours prior to use. PLL was removed and coverslips were washed with autoclaved Milli-Q H_2O and left to dry for 30 minutes. Then, 30 µl of 1:100 of Laminin (1-2 mg/ml)(Sigma, L2020) in Ham's F12 (Life technologies, 17502-048) were put on the coverslips and incubated for 2 hours in the tissue culture incubator.

Mice were sacrificed according to Schedule 1. DRGs from all levels and both sides were harvested into Ham's F12 on ice. Ham's F12 was removed and the 3 ml of dissociation enzyme cocktail (3mg/ml dispase (Sigma, 4942078001), 0.1% collagenase (Sigma, C9891) and 200 units/ml DNAse (Sigma, 10104159001), diluted in Ham's F12) was added to dissociate the DRGs and placed into the incubator for 45 minutes.

Enzyme cocktail was removed and 1 ml of Ham's F12 was added, followed by mechanical trituration of DRGs using a P1000 pipette. Cells were then centrifuged at 1000 RPM for 10 seconds and the supernatant containing the dissociated cells was moved to a new tube. The dissociation process was then repeated 4 more times. The final cell suspension was passed through a 70 µm filter to remove debris. The filtered cell suspension was centrifuged at 1000 RPM for 7 minutes, and cells were resuspended in BS medium (10% FBS (Sigma, F9665), 1% N-2 supplement (Life technologies, 17502-048) in Ham's F12). Laminin was aspirated off the coverslips and 20 µl of cell suspension was plated onto the coverslips. Cells were left in the

incubator for 30 minutes, after which 500 µl BS media was added. If cells were not used the next day, half the medium in the wells was replaced with fresh BS media.

For immunocytochemistry, warm (37 °C) 4% PFA was added to the wells with coverslips, for a final concentration of 2% PFA, and incubated for 20 minutes at 37 °C. Coverslips were then washed three times with PBS, and then incubated in the blocking medium (1xPBS with 10% normal donkey serum (Sigma, S30-M) and 0.01% sodium azide) for 1 hour at RT. Coverslips were then washed 3 times with PBS for 5 minutes each, before incubating in 300 µl of primary antibody solution (see **Table 2.3**) diluted in PBS with 0.1% Triton X and 0.01% sodium azide for 1 hour in the dark at RT. After that, coverslips were washed three times with PBS for 5 minutes each, and then incubated in 300 µl of secondary antibody solution (see **Table 2.3**) diluted in PBS with 0.1% Triton X and 0.01% sodium azide for 1 hour in the dark at RT. Finally, coverslips were washed 3 times in PBS for 5 minutes each, before mounting the coverslips onto microscope slides using Fluoromount-G with 4',6-diamidino-2-phenylindole (DAPI) (Thermo Fisher, 00-4959-52) and left to dry overnight.

Three non-overlapping mosaic images were taken per coverslip, ensuring the maximum number of cells in the FOV. Image acquisition and method of quantification was identical to the IHC, using the β-III-tubulin staining to create a mask which is then used to calculate the proportion of transduced neurons per image, and then averaged for each coverslip (see **2.2.7**).

2.2.10 Neuronal enriched cultures using magnetic-assisted cell sorting (MACS)

This technique has first been optimised by Dr J. Kelleher (Thakur *et al.*, 2014). Coverslips were coated with PLL in the same way as for mixed cell cultures (described above). After washing, 30 µl of Matrigel (BD bioscience, 356230) dissolved in Ham's F12 was applied to the coverslips before they were placed in an incubator for 2 hours in 4 well dishes. Dissection, dissociation, trituration, and centrifugation were carried out in the same way to mixed culture. After centrifugation, cells were resuspended in 2 ml Dulbecco's phosphate-buffered saline (DPBS) (Gibco, 14190144) and centrifuged for 7 minutes at 1000 RPM. DPBS was replaced with 130 µl

of 0.5% w/v bovine serum albumin in MACS buffer + 30 µl of biotin-conjugated antibody cocktail that binds to non-neuronal cells, including astrocytes, oligodendrocytes, satellite glia cells, fibroblasts and epithelial cells (MACS kit (Miltenyi biotec, 130-098-752)). Suspension was left at 4 °C for 5 minutes to allow antibody binding. 1840 µl of MACS buffer were added and suspension centrifuged at 1000 rpm for 7 minutes. Supernatant was discarded, and cells were resuspended in 130 µl MACS buffer and 30 µl of anti-biotin microbeads, followed by incubation at 4 °C for 10 minutes. After that, 340 µl of MACS buffer was added. LD columns were primed with 2 ml of MACS buffer, after which the cell suspension was added to them. Columns were washed through with 1 ml of MACS buffer before the elute was centrifuged for 8 minutes at 1000 rpm. Cells were then resuspended in a desirable amount of BS before being plated onto the Matrigel-coated coverslips.

2.2.11 In vitro viral transfection

Cells were processed for culture as described above. After resuspending them in the desired volume of BS, various amounts of AAV9-eGFP, AAV9-Cre or AAV9-GCaMP6s were added to reach the desired virus concentration (see **2.3.7**) and left to incubate at 37 °C for 20 minutes in suspension before plating cells onto the coverslips.

2.2.12 Flow cytometry

Mice were intrathecally injected with either AAV9-eGFP or vehicle and left to incubate for 14 days. DRGs were extracted, enzymatically digested and passed through a 70 µm filter as described above. Cells were suspended in 50 µl Live/Dead fixable yellow dye (L-34959, Life Technologies) and incubated in the dark for 15min on ice. 2x 50ul antibody mix was then added, consisting of mFACS buffer (HBSS with 0.4% BSA, 15 mM HEPES and 2 mM EDTA), 1:10 Fc block (purified anti-mouse CD16/32, Cambridge Bioscience, 101302, 1:20) and 1:150 of the following antibodies from Biolgened: CD45 (immune cells) – PercPCy5.5 (103108); CD11b (myeloid lineage) – APC-Cy7 (101212); Ly6G (neutrophils, granulocytes) – Pac blue (127612);

Ly6C (monocytes) – PE (128007); CD11c (dendritic cells) – APC (117328); CD19 (B cells) – BV605 (115540); TCRβ (T cells) – PE-Cy7 (109222).

Cells were incubated a further 15min on ice in the dark and centrifuged at 1500 rpm at 4 °C for 3 minutes. Supernatant was removed, and cells were fixed with 50 µl of 4% PFA for 5 minutes on ice. Finally, cells were centrifuged at 1500 rpm at 4 °C for 3 minutes and resuspended in 50 µl mFACS. Cells were then processed using a BD SORP Fortessa at the NIHR BRC flow core facility at King's College London. Unstained cells, cells stained with viability dye only and controls beads (BD Bioscience Comp beads, rat and hamster, cat. # 552845) stained with each antibody on its own were used for compensation. FlowJo was used to analyse the data. Basic gating for all events was as follows: all cells based on forward (FSC) and side scatter (SSC); single cells based on SSC area and width; live cells based on FSC and viability dye and finally FSC and CD45 for all immune cells. For quantification, all gates were kept constant between conditions (Lopes *et al.*, 2017).

2.2.13 Statistics

All statistical analysis and data visualisations were performed using GraphPad Prism 7 (GraphPad). Paired and unpaired Two-tailed T-tests were used when comparing means of two groups. Dunnett, Tukey and Sidak multiple comparisons correction post-hoc tests were used after One-Way ANOVA, and the choice of the test was based on the dataset and the type of comparison required. When multiple means were compared to one control mean, Dunnett post-hoc test was used. When means of all columns were compared to each other, and when the number of entries per column was not the same, Tukey's post-hoc method was used. When a select set of means out of the whole dataset was compared, Sidak post-hoc test was used. Non-parametric Kolmogorov-Smirnov test was used to assess the neuronal diameter distribution for eGFP-positive and all neurons in L4 DRG following intrathecal administration of AAV9-eGFP. Individual two-tailed t-tests were used to compare the transduction efficiency for each DRG level between 30 days and 14 days after AAV9-eGFP injection timepoints, and for 30

days and 7 days after AAV9-eGFP injection timepoints. Similarly, two-tailed t-tests were used to compare transduction at each DRG level between 30 days and 14 days after AAV9-GCaMP6s injection, as well as AAV9-Cre. One-Way ANOVA with Sidak multiple comparisons correction was used to compare the L4 transduction after injection of AAV9-eGFP at different titres. Individual two-tailed t-tests were used to compare the transduction in L4, T and C DRGs after AAV9-eGFP injection between high ($2.5x10^{13}$ gc/ml) and lower ($6.39x10^{12}$ gc/ml) titres. One-Way ANOVA with Tukey's multiple comparisons was used to assess the AAV9 transduction in different neuronal subpopulations following AAV9-eGFP injection. For Von Frey behavioural test, One-Way ANOVA with Dunnett multiple comparisons correction was used to compare the mechanical thresholds at each timepoint to that of baseline, and One-Way ANOVA with Sidak multiple comparisons to compare the mechanical thresholds between the two groups at each timepoint. To compare the proportion of different immune cell types in the DRGs after AAV9-eGFP injection, One-Way ANOVA with Sidak multiple comparisons was used. Two-tailed t-tests were used to compare transduction after AAV9 and AAV8 injection, and after AAV9-eGFP and AAV9-mCherry injection. Two-tailed t-tests were used to compare transduction after intraneural, intraarticular and intraplantar injections. For *in vitro* ICC experiments, two-tailed t-tests were used to compare the proportion of transduced neurons after incubation with AAV9-eGFP or vehicle, same for AAV9-Cre. One-Way ANOVA with Tukey's multiple comparisons correction was used to compare *in vitro* transduction after incubating with different titres of AAV9-GCaMP6s.

For *in vitro* calcium imaging experiments, One-Way ANOVA with Tukey's multiple comparisons correction was used to compare the amplitude of neuronal responses for each stimulus before and after addition of sensitizer.

2.3 Results

2.3.1 AAV9-eGFP delivery by lumbar puncture transduced over 50% of L4 DRG neurons

Initially, we performed intrathecal delivery of AAV9-eGFP via a lumbar puncture to transduce DRG neurons. Mice were injected via percutaneous lumbar puncture with 5 µl of AAV9-eGFP at $2.5x10^{13}$ gc/ml and incubated for 30 days. We found that transduction efficiency was not uniform across DRG levels. It was highest at the lumbar (52.41% ± 5.07%) and cervical levels (52.97± 7.29%), while at the thoracic level it was considerably lower (24.73% ± 6.49%) (**Fig. 2.1 a-d**). Further, we investigated the cell size distribution of the transduced DRG neurons and found that there is no difference in size between AAV9-eGFP transduced and all L4 DRG neurons (**Fig. 2.1 e**), suggesting that AAV9 does not have a preference for neurons of a particular diameter. We also investigated transduction of the spinal cord. We observed a strong eGFP signal in the superficial laminae and white matter above the dorsal horns but not in the deeper laminae, suggesting that DRG projections into the spinal cord also fill up with eGFP. (**Fig. 2.1 f**).

Next, we evaluated the influence of the time post injection on the transduction efficiency. Mice were injected with 5 µl of AAV9-eGFP at $2.5x10^{13}$ gc/ml and incubated for 10, 20, 30 or 40 days. At the L4 DRG, we observed 0% transduction at 10 days, 21.5% ± 15.8% at 20 days, 52.41% ± 5.07% at 30 days and 28.9% ± 28.9% at 40 days (**Fig. 2.2 a-e**). Since there was no improvement of efficiency between 30 and 40 days post injection we chose to incubate the animals for 30 days in future experiments. Of note, there was a high level of variability in our results. The potential reasons for that are discussed in **2.4.1**.

Taken together, or data suggest that lumbar puncture delivery method has moderate transduction success with no value higher than 60%. However, the reliability and reproducibility were suboptimal (**Table 2.4**). Therefore, we decided to set up a different method of vector delivery to the intrathecal space, which had to allow greater control over the delivery rate as well as provide confirmation of intrathecal targeting.

Virus	*Time post injection*	*Total n*	*Successful transduction*	*Rate of success*
AAV9-eGFP	10 days	2	0	0%
AAV9-eGFP	20 days	2	1	50%
AAV9-eGFP	30 days	17	9	53%
AAV9-eGFP	40 days	2	1	50%
AAV9-mCherry	30 days	4	0	0%
AAV9-TurboRFP	30 days	2	0	0%
AAV9-GCaMP6s	30 days	5	3	60%
AAV9-Cre	30 days	4	1	25%
AAV8-eGFP	30 days	2	0	0%

Table 2.4 – Summary table for Percutaneous delivery success

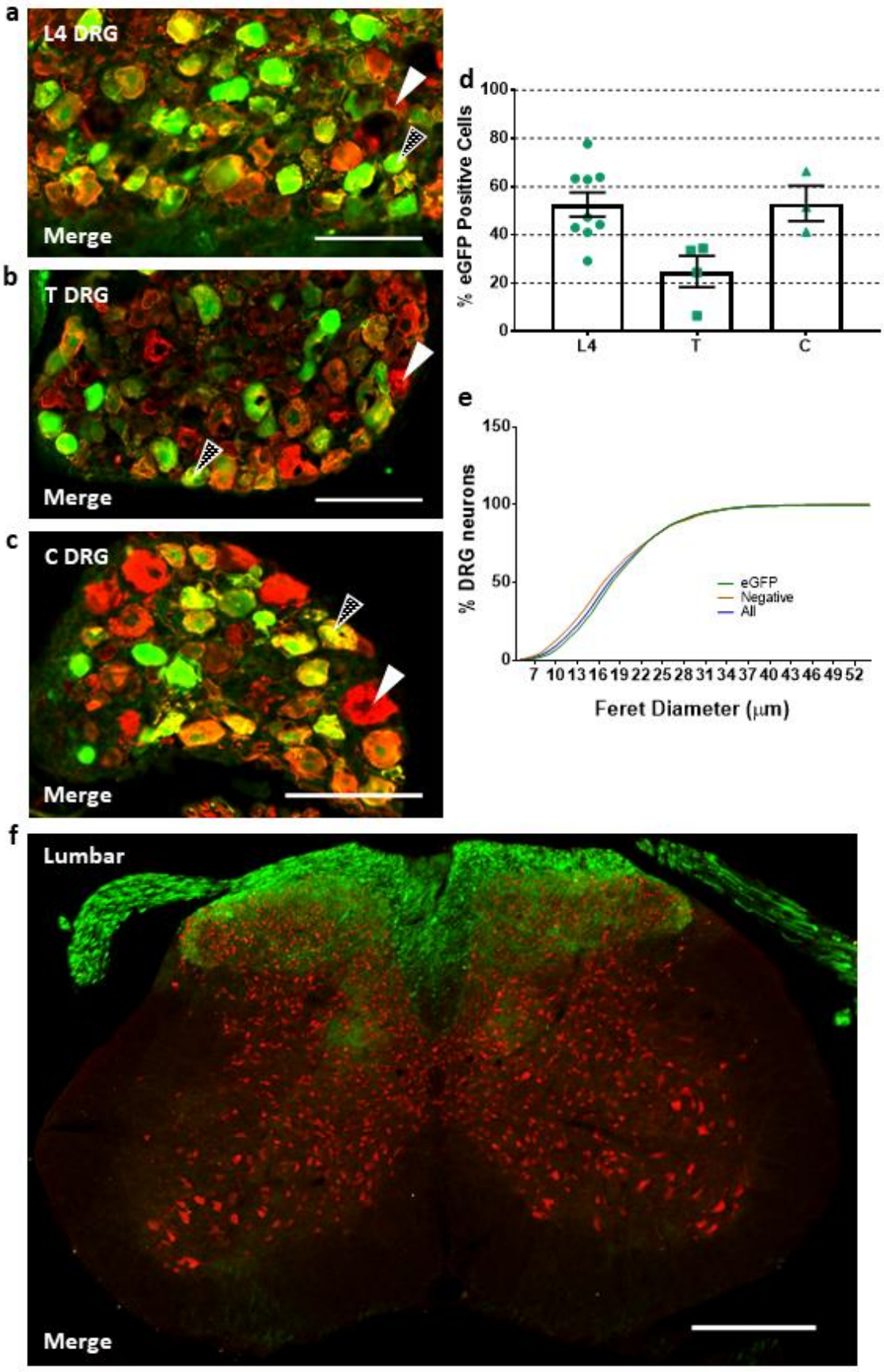

Figure 2.1 – Intrathecal delivery of AAV9 via percutaneous lumbar puncture results in DRG neuron transduction after 30 days. *Animals were injected with 5 ul AAV9-eGFP at 2.5x10^{13} gc/ml.* ***R****epresentative IHC images of* ***a****) lumbar 4,* ***b****) thoracic and* ***c****) cervical DRG sections.*

Sections were stained for β-III-Tubulin (red) and GFP (green). Example of transduced and non-transduced neurons are marked with black and white arrows respectively. Scale bar = 100 µm. ***d****) quantification of transduction efficiency for lumbar (52.51% ± 5.07%, n = 9), thoracic (24.73% ± 6.49%, n = 4) and cervical (52.97± 7.29%, n = 3) DRGs.* ***e****) cumulative frequency plot of neuronal diameters for all (blue), eGFP-negative (orange) and eGFP-positive (green) L4 DRG neurons. Kolmogorov-Smirnov test showed no significant difference in diameter distribution between all and eGFP-positive neurons, p-value = 0.146, n = 4.* ***f*** *Representative IHC image of lumbar spinal cord, stained for NeuN (red) and eGFP (green). Scale bar = 500 µm.*

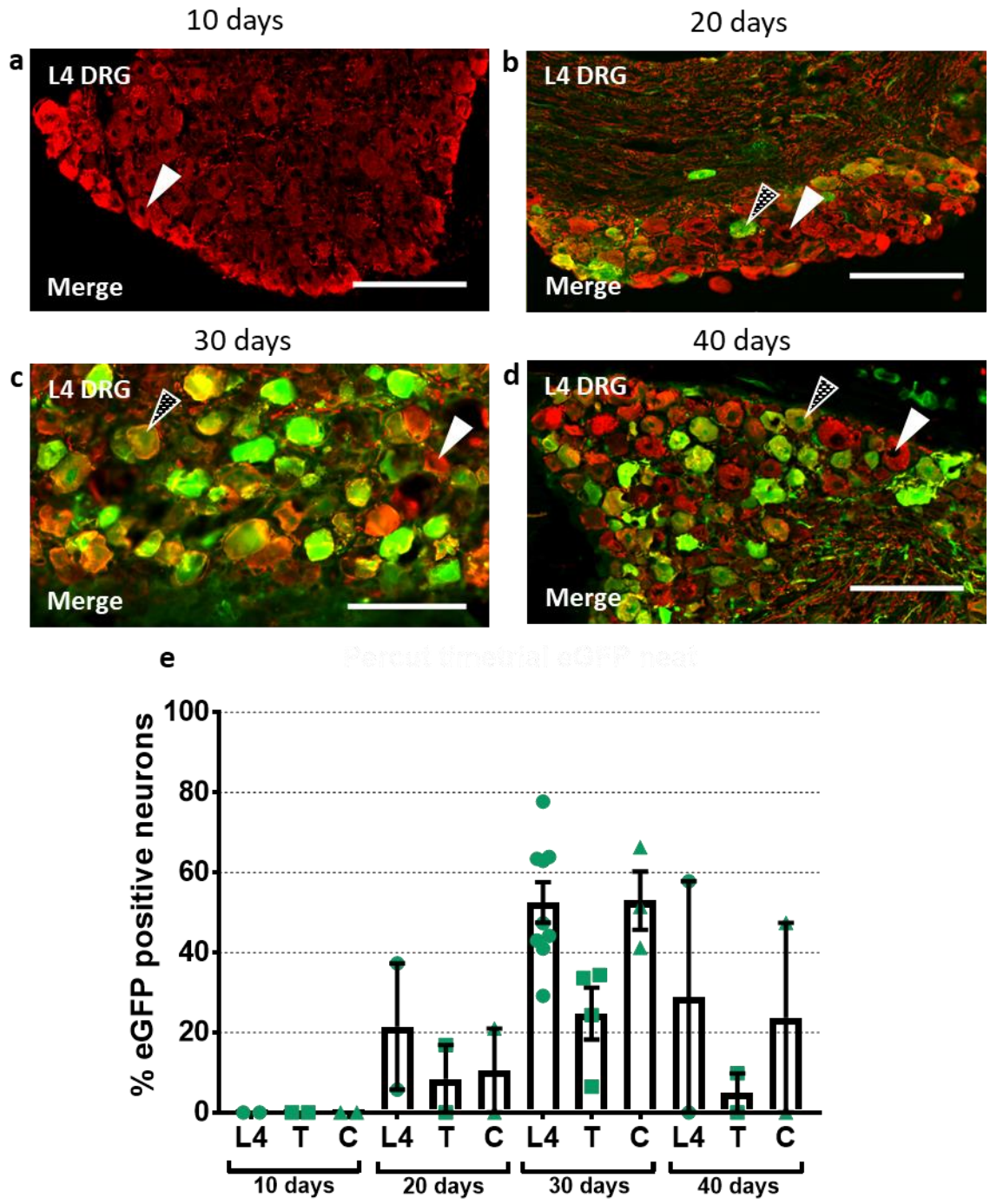

Figure 2.2 – Time after intrathecal delivery of AAV9-eGFP via lumbar puncture affects transduction efficiency. *Animals were injected with 5 ul AAV9-eGFP at 2.5x10^{13} gc/ml. Representative IHC images of lumbar 4 DRG **a**) 10, **b**) 20, **c**) 30 and **d**) 40 days after virus delivery. Sections were stained for β-III-Tubulin (red) and GFP (green). Example of transduced and non-transduced neurons are marked with black and white arrows respectively. Scale bar = 100 um. **e** quantification of transduction efficiency for lumbar, thoracic and cervical DRGs for 10 (0%, 0%, 0%, respectively, n=2), 20 (21.5% ± 15.8%, 8.45% ± 8.45%, 10.5% ± 10.5%, respectively, n=2), 30 (52.51% ± 5.07%, 24.73% ± 6.49%, 52.97% ± 7.29%, respectively, n = 3-9) and 40 (28.9% ± 28.9%, 4.9% ± 4.9%, 23.7% ± 23.7%, respectively, n = 2) day timepoints.*

.

2.3.2 Intrathecal delivery via a catheter achieves transduction efficiency similar to lumbar puncture

To achieve this, we designed and optimized an intrathecal catheter (see **2.2.4**). In this set up, the dura was cut after exposure and a thin (~0.2 mm outer diameter) catheter connected to a syringe pump was gently inserted into the intrathecal space of an anaesthetized mouse (**Fig. 2.3**). We then infused the virus at a set rate of 1.2 µl/min until all the loaded virus was infused. Intrathecal targeting was confirmed by insertion of the catheter into the cut in the dura. Connecting the catheter to a syringe gave us greater control over the rate of delivery compared to a hand-infused system.

Delivery of AAV9-eGFP using this method produced results similar to that of lumbar puncture, with good transduction efficiency at the lumbar (61% ± 6.06%) and cervical (49.86% ± 11.03%) DRG levels and worse efficiency at the thoracic (11.5% ± 3.33%) level (**Fig. 2.4 a-d**). Also, the cell size distribution of the transduced L4 DRG neurons closely resembled the cell size distribution for all L4 DRG neurons (**Fig. 2.4 e**, green and blue lines respectively). Although the Kolmogorov-Smirnov test showed statistically significant differences in the population distribution between eGFP neurons and all neurons ($p<0.05$, $n = 4$, **Fig. 2.4 e**), this may not be biologically significant as the difference is minimal. The central terminals of the DRG neurons were also labelled with eGFP, as shown by eGFP signal in the superficial dorsal horn and the white matter above and between the dorsal horns. There was little eGFP signal in the deeper laminae and little transduction of the spinal cord neurons (**Fig. 2.4 f**), which may indicate that the majority of the eGFP signal in the spinal cord comes from projections of transduced DRG neurons and not transduced spinal cord neurons.

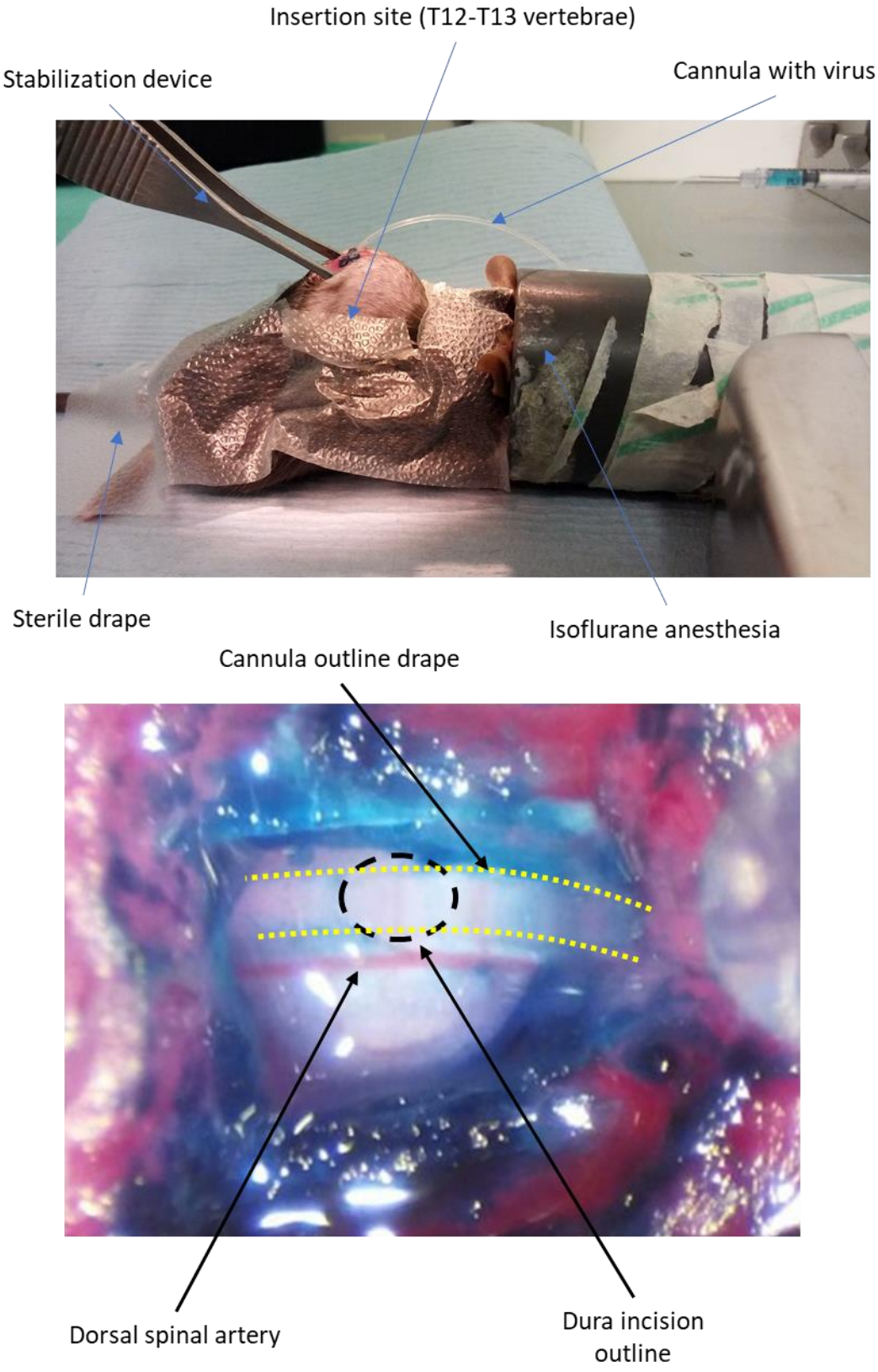

Figure 2.3 – Intrathecal cannula delivery set up. a) *Example picture of an intrathecal cannula viral delivery.**b)** Image taken through the surgery microscope objective, showing the cannula insertion site. The blue coloration is from the dye used to visualise the dura.*

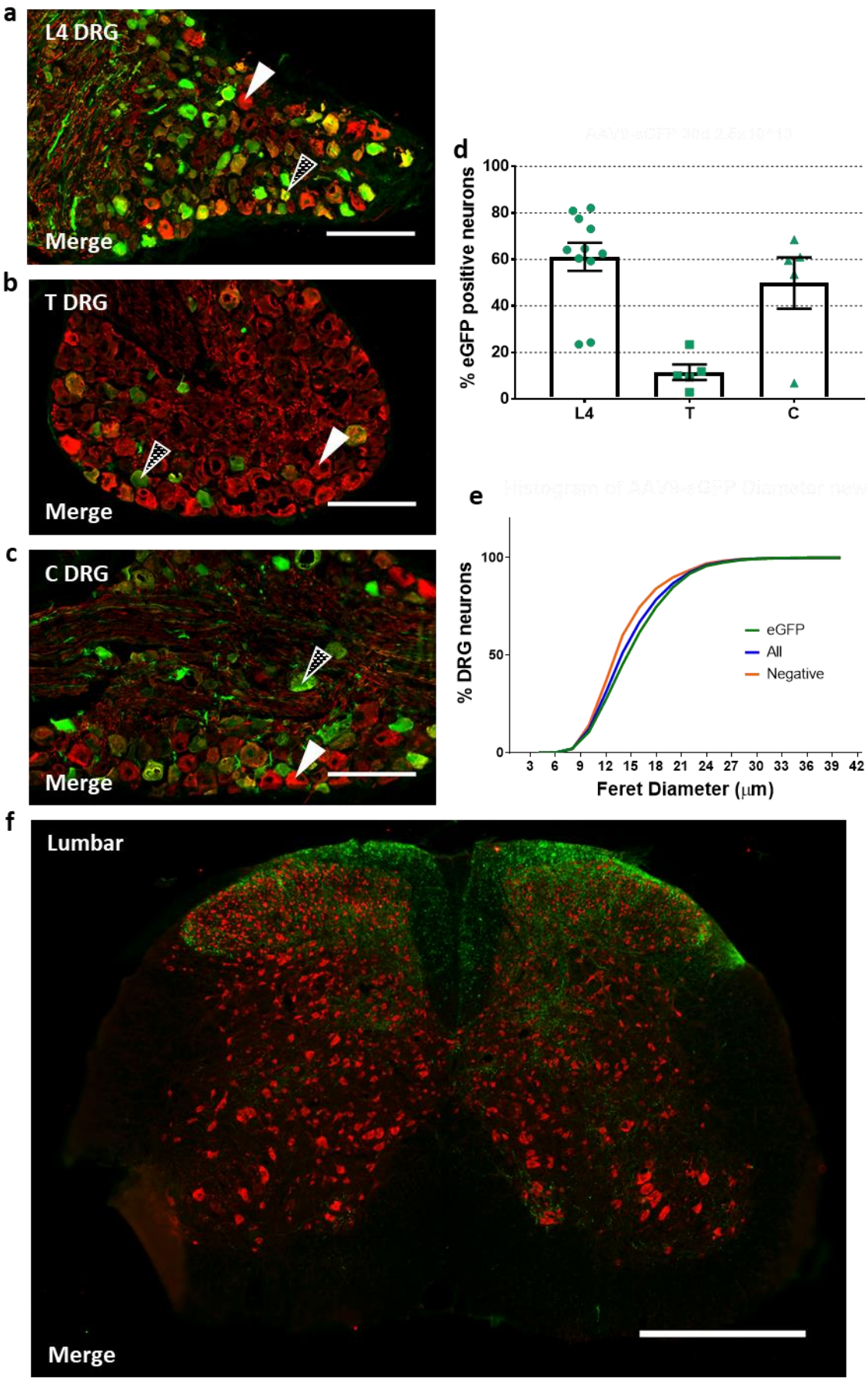
a
L4 DRG
Merge
b
T DRG
Merge
c
C DRG
Merge
d
% eGFP positive neurons
100
80
60
40
20
0
L4
T
C
e
% DRG neurons
100
50
0
3 6 9 12 15 18 21 24 27 30 33 36 39 42
Feret Diameter (μm)
eGFP
All
Negative
f
Lumbar
Merge

Figure 2.4 – Intrathecal delivery of AAV9 via intrathecal cannula results in DRG neuron transduction after 30 days. *Animals were injected with 5 ul AAV9-eGFP at 2.5x10^{13} gc/ml. Representative IHC images of **a**) lumbar 4, **b**) thoracic and **c**) cervical DRG sections. Sections were stained for β-III-Tubulin (red) and GFP (green). Example of transduced and non-transduced neurons are marked with black and white arrows respectively. Scale bar = 100 um. **d)** Quantification of transduction efficiency for lumbar (61.12% ± 6.06%, n = 11), thoracic (11.5% ± 3.33%, n = 5) and cervical (49.86% ± 11.03%, n = 5) DRGs. **e**) cumulative frequency plot of neuronal diameters for all (blue), eGFP-negative (orange) and eGFP-positive (green) in L4 DRG neurons. Kolmogorov-Smirnov test showed significant difference in diameter distribution between all and eGFP-positive neurons, approximate p-value < 0.0001, n = 4. **f)** Representative IHC image of lumbar spinal cord, stained for NeuN (red) and eGFP (green). Scale bar = 500 um.*

After confirming that intrathecal delivery via a cannula is as effective as the lumbar puncture at transducing L4 DRG neurons, we decided to investigate the influence of time post injection on this method. If successful, shorter time period would speed up experimental turn over and allow greater flexibility. Reducing the time post injection from 30 days to 14 days did not have a significant influence on transduction efficiency of L4 or thoracic DRG neurons (66% ± 3.41% vs 61% ± 6.06%, Two-tailed t-test, p = 0.625, n = 5 for L4 and 11.5% ± 3.33% vs 11.8% ± 2.8%, Two-tailed t-test, p = 0.96, n = 5 and 2 for thoracic) (**Fig. 2.4 e and 2.5 a-b,d**). Central terminals in the spinal cord were also positive for eGFP (**Fig. 2.5 e**). However, transduction in the cervical region was significantly lower compared to the 30 days post injection (16% vs 50%, Two-tailed t-test, p = 0.0439, n = 5) (**Fig. 2.4 e and 2.5 c-d**).

Further reduction of the post injection time period to 7 days did not significantly reduce transduction efficiency in either L4 (58% vs 61%, Two-tailed t-test, p = 0.77, n =6) or cervical (61% vs 50%, Two-tailed t-test, p = 0.971, n = 5) DRGs compared to 30 days (**Fig. 2.4 e and 2.6 a-c**). We did not check labelling in the thoracic DRGs. EGFP labelling of the central terminals was also present, but mostly restricted to the superficial laminae (**Fig. 2.6 d**). These experiments suggest that the previously observed lack of transduction at shorter post injection time periods with lumbar puncture delivery was not due to biological limitations of AAV9.

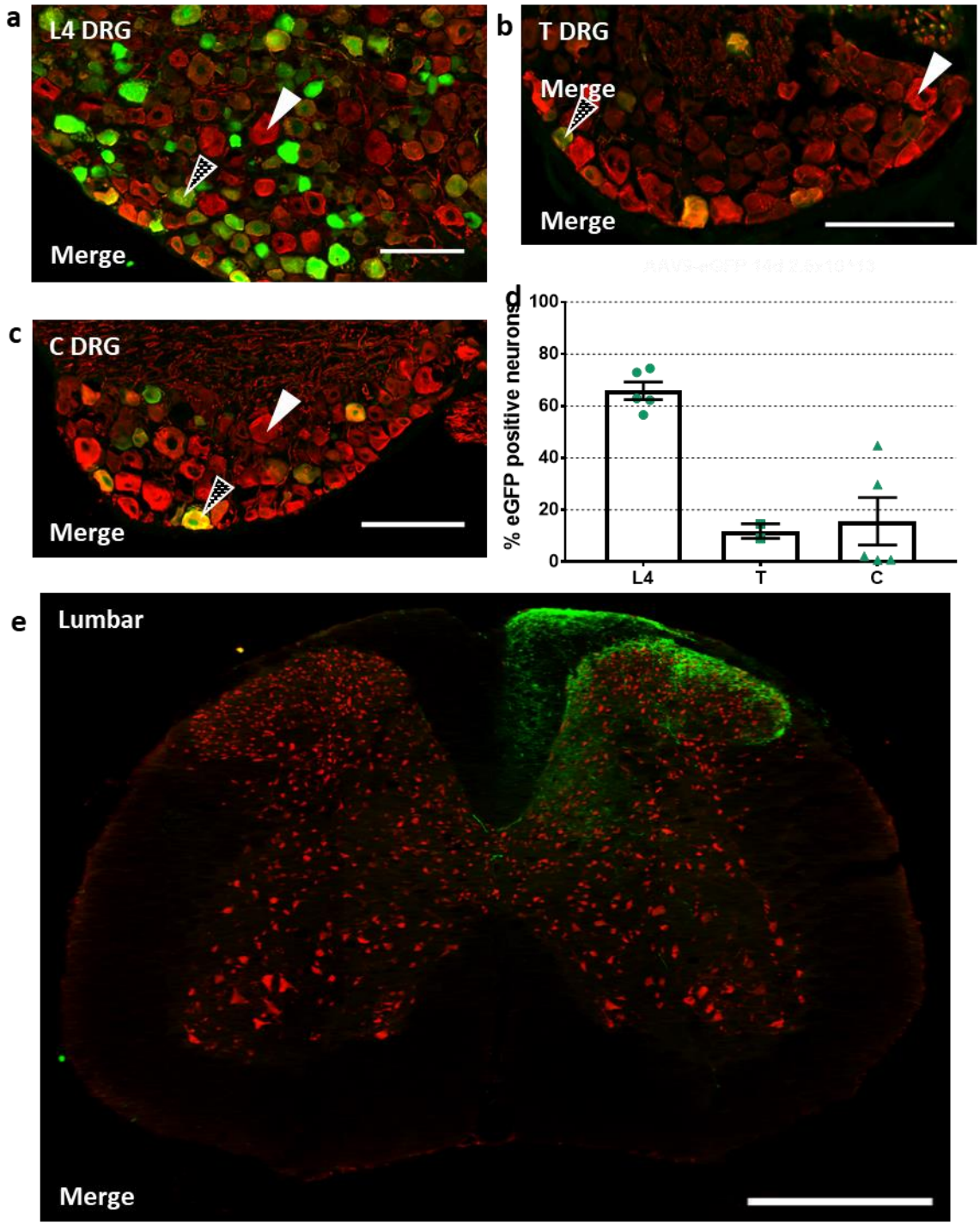

Figure 2.5 – L4 DRG neuronal transduction after 14 days is similar to that after 30 days. *Animals were injected with 5 µl AAV9-eGFP at 2.5x10^{13} gc/ml. Representative IHC images of **a**) lumbar 4, **b**) thoracic and **c**) cervical DRG sections. Sections were stained for β-III-Tubulin (red) and GFP (green). Example of transduced and non-transduced neurons are marked with black and white arrows respectively. Scale bar = 100 µm. **d**) Quantification of transduction efficiency for lumbar (65.83% ± 3.41%, n = 5), thoracic (11.08% ± 2.8%, n =2) and cervical (15.64% ± 9.14%, n = 5) DRGs. **e**) Representative IHC image of lumbar spinal cord, stained for NeuN (red) and eGFP (green). Scale bar = 500 µm.*

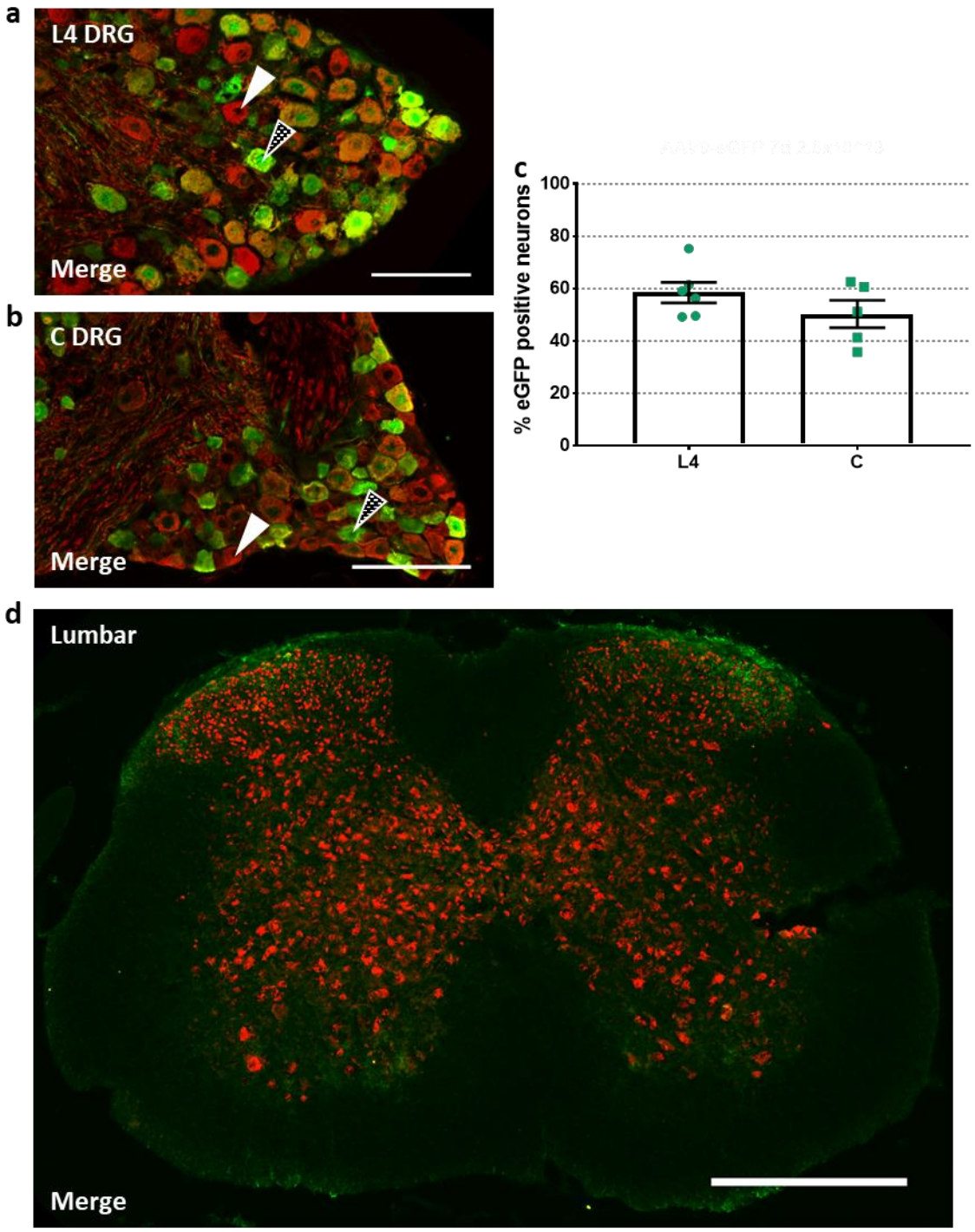

Figure 2.6 – Majority of lumbar and cervical DRG neurons are transduced 7 days after intrathecal injection of AAV9-eGFP using the intrathecal catheter method. *Animals were injected with 5 µl AAV9-eGFP at 2.5x10^{13} gc/ml. Representative IHC images of* ***a****) lumbar 4 and* ***b****) cervical DRG sections. Sections were stained for β-III-Tubulin (red) and GFP (green). Example of transduced and non-transduced neurons are marked with black and white arrows respectively. Scale bar = 100 µm.* ***c****) Quantification of transduction efficiency for lumbar (58.5% ± 3.93%, n = 6) and cervical (50.32% ± 5.25%, n = 5) DRGs.* ***d****) Representative IHC image of lumbar spinal cord, stained for NeuN (red) and eGFP (green). Scale bar = 500 µm.*

2.3.3 The viral titre of AAV9-eGFP influences the transduction efficiency in DRG neurons

Next, we wanted to know what effect the viral titre had on transduction efficiency. To evaluate this, we assessed the transduction efficiency of AAV9-eGFP 30 days after intrathecal cannula delivery of either 0.25, 0.5, 1.25 or 2.5 x10^{13} gc/ml. The L4 DRG transduction efficiencies with these titres were 32.53% ± 16.35%, 43.27% ± 9.99%, 61.48 % ± 4.36% and 61.12% ± 6.06%, respectively. Decreasing the titre had no significant impact on transduction efficiency in L4 DRG, however this may be due to high variability of lower-titre data (**Fig. 2.7 a-e**, One-Way ANOVA, p = 0.15, n = 3 - 11). In addition, linear regression of the percentage of transduced neurons in L4 DRG shows a positive trend with increasing titre, suggesting that titre and transduction efficiency may have a positive linear relationship (slope = 17.31 ± 3,635, R square = 0.919) (**Fig. 2.7 f**).

After carrying out characterization of AAV9-eGFP transduction, our stock of 2.5x10^{13} gc/ml AAV9-eGFP was depleted. The next batch that was purchased from the supplier was of lower titre (6.39x10^{12} gc/ml). Since our experiments suggested that lower titre may reduce the transduction efficiency, we investigated the transduction efficiency of the new AAV9-eGFP titre after 30 days post injection. The transduction efficiency in the L4 DRG 30 days after delivery did not significantly differ between 6.39x10^{12} gc/ml and 2.5x10^{13} gc/ml AAV9-eGFP (**Fig. 2.8 a,e**, 58% vs 61%, Two-tailed t-test, p = 0.61, n = 11-15). However, the transduction efficiency in thoracic and cervical regions was significantly reduced comparted to 2.5x10^{13} gc/ml AAV9-eGFP (0.6% ± 0.3% vs 11.5% ± 3.33%, Two-tailed t-test $p<0.05$, n = 5-14 for thoracic, 7.91% ± 4.23% vs 49.9% ± 11.03%, Two-tailed t-test $p<0.05$, n = 5-14 for cervical, **Fig. 2.4 b,c,e and 2.8 b-d**). We also investigated whether lowering the titre would impact eGFP signal in the spinal cord. Similar to high-titre AAV9-eGFP, there was eGFP signal in the lumbar dorsal spinal cord, but there was no evidence of eGFP-NeuN double-positive cells, suggesting that transduction with AAV9-eGFP is restricted to DRG neurons, and the eGFP signal observed in the spinal cord comes from the projections of DRG neurons (**Fig. 2.8 e**). These data suggest that the new lower-titre (6.39 x10^{12} gc/ml) AAV9-eGFP is as efficient at transducing L4 DRG

neurons as the high-titre virus, however transduction at thoracic and cervical levels is significantly worse.

Next, we wanted to investigate whether the serotype 9 of the AAV has a preference for a particular sub-population of DRG neurons, as we have found significant difference in the cumulative frequency distribution of the neuronal diameter of transduced neurons Therefore, we quantified transduction rates among the different sub-populations of DRG neurons, namely large (neurofilament 200 (NF200)-positive), small peptidergic (CGRP-positive) and non-peptidergic (IB4-positive) neurons in mice injected with AAV9-eGFP. We found no significant difference in the distribution of marker-positive neurons between eGFP-positive neurons and all DRG neurons (One-way ANOVA with Tukey's Multiple comparisons correction; 42.23% ± 4.34% vs 32.21% ± 2.16%, p = 0.124, n = 10 for CGRP; 32.21% ± 3.32% vs 31.19% ± 3.0%, p = 0.97, n = 10 for NF200; 24.98% ± 1.31% vs 27.54% ± 1.25%, p = 0.983, n = 10 for IB4; **Fig. 2.9 a-d,**). This suggests that AAV9 is effective in transducing a large proportion of L4 DRG neurons even at a lower titre and that it does not have affinity for a particular neuronal sub-population.

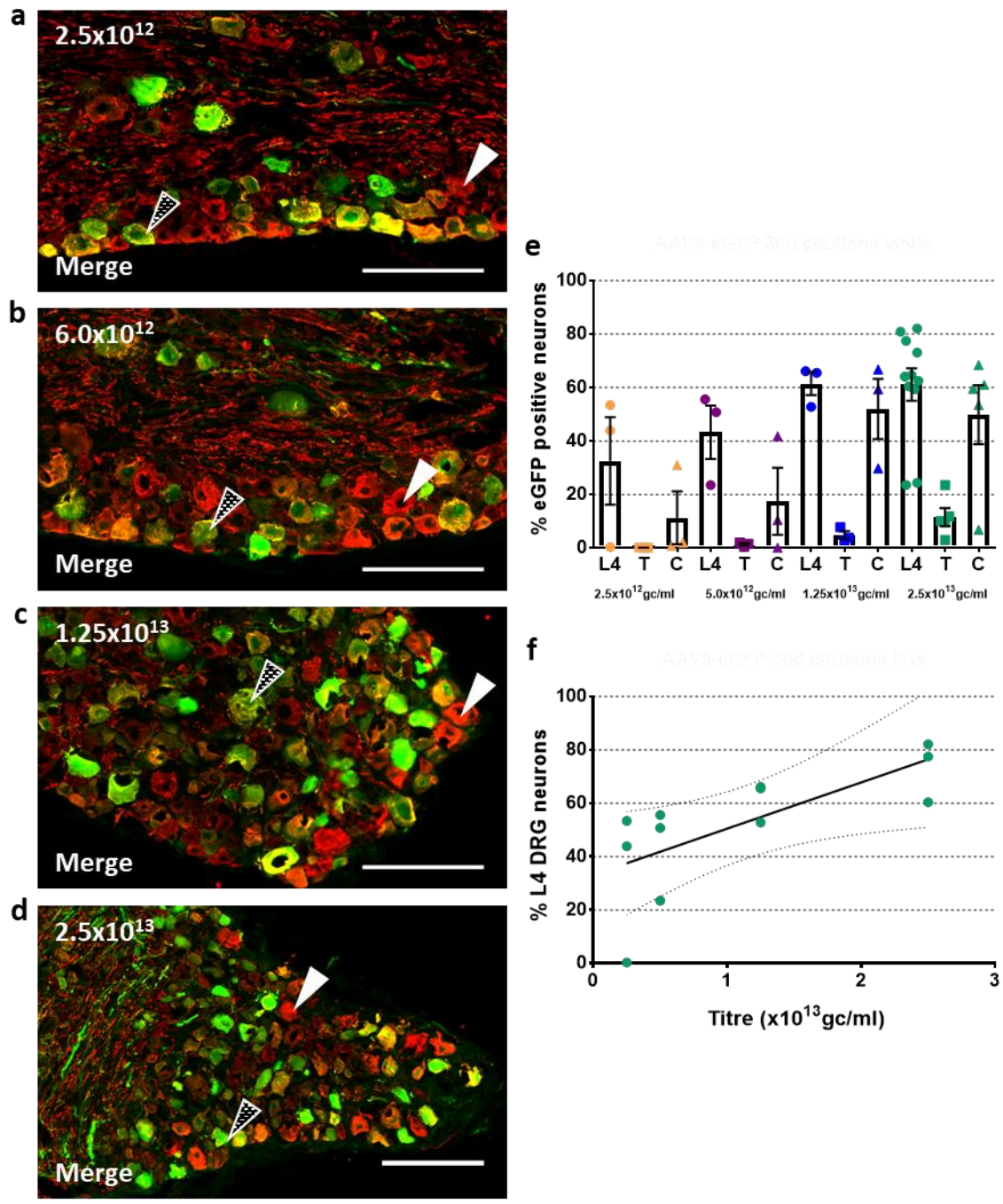

Figure 2.7 – Viral titre affects transduction efficiency after 30 days. *Representative IHC images of lumbar 4 DRG 30 days after 5 ml AAV9-eGFP injection at* ***a)*** *2.5x10^{12},* ***b)*** *5.0x10^{12} ,* ***c)*** *1.25x10^{13} and* ***d)*** *2.5x10^{13} gc/ml. Sections were stained for β-III-Tubulin (red) and GFP (green). Example of transduced and non-transduced neurons are marked with black and white arrows respectively. Scale bar = 100 µm.* ***e)*** *quantification of transduction efficiency for lumbar, thoracic and cervical DRGs at various virus titres. The number of L4 neurons transduced from lowest to highest titre were 32.53% ± 16.35% (n = 3), 43.27% ± 10% (n = 3), 61.48% ± 4.36% (n = 3) and 61.12± 6.06% (n = 11).* ***f)*** *Linear regression of L4 DRG transduction efficiency plotted against virus titre. R square = 0.919.*

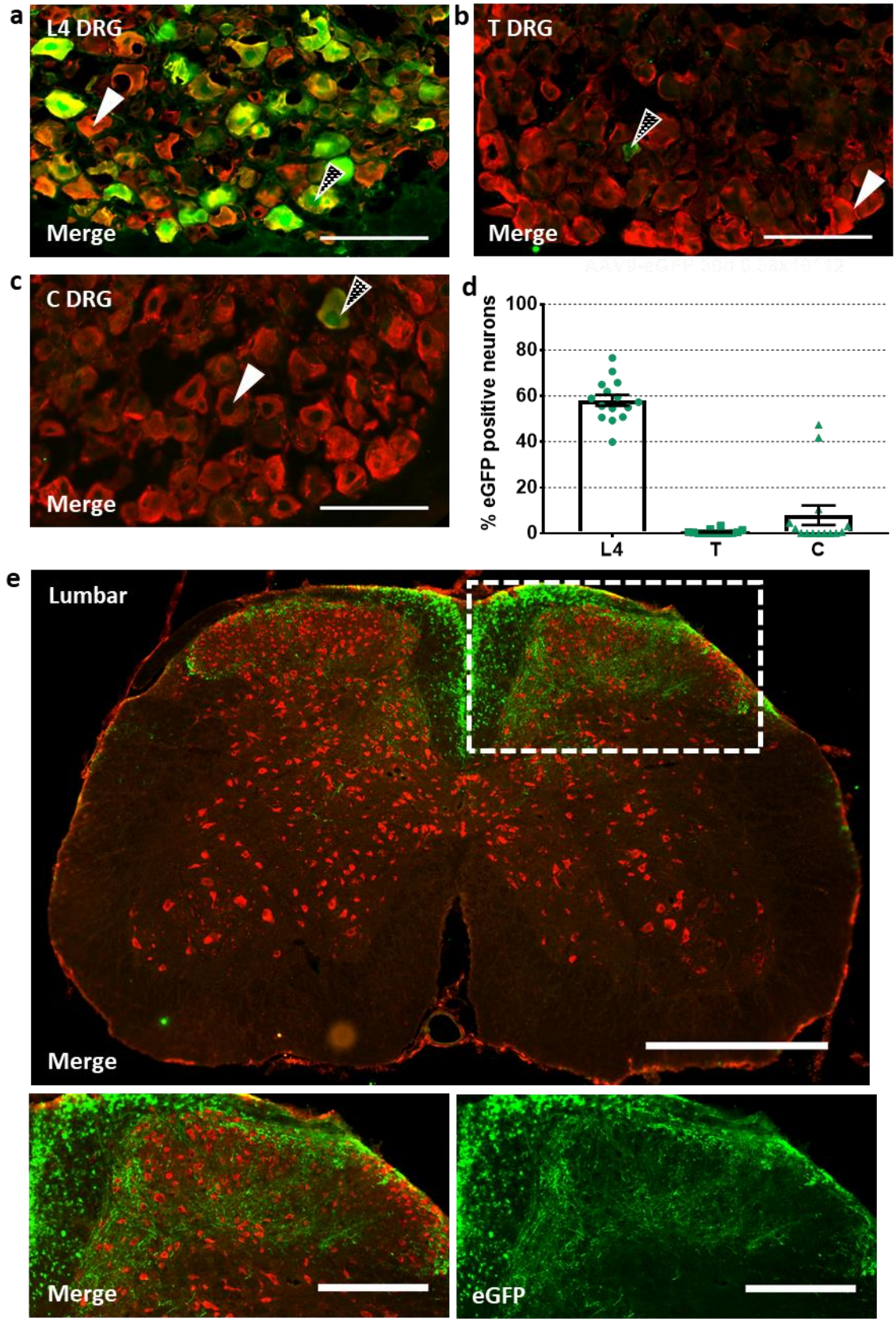

Figure 2.8 – Decreasing viral titre does not significantly impact lumbar transduction but reduces thoracic and cervical transduction. *Animals were injected with 5 µl AAV9-eGFP at 6.39x10^{12} gc/ml. Representative IHC images of* ***a)*** *lumbar 4,* ***b)*** *thoracic and* ***c)*** *cervical DRG sections. Sections were stained for β-III-Tubulin (red) and GFP (green). Example of transduced and non-transduced neurons are marked with black and white arrows respectively. Scale bar =*

100 µm. ***d)*** *Quantification of transduction efficiency for lumbar (58.1% ± 2.36%, n = 15), thoracic (0.636% ± 0.26%, n = 14) and cervical (7.91% ± 4.23%, n = 14) DRGs.* ***e)*** *Representative IHC image of lumbar spinal cord, stained for NeuN (red) and eGFP (green). Scale bar = 500 µm. The inserts show dorsal horn, with no NeuN – eGFP double-positive cells.*

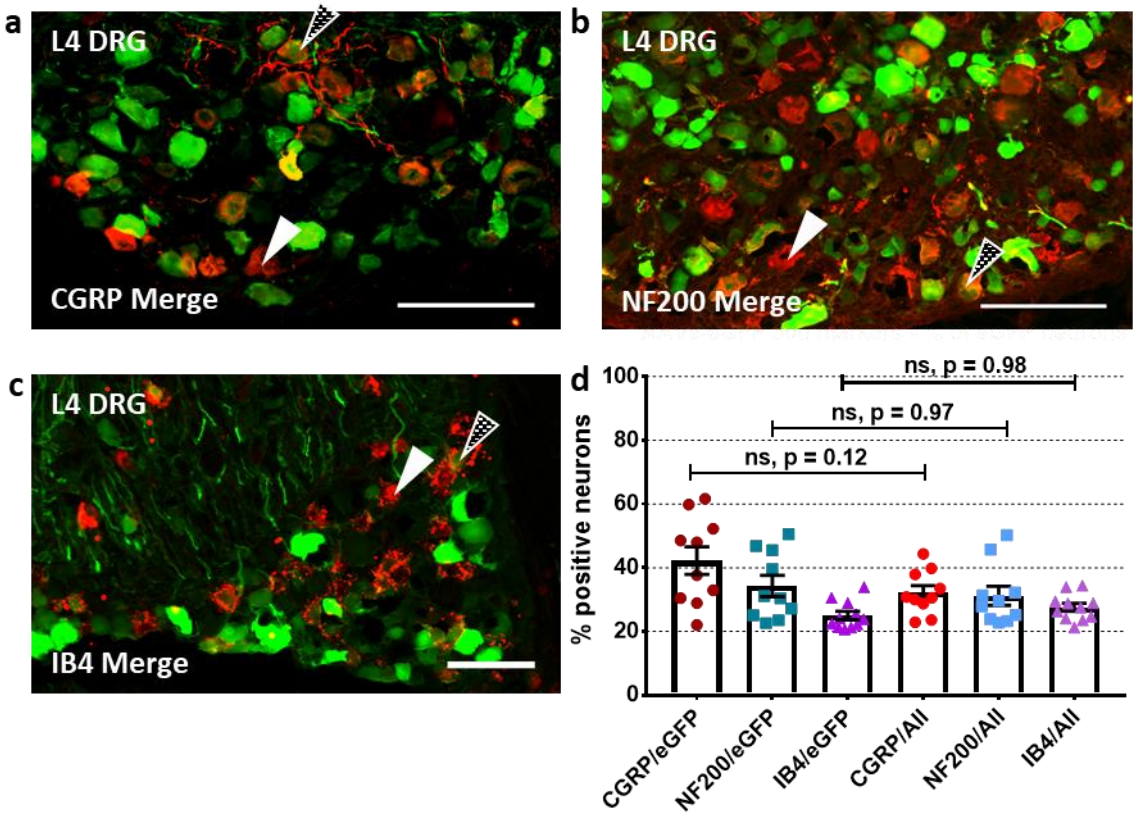

Figure 2.9 – Transduction is not selective for DRG neuronal subpopulations. *Animals were injected with 5 µl AAV9-eGFP at 6.39x10^{12} gc/ml. Representative IHC images of lumbar 4 DRG sections. Sections were stained for GFP (green) and* ***a)*** *CGRP (red),* ***b)*** *NF200 (red) or* ***c)*** *IB4 (red). Example of transduced and non-transduced neurons are marked with black and white arrows respectively. Scale bar = 100 µm.* ***d)*** *Quantification of the number of cells stained for the different markers. There was no significant difference in the proportion of total neurons and eGFP-positive neurons co-labelled with subpopulation markers (One-way ANOVA with Tukey's multiple comparisons correction, p = 0.12 (CGRP), 0.97 (NF200) and 0.98 (IB4), n = 10).*

2.3.4 Impact of surgical procedure and viral transduction on mechanical sensitivity and DRG immune cell composition

Further, we wanted to elucidate whether intrathecal delivery of AAV9-eGFP via an intrathecal cannula had any undesired side effects, such as pain or an immune response. Intrathecal delivery of AAV9 via a cannula is an invasive procedure. Extreme care must be taken when performing it, as the cannula insertion into the intrathecal space could compress or damage the spinal cord, potentially causing pathology, which would undermine the experiment. To minimise the potential damage to the spinal cord, we used the smallest cannula size possible. In order to evaluate the impact of the procedure and AAV9 transduction on mechanical sensitivity we used an established sensory test, the Von-Frey Test. After 3 baseline assessments over one week, mice were split into 2 groups of 8 and injected with either AAV9-eGFP or saline. Their mechanical thresholds were then assessed up to 34 days after injection (**Fig. 2.10**). This experimental set up also allowed us to evaluate the effect of the surgical procedure by comparing the baseline (0.66g ± 0.035) to the timepoint after surgery of the vehicle injected animals (0.66g ± 0.05, 0.74g ± 0.05, 0.7g ± 0.06, 0.63g ± 0.05, 0.64g ± 0.04 and 0.64g ± 0.02 for 4-, 7-, 14-, 20- 26- and 34-day timepoints). We found no significant difference between the baseline value and the value for any timepoint after vehicle injection (One-way ANOVA with Dunnett's multiple comparisons correction, $p = 0.71 – 0.99$, n=8). Our data suggest that our surgical procedure does not result in a mechanical sensory deficit. Furthermore, there was also no evidence that AAV9-eGFP infusion results in a mechanical sensory deficit, as there is no significant difference between the two groups at any timepoint (One-way ANOVA with Sidak's Multiple comparisons correction, $p = 0.08 – 0.99$, n = 8 per group).

Since expression of non-self protein in DRG neurons has been reported to cause an immune response in primates (Ciesielska *et al.*, 2013; Yang *et al.*, 2016) , we next investigated the immune cell composition of DRGs from mice injected with AAV9 compared to vehicle. We

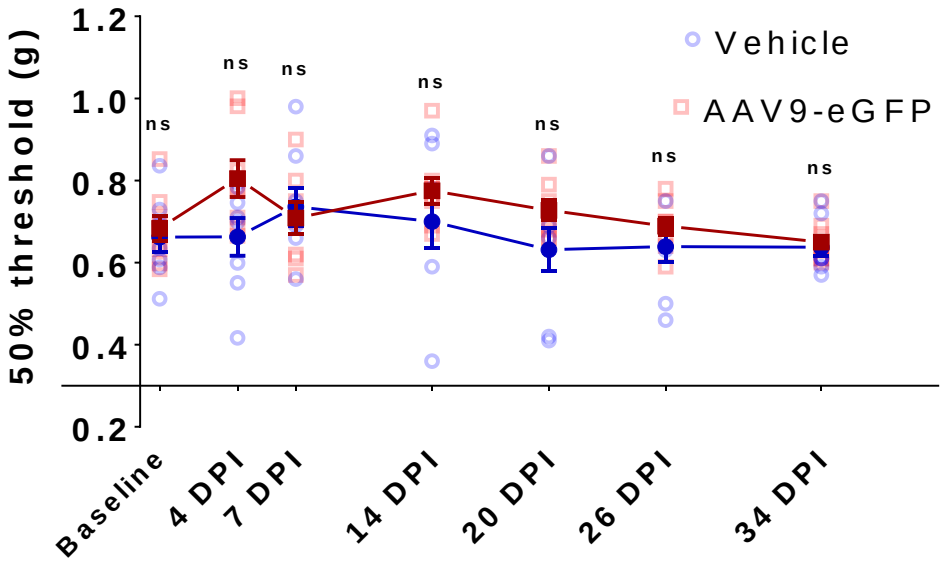

Figure 2.10 – Neither intrathecal cannula delivery nor AAV9-eGFP transduction change mechanical sensitivity. *Mechanical sensitivity was assessed using the Von Frey test. For the vehicle-treated group, there was no difference between any timepoint and the baseline, suggesting that the intrathecal cannulation procedure itself does not produce significant change in mechanical sensitivity (One-Way ANOVA with Tukey's Multiple comparisons correction, p > 0.76 – 0.99, n = 8). Additionally, there was no significant difference in mechanical thresholds between vehicle and AAV9-eGFP injected animals at any timepoint, up to 34 days post injection (DPI) (One-way ANOVA with Tukey's Multiple comparisons correction, p > 0.08, n = 8 animals in each group).*

proceeded to compare the immune cell composition of DRGs from virus- or vehicle-injected mice by flow cytometry. We harvested and dissociated lumbar DRGs 30 days after injection. Cells were then stained using a panel of immune cell markers (see **2.2.12**) and their absolute numbers were analysed using flow cytometry. Our gating strategy is shown in **Fig. 2.11 a.** There was no significant difference in the number of marker-positive cells between AAV- and vehicle-treated groups (CD45+ immune cells 66.9 vs 64.6; B cells 4.08 vs 4.6; T cells 28.9 vs 13.79; Neutrophils 0.13 vs 0.26; Dendritic cells 0.122 vs 0.09; Macrophages 28.13 vs 32.68; Monocytes 3.49 vs 1.85; One-way ANOVA with Sidak's Multiple comparisons correction, p = 0.11 – 0.99, n = 4 per group; **Fig. 2.11 b**), suggesting that viral transduction does not cause an immune response.

a

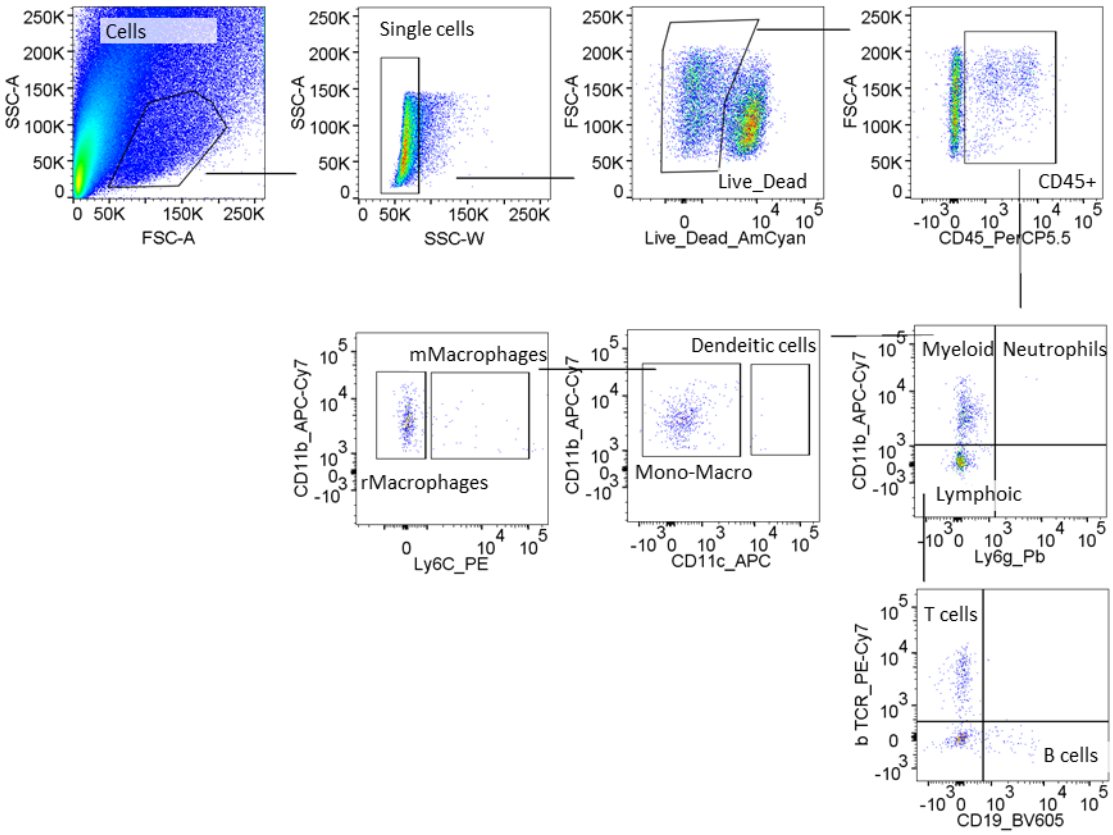
Cells
SSC-A
FSC-A
Single cells
SSC-W
Live_Dead
Live_Dead_AmCyan
CD45+
CD45_PerCP5.5
mMacrophages
rMacrophages
CD11b_APC-Cy7
Ly6C_PE
Dendeitic cells
Mono-Macro
CD11c_APC
Myeloid
Neutrophils
Lymphoic
Ly6g_Pb
T cells
B cells
b TCR_PE-Cy7
CD19_BV605

b

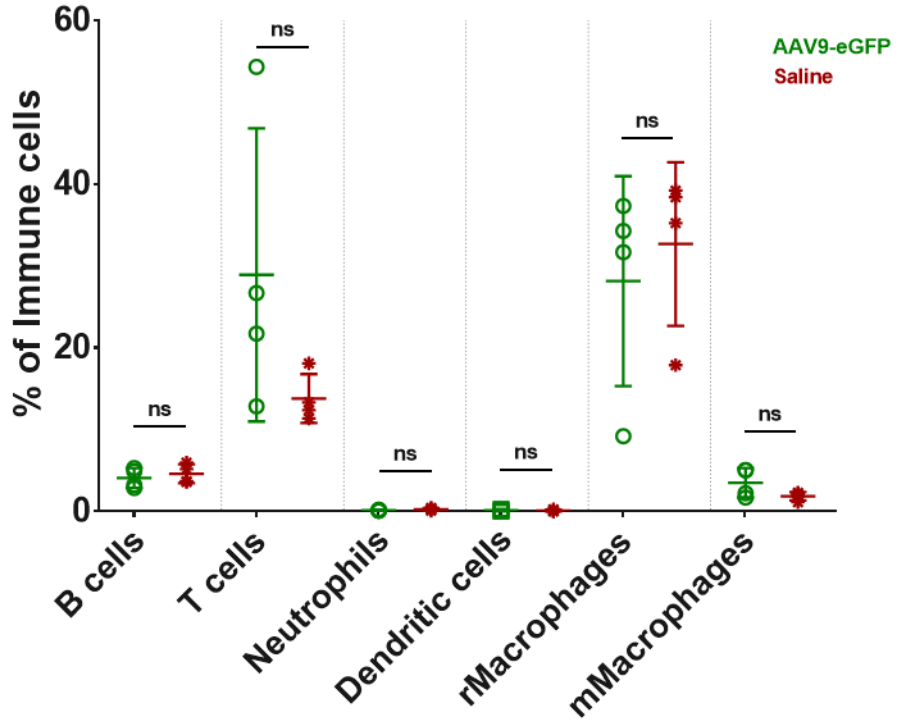
% of Immune cells
AAV9-eGFP
Saline
ns
B cells
T cells
Neutrophils
Dendritic cells
rMacrophages
mMacrophages

Figure 2.11 – Viral transduction does not cause significant changes in the immune cell profile of the L4 DRGs. *Mice were injected with 5 µl of 6.39x10^{12} gc/ml of AAV9-eGFP or vehicle 14 days before tissue collection for flow cytometry.* ***a)*** *Example of gating strategy that was used to obtain cell counts from AAV9-eGFP or vehicle-treated mice.* ***b)*** *Quantification of cell number for AAV9-eGFP and saline injected mice. There was no significant difference between any types of immune cells (One-Way ANOVA with Tukey's multiple comparisons correction, p> 0.12, n=4 each group).*

2.3.5 AAV8 is less efficient than AAV9 at transducing DRG neurons after intrathecal delivery

After establishing that AAV9 was efficient at transducing lumbar DRG neurons at different timepoints and titres, we next assessed DRG neuronal transduction with a different AAV serotype. We investigated the transduction efficiency of high titre ($1.78x10^{13}$ gc/ml) AAV8-eGFP 30 days after intrathecal injection. 35.16% ± 7.37% of L4 DRG neurons were transduced, which is significantly lower than the proportion of neurons transduced with AAV9-eGFP (58.1% ± 2.36%, Two-tailed t-test, p = 0.0009, n = 5). Cervical and thoracic transduction was very low, 5.72% ± 3.5%, and 0%, respectively (**Fig. 2.12**). The difference in transduction efficiency may be due to the difference in neuronal tropism between serotypes.

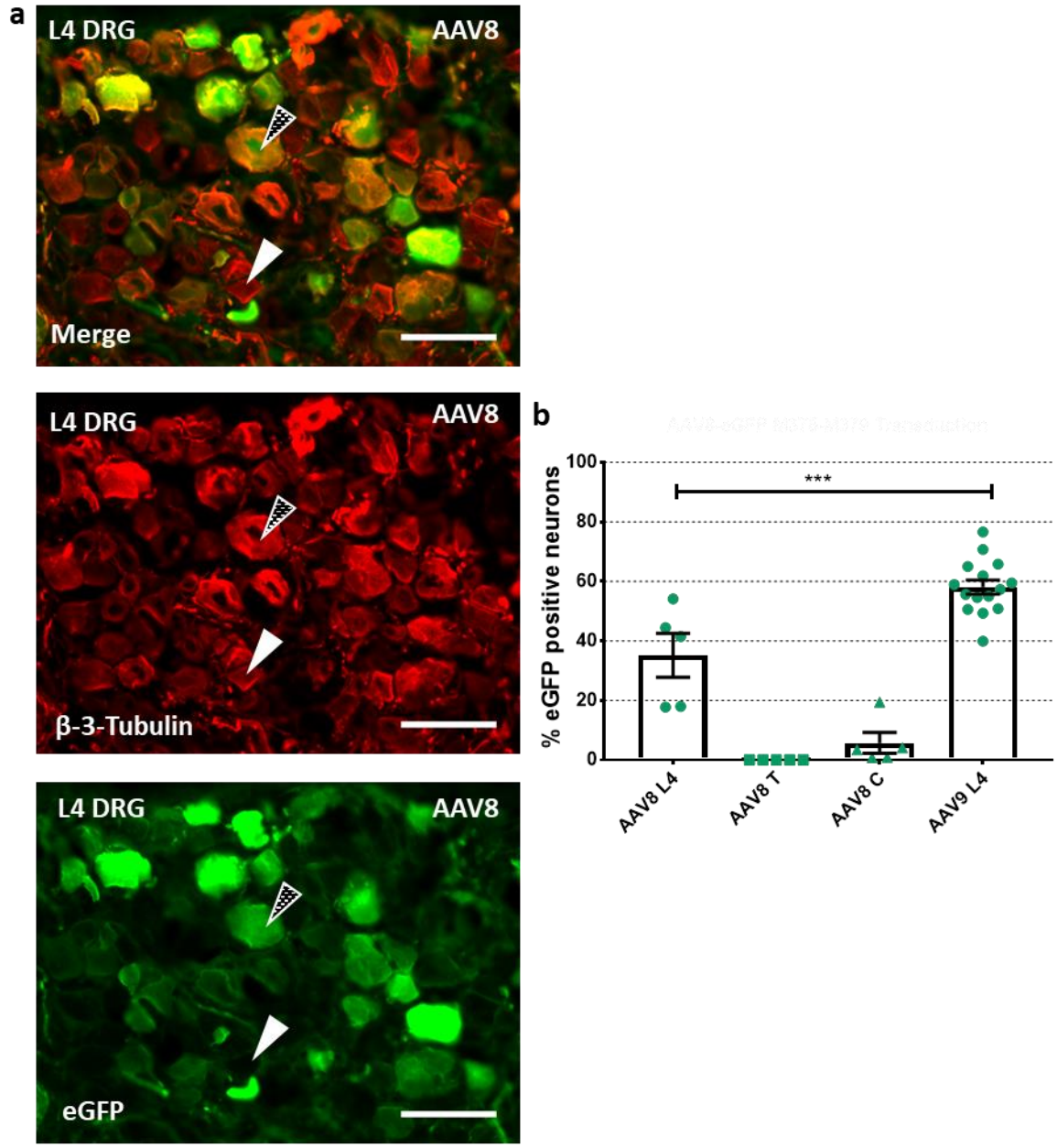

Figure 2.12 - Intrathecal delivery of AAV8-eGFP results in lower transduction of DRG neurons compared to AAV9. *Mice were injected with 5 µl of AAv8-eGFP at 1.78x10^{13} gc/ml.* ***a)*** *Representative IHC images of lumbar 4 DRG sections. Sections were stained for β-III-Tubulin (red) and GFP (green). Example of transduced and non-transduced neurons are marked with black and white arrows, respectively. Scale bar = 100 µm.* ***b)*** *Quantification of transduction efficiency of AAV8-eGFP for lumbar (35.16% ± 7.36%, n = 5), thoracic (0.00% ± 0.0%, n = 5) and cervical (5.72% ± 3.49%, n = 5) DRGs. There was a significant difference in L4 transduction compared to AAV9-eGFP (35.16% ± 7.36% vs 58.1% ± 2.36%, Two-tailed t-test, p = 0.0009 n = 5).*

2.3.6 AAV9 can deliver transgenes other than eGFP

As AAV8 was found to be less efficient at transducing DRG neurons, we decided to continue using AAV9. Next, we tested if a transgene other than eGFP could be successfully expressed and compared its expression to eGFP expression. We used AAV9-mCherry to express a red fluorophore in the DRGs. Expression of mCherry in the L4 DRG 30 days after injection was not significantly different from eGFP expression 30 days after AAV9-eGFP injection (64.48% ± 9.57% and 58.1% ± 2.36%, respectively, Two-tailed t-test, p = 0.345, n = 3) (**Fig. 2.13**).

After that, we investigated whether co-transduction of two different viral vectors was possible and how this would impact the transduction pattern. Animals were injected simultaneously with 2.5 µl each of AAV9-eGFP and AAV9-mCherry. Overall, percentage of L4 DRG neurons expressing either eGFP or mCherry following co-transduction was not significantly lower than after transduction with AAV9-eGFP or AAV9-mCherry alone (52.38 ± 11.25% vs 58.1 ± 2.36% and 59.9% ± 9.77% vs 64.5 ± 9.57%, respectively; One-way ANOVA with Sidak's multiple comparisons correction, p = 0.73 and 0.34, respectively, n = 4; **Fig. 2.14b and Fig. 2.13b**). The percentage of L4 DRG neurons that expressed both eGFP and mCherry was 39.28% ± 12.13% (**Fig. 2.14b**). The number of eGFP positive cells expressing mCherry and mCherry positive cells expressing eGFP was similar, 68.1% ± 7.92% and 71.45% ± 9.89%, respectively (**Fig. 2.14b**). Overall, there was no indication of one viral vector interfering with another.

Detailed above are a number of experiments investigating the efficacy of intrathecal infusion of AAV9 using a cannula, varying post injection time, virus titre and transgene. Our data shows that AAV9 is a good serotype to get roughly 60% transduction in the lumbar DRGs. We have shown that a titre of $2.5x10^{13}$ gc/ml is ideal but can be reduced to $6.39x10^{12}$ gc/ml without significant impact on transduction. We also found that post injection time of 30 days is sufficient, however this can also be reduced without significant impact on lumbar DRG transduction. Overall, this method of delivery of AAV9 resulted in the average success rate of 93.6% across all experimental conditions and ranged between 67% and 100% (**Table 2.5**).

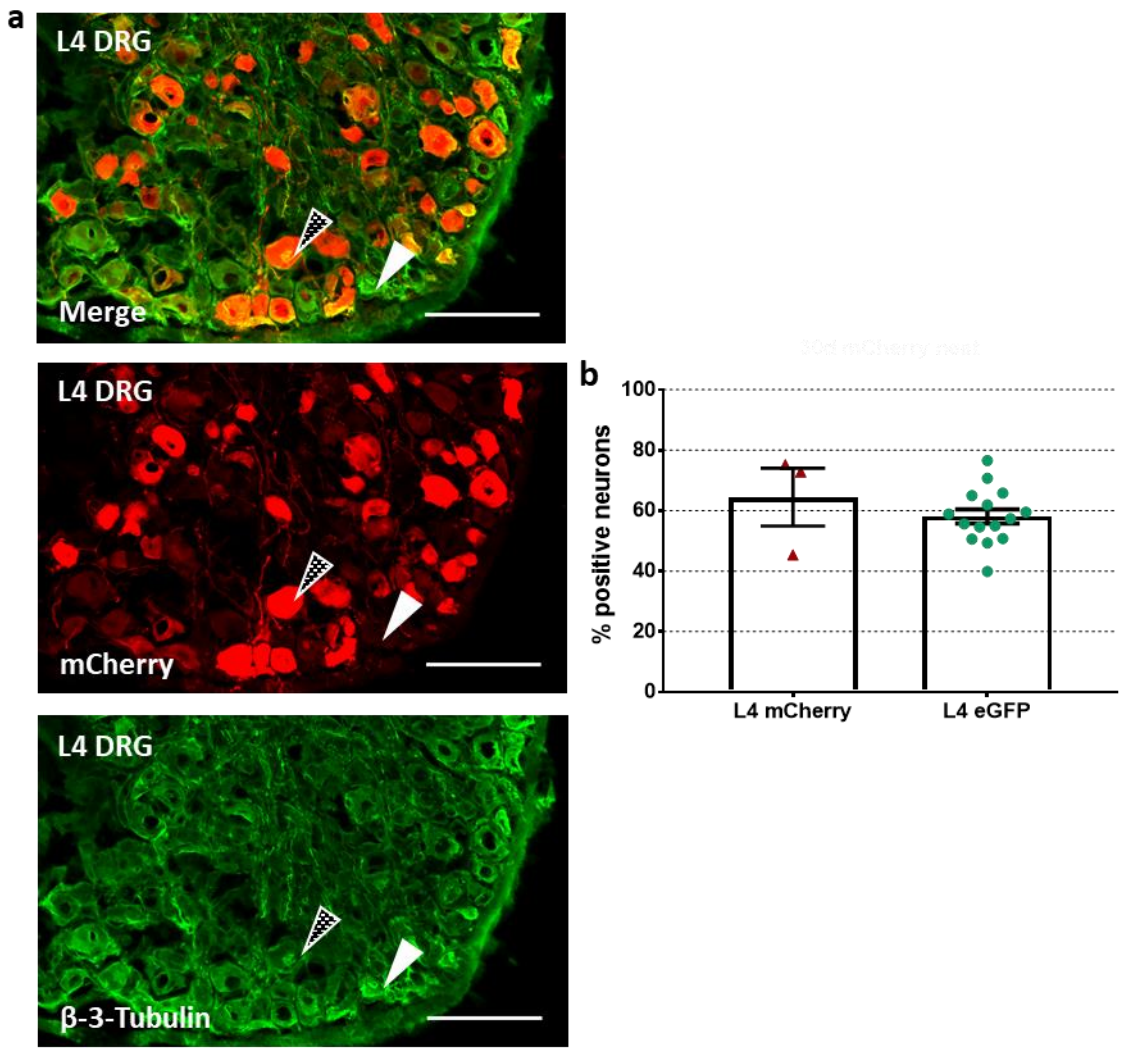

Figure 2.13 – AAV9-mCherry achieves transduction efficiency comparable to AAV9-eGFP in L4 DRG. *Animals were injected with 5 µl AAV9-mCherry at 1.49x10^{13} gc/ml and compared to our data for L4 DRG transduced with 6.39x10^{12} gc/ml AAV9-eGFP.* ***a)*** *Representative IHC image of lumbar 4 DRG section. Sections were stained for β-III-Tubulin (green) and RFP (red). Example of transduced and non-transduced neurons are marked with black and white arrows, respectively. Scale bar = 100 µm.* ***b)*** *Quantification of transduction efficiency for mCherry (64.48% ± 9.57%, n = 3). There was no significant difference compared to AAV9-eGFP transduction (Two-tailed t-test, p = 0.345, n = 3).*

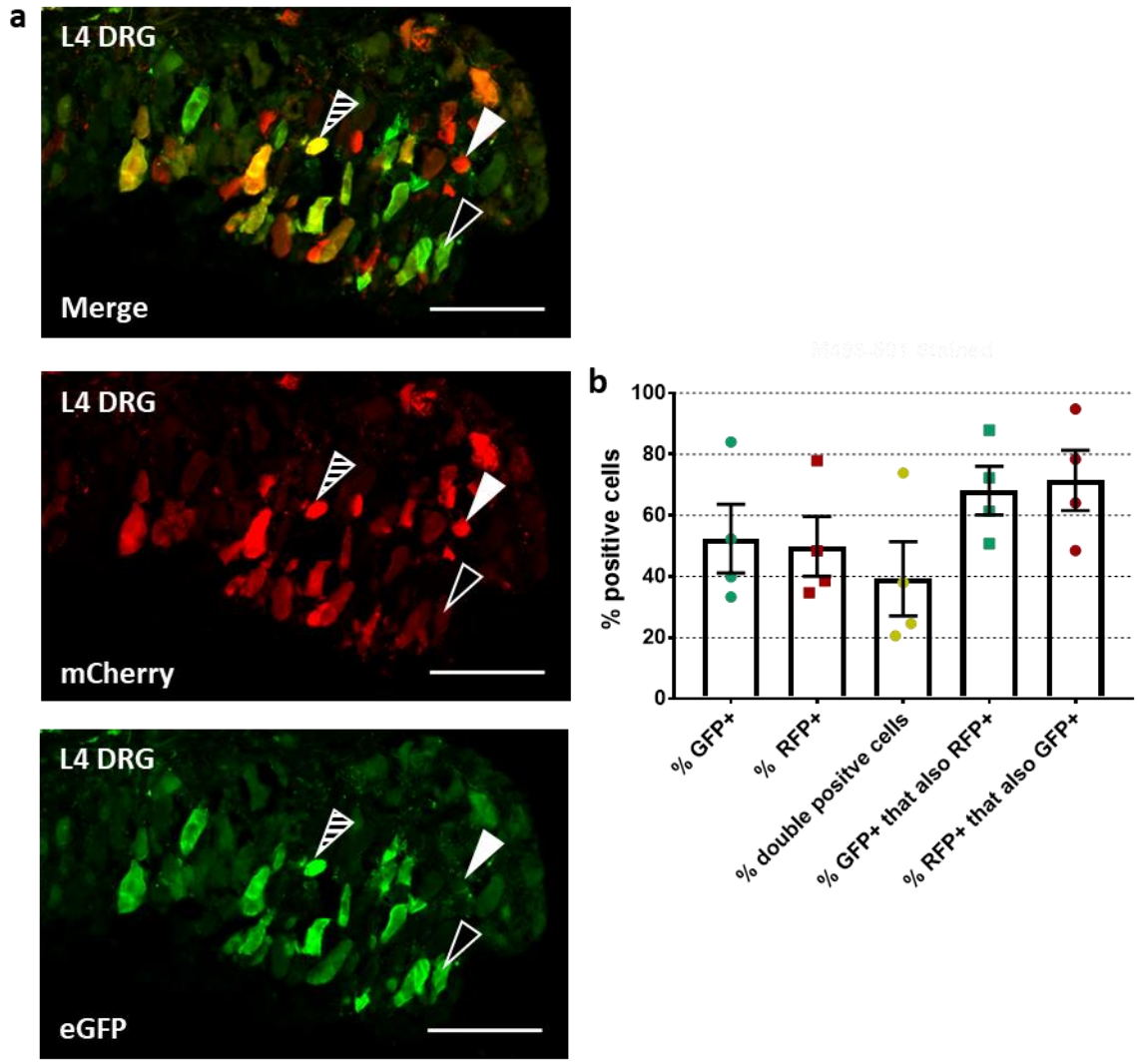

Figure 2.14 – Combined intrathecal delivery of AAV9-eGFP and AAV9-mCherry results in both fluorophores being expressed in L4 DRG neurons. *Animals were injected with 2.5 µl AAV9-eGFP at 6.39x10^{12} gc/ml and 2.5 µl of AAV9-mCherry at 1.49x10^{13} gc/ml.* ***a)*** *representative IHC image of lumbar 4 DRG section. Sections were stained for RFP (red) and GFP (green). Example of double-transduced and RFP+ and GFP+ neurons are marked with dashed, white and black arrows respectively. Scale bar = 100 µm.* ***b)*** *Quantification of transduction for fluorophores, both individually and as a proportion of co-transfected cells. No significant difference between GFP+ and RFP+ (Two-tailed T-test, p =0.22, n = 4) or %GFP+ cells that are RFP+ and %RFP+ cells that are GFP+ (Two-tailed T-test, p = 0.2, n = 4).*

Virus	*Titre, gc/ml*	*Time post injection*	*Total, n*	*Successful transduction, n*	*Successful transduction rate*
AAV9-eGFP	$2.5x10^{13}$	7 days	7	6	86%
AAV9-eGFP	$2.5x10^{13}$	14 days	7	5	71%
AAV9-eGFP	$6.39x10^{12}$	14 days	10	10	100%
AAV9-eGFP	$2.5x10^{13}$	30 days	10	10	100%
	$1.5x10^{13}$	30 days	3	3	100%
	$6.39x10^{12}$	30 days	13	12	92%
	$2.5x10^{12}$	30 days	3	2	67%
AAV9-mCherry	$1.49x10^{13}$	30 days	3	3	100%
AAV9-GCaMP6s	$1.69x10^{13}$	30 days	5	5	100%
AAV9-GCaMP6s	$1.69x10^{13}$	14 days	12	12	100%
AAV9-Cre	$3.29x10^{13}$	40 days	4	4	100%
AAV9-Cre	$3.29x10^{13}$	30 days	7	7	100%
AAV9-Cre	$3.29x10^{13}$	14 days	5	4	80%
AAV8-eGFP	$1.78x10^{13}$	30 days	5	5	100%

Table 2.5 – Summary table for intrathecal cannula delivery success.

2.3.7 Peripheral delivery of AAV9-eGFP successfully transduces DRG neurons

After our success with the intrathecal delivery method, we explored other avenues of AAV9 vector delivery. In particular, we were interested in transducing sensory neurons by virus injection into distinct anatomical structures. First, we injected 1 µl of AAV9-eGFP into the sciatic nerve. After 12 days, there was moderate labelling (21.48% ± 2.33%) in L4 DRG ipsilateral to the injection, while labelling on the contralateral side was absent (**Fig. 2.15 a-c**). This suggests that intraneural injections may be a feasible method of labelling an anatomically distinct population of DRG neurons.

We also performed intraarticular and intraplantar injections of AAV9-eGFP. Labelling on the ipsilateral side was present, however minimal, in L3 DRG neurons after intraarticular (1.05% ± 0.27%, **Fig. 2.16 a**) and in L4 DRG neurons after intraplantar (3.83% ± 1.44%, **Fig. 2.17 a**) injections. Furthermore, both intraarticular and intraplantar delivery methods resulted in labelling on the contralateral side (0.33% ± 0.14% and 4.57% ± 0.95%, respectively, **Figs. 2.16 b**

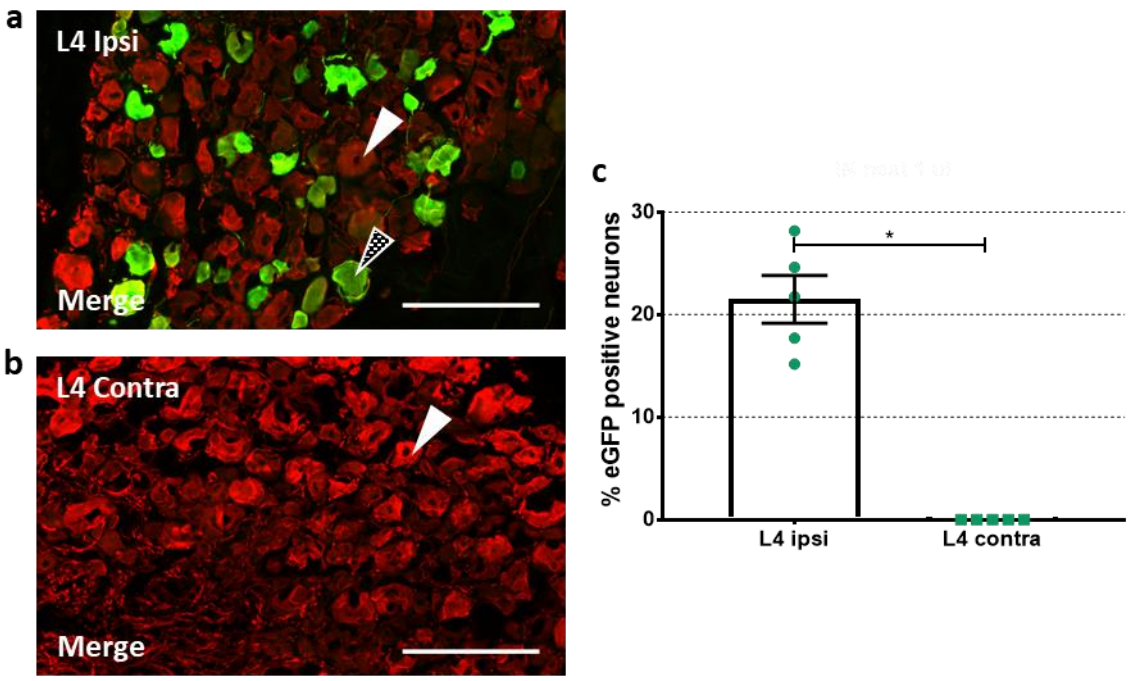

Figure 2.15 – Intrasciatic injection of AAV9-eGFP results in eGFP signal on the ipsilateral side 12 days after injection. *Animals were injected with 1 µl AAV9-eGFP at 6.39x10^{13} gc/ml. Representative IHC images of lumbar 4 DRG* ***a****) ipsilateral and* ***b)*** *contralateral to injection. Sections were stained for β-III-Tubulin (red) and GFP (green). Example of transduced and non-transduced neurons are marked with black and white arrows respectively. Scale bar = 100 µm.* ***c)*** *quantification of L4 transduction on ipsilateral (21.48% ± 2.33%, n = 5) and contralateral (0.00%, n = 5) sides. There was a significant difference between ipsilateral and contralateral L4 transduction (Two-tailed t-test, p < 0.0001, n = 5).*

and 2.17 b). Further refinement of the injection technique as well as the injection parameters, such as titre and volume, may increase the transduction efficiency and eliminate off-target labelling.

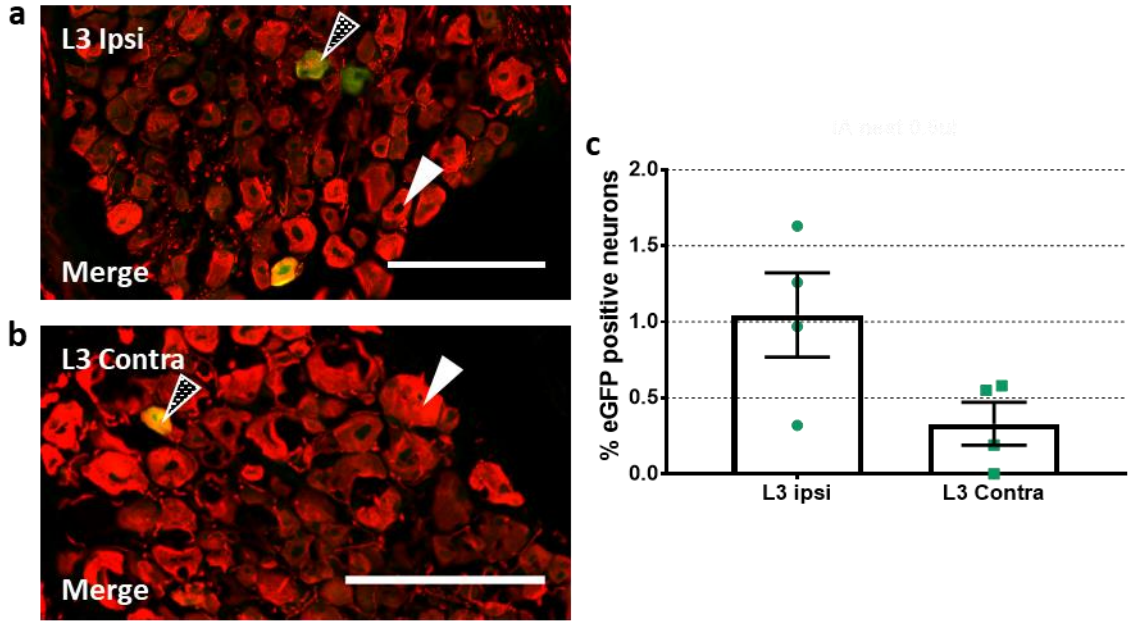

Figure 2.16 – Intraarticular injection of AAV9-eGFP results in low transduction efficiency on both ipsi- and contralateral sides 14 days after injection. *Animals were injected with 0.5 µl AAV9-eGFP at 6.39x10^{13} gc/ml. Representative IHC images of L3 DRG **a**) ipsilateral and **b**) contralateral to injection. Sections were stained for β-III-Tubulin (red) and GFP (green). Example of transduced and non-transduced neurons are marked with black and white arrows respectively. Scale bar = 100 µm. **c)** Quantification of L3 neuronal transduction on ipsilateral (1.045% ± 0.28%, n = 4) and contralateral (0.33% ± 0.14%, n = 4) sides. There was no significant difference between ipsilateral and contralateral L3 transduction (Two-tailed t-test, p = 0.061, n = 4).*

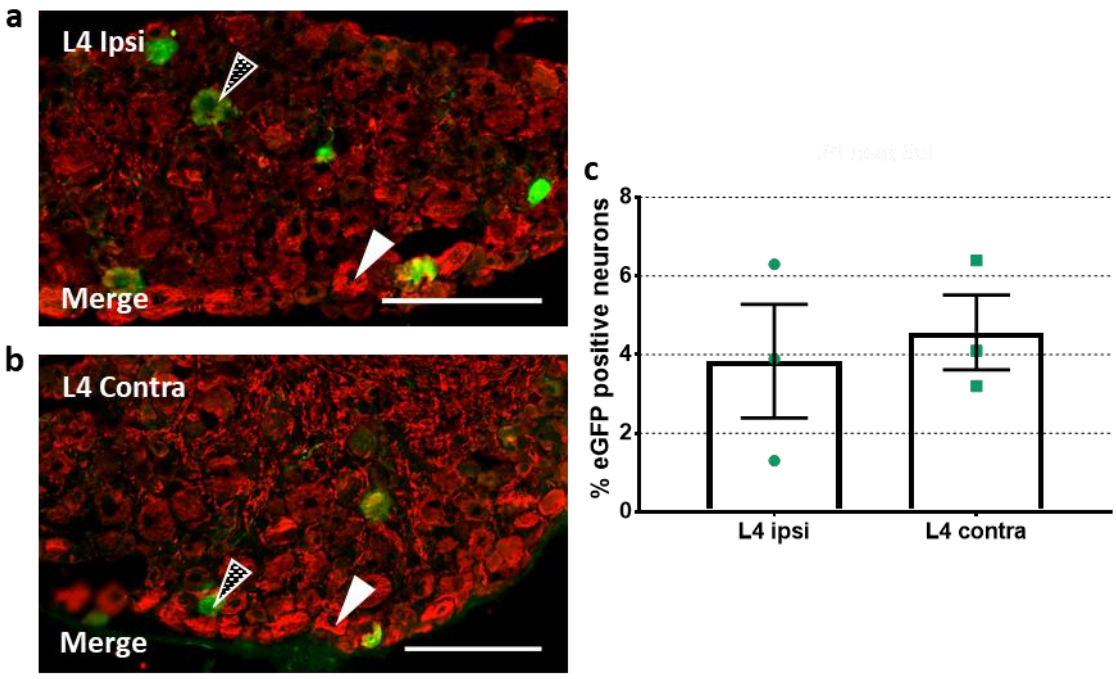

Figure 2.17 – Intraplantar injection of AAV9-eGFP results in low transduction efficiency on both ipsi- and contralateral sides 28 days after injection. *Animals were injected with 5 µl AAV9-eGFP at 6.39x10^{13} gc/ml. Representative IHC images of L4 DRG* ***a****) ipsilateral and* ***b****) contralateral to injection. Sections were stained for β-III-Tubulin (red) and GFP (green). Example of transduced and non-transduced neurons are marked with black and white arrows respectively. Scale bar = 100 µm.* ***c)*** *Quantification of L4 neuronal transduction on ipsilateral (3.83% ± 1.44%, n = 3) and contralateral (4.57% ± 0.95%, n = 3) sides. There was no significant difference between ipsilateral and contralateral L4 transduction (Two-tailed t-test, p = 0.693, n = 3).*

2.3.8 AAV9 transduces adult DRG neurons *in vitro*

In addition to *in vivo* applications, we studied AAV9 as a useful tool to transduce adult DRG neurons *in vitro*. To explore *in vitro* transduction efficiency, we first transduced MACS-purified DRG cultures, which are neuronally-enriched (Thakur *et al.*, 2014). We used these neuronally enriched cultures to maximise neuronal transduction by removing any non-neuronal cells that may reduce the number of viral particles available to neurons. After neurons were extracted and MACS-sorted, virus or vehicle was added to cell suspension and incubated for 20 minutes. A high number of viral particles ($6.39x10^9$ gc AAV9-eGFP per 100 µl cell suspension) was used to increase the chance of successful transfection. Transduction efficiency was evaluated three days after. 78.9% ± 0.6% of neurons were transfected and no eGFP positive neurons were detected in the control samples (**Fig. 2.18 a-c**).

Next, we transfected MACS purified adult DRG cultures using a vector that expressed a different transgene, the Cre-recombinase. Cre recombinases can be used to control gene expression by cutting out LoxP sites and therefore excising the DNA sequence located between LoxP sites. To assess the efficiency of AAV9-Cre transduction as well as Cre functionality *in vitro*, we used MACS purified and cultured DRGs from GCaMP6s-floxed-STOP-cassette mice. Cells that were successfully transduced and expressing a functional Cre-recombinase will lose the STOP sequence and express GCaMP6s. 3 days after virus treatment we fixed the cells and stained for GFP, which is a part of GCaMP6s and can be used to detect it. Analysis of the staining revealed that there was a high proportion (67.45% ± 6.75%) of GCaMP6s-positive neurons 3 days transfection. There was a low percentage of GFP-positive neurons in the control coverslips (1.4% ± 1.4%, **Fig. 2.19 a-c**).

Lastly, we tested whether neuronal transduction was affected by the presence of non-neuronal cells in the culture. We transfected mixed DRG cultures with varying titres of AAV9-GCaMP6s and examined GCaMP6s expression 24 hours later. We found highest transduction at the highest titre we used (66.89% ± 4.3% at $1.54x10^{13}$ gc/ml), while transduction efficiency

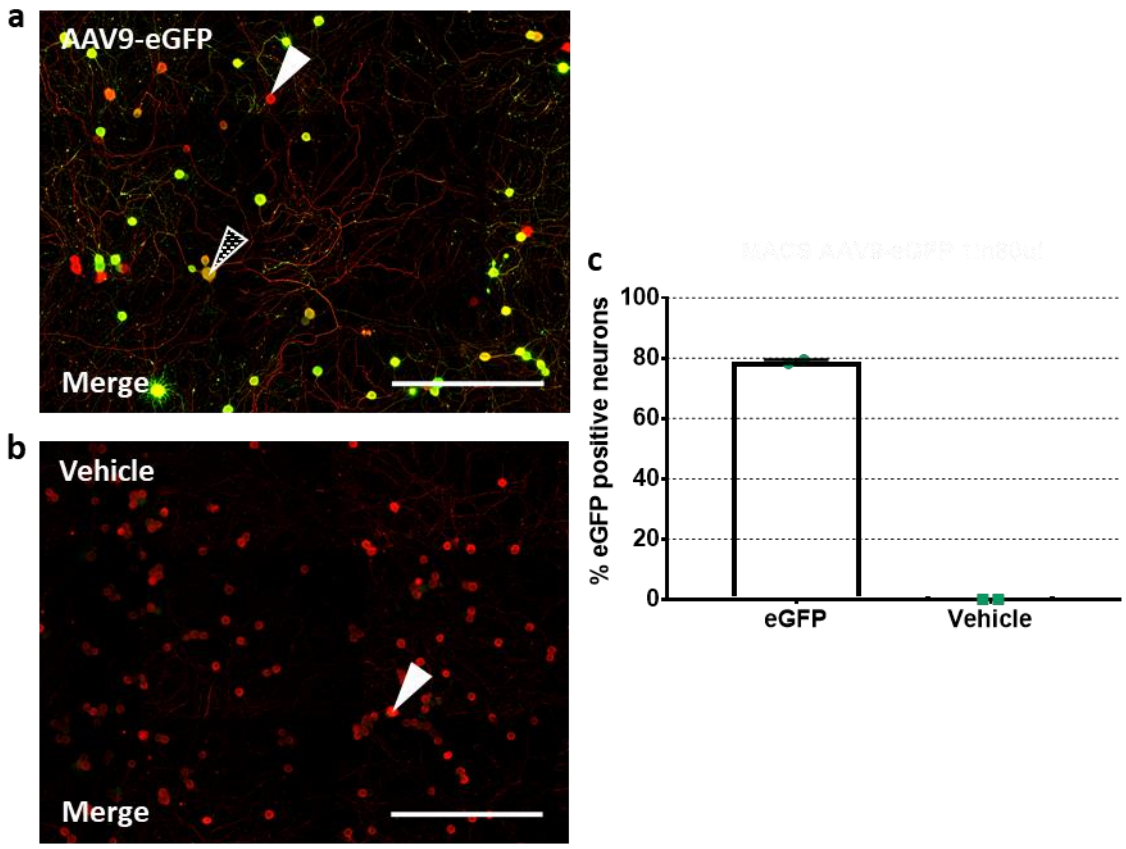

Figure 2.18 – AAV9-eGFP can transduce DRG neurons in vitro. *DRGs from all spinal levels were collected and MACS-purified before incubation with 6.39x10^9 gc of AAV9-eGFP or vehicle for 3 days. Total virus 6.39x10^9 gc per 100 µl. Representative ICC images of MACS DRG neurons in culture with **a**) AAV9-eGFP or **b**) vehicle after 3 days in vitro. Sections were stained for β-III-Tubulin (red) and GFP (green). Example of transduced and non-transduced neurons are marked with black and white arrows respectively. Scale bar = 100 µm. **c)** Quantification of transduction for cultures with eGFP (78.9% ± 0.6%) and vehicle (0.00%). There was a significant difference in transduction between vehicle and AAV9-eGFP cultures (Two-tailed t-test, p <0.0001, n = 3765 neurons, 2 coverslips each, 1 animal).*

decreased with lower viral titre (**Fig. 2.20 a-e**). Compared to a 3-day culture with AAV9-Cre, there was no significant difference in the percentage of transduced neurons (Two-tailed t-test, p = 0.95, n = 2 coverslips each), suggesting that 1 day incubation period is sufficient for transduction with AAV9 *in vitro.* It also suggests that the presence of non-neuronal cells does not reduce the percentage of transduced DRG neurons, which may be due to the neuronal tropism of AAV9.

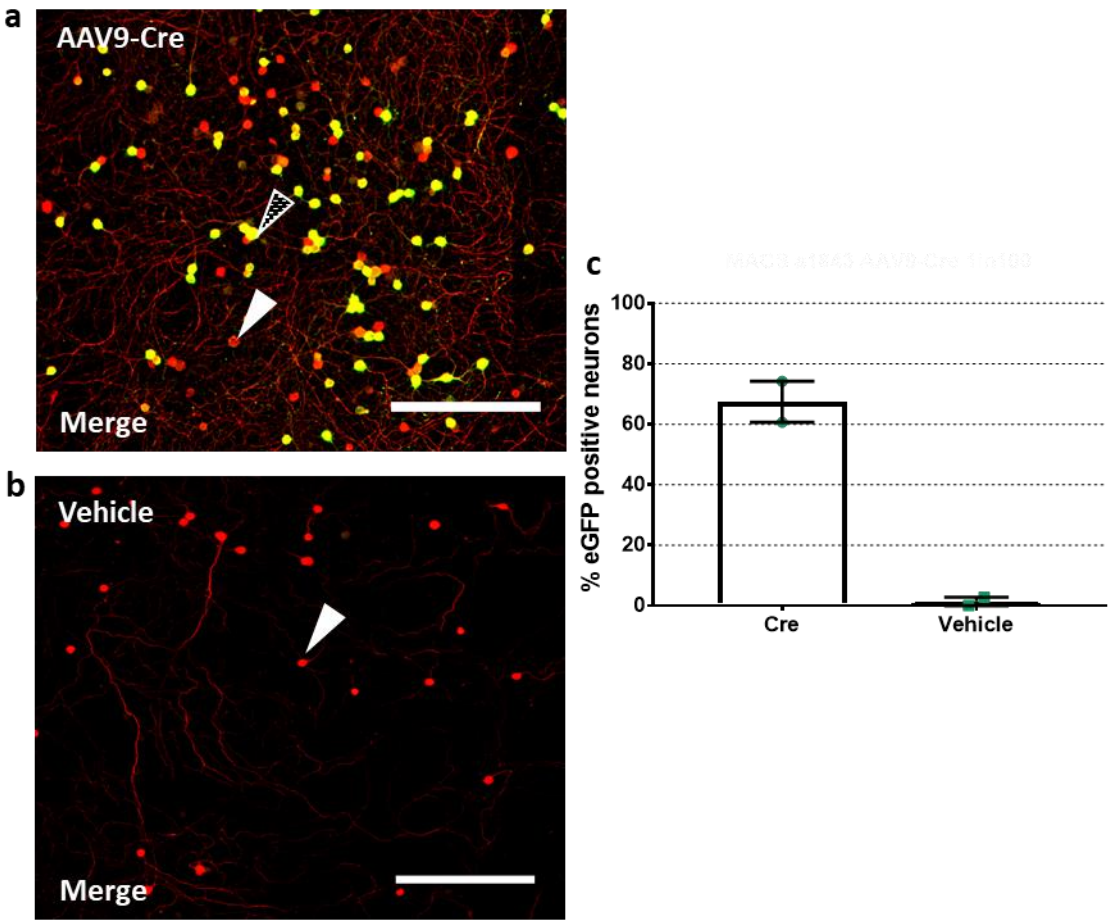

Figure 2.19 – Cre recombinase is functional in DRG neurons as early as 3 days after in vitro transduction with AAV9-Cre. *Transgenic mice where GCaMP6s expression is under control of a Cre recombinase were used to assess AAV9-Cre functionality in vitro. DRGs form all spinal levels were collected from GCaMP6s-floxed-STOP-cassette transgenic mice and MACS-purified before incubation with 3.29x10^{10} gc of AAV9-Cre. Total virus 3.29x10^{10} gc per 100 µl. Representative ICC images of MACS DRG neurons in culture with **a**) AAV9-Cre or **b**) vehicle after 3 days in vitro. Sections were stained for β-III-Tubulin (red) and GFP (green) (to enhance the green GCaMP6s signal). Example of transduced and non-transduced neurons are marked with black and white arrows respectively. Scale bar = 100 µm. **c)** Quantification of transduction efficiency for cultures treated with AAV9-Cre (67.45% ± 6.75%) and vehicle (1.4% ± 1.4%). There was a significant difference in transduction between vehicle and AAV9-eGFP cultures (Two-tailed t-test, p = 0.011, n =2414 neuron, 2 coverslips each, 1 animal).*

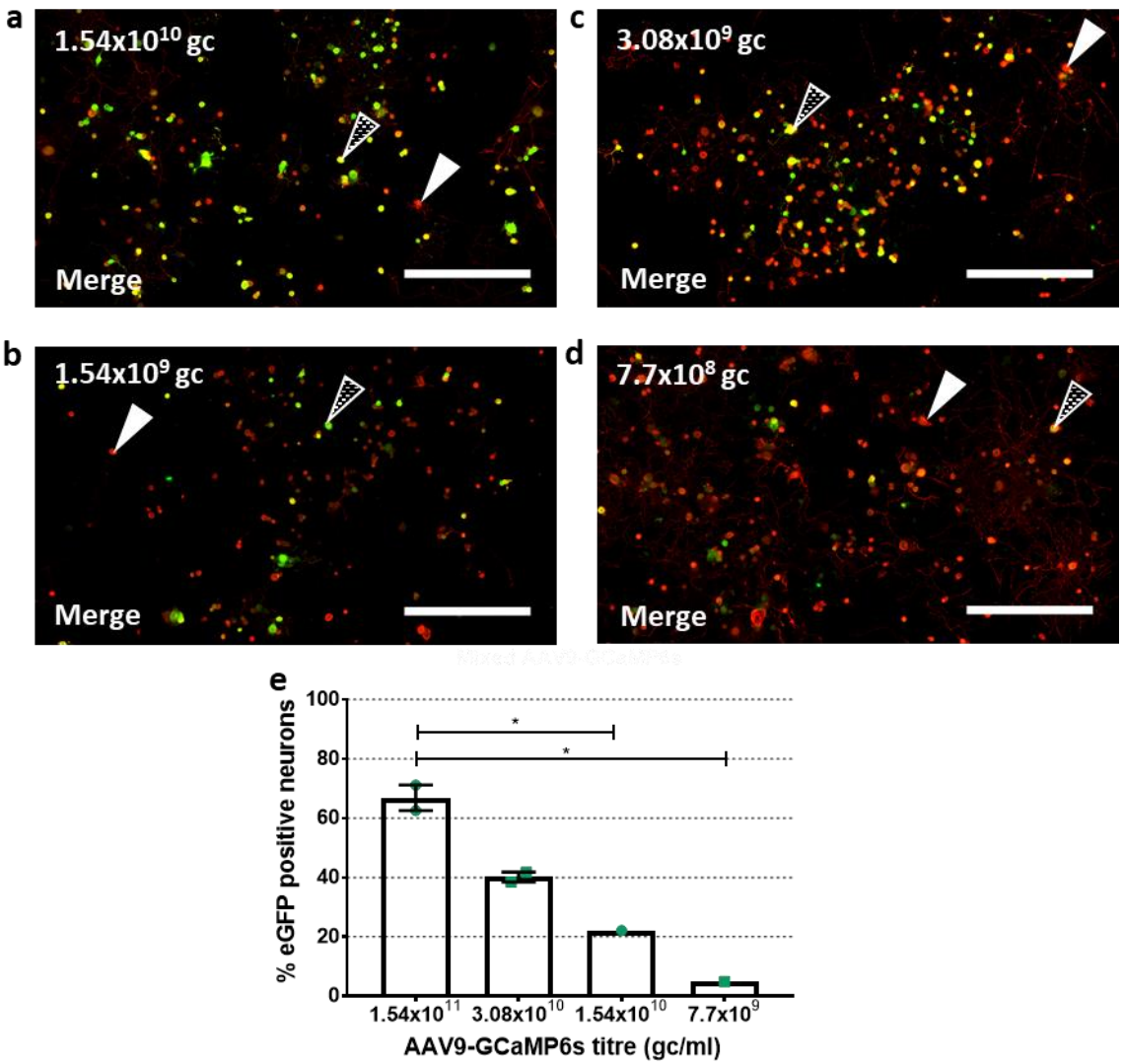

Figure 2.20 – Transgene expression in mixed DRG culture is present as early as 1 day in vitro following transduction with AAV9-GCaMP6s and is influenced by viral titre. *DRGs from all spinal levels were collected and cultured before addition of $1.54x10^{10}$, $3.08x10^{9}$, $1.54x10^{9}$ or $7.7x10^{8}$ gc of AAV9-GCaMP6s to 100 µl of cell suspension.* ***a-d)*** *Representative ICC images of mixed DRG neuronal culture with decreasing concentrations of AAV9-GCaMP6s after 1 day in vitro. Sections were stained for β-III-Tubulin (red) and GFP (green) (to enhance the GCaMP6s signal). Example of transduced and non-transduced neurons are marked with black and white arrows respectively. Scale bar = 100 µm.* ***e)*** *Quantification of neuronal transduction for cultures with decreasing AAV9-GCaMP6s titres. Transduction efficiency ranged from 66.89% ± 4.30% (n = 2971 neurons over 2 coverslips, 1 animal) for highest titre and 4.9% (n = 1007, 1 coverslip from 1 animal) for the lowest titre. There was a significant difference in transduction between highest and two lowest titres (One-way ANOVA, p = 0.04 and p = 0.02).*

2.4 Discussion

2.4.1 Methods of intrathecal delivery

The first intrathecal delivery method that we assessed in this study was LP. This is a well-established intrathecal delivery method that was applied in a large number of studies in several fields, including pain (Hayek and Hanes, 2014; Ver Donck *et al.*, 2014; Wang *et al.*, 2015).

It allows quick and relatively simple access to the intrathecal space and is applicable to a wide range of experimental species and humans. In mice, this method was first described by Hylden & Wilcox in 1980 (Hylden and Wilcox, 1980). The surgical procedure does not require extensive preparation or specialised equipment and only takes a couple of minutes, reducing the amount of stress the animal is subjected to. Furthermore, it is a relatively non-invasive procedure, compared to other methods of accessing CSF and CNS, e.g. ICV or CM. Lastly, with sufficient experience this technique can be used for repeated administration (Fairbanks, 2003). However, LP also has several disadvantages. For instance, it is not possible to confirm needle placement in the correct location. This increases the probability of positioning the needle outside of the intrathecal space, as well as possible spinal cord damage caused by inserting the needle too far into the intrathecal space. Finally, if the needle is withdrawn too fast the negative pressure will carry most of the injected substance back out of the intrathecal space.

In our hands, delivery of AAV9-eGFP via LP produced extensive transduction in the lumbar DRG, as well as cervical DRGs. However, the success rate for this technique was sub-optimal. We had to uncover the reason for the low success rate in order to try to improve the experimental technique. All injections were performed by Dr Clive Gentry, who is highly skilled in LPs. Therefore, we ruled out incorrect needle placement as the reason for low success rate. After consulting with Dr Gentry, we concluded that a probable cause was difficulty in accurate loading of the syringe and delivering such small volumes of virus.

To circumvent this problem, we then used an intrathecal catheter to deliver the AAV vector. Intrathecal catheter implantation is a technique that is often used to allow access to the intrathecal space for chronic treatments without the need for repeated surgery. We have adapted this technique to use a lumbar level catheter to deliver a single infusion of the virus into the intrathecal space, after which it is withdrawn. The strengths of this technique addresses some of the disadvantages listed above for LP. Firstly, by using methylene blue we could visualise the otherwise transparent dura, making it easier to manipulate. The coloured dura can be lifted, and the catheter inserted into the intrathecal space, allowing visual verification of placement. Secondly, by connecting the catheter to a syringe pump we could precisely control the injection speed, allowing us to infuse the virus at rates unachievable with hand-held syringes. This is important, since it has been shown that the virus infusion rate influences the transduction pattern (D. Li *et al.*, 2017). Furthermore, the syringe pump allowed us to keep the infusion rate consistent across all experiments. Thirdly, it is easier to ensure the correct volume of virus is delivered with this set up, as the catheter is transparent, and we can monitor the movement of the meniscus, stopping delivery as soon as it reaches the 5 µl mark. Finally, the speed at which the catheter is withdrawn can be controlled with more finesse, ensuring that little negative pressure is created and therefore minimising backflow.

However, this delivery method also has its disadvantages. The catheter insertion procedure is not as quick and simple as the LP delivery. It requires more equipment and a dedicated surgery set-up, which, combined with the time needed per injection, makes injecting many animals a considerable resource investment. Introduction of a catheter into the intrathecal space may exert pressure onto the spinal cord, or even damage it if the insertion was not done with the necessary care. Considering also the dura exposure and anaesthesia requirement, this procedure is quite invasive and stressful for the animal.

We addressed the mentioned shortcoming by: 1) choosing a catheter that was small enough to fit into the intrathecal space without causing damage, but with a large enough inner diameter

to avoid being clogged up, and thick walls to prevent excessive bending in the intrathecal space to avoid accidental spinal cord damage. 2) Securing the animal with a custom-made animal support device in a slightly elevated hunched position, which makes intrathecal space more accessible. In addition, it removes the need for the surgeon to support the animal, which allows more freedom of movement. This allowed the surgeon to more precisely manipulate the dura and place the catheter, further reducing the chance of the catheter damaging the spinal cord. 3) Performing the dura exposure in a way that avoids removing any bone, which is beneficial for animal recovery. 4) Monitoring all animals for behaviour indicating any spinal cord damage.

In general, the majority of the animals recovered well and showed no signs of spinal cord of dorsal root damage. However, spinal cord damage is known to affect mechanical sensitivity, so to further assess potential damage to the spinal cord we also tested for mechanical sensitivity changes after virus infusion using a Von Frey test (Hoschouer, Basso and Jakeman, 2010; Nees *et al.*, 2016). The analysis of our behavioural tests suggested that there is no spinal cord damage and that our surgical procedures are carried out with the necessary finesse. However, deficits in mechanical sensitivity is not the only sign of spinal cord damage, and further behavioural tests are needed to gain more insight into the impact of intrathecal cannulation on the animal. For instance, assessment of other sensory modalities, like Hargreaves test for heat sensitivity (Hargreaves *et al.*, 1988), as well as motor function tests, such as the beam walk test or rotarod (Brooks and Dunnett, 2009), may reveal effects that are not uncovered by the mechanical sensitivity Von Frey test.

Overall, we found that intrathecal delivery of AAV via a catheter produced more reliable and repeatable results than the LP delivery.

2.4.2 The transduction pattern in the DRGs and the spinal cord after intrathecal AAV delivery

The main aim of this part of my project was to characterise the transduction pattern of AAV9 in the DRGs and to identify the optimal parameters for variables such as titre or post injection time.

We found high transduction levels in L4 DRGs in almost all experimental conditions, which is in agreement with a number of studies (Towne *et al.*, 2009; VulchanovaDaniel, 2012; Xu *et al.*, 2012; Schuster *et al.*, 2014). When we tested if the viral titre affects the transduction efficiency we found evidence of a linear correlation between the viral titre and the transduction efficiency of L4 DRGs, with a trend for lower transduction with decreasing titre. However, the difference in the mean L4 transduction was not significant. Interestingly, there was almost no transduction the in the cervical region when the viral titre was decreased, suggesting that DRGs more distal from the injection epicentre are more sensitive to the viral titre. The limited transduction efficiency in the thoracic region might be explained by the fact the virus particles will be carried by the CSF and both lumbar and cervical levels, are surrounded by abundant CSF volumes, while the thoracic region is covered in relatively little CSF. This could result in thoracic DRGs being exposed to fewer AAV particles and therefore could explain the relatively low transduction efficiency in the thoracic DRGs observed across all our experiments.

Next, we explored the effect of the time after AAV9 delivery on transduction efficiency. Most studies using intrathecal AAV9 administration assessed transduction efficiency or its effect 3-5 weeks after injection (Snyder *et al.*, 2011; Hirai *et al.*, 2012; Schuster *et al.*, 2014; Bey *et al.*, 2017). Our first experiments showed high levels of transduction 30 days after injection (61%), so we wanted to explore the impact of shorter times post injection. Our results following LP delivery showed no transduction with AAV9-eGFP at 10 days and unreliable transduction at 20 days. In comparison, delivery of AAV9-eGFP via intrathecal cannula produced strong labelling in L4 DRG neurons as early as 7 days after injection (58%). This discrepancy may be explained

by the lower reliability of the LP method for delivery of small volumes of AAV9, as well as low number of animals tested at shorter post injection time periods. The fact that good transduction is achievable as soon as 7 days is a great asset, as this considerably speeds up experimental turnover, allowing quicker exploration of various experimental avenues, as well as reducing the cost of animal housing.

Most of the characterization in this chapter is performed with AAV9-eGFP. However, we also wanted to investigate if the transgene expressed by the AAV impacts the transduction efficiency. We assessed the efficiency of AAV9-mCherry at 30 days following intrathecal catheter delivery. mCherry is a modified red fluorescent protein (RFP), and, unlike eGFP, its signal is in a different spectral channel to neuronal autofluorescence. This makes its expression in neurons easier to detect. Our experiments showed that AAV9-mCherry has the same labelling efficiency as AAV9-eGFP in L4 DRGs. The red fluorophore is useful in settings where the green channel is already taken, such as transgenic lines expressing GFP in particular cell types. It's also possible to use it in combination with other AAVs, each of them delivering fluorophores of different colours, for instance for tracing experiments. However, it is important to keep in mind that mixing two AAVs for injection will lower each individual virus concentration. As the intrathecal injection has a limited volume, using an equal mix of two different viruses halves the amount of each individual virus. Our data supports this, as the percentage of DRG neurons transduced with either AAV9-eGFP or AAV9-mCherry alone is greater, compared to the mixed situation.

Next, we wanted to assess the effect of the viral serotype on transduction pattern and efficiency, since there is abundant evidence in the literature that the viral serotype plays a great role in determining these parameters (Mason *et al.*, 2010; Snyder *et al.*, 2011; VulchanovaDaniel, 2012). We compared transduction patterns of AAV8-eGFP and AAV9-eGFP and observed that AAV9 performed better in transducing sensory neurons. However, there is evidence in the literature of AAV8 having stronger tropism for large-diameter NF200 positive

DRG neurons (Jacques *et al.*, 2012), so for studies that focus on that DRG neuronal sub-population, AAV8 may be a more suitable serotype.

When we stained L4 DRG sections with markers for different neuronal DRG populations we discovered no preference of AAV9 for a specific neuronal subtype, implying that serotype 9 does not preferably transduce any DRG neuronal subtypes in the lumbar region and can therefore be used for studies including all neuronal subtypes. However, it has been reported that low AAV9 titre preferentially targets large DRG neurons (Schuster *et al.*, 2014), suggesting that transduction of DRGs at higher spinal levels may have a different transduction pattern since the virus concentration decreases with the distance from the infusion centre. Furthermore, other serotypes may have different transduction preferences that can be employed to study different neuronal sub-populations in the DRG. For example, AAV8, that has a preference for large-diameter DRG neurons (Jacques *et al.*, 2012), may be useful for studying proprioception.

Not only did we find eGFP signal in DRG neurons, but also in the lumbar spinal cord, in particular in the dorsal white and grey matter 30 days after AAV9-eGFP delivery. When sections were co-stained with NeuN to visualise the cell bodies of spinal neurons, we found little to no co-localisation of NeuN and eGFP in spinal neurons. This suggests that all the eGFP signal in the dorsal spinal cord came from afferents of transduced DRG neurons. This restriction of transduction to DRG neurons is significant, as it allows expression of functional transgenes in DRG neurons without impacting the physiology of cells harbouring their cell bodies in the spinal cord. However, this finding contradicts several other studies, where extensive spinal cord labelling was present after intrathecal delivery of AAV9 (Schuster *et al.*, 2014; Bey *et al.*, 2017; Hu *et al.*, 2018). There are several possible reasons for this discrepancy. Snyder et al investigated how the viral promoter of a transgene influenced the CNS transduction pattern after intrathecal delivery of AAV9-eGFP (Snyder *et al.*, 2011). They found that extensive labelling of primary afferent projections in the spinal cord can be achieved using

either a CBA or a CMV promoter, but labelling of CNS neurons, in particular motor neurons, was only observed with a CMV promoter. As the transgene promoter used in our study is CB7, a modified version of the CBA promoter, this may explain the absence of transduction of spinal cord neurons in our case. Another possible reason is the restrictive properties of the pia mater. Miyanohara et al have recently published a study comparing transgene expression after subpial or intrathecal delivery of AAV9-eGFP in rodents and pigs. They report extensive transduction of neurons and glia throughout the spinal cord segment after subpial delivery, while intrathecal delivery produced labelling restricted to the dorsal horn and white matter, with only few transduced CNS neurons (Miyanohara *et al.*, 2016). This suggests that the pia may form a protective barrier that prevents AAV9 particles from entering the deep spinal cord. Indeed, during the early stages of our study, when our technique was not yet refined and the risk of damaging the pia or spinal cord was higher, we did occasionally observe labelling of spinal cord neurons.

Interestingly, several studies have shown intrathecal delivery of AAV9 also results in transduction in the peripheral tissues, such as liver, heart and ileum (Haurigot *et al.*, 2013; Schuster *et al.*, 2014; Bailey *et al.*, 2018). This is likely to be a result of AAV9 leaking into the bloodstream and transducing these tissues, likely due to liver and heart having a high affinity for AAV9 particles (Sands, 2011; Haurigot *et al.*, 2013). Although we did not conduct a thorough experimental investigation of off-target transduction following intrathecal delivery of AAV9 using our delivery method, there is some anecdotal evidence encountered during mouse dissection that suggests that it results in some transduction in the liver. Further experiments looking at the transduction in the peripheral tissues are required to make any conclusions. Importantly, this off-target transduction may reduce the specificity of our approach, since cells other than primary afferent neurons are transduced. However, some studies would find this off-target transduction beneficial, for instance for correcting pathology such as both in the CNS and the periphery (Haurigot *et al.*, 2013).

One important aspect of the AAV9-eGFP transduction pattern characterization is the impact the eGFP transgene itself has on the transduced cells, and what effect that might have on the animal. While eGFP is a relatively simple protein that does not have any functions in the cell other than to fluoresce, the rapid increase in the number of foreign protein molecules, associated with AAV-driven expression of transgenes, may have a detrimental effect on the cell. There are a number of studies showing that overexpression of non-self-protein in both rodents and non-human primates with AAV9 can cause an immune response (Mays *et al.*, 2009; C. Yang *et al.*, 2013; Ciesielska *et al.*, 2013; Samaranch *et al.*, 2014; Hinderer *et al.*, 2018). Inflammation observed in these studies was centred around the brain region that was overexpressing the transgene. Importantly, the delivery methods utilised in these studies result in a very high concentration of viral particles immediately at the injection epicentre. In our model, this would cause inflammation and cell death in the DRGs and dorsal spinal cord, both targeted by the virus. If there was inflammation this should manifest in behavioural alterations, such as mechanical and thermal hyperalgesia. However, our Von Frey data show that there is no significant change in the mechanical threshold between AAV9-eGFP and vehicle infused groups, for up to 34 days post infusion. Additionally, an immune response would result in increased numbers of immune cells in the DRGs. However, when we assessed the numbers of several immune cell types in lumbar DRGs with flow cytometry, there was no significant difference in any major immune cell category, including lymphocytes and macrophages. These findings suggest that intrathecal delivery of AAV9-eGFP and transgene expression does not trigger an immune response. It is possible that this is the result of optimal transgene expression levels. They are high enough for the detection of a signal, but low enough to avoid triggering an immune response. Intrathecal injection of high titre AAV9, unlike direct CNS injections, does not restrict the viral particles to a small area, which would result in transduction with a higher number of viral particles per cell and stronger transgene overexpression. Instead, viral particles are diluted and spread out via the CSF, which helps to avoid excessive expression of the transgene. To further assess the immunogenicity of AAV9-

eGFP, longer-term exposures with regular assessments of mechanical and thermal sensitivity could be performed, as that would allow more time for an immune response to be triggered. In addition, it is possible that although there is no change in the immune cell composition of the DRG, the immune cells already present at the site are activated by the AAV transduction, for instance macrophages or microglia (Fischer *et al.*, 2011; Xu *et al.*, 2012). Therefore, future experiments must be conducted to assess whether immune cell activation profile in the DRG changes following AAV transduction after intrathecal delivery, for instance by assessing Iba1 immunoreactivity (Xu *et al.*, 2012).

2.4.3 Transgene expression in the DRG neurons after AAV delivery via different delivery routes

One of the ways that expression of a specific transgene using a viral vector differs from transgenic lines is that transduction patterns can be altered by using different delivery methods. Confining the virus spread to a specific anatomical structure results in transduction restricted to cells in that structure. Using viruses that are capable of retrograde transport, such as AAV9 or rAAV2-retro, allows transduction of sensory neurons via injection of the virus to the site where these neurons send their projections (Cearley and Wolfe, 2007; Castle, Perlson, *et al.*, 2014; Tervo *et al.*, 2016). This enables to study specific neuronal populations (e.g. knee-joint afferents) in more detail. For instance, expression of fluorescent proteins in specific anatomical subpopulations allows precise circuitry interrogation, while expression of functional transgenes such as ion channels or other genetically-encoded tools assists in studying their physiology.

We attempted to label specific anatomical subpopulations of sensory neurons by performing intraarticular and intraplantar AAV9 injections. Our results showed that a low level of transduction was present in both ipsilateral and contralateral DRGs. Expression in the contralateral side is likely the result of a virus leakage into the bloodstream, as in the literature there is evidence that intramuscular injection of AAV9 results in widespread transduction in

the CNS as well as in the contralateral muscle. In that case the cause was found in the virus leaking into the bloodstream (Benkhelifa-Ziyyat *et al.*, 2013). In the future, it may be possible to reduce off-target labelling by using smaller volumes of more concentrated virus, as well as by restricting animal movement right after the injection so that the virus suspension remains at the site of injection. Next, we performed intraneural injections of AAV9-eGFP into the sciatic nerve with AAV9-eGFP and observed moderate transduction in the ipsilateral L4 DRG with no labelling on the contralateral side. This is in line with the literature (Pleticha *et al.*, 2014). Similarly, high transduction in the DRG is found after intraganglionic injection of AAV (Fischer *et al.*, 2011). However, there is evidence that direct injection of AAV into the DRG causes neural damage resulting in behavioural alterations such as thermal hypersensitivity, mechanical allodynia and worse motor control (Fischer *et al.*, 2011).

Further to using different administration routes to target different subpopulations, it is also possible to change the transduction pattern of the same injection route by altering the parameters. For instance, when studying front limb function or migraine, it is beneficial to achieve high levels of transduction in the cervical and trigeminal ganglia. This should be possible to achieve by altering the intrathecal infusion route by infusing the virus through the atlanto-occipital membrane into the cisterna magna, as this moves the delivery epicentre closer to the target ganglia. This method has been used for AAV vector delivery in mice, with good transduction in the spinal cord and brain (Sinnett *et al.*, 2017). Unfortunately, the authors of this study did not investigate the transduction in the DRG.

The primary focus of this project was on the *in vivo* transduction of DRG neurons with AAV9. However, AAV9 is also capable of transducing adult neurons *in vitro.* We observed transgene expression after AAV9-GCaMP6s transduction after only 1 day in culture. Furthermore, we explored the specificity of transduction with AAV9 by incubating mixed DRG cultures with AAV9-GCaMP6s and observed no difference in the percentage of transduced neurons compared to neuronally-enriched cultures. We only observed a small percentage of GCaMP6s-

positive non-neuronal cells (data not shown), supporting the notion of neuronal tropism of AAV9. Transduction *in vitro* can be a valuable asset for a number of approaches, as it allows quick expression of a transgene in a system that can be precisely controlled. For instance, *in vitro* transduction with two fluorophores can be combined with a microfluidics system to study neuronal connectivity (Tsantoulas *et al.*, 2013). It can also be used to express proteins that may affect neuronal physiology, where a cellular response can be assessed later using readouts such as RNA analysis of gene expression and assess their responses with calcium imaging, or extract RNA and proteins for western blot/sequencing.

2.4.4 Methods of influencing transduction pattern

There are several variables not explored in this study that may influence AAV transduction in a way that is beneficial to studying DRG neurons and related neural circuits. Among them is the choice of transgene promoter.

By changing the promoter, it is possible to restrict expression to cells that express genes using that specific promoter. There are studies that use transgenes under a control of neuronal-specific promoter. This can eliminate the chance of off-target expression associated with some methods of AAV delivery, such as intravenous injection (Jackson *et al.*, 2016). Others tailored the promoter so that the transgene is only expressed in a subset of neurons, such as in the tyrosine hydroxylase (TH) positive neurons (Oh *et al.*, 2009; Gompf *et al.*, 2015). The TH positive neuron subpopulation in the DRG are small to medium sized neurons that have low CGRP and IB4 expression, and are known to play an important part in nociception, so targeting this subpopulation may be beneficial to pain research (Brumovsky, Villar and Hökfelt, 2006; Brumovsky, 2016). There are also promoters available that can restrict expression to non-neuronal cells such as glia, *e.g.* the glial fibrillary acidic protein (GFAP) promoter can be used to restrict expression to astrocytes (Dashkoff *et al.*, 2016), or the myelin associated glycoprotein (MAG) promoter restricts expression to oligodendrocytes (von Jonquieres *et al.*, 2016).

Moreover, even the use ubiquitously-expressed promoters, such as the CMV or CBA promoters, can produce different transduction pattern. One study reported that expression of transgenes under the CMV promoter diminishes overtime in the CNS and DRGs. In addition, this study reported that the CBA promoter achieved higher transduction in the CNS compared to the CMV promoter (Gray, Foti, *et al.*, 2011).

2.4.5 Conclusion

In this chapter we have shown that extensive labelling of DRG neurons in mice can be achieved by a single intrathecal injection of 5 µl of AAV9-eGFP. Transduction was more reliable and consistent when the virus was delivered via an intrathecal catheter compared to by lumbar puncture. We found that 60-70 % of L4 DRG neurons were transduced after intrathecal injection of AAV9-eGFP ($6.39x10^{12}$ gc/ml), while cervical DRGs required a higher titre of AAV9 for efficient transduction. AAV9 also showed no preference for any neuronal DRG sub-population. We further demonstrated that the transduction profile can be influenced by several factors, including titre, post injection time and AAV serotype. Finally, we confirmed that intrathecal delivery of AAV9-eGFP via a cannula did not result in adverse side-effects, as it did not elicit mechanical hypersensitivity or trigger an immune response in transduced DRGs. Overall, this technique is applicable to a wide variety of studies investigating the function and pathology of DRG neurons, as it can be used to deliver a wide variety of transgenic tools to expand our understanding of pain circuitry. Furthermore, intrathecal infusion can be used to deliver functional transgenes, such as a Cre recombinase, that can be used to study various aspects of cell physiology, such as gene expression and activity.

Chapter 3: Assessing acute neuronal sensitisation *in vitro* using electrical stimuli

3.1 Introduction

In the previous chapter we explored AAV9 transduction capabilities in DRG neurons with relatively simple transgenes encoding fluorophores like eGFP or mCherry. We found that both *in vivo* and *in vitro* application of AAV9 to DRG results in a high proportion of transduced neurons. AAV vectors that encode fluorophores are useful for the initial characterisation of the AAV transduction, as the use of these transgenes produces an unambiguous and easy-to-detect indication of successful transduction. In addition, the transgene fills the whole cell, making it useful in anatomical interrogations of the nervous system, for instance by transducing select neuronal sub-populations via targeted peripheral injections and then assessing their central projections in the spinal cord. However, this experimental approach does not use one of the core strengths of viral vectors – the ability to deliver a wide variety of functional transgenes. AAV vectors are capable of delivering complex transgenic tools that can be used in a wide variety of experiments, from those that report neuronal activity (like genetically encoded calcium indicators (GECIs)) to those that can influence gene expression (like Cre recombinase). To assess how suitable the AAV9 vector is for delivery of these "functional" transgenic tools into the DRG neurons, we decided to use AAV9 to deliver a GECI GCaMP6s to primary afferent neurons and to explore its use for *in vitro* calcium imaging.

3.1.1 The Importance of calcium ions in neurons

Calcium ions play a crucial role in regulating a vast number of cellular processes, from exocytosis to gene transcription (Berridge, Lipp and Bootman, 2000). In neurons, a sharp increase in calcium levels is associated with membrane depolarisation (Clapham, 2007; Simms and Zamponi, 2014). For instance, as seen in dendritic spines after neurotransmitter binding (Malinow *et al.*, 1994; Yuste and Denk, 1995), or in the cell body after the initiation of an

action potential (Bolsover and Spector, 1986; Simons, 1988; Smetters, Majewska and Yuste, 1999). These rapid changes in intracellular calcium levels are crucial for neuronal physiology. Calcium signalling is of great importance for the generation of post-synaptic potentials in dendritic spines after detection of neurotransmitter (Kovalchuk *et al.*, 2000; Bloodgood and Sabatini, 2007). Calcium signalling in cell soma is important for modulating neuronal activity (Sterratt *et al.*, 2012; Tonini *et al.*, 2013). Moreover, the ability of neurons to communicate to each other through the release of neurotransmitters is dependent on local, transient changes in presynaptic terminal calcium ion concentration (Adler *et al.*, 1991; Stanley, 1993; Bucurenciu *et al.*, 2008; Neher and Sakaba, 2008). It is also crucial for activity-dependent regulation of gene transcription that is vital for controlling synaptic strength and long-term plasticity (Lyons and West, 2011; Brini *et al.*, 2014). These and many other functions make calcium ions one of the most important signalling molecules in neurons (Berridge, Bootman and Roderick, 2003; Clapham, 2007).

There are several sources of calcium in neurons that can contribute to calcium signalling. These include both the entry of extracellular calcium ions via ion channels and the release of calcium ions from intracellular stores such as endoplasmic reticulum (ER) and mitochondria (Verkhratsky and Petersen, 1998; Brini *et al.*, 2014). One of the major contributors to neuronal activity-associated rise in intracellular calcium are Voltage-Gated Calcium Channels (VGCC). These ion channels are located on the extracellular membrane and are activated by membrane depolarization, which allows extracellular calcium ions to enter the cytoplasm (Simms and Zamponi, 2014). VGCCs can be divided into high and low voltage-activated channels (HVA and LVA, respectively) (Catterall, 2000). Both types have several functions in the neuron. For instance, LVA channels can create a positive-feedback loop of small membrane depolarisations causing more LVA calcium channels to open and increase the influx of calcium ions, depolarising the membrane further until voltage-gated sodium channels are activated and an action potential is triggered (Molineux *et al.*, 2006; Alviña, Ellis-Davies and Khodakhah, 2009). HVA channels facilitate calcium ion entry into the presynaptic terminal, where it interacts with

the SNARE complex and facilitates exocytosis of neurotransmitter vesicles (Südhof, 2004; Catterall, 2011). Calcium ions may also enter a neuron as a direct consequence of a neurotransmitter binding to its receptors, for example through N-Methyl-D-Aspartate (NMDA) or α-Amino-3-Hydroxy-5-Methyl-4-Isoxazolepropionic Acid (AMPA) receptors that respond to glutamate (Kyrozis *et al.*, 1995; Reichling and MacDermott, 1996; Bloodgood and Sabatini, 2009). These channels are typically found on postsynaptic dendritic spines, and calcium entry through these channels is important for long-term regulation of synaptic strength, often in the form of long-term potentiation (LTP) (Man, 2011; Wang and Peng, 2016).

Neurons also possess intracellular calcium stores, mostly in the endoplasmic reticulum (ER) and mitochondria, that retain calcium ions within the cell but are isolated from the cytosol, preventing them from participating in calcium signalling (Verkhratsky and Petersen, 1998; Brini *et al.*, 2014). Release of calcium from these stores can be triggered by neurotransmitters, such as glutamate, binding to receptors that can trigger production of a secondary messenger molecule, such as inositol-triphosphate production after metabotropic glutamate receptor (mGluR) activation (Zirpel, Lachica and Rubel, 1995; Rose and Konnerth, 2001). This secondary messenger cascade results in release of calcium ions from the ER, which makes these ions available for various signalling pathways in the cell (Coutinho and Knöpfel, 2002; Valenti, Jeffrey Conn and Marino, 2002; Niswender and Conn, 2010).

As calcium signalling is involved in many cellular processes, the calcium ion levels in the cell must be tightly regulated. In neurons, the calcium ion concentration is maintained around 100 nM, but it can increase up to 100-fold during electrical activity associated with neuronal firing (Berridge, Lipp and Bootman, 2000). Therefore, the excess calcium ions following neuronal firing should be cleared from the cytosol as quickly as possible. The main methods to clear cytosolic calcium is to transport it outside of the cell or into cellular compartments that restrict its participation in signalling, such as the ER and mitochondria (Brini *et al.*, 2014). The two main transmembrane proteins responsible for transporting calcium ions out of the cells are Plasma

Membrane Ca^{2+} ATPase (PMCA) and the Na^{+}/Ca^{2+} exchanger (NCX). PMCA has high affinity for calcium ions but low capacity, therefore its function is mostly to maintain a low concentration of intracellular calcium ions at rest. On the other hand, NCX is a low affinity, high capacity exchanger that is mostly responsible for quickly reducing high intracellular calcium concentration back to resting levels following calcium entry into the cell, e.g. following an action potential (Roome, Knöpfel and Empson, 2013; Brini *et al.*, 2014). These two proteins are crucial for normal neuronal functioning, and their malfunction is associated with several diseases, including Parkinson's (Kip and Strehler, 2007; Kurnellas, Donahue and Elkabes, 2007; Brendel *et al.*, 2014). Another way for the excess calcium ions to be cleared is by uptake into endoplasmic reticulum and mitochondria. The main proteins that mediate this are sarco/endoplasmic reticulum calcium ATPase (SERCA) for the ER and the mitochondrial calcium uniporter (MCU) for the mitochondria (Verkhratsky, 2004; Mammucari *et al.*, 2018). These proteins make it possible for ER and mitochondria to act as readily-available calcium ion pools that can help fine-tune the calcium signalling pathways in the cell (Gunter and Pfeiffer, 1990; Dupont and Combettes, 2016).

The cellular machinery described above ensures that the concentration of calcium ions in a neuron is tightly regulated. In neurons, the quick rise and fall of calcium that correlates with action potential firing makes cytosolic calcium concentration a good proxy for measuring neuronal activity.

3.1.2 Imaging calcium dynamics in neurons

In the nervous system, neurons communicate with each other via action potentials. This communication lies at the core of virtually every aspect of the nervous system and is the cornerstone of correct functioning of the whole organism. Recording and studying neuronal activity is one of the most widely used methods to interrogate nervous system physiology and pathology. Electrophysiological recordings have given us insight into neuronal activity patterns in health and disease (Kucyi and Davis, 2017), however they are limited by the low number of

neurons that can be recorded simultaneously. To record activity of a large number of neurons or neuronal networks, a different approach has to be taken.

As discussed above, a rise in calcium ion levels in the neuronal cytosol can serve as a proxy for action potential and, therefore, neuronal activity. Tools known as calcium indicators provide a visual readout of the levels of calcium ions within the cell, and therefore have been widely used to study neuronal activity (Grienberger and Konnerth, 2012). When calcium binds to a calcium indicator molecule, it causes a conformational change in the indicator molecule that results in either emission of light or a change in its fluorescence properties (Grienberger and Konnerth, 2012). Optical imaging of neuronal activity holds several advantages over electrophysiological techniques. Firstly, it enables simultaneous imaging of many neurons (Ahrens *et al.*, 2013; Ziv *et al.*, 2013; Lecoq *et al.*, 2014). Secondly, it is possible to study a specific cell compartment, such as dendritic spines (Korkotian and Segal, 1998; Chiu *et al.*, 2013; Siegel and Lohmann, 2013). Lastly, electrophysiological techniques often require electrode placement close to, or onto the cells of interest, which inevitably damages the tissue. Optical recordings using calcium indicators do not require tissue damage past initial exposure *in vivo*, or tissue processing *in vitro*. There are two types of calcium indicators: calcium dyes and genetically encoded calcium indicators (GECI). They are different in the way that they are introduced into the cells. Calcium dyes can either be directly loaded into the cell via micropipettes, or can be taken up into the cell from the extracellular space (Paredes *et al.*, 2008; Grienberger and Konnerth, 2012). On the other hand, GECI are transgenic tools that are produced by the cell itself, however the sequence encoding them has to be first introduced into the cell, either by inserting the sequence directly into the DNA or by using viral vectors for its delivery into the cell (Broussard, Liang and Tian, 2014).

One of the first calcium indicators developed was aequorin, a bioluminescent protein that emits a photon of around 470 nm wavelength upon the binding of calcium ions (Shinomura, Johnson and Saiga, 1962; Ohmiya and Hirano, 1996). In comparison to fluorescent dyes,

aequorin is bioluminescent. This means that the cells are not required to be exposed to light at an excitation wavelength in order for the signal to be detected. In turn, this helps to avoid phototoxicity and noise due to autofluorescence. In addition, it can be modified to have different affinities for calcium ions or to target different subcellular compartments (Montero *et al.*, 1995; Alonso, Manjarrés and García-Sancho, 2009). However, only one photon of light is produced per aequorin molecule, and the regeneration time of aequorin is relatively long, meaning that the emitted light is very dim (Shimomura, Kishi and Inouye, 1993; Baubet *et al.*, 2000). In addition, aequorin does not readily cross the cell membrane, making its delivery into cells problematic. Initially, it had to be loaded into cells through micropipettes or by permeabilization procedures, restricting its use to large cells such as muscle fibres (Ridgway and Ashley, 1967; Brini, 2008). Since then, the aequorin cDNA has been cloned, making it possible to direct its expression to the cells of interest. Many variations of aequorin exist, each having different properties and mostly being administered into cells via genetic methods, essentially making them a part of the GECI family (Chiesa *et al.*, 2001; Brini, 2008; Bakayan *et al.*, 2011).

Another type of calcium indicators that has been broadly used to study *in vitro* and *in vivo* neuronal activity are chemical calcium indicators. These are chemically engineered molecules that change their fluorescent properties when bound to calcium (Paredes *et al.*, 2008). There are many different chemical calcium indicators, each having their own affinity for calcium ions and fluorescent properties. Perhaps the most widely used one is Fura-2, a chemical calcium dye that can be taken up by the cells from the extracellular environment (Grynkiewicz, Poenie and Tsien, 1985). Fura-2 is a ratiometric dye, meaning that it changes the peak excitation or emission wavelengths upon calcium binding. Fura-2 that is not bound to calcium is excited by light at 340 and 380 nm wavelengths, and emission is between 505 and 520 nm, respectively (Tsien, Rink and Poenie, 1985). However, upon calcium binding, excitation shifts towards 340 nm wavelength, emitting less light at 380 nm excitation wavelength. The change in the ratio of emission at 340 and 380 nm is used to quantify the changes in the levels of intracellular

calcium ions (Tsien, Rink and Poenie, 1985). The ratiometric nature of Fura-2 means that its signal is unaffected by uneven dye distribution between cells, dye leakage and photobleaching, as the ratio will stay the same independent of the number of Fura-2 molecules (Paredes *et al.*, 2008). Furthermore, Fura-2 has been modified to create Fura-2-acetoxymethyl ester (Fura-2 AM), a dye that can readily cross the cell membrane, significantly increasing the efficiency of the dye uptake into the cells (Tsien, 1981; Grynkiewicz, Poenie and Tsien, 1985). This cell membrane permeability, coupled with a high signal to noise ratio and ratiometric properties has made Fura-2 AM one of the widely used calcium dyes both for *in vitro* and *in vivo* calcium imaging (Paredes *et al.*, 2008). It has been used to image cortical neurons *in vitro* (Barreto-Chang and Dolmetsch, 2009; Mauleon *et al.*, 2013; Calvo-Rodríguez, Villalobos and Nuñez, 2015; Cameron *et al.*, 2016; Chen *et al.*, 2017), as well as *in vivo* (Stosiek *et al.*, 2003; Sohya *et al.*, 2007). It has also been used to image neuronal activity in DRG neurons *in vitro*, especially in response to addition of various molecules and compounds used in pain research, including capsaicin and PGE2 (Thayer, Perney and Miller, 1988; Walker *et al.*, 1988; Eun *et al.*, 2001; Ma *et al.*, 2005; Lu and Gold, 2008; Barabas, Kossyreva and Stucky, 2012).

3.1.3 The use of Genetically Encoded Calcium Indicators (GECI) to image neuronal activity

Despite being popular, chemical calcium dyes have several disadvantages that impede their usefulness. For instance, their expression cannot be targeted to a specific sub-population of cells, and the sole determinant of the cells labelled is the delivery of the dye (Paredes *et al.*, 2008; Grienberger and Konnerth, 2012). Furthermore, long-term or chronic imaging of neuronal activity *in situ* or *in vivo* requires repeated injections of the dye that are damaging to the tissue and may reduce the quality of data (Tian *et al.*, 2012; Tian, Hires and Looger, 2012; Broussard, Liang and Tian, 2014). However, it is possible to overcome these drawbacks with the use of genetically encoded calcium indicators (GECI).

GECI are a group of calcium indicators that instead of having to be delivered into the cell can be expressed by the cell itself. Therefore, repeated imaging of GECI does not require repeated dye application that would be damaging to the tissue, and enables chronic imaging of neuronal activity (Mank *et al.*, 2008; Sadakane *et al.*, 2015; Silasi *et al.*, 2016). GECI expression is achieved either by inserting the GECI DNA sequence through genetic manipulation into the host DNA, e.g. transgenic mouse line generation, or by viral vector-mediated delivery of a plasmid carrying the GECI sequence (Grienberger and Konnerth, 2012; Brini *et al.*, 2014). This makes it possible to target the GECI expression to a specific cell type or anatomical subset of cells. For instance, crossing mice that express GECI under the control of Cre with transgenic lines that express Cre in parvalbumin-positive interneurons or retinal neurons will result in GECI expression only in those cells (Ivanova, Hwang and Pan, 2010; Madisen *et al.*, 2010; Zariwala *et al.*, 2012). In addition, it is possible to use viral vectors such as AAVs to deliver GECI sequence to specific cells. In this case the AAV delivery method and serotype will determine the transduction pattern (Komiyama *et al.*, 2010; Harvey, Coen and Tank, 2012; Sekiguchi *et al.*, 2016). Furthermore, the expression of the GECI protein can be put under the control of a cell-specific promoter to ensure targeted transgene expression. For example, it is possible to restrict expression of the GECI to pyramidal neurons in the hippocampus through the use of AAV-delivered GECI that is under the control of the *CaMKIIα* promoter (Ziv *et al.*, 2013).

All GECI can be split into two groups according to their mode of action: those that use Förster resonance energy transfer (FRET) and those that rely on a single fluorescent protein to produce signal. FRET-based GECI use two fluorophores that are tethered to each other, with the donor fluorophore emitting light of a particular wavelength upon excitation with a laser. When calcium binds to a FRET GECI molecule, the conformational change brings the fluorophores close together. The close proximity allows the donor to transfer the energy to the acceptor fluorophore, making it emit light at a different wavelength from the one emitted by the donor. Therefore, upon calcium detection donor fluorescence diminishes while acceptor fluorescence increases. The change in the ratio of emissions before and after calcium binding is

used to quantify the changes in the intracellular calcium (Jares-Erijman and Jovin, 2003). The ratio-based signal means that FRET GECI are ratiometric indicators, which makes them more resistant to motion- and uneven loading-related artefacts, which is especially important in live animal imaging (Lütcke *et al.*, 2010; Thestrup *et al.*, 2014). The most popular FRET-based GECI belong to the Cameleon family, members of which are mostly made up of two fluorescent proteins linked together by calmodulin and calmodulin-binding peptide M13, which facilitates a conformational change upon calcium binding (Miyawaki *et al.*, 1997). Since its initial development in 1997, many different variants of the original Yellow Cameleon (YC) with better stability and stronger signal have been designed (Palmer *et al.*, 2011). In addition, new variants of Cameleon family GECI have been developed that use Troponin C instead of calmodulin as a calcium binding site, reducing the probability of unwanted interactions with endogenous proteins (Mank *et al.*, 2006, 2008; Thestrup *et al.*, 2014). However, they have several drawbacks. FRET-based GECI suffer from low signal-to-noise ratio and often use blue-yellow light that has poor tissue penetrance and is prone to scatter (Miyawaki, 2011; Tian, Hires and Looger, 2012; Lin and Schnitzer, 2016). In addition, the use of two fluorescent proteins each with a separate set of excitation-emission wavelengths makes FRET-based GECI difficult to use in conjunction with any other fluorophores due to signal interference (Miyawaki, 2011).

In comparison to FRET-based GECI, single fluorescent protein indicators are not ratiometric. This class of GECI have only one fluorescent protein in their structure, whose fluorescence changes upon calcium binding (Brini, 2008; Grienberger and Konnerth, 2012). Single-fluorophore GECIs typically show greater signal-to-noise ratio, as well as larger responses than FRET-based GECIs. (Lin and Schnitzer, 2016). However, since single-fluorophore GECI are not ratiometric, they are more prone to movement artefacts as well as signal variation due to differential expression of the GECI (Anderson, Zheng and Dong, 2018).

The most popular class of single fluorophore GECI is the GCaMP family. The basic structure of GCaMP is made up of a circular permutated enhanced green fluorescent protein (cpEGFP),

with its N-terminus connected to the M13 fragment of the myosin light chain kinase and the C-terminus of calmodulin (Nakai, Ohkura and Imoto, 2001). Binding of calcium to calmodulin allows it to interact with the M13 fragment, inducing a conformational change in the cpEGFP that greatly increases its fluorescence (Baird, Zacharias and Tsien, 1999; Nakai, Ohkura and Imoto, 2001). GCaMP has gone through several iterations, each improving its fluorescence properties such as basal fluorescence and dynamic range, as well as increasing sensitivity, calcium affinity and pH stability (Ohkura *et al.*, 2005; Tallini *et al.*, 2006; Tian *et al.*, 2009; Akerboom *et al.*, 2012). Currently, the most widely used iteration of GCaMP is the GCaMP6 series (T. W. Chen *et al.*, 2013). The GCaMP6 members show fluorescence increases that are an order of magnitude greater than those of FRET-based GECI, and 5 to 10-fold greater than previous GCaMP iterations (T. W. Chen *et al.*, 2013; Lin and Schnitzer, 2016). There are three types of GCaMP6, distinguished based on their kinetics: slow (GCaMP6s), medium (GCaMP6m) and fast (GCaMP6f) (T. W. Chen *et al.*, 2013). GCaMP6s has the highest dynamic range and saturated fluorescence out of all GCaMP6 family members (T. W. Chen *et al.*, 2013). GCaMP6f and its variant GCaMP6fRS09 are one of the fastest GECI available, with half-decay times *in vitro* of 71 s and 20 ms, respectively (Badura *et al.*, 2014). These are comparable to the half-decay times of calcium ion transients after a single action potential, which are 50-60 ms (Helmchen, Borst and Sakmann, 1997). These properties of GCaMP GECI have made them one of the most popular GECI, with hundreds of studies using them. In the neuroscience field, GCaMP indicators have been used to study neuronal activity associated with multiple physiological and pathological processes in various organisms. For instance, GCaMP1 was used to study activity patterns in the fly brain in response to different odours (Wang *et al.*, 2003). In *C. elegans* GCaMP6s has been used to visualise neuronal activity associated with locomotion (Venkatachalam *et al.*, 2016). In mice, GCaMP has been used in studies of many processes, including olfaction, memory, navigation and sensation (Fletcher *et al.*, 2009; Dombeck *et al.*, 2010; O'Connor *et al.*, 2010; Mittmann *et al.*, 2011; Harvey, Coen and Tank, 2012; Huber *et al.*, 2012). Furthermore, GCaMP has been used to monitor the activity of DRG and TG neurons in

the context of chronic pain in rodents, and uncovered strong neuronal coupling between neuronal cell bodies after tissue injury (Y. S. Kim *et al.*, 2014; Kim *et al.*, 2016; Anderson, Zheng and Dong, 2018).

In this study, we wanted to use intrathecal delivery of AAV9 to express GCaMP in DRG neurons. This will allow us to study their activity *in vivo* in healthy animals and in pain pathologies such as neuropathic pain. Since GCaMP6s showed the greatest dynamic range and fluorescence, we decided to use it for our experiments. However, before transitioning into an *in vivo* setting, we first wanted to explore GCaMP6s properties *in vitro*. When cultured, neurons change their properties, and the longer they spend in culture the more their phenotype differs from that *in vivo*. Typically, cultured DRG neurons for calcium imaging experiments with chemical dyes are used after a day in culture. This allows them to attach to the coverslip but does not give them enough time to significantly change their phenotype. In the previous chapter we have shown that cultured DRG neurons incubated with AAV9-GCaMP6s express the GCaMP6s transgene in less than 24 hours (see 2.3.8). This short incubation time means that these neurons can express the transgene before their phenotype significantly changes in culture, making *in vitro* transduction with AAV9 compatible with calcium imaging.

3.1.4 Aim

In this chapter, we wanted to explore the use of virally-delivered GCaMP6s for calcium imaging of adult DRG neurons. We used *in vitro* delivery of AAV9-GCaMP6s to ensure high levels of transduction and quick turnover of experiments. We aimed to investigate whether virally-delivered GCaMP6s can be used to visualise the responses of adult DRG neurons to electrical field stimulation, and whether this can be enhanced by acute application of sensitising agents, such as Prostaglandin E2.

3.2 Methods

3.2.1 DRG Culture for calcium imaging

Cell culture dishes with glass coverslips attached to the bottom of the dish (MatTek, P35G-0-14-C) were used for calcium imaging. Their treatment and the rest of the cell culture protocol were identical to that of a standard mixed DRG culture protocol outlined in chapter 2 (**2.2.9**). Cells were imaged the day after they were cultured.

3.2.2 Calcium imaging

For imaging with Fura-2, cells were loaded with a mix of 2 µM Fura-2 AM (Invitrogen, F1201) and 1mM probenecid, each dish being treated with 400 µl and incubated for 1 hour, then the cells were immediately imaged. For GCaMP6s imaging, cells were transfected with AAV9-GcaMP6s on the day of the culture, as described in chapter 2 (**2.2.11**).

Immediately prior to imaging, media was replaced with 200 µl of Calcium Imaging Buffer (1X HBSS with $MgCl_2$ and Ca^{2+} (Thermo Fisher, 14065072) + 10 mM Hepes, (pH 7.4)). The cell culture dish was placed onto the imaging stage and secured. A custom-made electrode holder was placed on top, ensuring the electrodes were on the same level as the cells and in parallel. Electrical stimuli were created with a Neurolog Digitimer unit connected to a biphasic stimulus isolator (Warner Instruments, SIU-102B). Calcium imaging was performed on a PTI EasyRatioPro Fluorescence Calcium Imaging (Horiba Scientific), Fura-2 dye fluorescence was measured at 340 and 380 nm excitation wavelengths.

3.2.3 Imaging protocol

The protocol is illustrated in **Fig. 3.1**. After the desired field of view was found, the baseline was recorded for 75 seconds. Next, the threshold was determined. This was done by keeping the stimulation frequency at 5 Hz and increasing the current slowly from 0 up to the point when at least one neuron starts responding. This current was then taken as the threshold for that coverslip. Cells are then stimulated at 1.5, 2, 2.5 and 3 times the threshold. Each train of stimuli was at 5 Hz and contained 10 stimuli. Cells were allowed to recover for 1 minute

between trains of stimuli. After 4 trains of stumuli, 20 µl of buffer was removed and 20 µl of vehicle or sensitizer was added to the coverslip.

Cells were incubated with the sensitizer for 5 minutes, and then the trains of stimuli were repeated. Sensitizers used were: Prostaglandin E2 (PGE2) 5 or 10 µM (Sigma, P5640), Bradykinin (BK) 5 µM (Sigma, B3259), Inflammatory soup (PGE2, BK, serotonin (Sigma, H9523) 2.5 or 5 µM each), Nerve Growth Factor (NGF) 50 ng/ml (Cambridge Bioscience, GFM11-1000) and Forskolin (Fsk) 10 µM (Sigma, 93049). Finally, 20 µl of 50 mM KCl was added to the coverslip to stimulate all neurons to serve as positive control.

3.2.4 Quantification

Images were processed using Fiji distribution of ImageJ. The background was subtracted, and the 340 nm fluorescence channel signal was divided by the 380 nm fluorescence channel to obtain the Fura-2 ratio signal. Neurons that responded to KCl were circled and the intensity measured for each frame. All values for an individual neuron were divided by the mean of that neuron's baseline intensity as a way of normalising the data. Data for each neuron were then individually plotted and screened for any abnormalities. Abnormal neurons were excluded from analysis. The remaining data were then used to analyse neuronal responses to stimuli and the impact of the sensitizers on their responses. Analysis parameters and rationale are elaborated on in the results section (**3.3.1**).

3.3 Results

3.3.1 *In vitro* calcium imaging set-up and experimental protocol

The basic concept applied in this study was to record neuronal response to several trains of electrical stimuli of increasing strength, add a potential sensitizer and then reassess neuronal responses to the same trains of stimuli. The effect of the sensitizer could then be assessed as the change in neuronal response, as well as the change in the number of neurons responding. To assess neuronal sensitization using electrical field stimulation *in vitro* the calcium imaging set-up had to be modified. Cells were cultured in a Petri dish with glass coverslip bottom to allow visualisation of cells on the calcium imaging stage without the need to transfer the cells into an imaging chamber. The top of the dish contained electrodes positioned in parallel to each other. (**Fig. 3.1 a-b**). Electrodes were then connected to a stimulus isolator that delivered biphasic current stimuli of varied intensity. The volume of the calcium imaging buffer was kept the same between coverslips, to minimize the impact of the liquid volume on the spread of electrical current. Each train of stimuli comprised of 10 shocks of 2 ms duration delivered at 5 Hz frequency. However, we decided against using set stimuli intensities, as the variations in the electrode alignment, imaging solution volume and cell position relative to electrodes will result in inconsistent stimuli intensities across different coverslips. To ensure that the relative intensity of the stimulus was similar for all coverslips we used multiples of each coverslip's electrical threshold (e.g. 1.5, 2.0, 2.5, and 3.0 times threshold) to determine the stimulus intensities instead of a set current value. The threshold was determined as the minimum current sufficient to activate at least one neuron in the field of view (see **3.2.3**). Using relative threshold instead of set current reduces the variability that is introduced by the liquid volume and electrode arrangement. The imaging protocol is illustrated in **Fig. 3.1 c**.

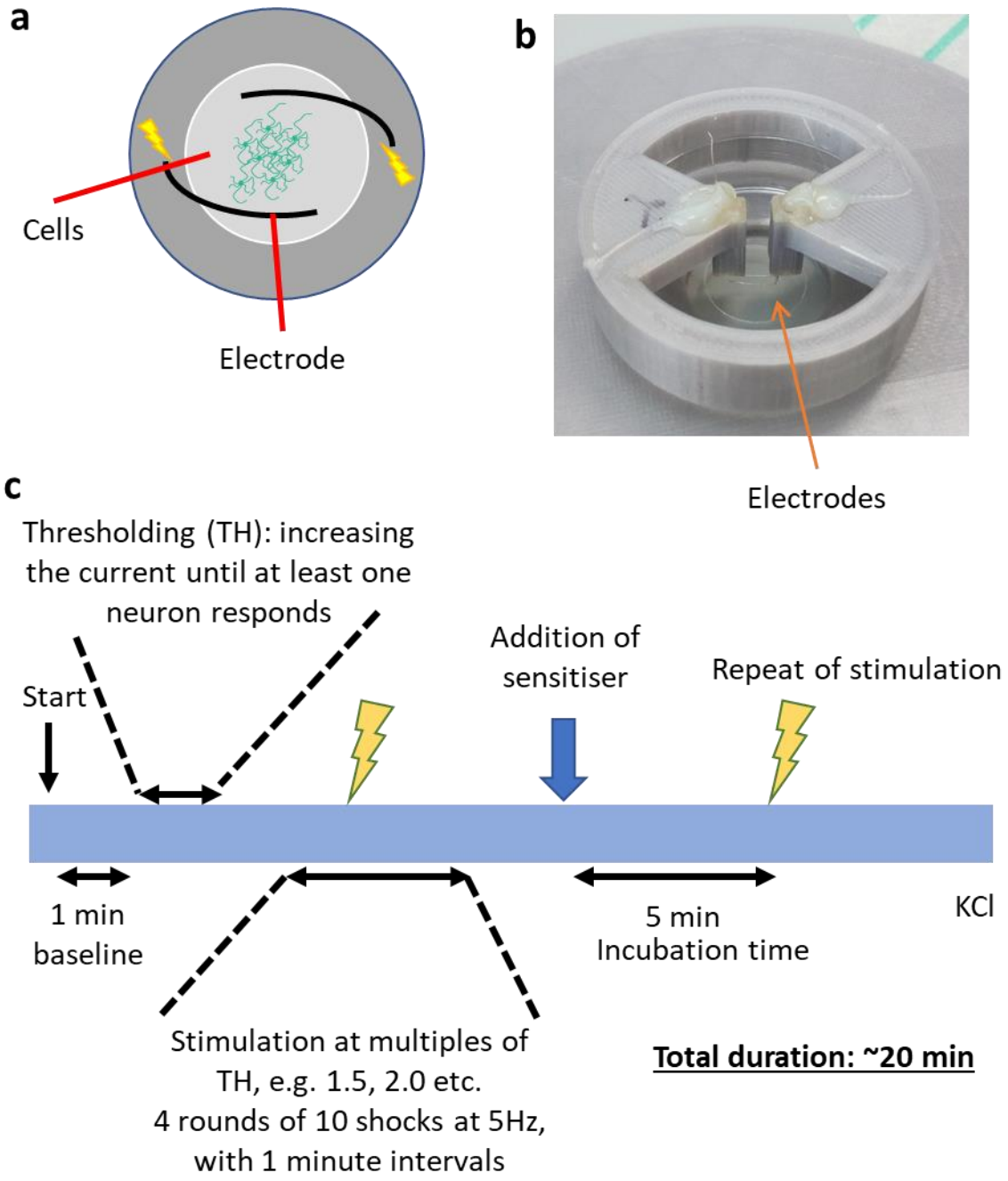

Figure 3.1 – In vitro calcium imaging dish with electrodes and experimental protocol. a) *Diagram and* ***b)*** *photograph of the calcium imaging glass-bottom dish with electrodes attached.* ***c)*** *Experimental protocol typically used in a calcium imaging session. Neuronal responses to electrical stimuli of increasing amplitude were assessed before and after incubation with a sensitising agent. KCl is added at the end to identify all viable neurons.*

Example images of an AAV9-GCaMP6s transfected culture before and after an electrical stimulus was applied is depicted in **Fig. 3.2 a, b**. Cells responding to the electrical stimulus are marked with black arrows. An example of overlaid traces of several responding and non-responding neurons is shown in **Fig. 3.2 c**. The difference between the minimum and maximum fluorescence signal during stimulus application (ΔF) was used to quantify neuronal responses (**Fig. 3.2 d**). To determine whether a neuron is activated by a specific stimulus, the ΔF was compared to the relative baseline activity of that neuron in the period between 20 and 15 seconds prior to the stimulus (Fpr, **Fig. 3.2 d**). If the ΔF was greater than Fpr + 5 times Fpr SEM, then that neuron was counted as a responder for that particular stimulus. After addition of sensitizer cells were left to incubate for 5 minutes before the stimulation was repeated. The difference in this response before and after sensitizer addition was used to assess neuronal sensitization. In addition, we can assess the percentage of neurons responding to each electrical stimulus before and after the addition of the sensitizer or the vehicle. We can then derive the change in the percentage of neurons responding to each electrical stimulus caused by the addition of the sensitizer or vehicle. After that, we can compare this change between the sensitizer and the vehicle groups for each electrical stimulus to assess whether that particular sensitizer caused an increase in the proportion of the neurons responding.

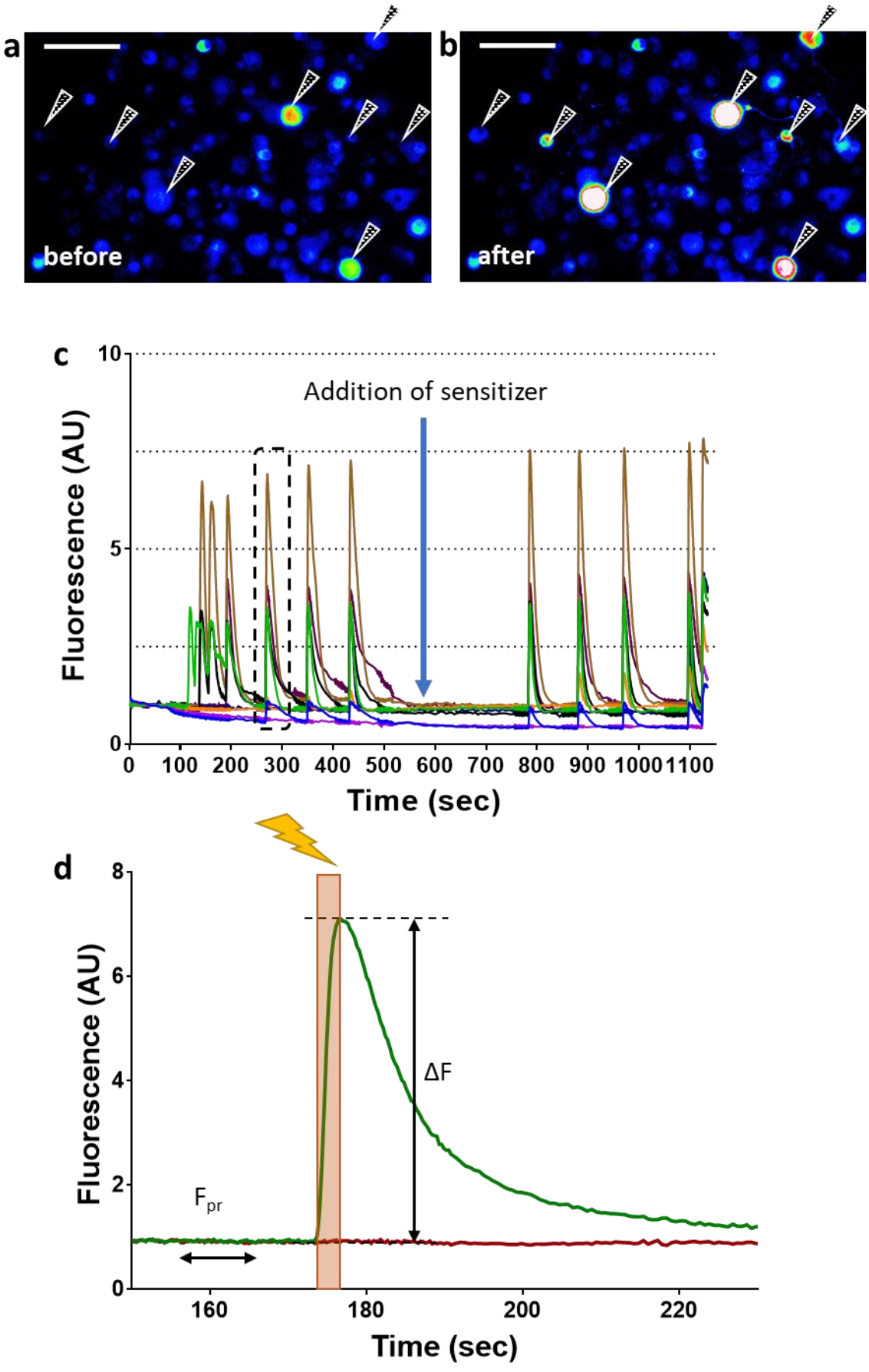
a
before
b
after
c
Addition of sensitizer
Fluorescence (AU)
Time (sec)
d
Fluorescence (AU)
ΔF
F_{pr}
Time (sec)

Figure 3.2 – Examples of neuronal responses and fluorescence traces. *Mixed DRG neurons were cultured and incubated with AAV9-GCaMP6s for 24 hours and neuronal responses to electrical stimuli were assessed. An increase in GCaMP6s fluorescence was observed in transduced neurons that responded to a given stimulus (black arrows,* ***a)*** *before stimulus,* ***b)*** *immediately after stimulus).* ***c)*** *Example fluorescence traces from neurons that responded to KCl at the end of the protocol.* ***Dashed area: d)*** *example traces of one neuron that responded to a particular electrical stimulus and one that did not. The neuronal response is quantified as the difference between the minimum and maximum fluorescence signal during the 5 second application of the stimulus (**ΔF**). If the ΔF is larger than the average fluorescence of that given neuron 15 seconds prior to the stimulus (**F_{pr}**) + 5xSEM, then the neuron is classified as a "responder". The number of responsive neurons as well as magnitude of neuronal responses to each stimulus were compared before and after the incubation with a sensitising agent.*

3.3.2 *In vitro* transduction with AAV9-GCaMP6s can be used to assess sensitisation of neurons by application of sensitising agents

To investigate whether virally-delivered GCaMP6s in neurons could be used to investigate neuronal sensitization, we assessed neuronal responses of the mixed DRG cultures to electrical field stimulation before and after addition of 5 µM of PGE2. The difference in neuronal responses to the same stimuli was used to assess neuronal sensitization after PGE_2 or vehicle addition. There was a significant increase in neuronal response to the strongest stimulus (3 times threshold) after PGE2 compared to vehicle (3 Con vs 3 PGE2, 200.1% ± 23.13% vs 499.4% ± 96.9%, One-Way ANOVA with Tukey's multiple comparisons, p = 0.038, n = 115 PGE2 neurons and 189 vehicle neurons, **Fig. 3.3 a**). However, the data spread was very large, which may reduce the biological significance. When we split the neurons into large diameter (> 20 µm) and small diameter (<20 µm), the difference in response to the strongest stimulus was no longer significant (3 Con vs 3 PGE2, One-Way ANOVA with Tukey's multiple comparisons, p >0.05, n = 35 PGE2 neurons and 77 vehicle for large neurons, 38 PGE2 neurons and 50 vehicle for large neurons, **Fig 3.3 b,c**). Interestingly, small neurons exhibited a significant increase in a response to 2.5 times threshold (2.5 CON vs 2.5 PGE2, 100.3% ± 11.56% vs 482.2% ± 152.7%, One-Way ANOVA with Tukey's multiple comparisons, p = 0.0316, n = 38 PGE2 neurons and 50 vehicle neurons, **Fig. 3.3 b**). The responses for large neurons to all stimuli intensities did not significantly differ between PGE2 and vehicle (Con vs PGE2, all intensities, One-Way ANOVA

with Tukey's multiple comparisons, p > 0.05, n = 35 PGE2 neurons and 77 vehicle neurons, **Fig. 3.3 c**). Unfortunately, the neuronal diameter data was not available for some neurons, resulting in reduced number of neurons in the two diameter groups. Lastly, there was no significant difference between PGE2 and vehicle in the change in the percentage of neurons responding to stimuli for all three groups (Con vs PGE2, all intensities, One-Way ANOVA with Tukey's multiple comparisons, p >0.05, **Fig. 3.3 d**).

As PGE2 is a known neuronal sensitizer we were surprised by a relatively weak effect it had on the neuronal responses. To assess if a stronger effect could be achieved, we tested a mix of 10 µM PGE2 and 10 µM Bradykinin (BK), both of which are known sensitizers for DRG neurons. However, there was no significant difference in response change for all stimuli intensities between sensitizer mix and vehicle for all diameters (Con vs PGE2 + BK, all intensities, One-Way ANOVA with Tukey's multiple comparisons, p >0.05, n = 104 PGE2 + BK neurons and 176 vehicle neurons, **Fig. 3.4 a**), small diameter (Con vs PGE2 + BK, all intensities, One-Way ANOVA with Tukey's multiple comparisons, p >0.05, n = 23 PGE2 neurons + BK and 95 vehicle neurons, **Fig. 3.4 b**) or large diameter groups (Con vs PGE2 + BK, all intensities, One-Way ANOVA with Tukey's multiple comparisons, p >0.05, n = 81 PGE2 + BK neurons and 81 vehicle neurons, **Fig. 3.4 c**). In addition, there was no significant change in the percentage of neurons responding to electrical stimuli after addition of sensitizer or vehicle for all three groups of neurons (Con vs PGE2 + BK, all intensities, One-Way ANOVA with Tukey's multiple comparisons, p >0.05, **Fig. 3.4 d**).

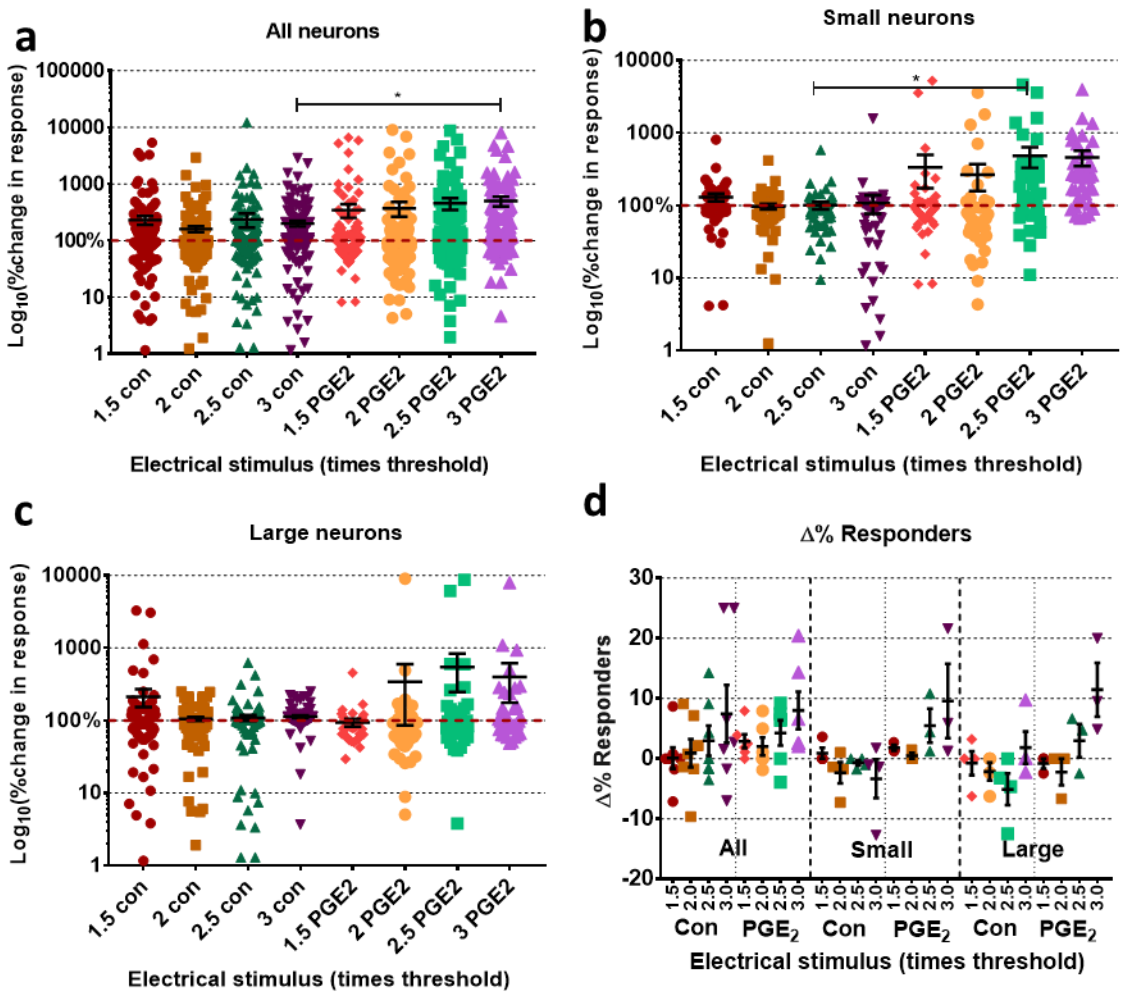

Figure 3.3 – Impact of 5 µM PGE2 on the average GCaMP6s responses of DRG neurons in vitro following electrical filed stimulation. *Mixed cultures of DRG neurons from all spinal levels incubated with AAV9-GCaMP6s 24 hours prior to imaging (total n = 115 PGE2 neurons, n = 189 vehicle neurons, 6-7 coverslips per group, 2 animals total).* ***a – c*** *Average change in response of* ***a)*** *all,* ***b)*** *small diameter (<20 µm), and* ***c)*** *large diameter (>20 µm) neurons to electrical stimuli after addition of 5 µM PGE2 or vehicle (Con). Following addition of PGE2, there was a significant increase in the neuronal response to 3 times the threshold stimulus for all neurons (**a**, 3 CON vs 3 PGE2, 200.1 % ± 23.13 % vs 499.4 % ± 96.9 %, One-Way ANOVA with Tukey's multiple comparisons, p = 0.038). Small diameter neurons showed increased responses following PGE2 addition to 2.5 times the threshold stimulus (**b**, 2.5 CON vs 2.5 PGE2, 100.3 % ± 11.56 % vs 482.2 % ± 152.7 %, One-Way ANOVA with Tukey's multiple comparisons, p = 0.0316, n = 38 PGE2 and 50 vehicle). There was no significant difference in responses of large diameter neurons (**c**, One-Way ANOVA with Tukey's multiple comparisons, p >0.05, n = 35 PGE2 and 77 vehicle). Unfortunately, neuronal diameter data were unavailable for one of the animals, so the small and large diameter neuron analysis was performed only on 3-4 coverslips per group, 1 animal total* ***d)*** *Average change in the percentage of neurons responding to electrical stimuli after addition of 5 µM PGE2 or vehicle. No significant difference in the change in the percentage of neurons responding to the same stimulus was observed for all, small diameter (<20 µm) and large diameter (>20 µm) neurons (**d**, One-Way ANOVA with Tukey's multiple comparisons, p >0.05).*

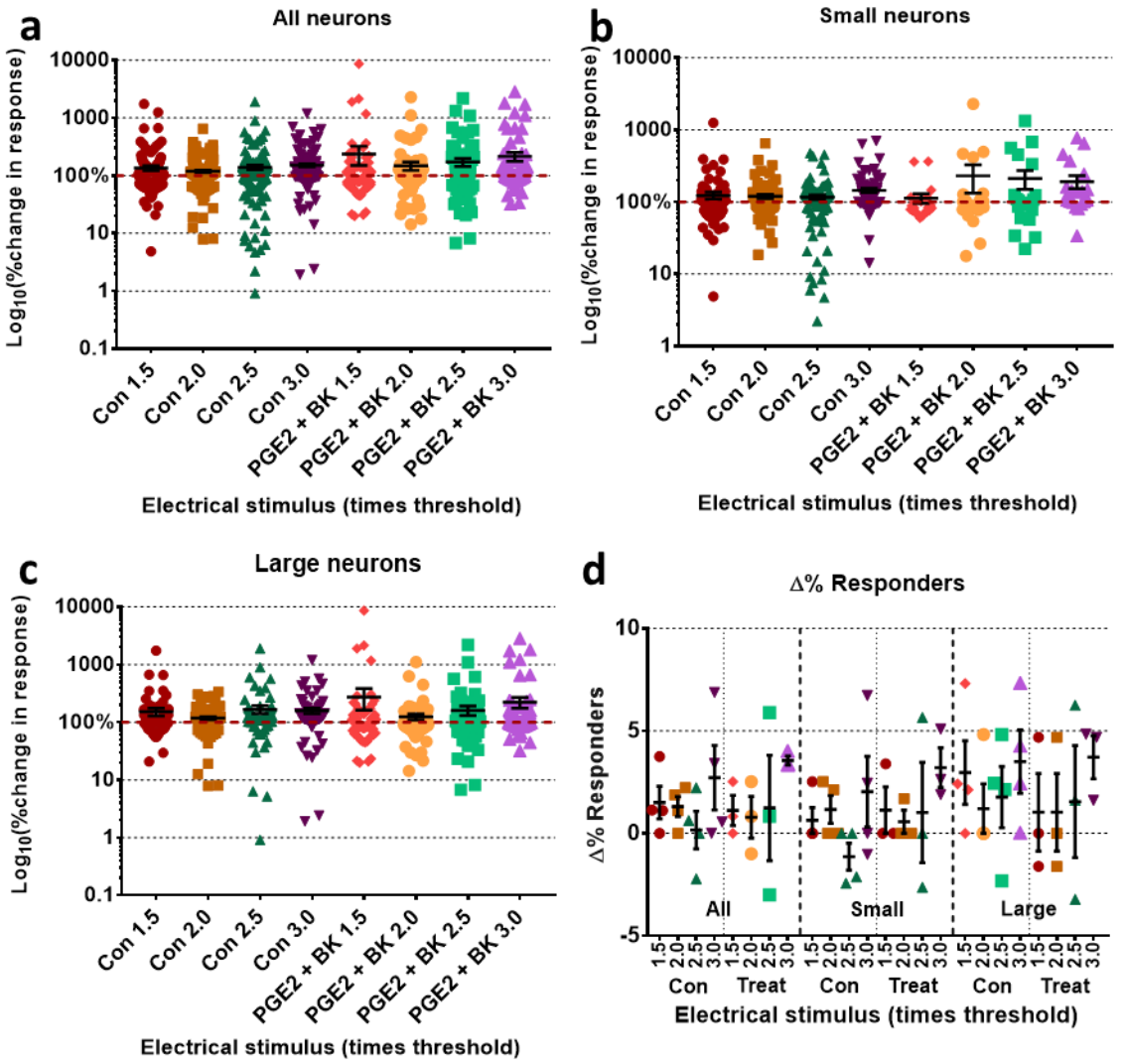

Figure 3.4 – Impact of 10 µM PGE2 + bradykinin (BK) mix on the average GCaMP6s responses of DRG neurons in vitro following electrical filed stimulation. *Mixed cultures of DRG neurons from all spinal levels incubated with AAV9-GCaMP6s 24 hours prior to imaging (total n = 104 PGE2 + bradykinin (BK) neurons, n = 176 vehicle neurons, 3-4 coverslips per group, 1 animal total).* ***a – c*** *Average change in response of* ***a)*** *all,* ***b)*** *small diameter (<20 µm), and* ***c)*** *large diameter (>20 µm) neurons to electrical stimuli after addition of 10 µM PGE2 + BK mix or vehicle. Following addition of the sensitising mix, there was no significant increase in the neuronal responses to electrical stimuli for all (**a**, One-Way ANOVA with Tukey's multiple comparisons, p >0.05, n = 104 PGE2 + BK and 176 vehicle), small diameter (**b**, One-Way ANOVA with Tukey's multiple comparisons, p >0.05, n = 23 PGE2 + BK and 95 vehicle) or large diameter neurons (**c**, One-Way ANOVA with Tukey's multiple comparisons, p >0.05, n = 81 PGE2 + BK and 81 vehicle).* ***d)*** *Average change in the percentage of neurons responding to electrical stimuli after addition of 10 µM PGE2 + BK mix or vehicle. No significant difference in the change in the percentage of neurons responding to the same stimulus was observed for all, small diameter (<20 µm) and large diameter (>20 µm) neurons (**d**, One-Way ANOVA with Tukey's multiple comparisons, p >0.05).*

3.3.3 Assessment of neuronal responses following addition of sensitizers using a chemical calcium indicator Fura-2 AM

The lack of response with the PGE2 + BK mix could be due to the nature of the trigger stimulus (electrical vs. chemical, e.g. capsaicin), and prompted us to investigate a broader selection of possible sensitizers. We decided to use Fura-2 AM dye instead of AAV9-GCaMP6s virus to test the effect of a number of sensitising agents *in vitro*, using the electrical field stimulation set up. Fura-2 AM is easier to use and produces more consistent labelling, as well as being considerably cheaper. First, we reassessed the effect of 5 µM PGE2 on the neuronal responses to electrical stimuli in neurons loaded with Fura-2 AM instead of GCaMP6s. We found no significant difference in the change in neuronal responses to all electrical stimuli after addition of 5 µM PGE2 for all diameter neurons (Con vs PGE2, all intensities, One-Way ANOVA with Tukey's multiple comparisons, $p > 0.05$, n = 140 PGE2 neurons and 121 vehicle neurons, **Fig 3.5 a**). When neurons were split into small and large diameter groups, we found no significant difference for all electrical stimuli in the small diameter group (Con vs PGE2, all intensities, One-Way ANOVA with Tukey's multiple comparisons, $p > 0.05$, n = 66 PGE2 neurons and 45 vehicle neurons, **Fig 3.5 b**) and the large diameter group (Con vs PGE2, all intensities, One-Way ANOVA with Tukey's multiple comparisons, $p > 0.05$, n = 74 PGE2 neurons and 76 vehicle neurons, **Fig 3.5 c**). Furthermore, no significant difference in the change in the percentage of responding neurons for all electrical stimuli was observed between the 5 µM PGE2 and vehicle treatment in any of the three neuronal groups (Con vs PGE2, all intensities, One-Way ANOVA with Tukey's multiple comparisons, $p > 0.05$, **Fig 3.5 d**). We also tested 10 µM PGE2 to see whether the higher concentration would have a stronger effect. However, the results with 10 µM PGE2 were similar to 5 µM PGE2. We found not significant difference in the change in neuronal responses to all electrical stimuli for all three groups of neurons (All neurons: Con vs PGE2, all intensities, One-Way ANOVA with Tukey's multiple comparisons, $p > 0.05$, n = 96 PGE2 neurons and 123 vehicle neurons, **Fig 3.6 a;** Small neurons: Con vs PGE2, all intensities, One-Way ANOVA with Tukey's multiple comparisons, $p > 0.05$, n = 64 PGE2 neurons and 56

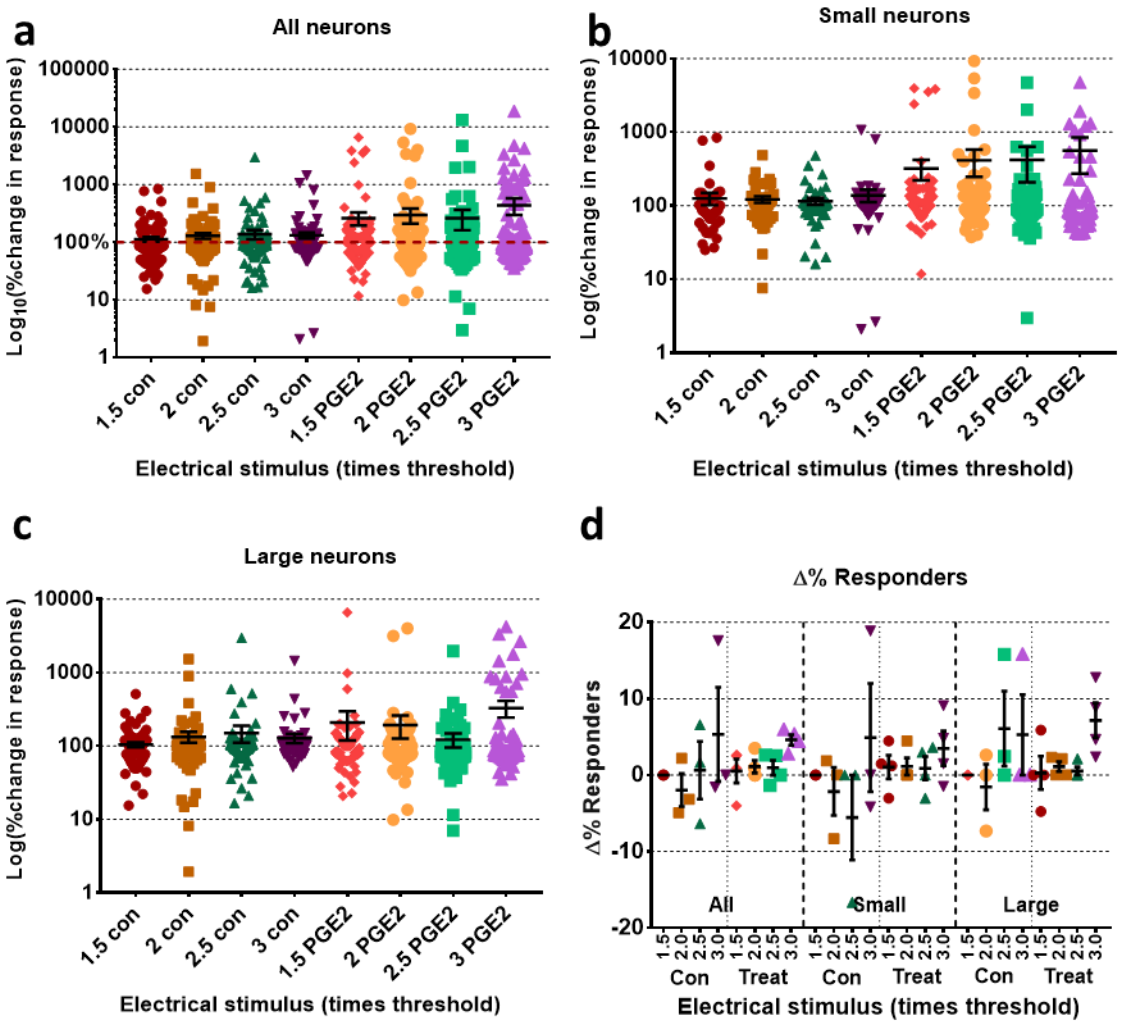

Figure 3.5 – Impact of 5 µM PGE2 on the average Fura-2 AM responses of DRG neurons in vitro following electrical filed stimulation. *Mixed cultures of DRG neurons were prepared 24 hours prior to imaging and loaded with 2 µM Fura-2 AM 1 hour before imaging (total n = 140 PGE2 neurons, n = 121 vehicle neurons, 3-4 coverslips per group, 1 animal total).* ***a – c*** *Average change in response of* ***a)*** *all,* ***b)*** *small diameter (<20 µm), and* ***c)*** *large diameter (>20 µm) neurons to electrical stimuli after addition of 5 µM PGE2 or vehicle. Following addition of the PGE2, there was no significant increase in the neuronal responses to electrical stimuli for all (**a**, One-Way ANOVA with Tukey's multiple comparisons, p >0.05, n = 140 PGE2 and 121 vehicle), small diameter (**b**, One-Way ANOVA with Tukey's multiple comparisons, p >0.05, n = 66 PGE2 and 45 vehicle) or large diameter neurons (**c**, One-Way ANOVA with Tukey's multiple comparisons, p >0.05, n = 74 PGE2 and 76 vehicle).* ***d)*** *Average change in the percentage of neurons responding to electrical stimuli after addition of 5 µM PGE2 or vehicle. No significant difference in the change in the percentage of neurons responding to the same stimulus was observed for all, small diameter (<20 µm) and large diameter (>20 µm) neurons (**d**, One-Way ANOVA with Tukey's multiple comparisons, p >0.05).*

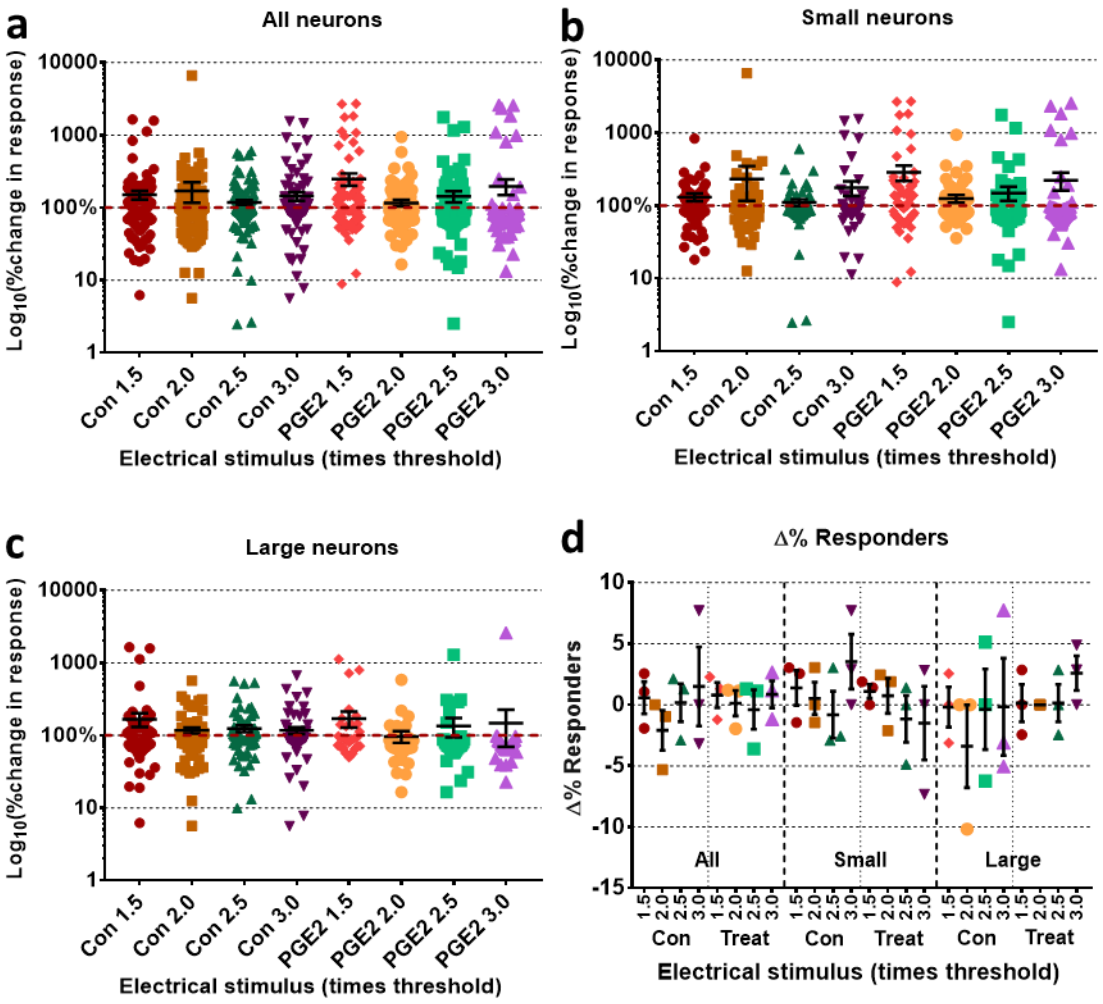

Figure 3.6 – Impact of 10 µM PGE2 on the average Fura-2 AM responses of DRG neurons in vitro following electrical filed stimulation. *Mixed cultures of DRG neurons were prepared 24 hours prior to imaging and loaded with 2 µM Fura-2 AM 1 hour before imaging (total n = 96 PGE2 neurons, n = 123 vehicle neurons, 3-4 coverslips per group, 1 animal total).* ***a – c*** *Average change in response of* ***a)*** *all,* ***b)*** *small diameter (<20 µm), and* ***c)*** *large diameter (>20 µm) neurons to electrical stimuli after addition of 10 µM PGE2 or vehicle. Following addition of the PGE2, there was no significant increase in the neuronal responses to electrical stimuli for all (**a**, One-Way ANOVA with Tukey's multiple comparisons, p >0.05, n = 96 PGE2 and 123 vehicle), small diameter (**b**, One-Way ANOVA with Tukey's multiple comparisons, p >0.05, n = 64 PGE2 and 56 vehicle) or large diameter neurons (**c**, One-Way ANOVA with Tukey's multiple comparisons, p >0.05, n = 23 PGE2 and 95 vehicle).* ***d)*** *Average change in the percentage of neurons responding to electrical stimuli after addition of 10 µM PGE2 or vehicle. No significant difference in the change in the percentage of neurons responding to the same stimulus was observed for all, small diameter (<20 µm) and large diameter (>20 µm) neurons (**d**, One-Way ANOVA with Tukey's multiple comparisons, p >0.05).*

vehicle neurons. **Fig 3.6 b;** Large neurons: Con vs PGE2, all intensities, One-Way ANOVA with Tukey's multiple comparisons, p >0.05, n = 23 PGE2 neurons and 95 vehicle neurons, **Fig 3.6 c**). Similar to 5 µM PGE2, we found no significant difference in the change in the percentage of responding neurons for all electrical stimuli between the 10 µM PGE2 and vehicle treatment for all three neuronal groups (Con vs PGE2, all intensities, One-Way ANOVA with Tukey's multiple comparisons, p >0.05, **Fig 3.6 d**). These results disagree with those obtained with AAV9-GCaMP6s, however that could be due to a large data spread in our AAV9-GCaMP6s experiments.

In addition, we also tested a number of other sensitizer which have been shown to produce neuronal sensitisation, including 10 µM bradykinin, 2.5 and 5 µM inflammatory soup (PGE2, Bradykinin and Serotonin), 10 µM forskolin and 50 ng/ml nerve growth factor (NGF). We found no significant difference in the change in neuronal responses between treatment with 10 µM bradykinin (BK) and vehicle for the all neurons group (Con vs BK, all intensities, One-Way ANOVA with Tukey's multiple comparisons, p >0.05, n = 64 BK neurons and 41 vehicle neurons, **Fig 3.7 a**). Both small and large diameter neuronal groups also showed no significant difference (Con vs BK, all intensities, One-Way ANOVA with Tukey's multiple comparisons, p >0.05, n = 27 small, 37 large BK neurons, 21 small and 20 large vehicle neurons, **Fig 3.7 b,c**). The change in the percentage of neurons responding to each electrical stimulus after BK addition was not significantly different from that after vehicle treatment (Con vs BK, all intensities, One-Way ANOVA with Tukey's multiple comparisons, p >0.05, **Fig 3.7 d**).

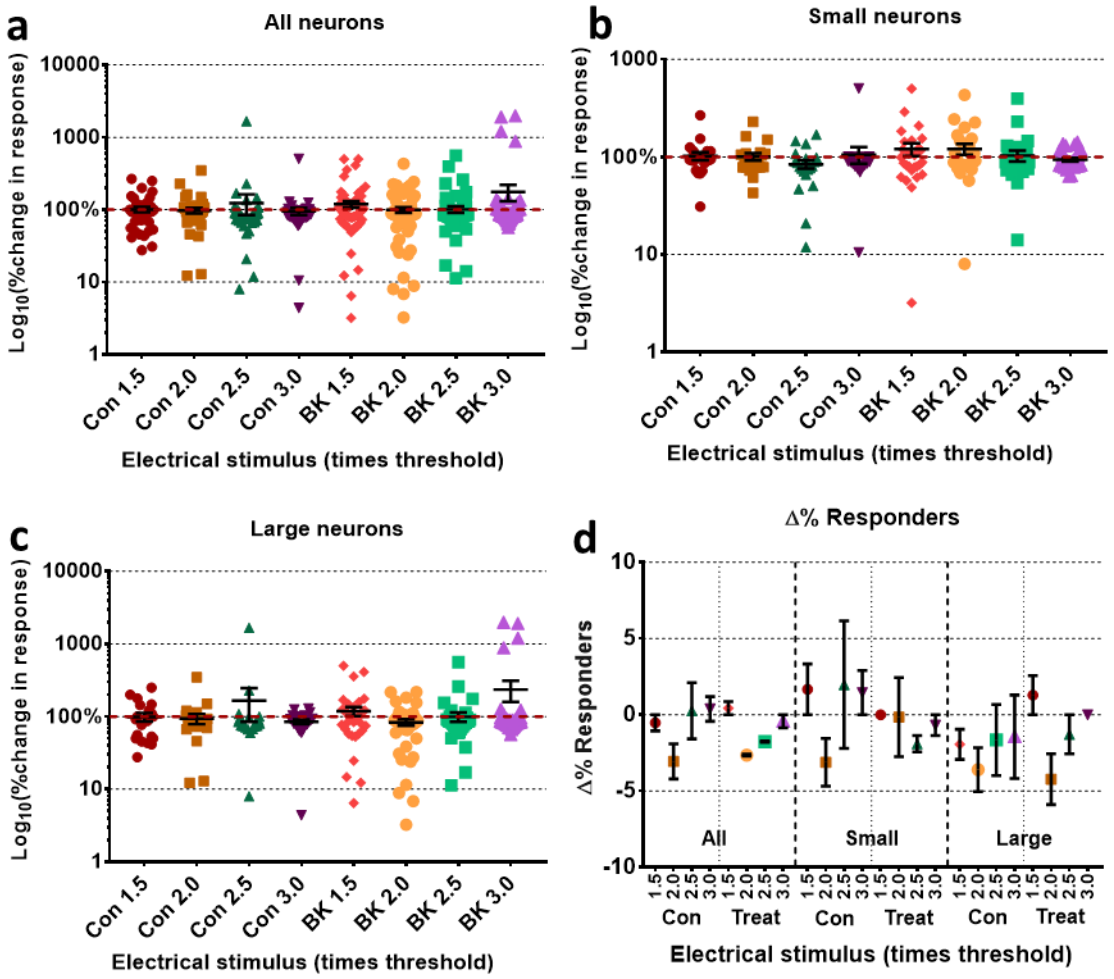

Figure 3.7 – Impact of 10 µM bradykinin (BK) on the average Fura-2 AM responses of DRG neurons in vitro following electrical filed stimulation. *Mixed cultures of DRG neurons were prepared 24 hours prior to imaging and loaded with 2 µM Fura-2 AM 1 hour before imaging (total n = 64 bradykinin (BK) neurons, n = 41 vehicle neurons, 3 coverslips per group, 1 animal total).* ***a – c*** *Average change in response of* ***a)*** *all,* ***b)*** *small diameter (<20 µm), and* ***c)*** *large diameter (>20 µm) neurons to electrical stimuli after addition of 10 µM BK or vehicle. Following addition of the BK, there was no significant increase in the neuronal responses to electrical stimuli for all (**a**, One-Way ANOVA with Tukey's multiple comparisons, p >0.05, n = 64 BK and 41 vehicle), small diameter (**b**, One-Way ANOVA with Tukey's multiple comparisons, p >0.05, n = 27 BK and 21 vehicle) or large diameter neurons (**c**, One-Way ANOVA with Tukey's multiple comparisons, p >0.05, n = 37 BK and 20 vehicle.* ***d)*** *Average change in the percentage of neurons responding to electrical stimuli after addition of 10 µM BK or vehicle. No significant difference in the change in the percentage of neurons responding to the same stimulus was observed for all, small diameter (<20 µm) and large diameter (>20 µm) neurons (**d**, One-Way ANOVA with Tukey's multiple comparisons, p >0.05).*

Next, we tested 2.5 µM and 5 µM inflammatory soup (IS). When we assessed all neurons together, we found no significant difference in the change in neuronal responses between 2.5 µM IS, 5 µM IS and vehicle (Con vs 2.5 IS vs 5 IS, all intensities, One-Way ANOVA with Tukey's multiple comparisons, $p > 0.05$, n = 86 2.5 µM IS neurons, 105 5 µM IS neurons and 95 vehicle neurons, **Fig 3.8 a**). However, assessment of the inflammatory soup (IS) effect on responses in small neurons revealed that 2.5 µM IS significantly increases the change in neuronal responses to 2.5 times the threshold electrical stimulation, compared to vehicle (3 Con vs 3 2.5 IS, 147.3% ± 35.86% vs 256.4% ± 107.1%, One-Way ANOVA with Tukey's multiple comparisons, $p = 0.036$, n = 50 2.5 µM IS neurons and 59 vehicle neurons, **Fig 3.8 b**). No sensitisation effect was observed after 5 µM IS treatment in small diameter group (Con vs 5 IS, all intensities, One-Way ANOVA with Tukey's multiple comparisons, $p > 0.05$, n = 53 5 µM IS neurons and 59 vehicle neurons, **Fig 3.8 b**), and after 2.5 µM and 5 µM IS treatment in large diameter neurons (Con vs 2.5 IS vs 5 IS, all intensities, One-Way ANOVA with Tukey's multiple comparisons, $p > 0.05$, n = 36 2.5 µM IS neurons, 52 5 µM IS neurons and 36 vehicle neurons, **Fig 3.8 c**). We also did not detect a significant difference in the percentage of neurons responding to any electrical stimuli between 2.5 µM IS, 5 µM IS and vehicle (Con vs 2.5 IS vs 5 IS, all intensities, One-Way ANOVA with Tukey's multiple comparisons, $p > 0.05$, **Fig 3.9 d**).

Forskolin (Fsk) treatment, compared to vehicle, did not significantly affect the change in neuronal responses to all electrical stimuli in all diameter, small diameter and large diameter groups (<u>All neurons</u>: Con vs Fsk, all intensities, One-Way ANOVA with Tukey's multiple comparisons, $p > 0.05$, n = 135 Fsk neurons and 123 vehicle neurons, **Fig 3.9 a;** <u>Small neurons</u>: Con vs Fsk, all intensities, One-Way ANOVA with Tukey's multiple comparisons, $p > 0.05$, n = 77 Fsk neurons and 56 vehicle neurons. **Fig 3.9 b;** <u>Large neurons</u>: Con vs Fsk, all intensities, One-Way ANOVA with Tukey's multiple comparisons, $p > 0.05$, n = 58 Fsk neurons and 67 vehicle neurons, **Fig 3.9 c**). Similar to other treatments, we did not observe a significant difference in the change in the percentage of neurons responding to any electrical stimulus between Fsk

and vehicle for all three neuronal diameter groups (Con vs Fsk, all intensities, One-Way ANOVA with Tukey's multiple comparisons, p >0.05, **Fig 3.9 d**).

Finally, we also assessed the effect of 50 ng/ml NGF on neuronal responses. Unfortunately, this experiment was done while the experimental paradigm was not in its final form, so the electrical stimuli used were higher than those in other experiments. We found that NGF treatment significantly decreased the change in the neuronal responses to 5 times the threshold stimulus, compared to vehicle (5 Con vs 5 NGF, 308.6% ± 17.51% vs 245.1% ± 6.386%, One-Way ANOVA with Tukey's multiple comparisons, p = 0.0001, n = 345 NGF neurons, 310 vehicle neurons, **Fig 3.10 a**). However, there was no significant difference in the change in percentage of neurons responding between NGF and vehicle treatment (Con vs NGF, all intensities, One-Way ANOVA with Tukey's multiple comparisons, p > 0.05, n = 345 NGF neurons, 310 vehicle neurons, **Fig 3.10 b**).

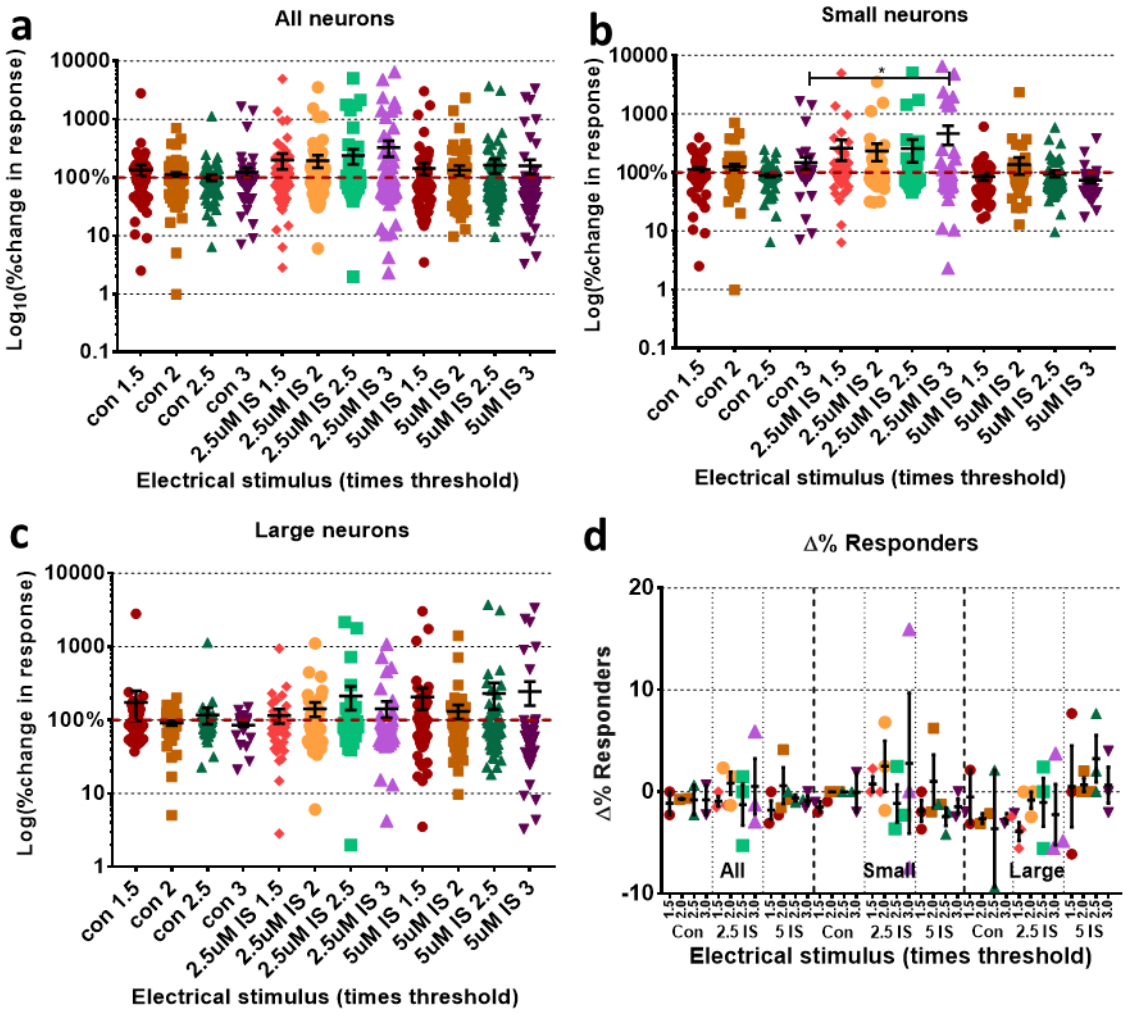

Figure 3.8 – Impact of 2.5 µM and 5 µM inflammatory soup (IS) on the average Fura-2 AM responses of DRG neurons in vitro following electrical filed stimulation. *Mixed cultures of DRG neurons were prepared 24 hours prior to imaging and loaded with 2 µM Fura-2 AM 1 hour before imaging (total n = 86-105 inflammatory soup (IS) neurons, 95 vehicle neurons, 2-3 coverslips per group, 1 animal total).* ***a – c*** *Average change in response of* ***a)*** *all,* ***b)*** *small diameter (<20 µm), and* ***c)*** *large diameter (>20 µm) neurons to electrical stimuli after addition of 2.5 µM and 5 µM IS or vehicle. Following addition of 2.5 µM IS, there was a significant increase in the neuronal response to 3 times the threshold stimulus for small diameter neurons (****b****, 3 CON vs 3 2.5 µM IS, 147.3% ± 35.86% vs 256.4% ± 107.1%, One-Way ANOVA with Tukey's multiple comparisons, p = 0.036, n = 50 2.5 µM IS and 59 vehicle). There was no significant difference in responses of all (****a****, One-Way ANOVA with Tukey's multiple comparisons, p > 0.05, n = 86 2.5 µM IS, 105 5 µM IS and 95 vehicle). or large diameter neurons (****c****, One-Way ANOVA with Tukey's multiple comparisons, p > 0.05, n = 36 2.5 µM IS, 52 5 µM IS and 36 vehicle).* ***d)*** *Average change in the percentage of neurons responding to electrical stimuli after addition of 2.5 µM and 5 µM IS or vehicle. No significant difference in the change in the percentage of neurons responding to the same stimulus was observed for all, small diameter (<20 µm) and large diameter (>20 µm) neurons (****d****, One-Way ANOVA with Tukey's multiple comparisons, p >0.05).*

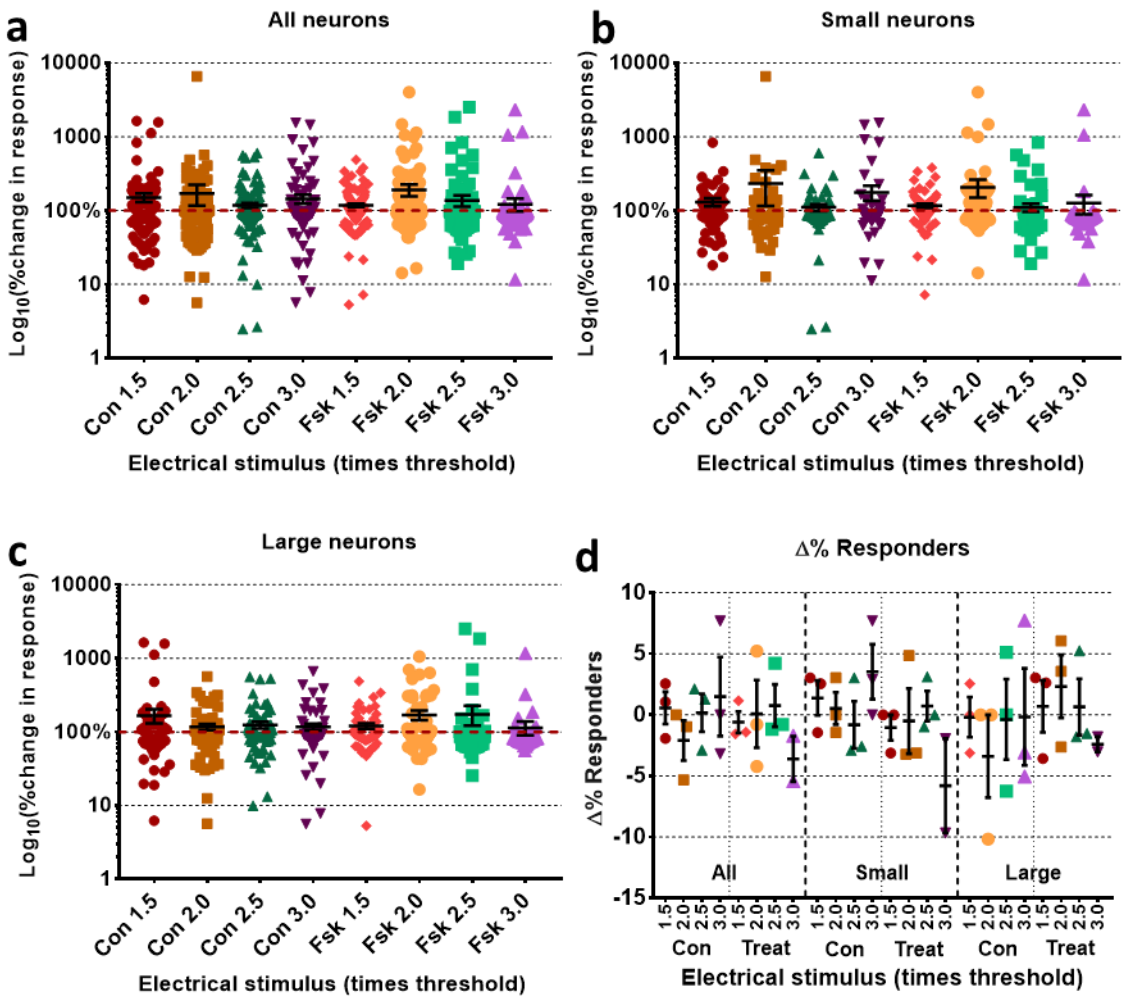

Figure 3.9 – Impact of 10 µM forskolin (Fsk) on the average Fura-2 AM responses of DRG neurons in vitro following electrical filed stimulation. *Mixed cultures of DRG neurons were prepared 24 hours prior to imaging and loaded with 2 µM Fura-2 AM 1 hour before imaging (total n = 135 Fsk neurons, 123 vehicle neurons, 3 coverslips per group, 1 animal total).* ***a – c*** *Average change in response of* ***a)*** *all,* ***b)*** *small diameter (<20 µm), and* ***c)*** *large diameter (>20 µm) neurons to electrical stimuli after addition of 10 µM BK or vehicle. Following addition of the Fsk, there was no significant increase in the neuronal responses to electrical stimuli for all (**a**, One-Way ANOVA with Tukey's multiple comparisons, p >0.05, n = 135 Fsk and 123 vehicle), small diameter (**b**, One-Way ANOVA with Tukey's multiple comparisons, p >0.05, n = 77 Fsk and 56 vehicle) or large diameter neurons (**c**, One-Way ANOVA with Tukey's multiple comparisons, p >0.05, n = 58 Fsk and 67 vehicle.* ***d)*** *Average change in the percentage of neurons responding to electrical stimuli after addition of 10 µM Fsk or vehicle. No significant difference in the change in the percentage of neurons responding to the same stimulus was observed for all, small diameter (<20 µm) and large diameter (>20 µm) neurons (**d**, One-Way ANOVA with Tukey's multiple comparisons, p >0.05).*

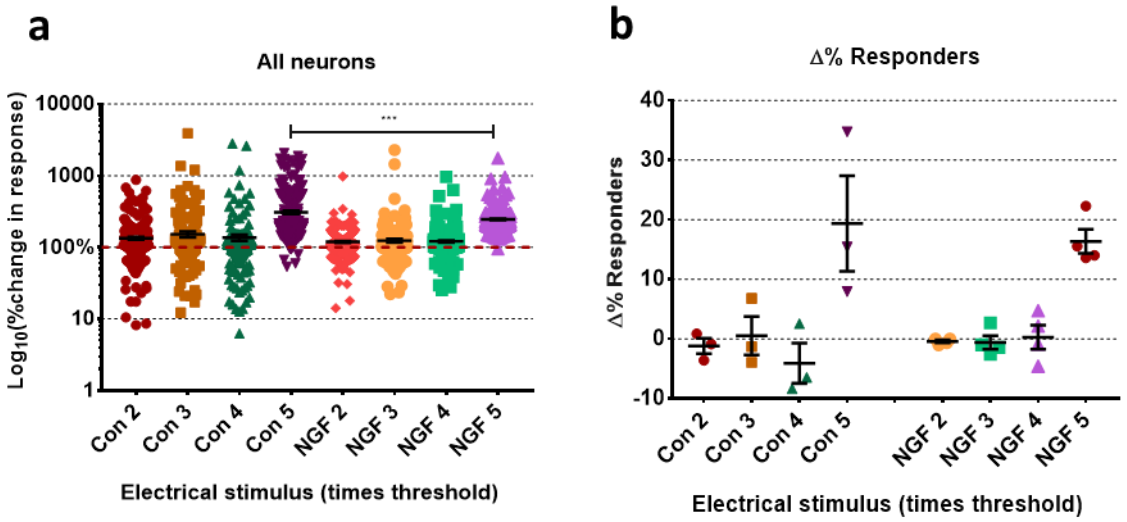

Figure 3.10 – Impact of 50 ng/ml nerve growth factor (NGF) on the average Fura-2 AM responses of DRG neurons in vitro following electrical filed stimulation. *Mixed cultures of DRG neurons were made 24 hours prior to imaging and loaded with 2 µM Fura-2 AM 1 hour before imaging (total n = 345 NGF neurons, n = 310 vehicle neurons, 3-4 coverslips per group, 1 animal total).* ***a)*** *Average change in response of all DRG neurons to electrical stimuli after addition of 50 ng/ml NGF or vehicle. Following addition of NGF, there was a significant decrease in the neuronal response to 5 times the threshold stimulus (**a**, 5 CON vs 5 NGF, 308.6% ± 17.51% vs 245.1% ± 6.386%, One-Way ANOVA with Tukey's multiple comparisons, p = 0.0001). Unfortunately, there is no neuronal diameter data available for this experiment.* ***b)*** *Average change in the percentage of neurons responding to electrical stimuli after addition of 50 ng/ml NGF or vehicle. No significant difference in the change in the percentage of neurons responding to the same stimulus was observed (**b**, One-Way ANOVA with Tukey's multiple comparisons, p >0.05).*

3.4 Discussion

Here, we have described our results following *in vitro* imaging of adult DRG neuron activity in response to short term application of various sensitising agents. In our setup, we used trains of electrical field stimuli of varying strength to evoke responses in cultured DRG neurons. Various known sensitizers, such as PGE2, were then applied to the cells and the electrical stimuli were repeated to assess the effect of the sensitising agent on the neuronal responses to each stimulus strength. However, before discussing the results I would like to address the reasons behind our choice of the electrical field stimulation as the trigger for neuronal activity.

3.4.1 Triggering neuronal activity *in vitro*

Calcium imaging is used to visualise fluctuations in intracellular calcium, which in neurons serves as a proxy for action potential firing (see **3.1.1**). However, uninjured adult DRG neurons in culture are not spontaneously active (Ma and LaMotte, 2007; Xie, Strong and Zhang, 2010; Djouhri *et al.*, 2015). Unless a compound elicits neuronal activity, its sensitising or desensitising effect on a cell cannot be easily observed during calcium imaging. Therefore, a trigger stimulus needs to be applied to elicit neuronal activity before and after addition of a compound to see its modulatory effect. An ideal trigger allows control of the strength and temporal profile of the stimulus, has to be easy to apply, and does not affect the neurons in any other way, i.e. repeated applications of the stimulus would trigger the same amount of activity. In pain research, different types of chemical, thermal and electrical triggers are used.

Perhaps the most widely-used chemical trigger in pain research for *in vitro* DRG calcium imaging is capsaicin, a transient receptor potential vanilloid 1 (TRPV1) agonist (Caterina *et al.*, 1997). TRPV1 is expressed in small and medium sized peptidergic and non-peptidergic nociceptors in the DRG (Guo *et al.*, 1999; Caterina and Julius, 2001; Hwang and Valtschanoff, 2003). Its application elicits pain *in vivo* and can activate DRG neurons *in vitro* (Heyman and Rang, 1985; Marsh *et al.*, 1987; Bleakman, Brorson and Miller, 1990; Szallasi and Blumberg, 1999). Due to capsaicin's robust activation of nociceptors, as well as a quick return of neuronal

activity to baseline after its removal, capsaicin has been widely used as a trigger for neuronal activity in numerous studies. For instance, it has been used to investigate the mechanisms of neuronal sensitisation to various endogenous compounds, such as bradykinin, nerve growth factor (NGF) and adenosine triphosphate (ATP) (Piper and Docherty, 2000; Eun *et al.*, 2001; Vellani *et al.*, 2001; Bonnington and McNaughton, 2003; Zhang, Huang and McNaughton, 2005; Vellani, 2006; Honan and McNaughton, 2007; Malin *et al.*, 2008). However, use of capsaicin as a neuronal activity trigger is not without its downfalls. Only a small proportion of large-diameter neurons express TRPV1 under normal physiological conditions, so most of them cannot be activated by capsaicin (Yu *et al.*, 2008). Furthermore, capsaicin-induced neuronal activity exhibits tachyphylaxis, diminishing with every successive application of capsaicin (Caterina *et al.*, 1997; Koplas, Rosenberg and Oxford, 1997; Shu and Mendell, 2001; Mohapatra and Nau, 2005; Maurer *et al.*, 2014). Therefore, care must be taken when comparing capsaicin-evoked neuronal activity after application of a potential activity-modulating compound. Finally, the application of capsaicin and its wash-off are not instantaneous, reducing the amount of temporal control over the stimulus.

In our set up, we used electrical field stimulation to trigger neuronal responses, instead of a chemical stimulus. Electrical stimulation has an advantage over chemical triggers in that its parameters such as duration and strength, as well as precise time of stimulation start and end can be easily controlled. In addition, the stimulation does not require perfusion, and therefore is not affected by the fluid movement. However, field stimulation is affected by the total amount of liquid in the dish as well as electrode arrangement. Electrical field stimulation using two parallel platinum electrodes has been shown to trigger consistent intracellular calcium responses in DRG neurons that did not show desensitisation, in contrast to capsaicin tachyphylaxis (Duflo, Zhang and Eisenach, 2004). It is important to note that prolonged electrical field stimulation (~60 seconds) of DRG neurons has been shown to reduce neuronal excitability (Koopmeiners *et al.*, 2013). Therefore, the stimulation parameters play an important role on the effect the electrical stimuli have on DRG neurons.

Electrical filed stimulation has been used to trigger activity in DRG neurons to study aspects of their physiology and pathology. For instance, prolonged electrical field stimulation has been used to elicit substance P release from DRG neurons and study the action of opioids (Holz, Dunlap and Kream, 1988; Chang *et al.*, 1989). It has also been used as a trigger during calcium imaging to investigate mitochondrial buffering of intracellular calcium ions and release of protons in rat DRG neurons (Werth and Thayer, 1994). Finally, Eisenach and colleagues used electrical field stimulation as a trigger during *in vitro* calcium imaging to look at the actions of α2-adrenoreceptor agonists and antagonists on DRG neurons from wild-type or spinal nerve-ligated rats (Eisenach, Zhang and Duflo, 2005; Ma *et al.*, 2005).

In our experiments, we opted for the use of electrical field stimulation over capsaicin stimulation because it showed much tighter control over neuronal activation parameters as well as uniform activation of neurons regardless of their TRPV1 expression. After identifying the coverslip threshold, we use a train of stimuli of increasing strength, and we found proportional increase in the number of neurons responding to stimuli, both with GCaMP6s and Fura-2 AM, suggesting that virally-delivered GCAMP6s performance is comparable to that of Fura-2 AM. In the literature, GCaMP6 has been shown to have equal or superior performance when compared to chemical dyes (T. W. Chen *et al.*, 2013). However, further experiments are needed to evaluate how various parameters of GCaMP6s, such as decay times and signal-to-noise ratio, compare to those of Fura-2 AM.

3.4.2 Selection of potential sensitizers

The aim of this chapter was two-fold: to assess performance of the GCaMP6s GECI in DRG neurons, and to set up an *in vitro* model of neuronal sensitisation to be used in future experiments. After showing that electrical stimulation can be used as a trigger for neuronal activity, we aimed to find a sensitizer that would either increase the number of neurons responding to each stimulus or increase the magnitude of neuronal responses.

Our first choice was prostaglandin E2 (PGE2). PGE2 is known to increase the frequency of neuronal firing by lowering the threshold of a voltage-gated sodium channel $Na_v1.8$ that is specific to nociceptors, in addition to playing a role in reducing the time between depolarisations (Gold *et al.*, 1996; Momin *et al.*, 2008). This is achieved through activation of the cAMP-PKA pathway that results in phosphorylation of the sodium channel (England, Bevan and Docherty, 1996; Gold, Levine and Correa, 1998; Fitzgerald *et al.*, 1999). Furthermore, PGE2 is a known sensitizer of the TRPV1 channel, increasing neuronal responses to capsaicin and heat (Pitchford and Levine, 1991; Moriyama *et al.*, 2005; Zhang, Li and McNaughton, 2008). Application of PGE2 has been shown to enhance action potential firing in small DRG neurons in response to a depolarising current injection and capsaicin application (Lopshire and Nicol, 1997; Gu, Kwong and Lee, 2003; Momin *et al.*, 2008). Mimicking PGE2 action by activating cAMP with forskolin has also been shown to sensitise DRG neurons (Smith, Davis and Burgess, 2000; Nicolson *et al.*, 2007). Taken together, these and many other studies show that PGE2 is a potent sensitizer of DRG neurons (McMahon, Cafferty and Marchand, 2005).

Another sensitizer whose effect on DRG neuronal activity we assessed during this study was bradykinin. Bradykinin has been shown to both excite nociceptive fibres and sensitise them to capsaicin, heat and mechanical stimuli (Lang *et al.*, 1990; Khan *et al.*, 1992; Cesare and McNaughton, 1996; Banik *et al.*, 2001; Koda and Mizumura, 2002). Bradykinin exerts its excitatory effect through release of calcium from intracellular stores via the PLC pathway (Bandell *et al.*, 2004; Ferreira, Da Silva and Calixto, 2004; Tang *et al.*, 2004; Liu *et al.*, 2010). In addition, it induces activation of the PKC and PKA pathways, which results in sensitization of TRPV1 and TRPA1 channels (Mizumura, Koda and Kumazawa, 1997; Wang *et al.*, 2008; Mizumura *et al.*, 2009). These and many other studies show that bradykinin can sensitise DRG neurons (Petho and Reeh, 2012).

In addition to assessing these sensitizers separately, in this study we investigated the sensitisation of the DRG neurons following an application of the PGE2, bradykinin and

serotonin mix, to mimic the "inflammatory soup" released upon injury *in vivo* (Basbaum *et al.*, 2009). Serotonin on its own has been show to excite as well as sensitize DRG neurons via its action on the TRPV1 channel (Linhart, Obreja and Kress, 2003; Salzer *et al.*, 2016). When applied together with PGE2 and bradykinin, the application of this "inflammatory soup" has been shown to activate TRPV1-positve DRG neurons *in vitro* and result in augmented capsaicin responses (Vyklický *et al.*, 1998; Ma, Greenquist and Lamotte, 2006).

The last potential sensitizer that we used in our experiments was nerve growth factor (NGF). NGF is released at the site of injury from non-neuronal cells such as fibroblasts and inflammatory cells (Ringkamp *et al.*, 2013). It is known to target TRPV1 through the PLC pathway, inducing sensitization to heat and capsaicin, in addition to promoting increased expression of TRPV1 (Chuang *et al.*, 2001; Ji *et al.*, 2002; Bonnington and McNaughton, 2003; Galoyan, Petruska and Mendell, 2003; Pezet and McMahon, 2006).

3.4.3 Effect of sensitizers on neuronal responses triggered by electrical field stimulation

Unfortunately, the sensitization to the electrical field stimulation produced by these compounds was moderate at best. In DRG cultures incubated with AAV9-GCaMP6s, we recorded a significant increase in the neuronal response to 3 times threshold stimulation after 5 µM PGE2 treatment (**Fig. 3.3a**). In addition, when we investigated at a subset of neurons with diameter of less than 20 µm, we recorded a trend towards an increased neuronal response for all stimulation intensities, with 2.5 times threshold intensity reaching significance (**Fig. 3.3b**). However, repeating the same experiment with Fura-2 AM did not show any significant sensitisation of neuronal activity for all neurons (**Fig. 3.5a**). Nevertheless, there was a trend towards increased response in the small diameter neuronal population, which is also evident in the GCaMP6s experiments (**Fig. 3.3b and 3.5b**). This discrepancy between the results with different calcium indicators is likely to be caused by a large data spread. There was no significant change in the percentage of neurons responding to each electrical trigger after PGE2 treatment. This is discordant with the literature, which shows that PGE2 increases the

number of neurons responding to chemical triggers, such as bradykinin (Smith, Davis and Burgess, 2000). This disagreement could be due to the nature of the stimulus, as electrical activity directly depolarises neurons, while chemical triggers exert their action via specific receptors and signalling pathways (see 3.4.1).

Interestingly, increasing the concentration of PGE2 to 10 µM did not significantly enhance neuronal responses (**Fig 3.6**). This could suggest that increasing PGE2 concentration reduced the sensitisation of DRG neurons to the electrical field stimulation. Alternatively, it could mean that the results we obtained with lower PGE2 (5 µM) concentration were false positives, appearing significant as a result of a large data spread. We did not see any neuronal sensitisation to electrical stimuli following an application of forskolin, an activator of cAMP that mimics PGE2 action and can sensitise sensory neurons to capsaicin (England, Bevan and Docherty, 1996; Lopshire and Nicol, 1998)

We found no potentiation of neuronal responses following treatment with 10 µM bradykinin alone, or in conjunction with 10 µM PGE2 (**Fig. 3.8 and 3.4**). However, we observed neuronal activation directly after application of bradykinin. As our set up does not allow for removal of the sensitizer once it has been introduced, it is possible that persistent activation of the DRG neurons by bradykinin masked the potential sensitisation to electrical stimuli.

When we assessed the sensitizing effect of the "inflammatory soup" on the DRG neurons, we found a trend towards potentiation of neuronal activity in DRG neurons (**Fig. 3.8 a**). It was even more pronounced in the small diameter sub-population of DRG neurons, reaching significance at 3 times the threshold stimulation (**Fig 3.8 b**). Surprisingly, this effect was only observed with 2.5 µM IS, and was completely gone when the concentration was increased to 5 µM. This dampening of neuronal sensitisation with increasing concentrations is similar to that seen of PGE2 (see above).

We also investigated the potential sensitising effect that NGF might have on the DRG neurons. In these experiments we used higher stimulation intensities to trigger responses in a larger

number of neurons. We did not see any potentiation of neuronal responses after NGF treatment compared to vehicle. In fact, there was a small but significant decrease in neuronal response to the highest stimulation intensity (**Fig. 3.10 a**). However, this may be a false positive due to the large data spread. Unfortunately, cell size information was not available during analysis, so we could not analyse small and large diameter sub-populations individually. It is also important to note that as these experiments follow a different stimulation protocol. Therefore, we cannot compare NGF with other sensitising agents shown here. In order to do so this experiment must be repeated with the final stimulation protocol.

3.4.4 Potential reasons for the lack of sensitisation effect

Overall, out of all sensitizer compounds we tested, we found weak sensitisation only with 5 µM PGE2 and 2.5 µM inflammatory soup. This was unexpected, as all tested sensitizers have been shown in the literature to sensitise sensory neurons *in vitro* and *in vivo* (Huang, Zhang and McNaughton, 2006; Basbaum *et al.*, 2009). There are several possible reasons for the lack of sensitisation observed in our setup, including analysis method, stimulation and incubation parameters as well as the nature of activity trigger.

Our data shows a high degree of variability, with a large spread of neuronal response changes. This could be due to our method of analysis. Our method corrects for signal degradation and baseline drift by calculating the difference between minimum and maximum values during each stimulation period instead of the absolute calcium indicator signal. The response to the same strength of field stimulation for the same neuron is then compared before and after the addition of a sensitizer. This difference in responses is then expressed as a percentage of the first response, with values less than 100% indicating a decreased neuronal response following addition of the sensitising agent. However, this can lead to small changes in calcium signal producing large differences in percentage response. For instance, a neuron that did not respond to a stimulus before the addition of the sensitizer but responded to the same stimulation after the addition of the sensitising agent. If the arbitrary change in the Fura-2 AM

signal is 0.015 before and 0.45 after the sensitizer addition, the difference between these two values is 0.435. By taking the first response as a 100%, the percentage change is $\frac{0.45}{0.015} \times 100 = 3000\ \%$ for this neuron. Using the percentage change for each neuron as the final readout increases the sensitivity of the analysis, making sure that even small changes in neuronal responses are detected. However, the caveat of the increased sensitivity is that it can also increase the data variability by potentially misrepresenting the extent of the change in neuronal responses, making small differences appear greater. This could result in masking a potentially significant difference.

It is also possible that these sensitizers do not potentiate neuronal responses to electrical field stimulation. All of the compounds we used in our experiments have been shown to potentiate neuronal responses to chemical stimuli. Most of these compounds were shown to exert their effect through modulation of the TRPV1 channel, so the majority of studies that use these sensitizers also use capsaicin as the trigger for neuronal activity (Chuang *et al.*, 2001; Shu and Mendell, 2001; Moriyama *et al.*, 2005; Ohta *et al.*, 2006; Sugiura *et al.*, 2014). We used electrical field stimulation, which does not require the activation of TRPV1 to trigger neuronal activity. Thus, it might not exhibit robust sensitisation as seen in studies using capsaicin. Interestingly, PGE2 has been shown to exert its sensitising effect by lowering the depolarisation threshold for the action potential generation as well as increasing resting membrane potential (Momin and McNaughton, 2009). As this effect is independent of TRPV1, it could explain the potentiation of neuronal activity we see with PGE2 and IS. However, it would not explain why this was not potentiated at higher concentrations.

There are other possible reasons for the lack of sensitization. Firstly, as these experiments were exploratory, we used a small sample size. In future experiments, larger animal and coverslip numbers may help improve the reliability of the data. Secondly, the strength of electrical field stimulation in a cell bath is influenced by the electrode arrangement as well as the amount of liquid in the bath. It is possible that non-uniform strength of electrical

stimulation resulted in biased neuronal activation. We attempted to control these factors by ensuring identical liquid volume for all experiments as well as using reusable electrode holders to keep electrodes in the same arrangement. Furthermore, it is possible that stimulation parameters were suboptimal for DRG stimulation. Unfortunately, it was beyond this thesis to further optimise each individual parameter used.

Longer incubation times may enhance the sensitising effect of the potential sensitizers on the sensory neurons, making it detectible with electrical field stimulation. Finally, a different sensitisation protocol that does not rely on acute sensitizer treatment may be required. For example, DRG neurons have been shown to become sensitised to mechanical and electrical stimuli after spinal nerve ligation (Djouhri, 2016). It may be beneficial to assess whether this effect is present in response to electrical field stimulation, and whether it can be used as a sensitisation model for studying effects of various compounds.

3.4.5 Conclusion

In this chapter, we used electrical field stimulation as a trigger for neuronal activity during *in vitro* calcium imaging. We used this setup to assess performance of virally-delivered GCaMP6s, which was capable of accurately reporting neuronal activity. We also used electrical field stimulation of DRG cultures to create a model of neuronal sensitization by applying several known sensitizer compounds and assessing their effects on the electrical field stimulation-triggered neuronal response. Only 5 µM PGE2 and 2.5 µM inflammatory soup enhanced neuronal response. The rest of the sensitizers did not produce sensitization. This may be due to the TRPV1-dependant mechanism of sensitisation produced by these compounds, which is not targeted by the electrical field stimulation.

Chapter 4: Exploring the use of AAV9-delivered functional transgenes *in vivo*

4.1 Introduction

AAV vectors have been used to deliver a variety of transgenic tools, in addition to relatively simple fluorophores whose use as markers has been described in chapter 2. Among these tools are transgenes that can be used to visualise neuronal activity in real time (such as GECI), control gene expression (Cre/Dre/Flp/CRISPR/ZFN etc.), and control neuronal activity (opto/chemogenetic tools such as DREADDs). All these tools are invaluable for studying the physiology and pathology of the nervous system, including peripheral and central pain circuitry and signal processing. Below, a number of these tools are described, and I present the results we obtained when using them in synergy with the intrathecal delivery method described in chapter 2.

4.1.1 Real-time visualisation of neuronal activity *in vivo*

Dysregulation of the neuronal activity is prominent in many neurological disorders, including chronic pain (Basbaum *et al.*, 2009; Todd, 2010). There are numerous studies that successfully used *in vivo* electrophysiological recordings in the context of pain (Holle, Obermann and Katsarava, 2009; Lelic, 2014; Lin *et al.*, 2014; Zhao *et al.*, 2014; Kucyi and Davis, 2017; Bell and Dallas, 2018). This approach, however, has several drawbacks, including its inability to simultaneously record the activity of a large number of neurons with high spatial resolution, as well as the tissue damage caused by electrode insertion (Anderson, Zheng and Dong, 2018).

These drawbacks can be overcome by using GECI that provide a visual readout of calcium transients associated with activity. Currently, the most popular type of GECI is GCaMP, which is a single-fluorophore calcium indicator that changes its fluoresce in response to a rapid increase in the intracellular calcium concentration that in a neuron is associated with an action potential (Nakai, Ohkura and Imoto, 2001; Grienberger and Konnerth, 2012; Yingxiao Chen *et*

al., 2013; Girven and Sparta, 2017). The use of GECI and GCaMP *in vitro* was introduced in chapter 3, however these tools can also be used *in vivo*, and they have several advantages over *in vivo* electrophysiological approaches. Firstly, the use of GCaMP eliminates the need for electrode insertion into the neuron or the surrounding tissue. Secondly, it allows simultaneous recording from a large number of neurons. The exact number of cells recorded is dependent on the field of view, which varies depending on the imaging setup and GCaMP expression. However, several studies that used GCaMP to elucidate pain-related neuronal activity have reported simultaneous recordings from over 100 DRG neurons (Emery *et al.*, 2016; Kim *et al.*, 2016; Chisholm *et al.*, 2018). Lastly, as GCaMP is a transgenic tool, its expression can be tailored to specific cell types. This can be achieved by using specific promoters, such as *Thy1* for neuronal expression (Q. Chen *et al.*, 2012), *Pirt* promoter for specific expression in DRG and TG neurons (Y. S. Kim *et al.*, 2014) and *Aldh1l1* promoter for astrocyte-specific expression (Srinivasan *et al.*, 2016).

Global and cell-specific GCaMP expression can be achieved by using transgenic lines (Zariwala *et al.*, 2012; Dana *et al.*, 2014; Sato *et al.*, 2015; Anstötz, Lee and Maccaferri, 2018). However, a large number of studies instead use AAV vectors to deliver GCaMP to the cells of interest (T. W. Chen *et al.*, 2013; Yu *et al.*, 2016; Ozbay *et al.*, 2018; Yoshida *et al.*, 2018). Using AAVs for GCaMP delivery offers several advantages. For instance, transgenic lines require a lot of time and resources to expand and maintain. Furthermore, as promoters for targeting different cell types are still under development, some cell types do not yet have a suitable promoter for cell-specific GCaMP expression in mice. This is a major confounding factor in studies that require expression of a transgene in a subset of neurons, for example DRG or spinal cord neurons. This can be circumvented by using local administration of AAVs. Depending on the delivery method, it is possible to restrict GCaMP expression only to the cells of interest. For instance, intramuscular injection in mice have been used to image axons of sensory afferents in the peroneal nerve (Anderson *et al.*, 2018). Direct injection into the dorsal horn of the spinal cord has been used to express GCaMP6f in mice and image activity in the spinal cord neurons in

awake behaving animals (Sekiguchi *et al.*, 2016). Therefore, viral delivery of GCaMP could be an asset for studying nociceptive circuitry. As shown in chapter 2 intrathecal injection of AAV9-eGFP results in transduction of the majority of L4 DRG neurons. Intrathecal delivery of AAV9-GCaMP6s could make it possible to image responses of these neurons to various stimuli.

4.1.2 Control of gene expression with transgenic tools

Every living cell has a specific gene expression profile at any one time. Cell gene expression profiles change to adapt to different requirements, e.g. maturation, proliferation and apoptosis (Hamatani *et al.*, 2004; Reik, 2007; Sato *et al.*, 2008). Furthermore, various external factors like chemical messengers, temperature fluctuations, external stress, damage and neuronal activity all influence the expression profile (Reik, 2007). Changes in gene expression are part of the normal functioning of the cell, for instance upregulation of genes in neurons during late-phase long-term potentiation (Nedivi *et al.*, 1993; Lee *et al.*, 2005). However, some changes can be a result of pathology, such as increased expression of voltage-gated sodium channels in sensory neurons after nerve injury (Cardoso and Lewis, 2017). These changes often contribute to symptoms of pathology, e.g. upregulation of HCN1 and HCN3 channels in IB4 negative Aδ afferents leads to increased I_h current, which brings the membrane potential close to the action potential threshold and makes the neuron hypersensitive (Liu *et al.*, 2015). Furthermore, preventing gene upregulation in pathology may attenuate the symptoms (Sun *et al.*, 2018).

For the gene to be expressed, it first has to be transcribed from DNA to mRNA, and then translated into a protein. Apart from direct replacement of the gene's DNA sequence, there are several transgenic tools that can influence gene expression at various points in this pathway. Recombinases, such as Cre, can excise parts of the gene's DNA that are flanked by pre-inserted LoxP sites. Excision can disrupt gene transcription and result in a protein that is truncated or misfolded, and is not functional (Hoess, Ziese and Sternberg, 1982; Hoess, Wierzbicki and Abremski, 1986). The recently developed CRISPR/Cas9 system can be used to

excise specific parts of the DNA, effectively silencing genes (Doudna and Charpentier, 2014; Sander and Joung, 2014). Moreover, RNA interference tools, such as shRNA or miRNA can cause degradation of the gene's mRNA before it can be translated (Fire *et al.*, 1998; Boudreau, Martins and Davidson, 2009).

These genetic tools can be controlled so that they are expressed only in a specific cell type or in a particular temporal pattern. For instance, by using cell-specific promoter it is possible to restrict expression of Cre recombinase to specific cell types, such as small and medium diameter sensory fibres using the $Na_v1.8$ promoter (Stirling *et al.*, 2005). Furthermore, it is possible to achieve temporal control over Cre expression, e.g. by fusing the Cre recombinase with a mutated binding domain of the human oestrogen receptor (ERT2) which sequesters it in the cytoplasm. Upon tamoxifen interaction with CreERT2, the Cre enters the nucleus and excises the DNA sequence between the LoxP sites (Feil *et al.*, 1997; Feil, Valtcheva and Feil, 2009). Therefore, it is possible to exert temporal control over Cre activity through timing of tamoxifen administration. Using CreERT2 with transgenic lines that have regions of interest flanked by the LoxP sites has made it possible to study genes whose knockout *in utero* with a normal Cre is lethal, or severely reduces animal lifespan. For instance, conventional knockout in mice of histone deacetylase 4 protein (HDAC4) results in severely reduced life expectancy due to developmental defects (Vega *et al.*, 2004; Majdzadeh *et al.*, 2008). However, it is possible to study the importance of this gene in adult pain sensation by using the CreERT2 system (Crow *et al.*, 2015). Lastly, it is possible to place a STOP cassette flanked by LoxP sites before a gene of interest or a transgene. In that case, administration of Cre will excise the STOP signal, allowing gene expression (Sauer, 1998). This can be used in conjunction with transgenic lines that express Cre recombinase in specific cell types to achieve selective gene expression in these cells (Sauer, 1998).

Gene expression can be readily manipulated using transgenic lines that already express these transgenic tools. However, the desired transgenic lines are not always readily available as

mentioned above. Moreover, temporal regulation of these tools is not always without side-effects. For instance, tamoxifen used in Cre-ERT2 system has been show to induce cellular stress in the nervous system (Denk *et al.*, 2015). Delivery of Cre recombinase using AAV vectors is one way to overcome these drawbacks. By varying the delivery time of AAV it is possible to achieve temporal control over expression of the Cre without the use of tamoxifen (see chapter 2.3). Furthermore, it is possible to express the Cre in cells of interest by using cell-specific promoters and injecting AAV vectors at the desired location. For instance, intraganglionic and intrathecal AAV injections in rats have been successfully used to deliver shRNA to silence $Na_v1.3$ in dorsal horn neurons and DRG neurons (Samad *et al.*, 2013). Injection of AAV-Cre into the brain has been shown to successfully knock out P phosphatase and tensin homolog (PTEN) in PTEN-floxed mice (Yang *et al.*, 2015). Furthermore, intrathecal injection of AAV5-Cre in $Na_v1.6$-floxed mice resulted in $Na_v1.6$ knockdown and attenuation of neuropathic pain behaviour (Chen *et al.*, 2018).

It is important to note, however, that using AAVs for delivery of these transgenic tools for gene expression modulation is not without pitfalls. The proportion of transduced cells depends heavily on the method of delivery and is rarely 100% (see chapter 2.3). This may obscure the effect of gene knockout by only knocking the gene out in some, but not all, cells. Therefore, it is essential to use the most efficient delivery strategy possible.

4.1.3 Control of neuronal activity with transgenic tools

One last example of a method of neural function interrogation in health and disease is to directly control neuronal activity by activating or silencing neurons. Modulating neuronal activity can help elucidate function of a particular neural circuit, or can counteract or exacerbate existing pathology, making it useful for identifying potential therapeutic targets (Roth, 2016; Wiegert *et al.*, 2017). This can be achieved with the use of optogenetic and chemogenetic tools. Optogenetic tools are activated by light of a particular frequency and undergo changes that result in alterations in the cell's physiology, most commonly changing

membrane conductivity and depolarising or hyperpolarising the cell (Boyden *et al.*, 2005; Chow *et al.*, 2010). Optogenetic tools are commonly used in the neuroscience field, including pain research, to interrogate circuit function and to modify an underlying pathology (Xie, Wang and Bonin, 2018). For instance, by expressing channelrhodopsin or archaerhodopsin in primary nociceptors it is possible to elicit or inhibit nocifensive behaviour, respectively, by shining light of a specific frequency onto the rodents skin (Daou *et al.*, 2013; Li *et al.*, 2015). Optogenetic tools respond to light stimuli within milliseconds, and are only active as long as the stimulus is present (Rein and Deussing, 2012). However, this may make optogenetic tools less viable for prolonged neuronal activity modulation. In addition, use of optogenetics requires a complex set up for light delivery, that depending on the target, may have to be implanted into the animal (Towne *et al.*, 2013; Montgomery *et al.*, 2015). In studies where access to the target tissue is restricted or that require prolonged activation of a large number of cells, chemogenetics may be a better option.

There are many various chemogenetic tools, but they all operate in a similar way. All of them are receptors that are engineered to respond to a single exogenous ligand (Sternson and Roth, 2014). When their respective ligand binds to these receptors, one type can initiate a secondary messenger cascade that in turn will depolarise or hyperpolarise a neuron (Alexander *et al.*, 2009). Another type of chemogenetic tool are ligand-gated ion channels (LGICs). Created by mutating the ligand binding domain of α7 nicotinic acetylcholine receptor (nAchR) to respond only to specific exogenous molecules, LGICs open an ion pore upon ligand binding, allowing flux of ions across the membrane (Magnus *et al.*, 2011). By transplanting the nAchR ligand binding domain to other ion channels it is possible to influence the specific ions that LGICs are permeable to, therefore enabling both excitatory and inhibitory LGICs (Magnus *et al.*, 2011; Wiegert *et al.*, 2017). Another type of a potent chemogenetic tools is an engineered invertebrate-derived Ligand-Gated Chloride Channel (LGCC). LGCC allows ion flux across the membrane like the LGICs but does not rely on the nAchR domain to be activated. Instead, this glutamate-activated chloride channel that is inactive in mammals has been mutated to

respond only to Ivermectin (IVM), an anti-malaria drug that is inert in mammals (Cully *et al.*, 1994; Li, Slimko and Lester, 2002). Upon activation, LGCC opens an ion pore and allows chloride ions to pass across the cell membrane. In most neurons, this creates an inward flux of chloride ions, hyperpolarising the neuron and effectively silencing it (Slimko *et al.*, 2002). An improved version of LGCC was developed in 2013, when Frazier and colleagues improved its structure by introducing two point-mutations that substantially improved sensitivity to IVM, as well as reduced degradation of LGCC protein within the cell (Frazier, Cohen and Lester, 2013).

Both optogenetic and chemogenetic tools can be expressed using transgenic mouse lines, but most commonly these tools are delivered via viral vectors. As previously described, viral vectors can provide spatial and temporal control over the transgene expression. AAV vectors have been successfully used to target specific groups of cells, for instance the entorhinal cortex projection neurons (Ge *et al.*, 2017). Furthermore, tighter restriction of expression can be made by using the Cre-dependent viral vectors and Cre-expressing transgenic lines, for example to target parvalbumin-expressing interneurons or GABAergic inhibitory neurons (Chandrasekar *et al.*, 2018; T. Zhang *et al.*, 2018).

4.1.4 Chapter Aim

In this chapter we show the assessment of GCaMP6s expression in DRG neurons after intrathecal infusion of AAV9-GCaMP6s, as well as characterisation of GCaMP6s responses to electrical stimuli, recorded using an *in vivo* calcium imaging setup. For a more extensive study, please see Chisholm et al. 2018. We were also interested in elucidating whether intrathecal delivery of AAV9-Cre using the method described in chapter 2 results in Cre expression that is sufficient to be useful in further studies. We investigated the activity of virally-delivered Cre in the TdTomato-floxed-STOP-cassette mice. Finally, we also investigated whether our method of viral delivery would be suitable for expressing chemogenetic tools in DRG neurons, and whether the expression level is high enough to be able to influence nocifensive behaviour. This

has been done in collaboration with Dr Weir of Prof Bennett's group at the Oxford University

Here we present data that is relevant for this thesis. For full study, please see Weir et al. 2017.

4.2 Methods

4.2.1 Animals

All procedures were in accordance with the UK Home Office guidelines and Animals (Scientific Procedures) Act 1986. Wild type C57Bl/6J mice, 6-8 weeks old, were obtained from Charles River or University of Oxford Breeding Unit. Transgenic mice were bred in King's College London Biological Services Unit. Initially, 2 GCaMP6s-floxed-STOP-cassette heterozygous males were obtained from JAX (stock number 024106). These males were used to establish a homozygous colony. Homozygous 3-5 months old GCAMP6s-floxed-STOP-cassette males and females were used for *in vivo* calcium imaging experiments. TdTomato-floxed-STOP-cassette mice were obtained from JAX (stock number 007909).

4.2.2 Genotyping of GCaMP6s-floxed-STOP-cassette mice

To genotype animals from the GCaMP6s-floxed-STOP-cassette colony, ear biopsies were performed. Biopsies were dissociated in 450 µl of earclip lysis buffer (50 mM KCl, 1.5 mM $MgCl_2$, 10 mM Tris, 0.45% Tergitol, 0.45% Tween-20) and 15 µl of 10mg/ml Proteinase K on a heat block at 55 °C for 3 hours. Samples were then heated up to 95 °C for 15 minutes to inactivate the Proteinase K. Samples were either stored at 4 °C for later processing or directly used in a PCR reaction. PCR plates were used for genotyping. Each reaction contained 12.35 µl of MQ H_2O, 4 µl of 5x buffer, 0.4 µl of 200nM nucleotide mix (Promega, U1330), 1 µl of primers, 0.25 of Taq Polymerase (Promega, M3175) and 2 µl of biopsy DNA. The plate was sealed and placed in a thermocycler. The cyclic program was as follows: 95 °C for 5 minutes, 35 cycles of 95 °C for 30 seconds, 58 °C for 30 seconds, 72 °C for 30 seconds and then 72 °C for 7 minutes. Completed PCR reactions were run on a 2% w/v agarose (Sigma, A9539) gel with $4x10^{-5}$ % v/v ethidium bromide (Sigma, E1510-10ML). DNA bands were visualised under UV light. Primers used were:

GGGAGTTCTCTGCTGCCTCCT – forward wild-type primer

CTGTGGGAAGTCTTGTCCCTCCAA - reverse wild-type primer

GCATCAAGGCGAACTTCCAC – forward GCaMP6s primer

CTCAGGTAGTGGTTGTCGGG – reverse GCaMP6s primer

4.2.3 Intrathecal injections

Intrathecal delivery procedure of AAV9-GCaMP6s and AAV9-Cre was identical to that of AAV9-eGFP described in chapter 2 (**2.2.4**) and performed by me. Injections of AAV9-GluCl were performed together with Dr Weir. Transduction efficiency quantification for different times post injection and neuronal sub-population transduction was assessed by me.

4.2.4 *In vivo* procedure

For *in vivo* calcium imaging, exposure surgery and imaging was performed by Dr K. Chisholm, as described in (Chisholm *et al.*, 2018). Briefly, mice were anaesthetised with 12.5% w/v urethane in saline. Initially 37.5 mg urethane was injected intraperitoneally. Subsequent doses were given until the mouse reached surgical depth of anaesthesia, which was then monitored throughout the procedure. Mice were kept at 37 °C and hydrated with 0.5 ml sterile saline subcutaneously. A tracheal catheter was used to improve survival. An incision was made over the L3, L4, and L5 DRGs and the underlying muscle removed. Next, the bone around the L4 DRG was carefully removed. The animals were rotated to achieve a more horizontal orientation of the L4 DRG, which was then stabilised by clamping it to the neighbouring vertebrae using spinal clamps. DRG and exposed spinal cord were covered with silicone elastomer to prevent them from drying out. Then the animals were placed under the Eclipse Ni-E FN upright confocal/multiphoton microscope (Nikon). GCaMP6s signal in the L4 DRG was imaged using the 10x dry objective and 488 nm Argon ion laser.

4.2.5 *In vivo* imaging stimuli

Electrical stimulation was used to assess the sensitivity of GCaMP6s *in vivo*, fully described in (Chisholm *et al.*, 2018). Electrical stimuli were applied directly to the ipsilateral sciatic nerve using custom-made cuff electrodes with Teflon coated silver wire. A biphasic stimulator was used to deliver individual or trains of stimuli at varying frequencies and intensities. Images

were processed and quantified using NIS Elements 4.30.01 (Nikon) and Fiji repack of ImageJ software. Cell bodies were selected, and their intensity measured in Fiji. Data were further processed by subtracting background signal and changes in fluorescence were calculated as a percentage of baseline fluorescence, 100% representing a signal that has an intensity of double the baseline fluorescence. To determine whether a neuron responded to a particular stimulus, a cut-off was used. The response had to be 70% above the baseline + 4 standard deviations for it to be counted as positive.

4.2.6 GluCl transgene study

Adapted from (Weir *et al.*, 2017). Intrathecal injections were performed as described in **2.2.4**, with the only difference being that the animals were injected with 8 µl of vector cocktail, containing 4 µl AAV9-GluClα and 4 µl AAV9-GluClβ. 3 weeks after injection, mice were used for histological or behavioural analysis. Ivermectin was used to activate GluCl channel. Intraperitoneal injection of 1 µl/g of 0.5 % ivermectin in sterile propylene glycol was performed. Hargreaves test was performed to assess thermal thresholds. An infrared light source was applied to the plantar surface of each hindpaw. Latency to withdrawal was measured three times per paw and averaged. Von Frey test was used to assess the mechanical threshold. The test was performed as described in **2.2.8**. Tissue preparation for immunohistochemistry was identical to that described in **2.2.7**.

Detailed electrophysiological methods can be found in (Weir *et al.*, 2017). Briefly, for *ex vivo* cell conductance assessment, DRG neurons were extracted from mice injected with AAV9-GluClα and AAV9-GluClβ or AAV9-GluClβ alone. To assess conductance, voltage clamp ramp from -40mV to -90mV was used. Conductance was then derived from the linear part of the current response curve. For neuronal excitability assessment, the rheobase value was used. To determine the rheobase, cells were slowly depolarised from their resting membrane potential (-60mV) by a depolarising current of increasing magnitude until an action potential was elicited. Cell were then divided into three groups based on their rheobase value, compared to the value

of the control group (mean = 160.1 ± 160.6 pA): excitable (<3 SD above the control group rheobase), partial silencing (3-10 SD above the control group rheobase) and full silencing (>10 SD above the control group rheobase).

4.3 Results

4.3.1 AAV9-GCaMP6s is effective in transducing DRG neurons *in vivo*

To explore the use of various functionally interesting transgenes we first had to establish their transduction efficiency *in vivo*. The first transgene we investigated was GCaMP6s, a member of GECI. We assessed the transduction pattern 30 and 14 days after intrathecal delivery of AAV9-GCaMP6s. Each injection consisted of 5 µl of AAV9-GCaMP6s, with a titre of $1.69x10^{13}$ gc/ml. The transgene was detected in the majority of L4 DRG neurons 30 days (64.98% ± 6.91%, n = 5, **Fig. 4.1 a,d**) and 14 days (51.82% ± 6.87%, n = 4, **Fig. 4.2 a,c)** after injection. Transduction in L4 DRG 30 days after AAV9-GCaMP6s injection was similar to that observed with AAV9-eGFP (Two-tailed t-test, p = 0.71, n = 5, **Fig 4.1 d**). In addition, although the transduction in the L4 DGR 14 days after AAV9-GCaMP6s injection was lower than that after 30 days, there was no significant difference between them (Two-tailed t-test, p = 0.227, n = 5-8, **Fig. 4.2 c**). There was little to no transduction in thoracic and cervical DRGs at 30 and 14 days (0.62% ± 0.4% and 9.7% ± 7.45%, respectively, for 30 days and 3.88% ± 3.68% cervical for 14 days, **Fig. 4.1 b-d, 4.2 b, c**).

We further investigated whether AAV9-GCaMP6s has a preference for transduction of specific DRG sub-populations. We found no significant difference between the distribution of GCaMP6s-positive neurons across CGRP, IB4 and NF200 neuronal sub-populations when compared to the distribution of all L4 DRG neurons across these sub-populations (One-way ANOVA with Tuckey's multiple comparisons correction p = 0.82 (CGRP), p > 0.99 (NF200), p = 0.13 (IB4), n = 4, **Fig. 4.3 a-d**). These results were similar to those obtained with AAV9-eGFP in chapter 2, suggesting that AAV9-GCaMP6s has a transduction efficiency comparable to that of AAV9-eGFP.

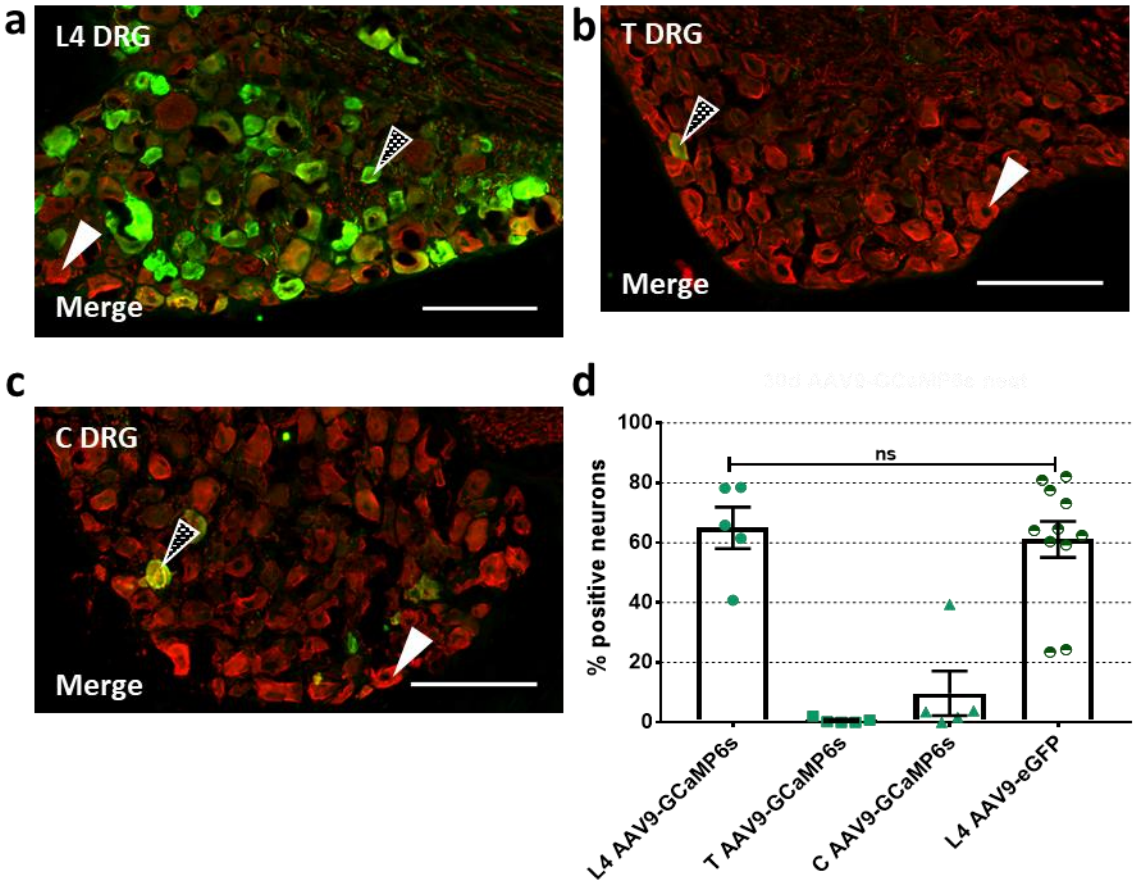

Figure 4.1 – Intrathecal delivery of AAV9-GCaMP6s results in DRG neuron transduction after 30 days comparable to that of AAV9-eGFP. *Animals were injected with 5 µl AAV9-GCaMP6s at 1.69x10^{13} gc/ml. Representative IHC images of* ***a)*** *lumbar 4,* ***b)*** *thoracic and* ***c)*** *cervical DRG sections. Sections were stained for ß-III-Tubulin (red) and GFP (green). Example of transduced and non-transduced neurons are marked with black and white arrows respectively. Scale bar = 100 µm* ***d)*** *quantification of transduction efficiency for lumbar 4 (64.98% ± 6.91%, n = 5), thoracic (0.62% ± 0.40%, n = 5) and cervical (9.7% ± 7.45%, n = 5) DRGs, as well as the transduction in L4 DRG after AAV9-eGFP administration (61.12% ± 6.06%, n = 11). There was no significant difference in the number of transduced L4 DRG neurons for AAV9-GCaMP6s and AAV9-eGFP (Two-Tailed t-test, p = 0.71, n = 5 for AAV9-GCaMP6s and 11 for AAV9-eGFP).*

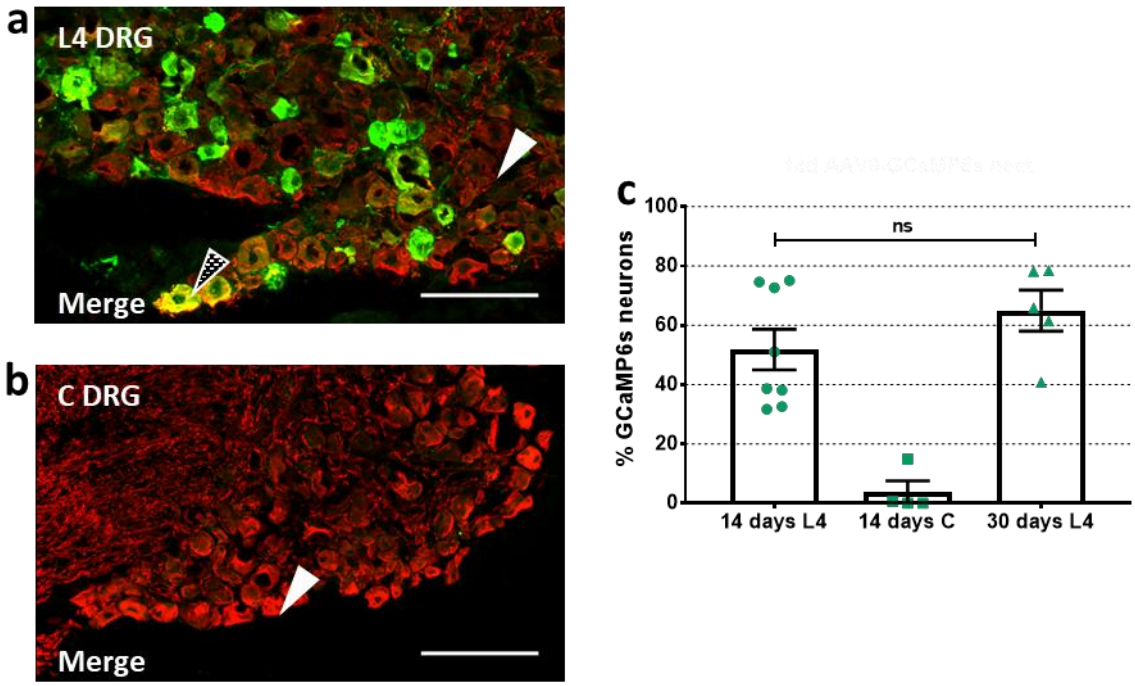

Figure 4.2 – Transduction with AAV9-GCaMP6s after 14 days is not statistically different from 30 days. *Animals were injected with 5 µl AAV9-GCaMP6s at 1.69x10^{13} gc/ml. Representative IHC images* ***a)*** *lumbar 4,* ***b)*** *cervical DRG sections. Sections were stained for β-III-Tubulin (red) and GFP (green). Example of transduced and non-transduced neurons are marked with black and white arrows respectively. Scale bar = 100 µm.* ***c)*** *Quantification of transduction efficiency for lumbar 4 (51.82% ± 6.87%, n = 8), cervical (3.88% ± 3.68%, n = 4) 14 days and L4 DRG 30 days after AAV9-GCaMP6s administration (64.98% ± 6.91%, n = 5). The difference in transduction between 14 and 30 days was not statistically significant (Two-tailed t-test, p = 0.227, n = 5-8 animals).*

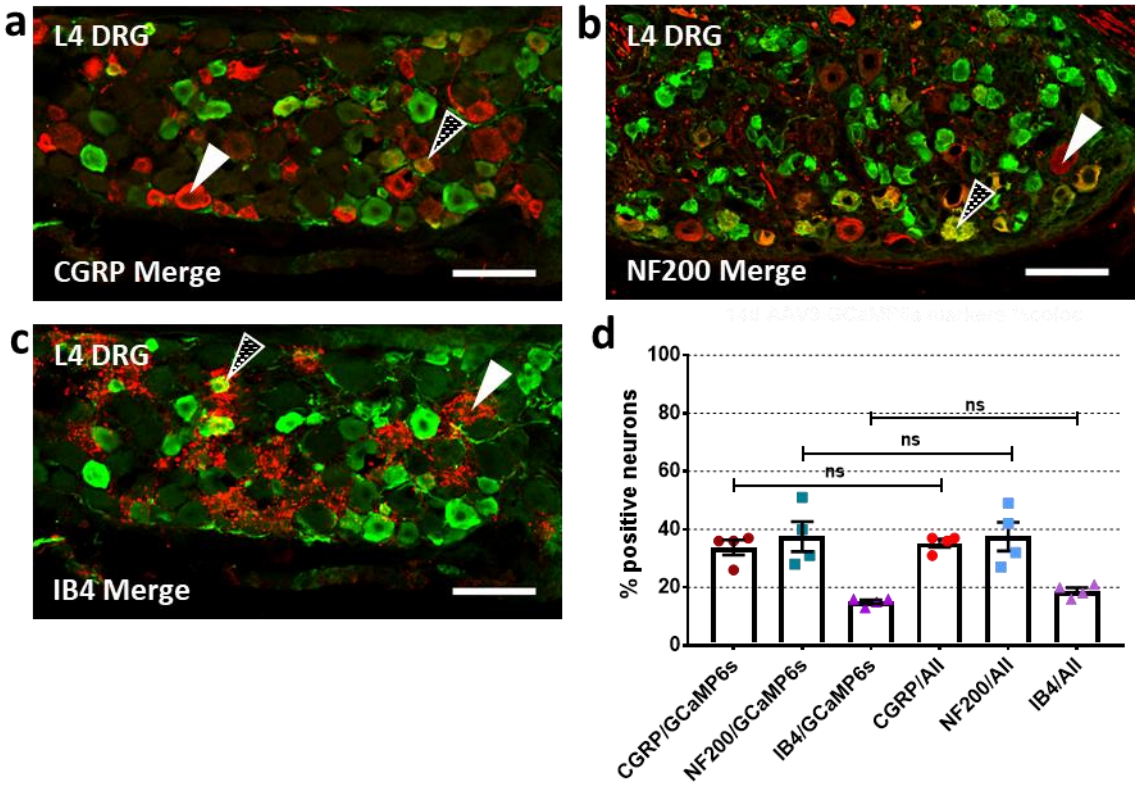

Figure 4.3 – AAV9-GCaMP6s is not selective for any specific DRG neuronal subpopulation. *Animals were injected with 5 µl AAV9-GCaMP6s at 1.69x10^{13} gc/ml. Representative IHC images of lumbar 4 DRG sections. Sections were stained for GFP (part of GCaMP6s, green) and* ***a)*** *CGRP (small diameter peptidergic population marker, red),* ***b)*** *NF200 (large diameter population marker, red) and* ***c)*** *IB4 (small diameter non-peptidergic population marker, red). Example of transduced and non-transduced neurons are marked with black and white arrows respectively. Scale bar = 100 µm.* ***d)*** *Quantification of marker labelling. There was no significant difference in the proportion of total neurons and GCaMP6s-positive neurons co-labelled with subpopulation markers (One-way ANOVA with Tukey's multiple comparisons, p = 0.82 (CGRP), p > 0.99 (NF200), p = 0.13 (IB4), n = 4).*

4.3.2 GCaMP6s retains its functionality and can be used for *in vivo* calcium imaging

Following confirmation of the transduction efficiency in L4 DRG neurons after intrathecal delivery of AAV9-GCaMP6s, we investigated the functionality of the GCaMP6s transgene for *in vivo* calcium imaging. All AAV9 delivery was done by me, however all *in vivo* calcium imaging was performed by Dr Chisholm. Below, the results relevant to this thesis are presented, however, detailed information about the experimental set up as well as full results can be found in Chisholm et al. 2018. Typically, mice were left to incubate for 14 days after intrathecal injection of AAV9-GCaMP6s before imaging. Preliminary experiments were performed to test the ability to detect the GCaMP6s signal in our *in vivo* calcium imaging set up. We used post mortem increase in the cytosolic calcium to test the signal strength and detection ability of the GCaMP6s fluorescence. There was a clear increase in fluorescence 30 minutes post mortem (**Fig. 4.4 b**).

After confirmation of the ability to visualize GCaMP6s in this system, we explored the use of external stimuli to drive neuronal activity. We used electrical stimulation of the sciatic nerve as a trigger and imaged ipsilateral L4 DRG to explore the limits of this set up. Electric stimuli at A-fibre (250 µsec duration and 250 µA amplitude) and C-fibre strengths (1 msec duration and 5 mA amplitude) were delivered to the ipsilateral sciatic nerve to see whether distinct populations of DRG neurons could be activated. We observed an increase in the number of active neurons that correlated with the increase in the stimulation frequency (**Fig. 4.5 a,b**). Interestingly, neurons responding to A-fibre stimulation also responded to C-fibre stimulation (**Fig. 4.5 c**). These results show that intrathecal administration of AAV9-GCaMP6s can be used to deliver functional GCaMP6s transgenes to the L4 DRG neurons. This technique can be used to study the neuronal activity *in vivo* in response to various stimuli in a wide variety of experimental conditions (expanded in Chisholm et al. 2018).

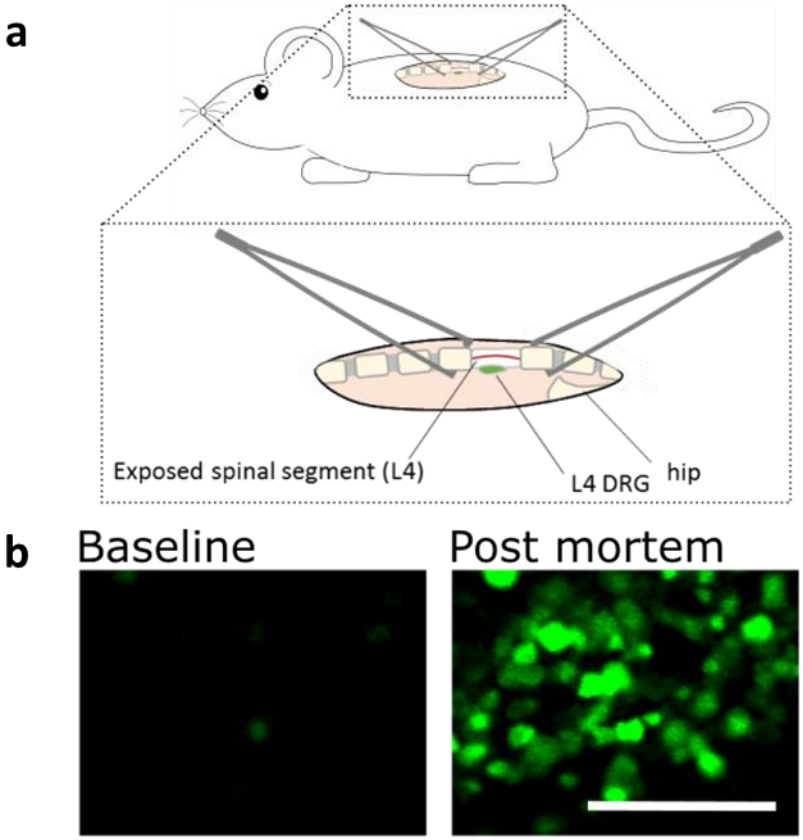

Figure 4.4 – Example of the in vivo experimental set up and GCaMP6s response in AAV9-GCaMP6s injected mice. *Animals were injected with 5 µl AAV9-GCaMP6s at 1.69x10^{13} gc/ml 14 days before in vivo calcium imaging.* ***a)*** *Diagram of the exposure procedure to access L4 DRG for confocal imaging. Preparation was stabilised by clamping the vertebra on either side of the exposure.* ***b)*** *Example of GCaMP6s fluorescence in DRG neurons at baseline and post mortem. Scale bar = 200 µm. Figure adapted from* (Chisholm *et al.*, 2018).

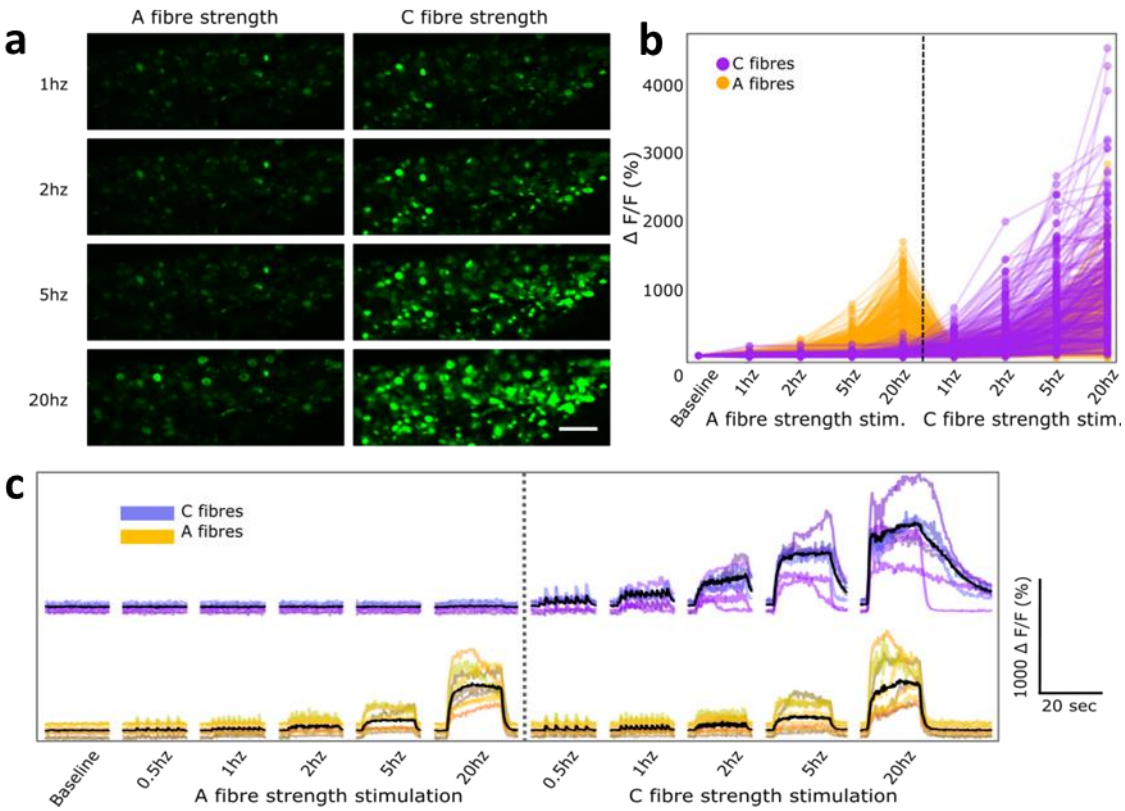

Figure 4.5 – Electrical stimulation of the sciatic nerve elicits robust frequency and intensity dependent GCaMP6s responses in DRG neurons in vivo. *Animals were injected with 5 µl AAV9-GCaMP6s at 1.69x10^{13} gc/ml 14 days before in vivo calcium imaging.* ***a)*** *DRG neuronal responses to sciatic nerve stimulation at various frequencies and A- and C-fibre strengths. Scale bar = 200 µm.* ***b)*** *Quantification traces of neuronal cell bodies responding to A- and C-fibre stimulation. Yellow traces indicate neurons responding both to A- and C-fibre strength, while purple traces indicate C-fibre strength responders only (n = 774 neurons, 6 mice).* ***c)*** *Example traces of neurons responding to C- and A-fibre stimulations. The black trace is the average response. Figure adapted from* (Chisholm *et al.*, 2018).

4.3.3 Transduction with AAV9-Cre is effective in regulating gene expression in transgenic animals

Another widespread transgenic tool that can be delivered using viral vectors is the Cre recombinase. Cre recombinase excises parts of the DNA that are flanked by LoxP sites, which can be used to delete critical segments of the genome to knock out a gene of interest (Van Duyne, 2015). Cre recombinase can also be used to excise a pre-inserted STOP sequence, thereby allowing temporal control over the transcription of a gene of interest. Cre delivery using AAV9 serves as an alternative to transgenic lines as a method of Cre expression.

To check whether Cre delivered via AAV9-Cre intrathecally retains its functionality, TdTomato-flanked-STOP-cassette mice were injected with 5 µl of AAV9-Cre at $3.29x10^{13}$ gc/ml, as described in chapter 2. This way, any cell that has a functional Cre recombinase in it will have the STOP cassette before the TdToamto gene excised, allowing expression of the TdTomato marker. We detected TdTomato protein in the majority of L4 (75.91% ± 2.6%, n = 4 **Fig. 4.6 a,d**) and minority of cervical (45.1% ± 10.85%, n = 4 **Fig. 4.6 c,d**) DRG neurons 30 days after the intrathecal administration of AAV9-Cre. We observed little signal in the thoracic DRGs (8.44% ± 1.65%, n =4 **Fig. 4.6 b,d**), so the overall transduction pattern of AAV9-Cre resembles that of AAV9-eGFP (**Fig. 2.4**).

Next, we injected AAV9-Cre into GCaMP6s-floxed-STOP-cassette mice to see if Cre-driven GCaMP6s expression is sufficient to be useful for *in vivo* calcium imaging. We found that transduction levels in the L4 and cervical DRGs were similar after 30-day (48.7% ± 6.1% and 0%, respectively, n = 4, **Fig. 4.7 a-c**) and 14-day post injection (45.95% ± 5.03% and 0%, respectively, n = 3, **Fig 4.8 a-c**), however the level of transduction was lower than that achieved with AAV9-GCaMP6s (**Fig 4.1 and 4.2**). One pilot GCaMP6s-floxed-STOP-cassette mouse injected with AAV9-Cre was used to test the performance of Cre-dependent GCaMP6s *in vivo* 14 days after AAV9 administration. We observed neuronal responses in ipsilateral L4

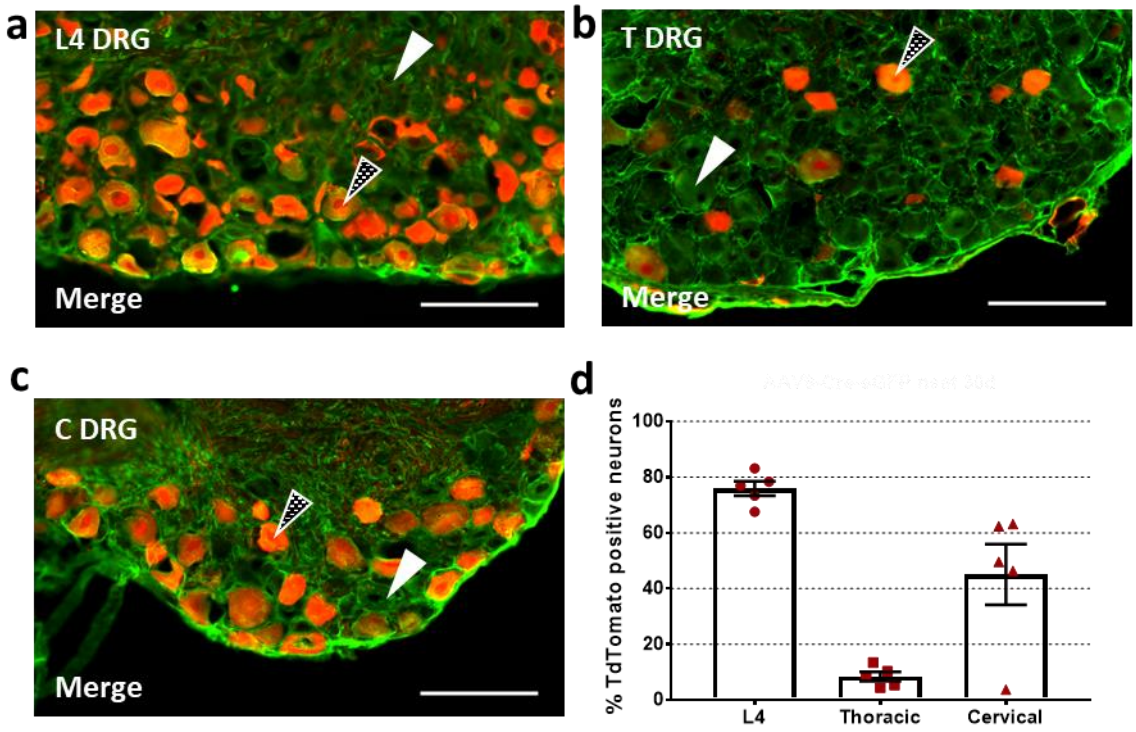

Figure 4.6 – Intrathecal delivery of AAV9-Cre into TdTomato-floxed-STOP-cassette mice results in TdTomato expression in DRG neurons after 30 days. *TdTomato-floxed-STOP-cassette animals were injected with 5 µl AAV9-Cre at 3.29x10^{13} gc/ml. Representative IHC images of* ***a)*** *lumbar 4,* ***b)*** *thoracic and* ***c)*** *cervical DRG sections. Sections were stained for β-III-Tubulin (green) and RFP (part of TdTomato, red). Example of transduced and non-transduced neurons are marked with black and white arrows, respectively. Scale bar = 100 µm.* ***d)*** *Quantification of transduction efficiency for lumbar (75.91% ± 2.6%, n = 4), thoracic (8.44% ± 1.65%, n =4) and cervical (45.1% ± 10.85%, n = 4) DRGs.*

DRG to mechanical and thermal stimuli applied to the plantar side of the hindpaw (**Fig. 4.9 a-c**).

Interestingly, same neurons could be seen responding to more than one modality of stimulus

(**Fig. 4.9 d**), suggesting a degree of polymodality (expanded in Chisholm et al. 2018).

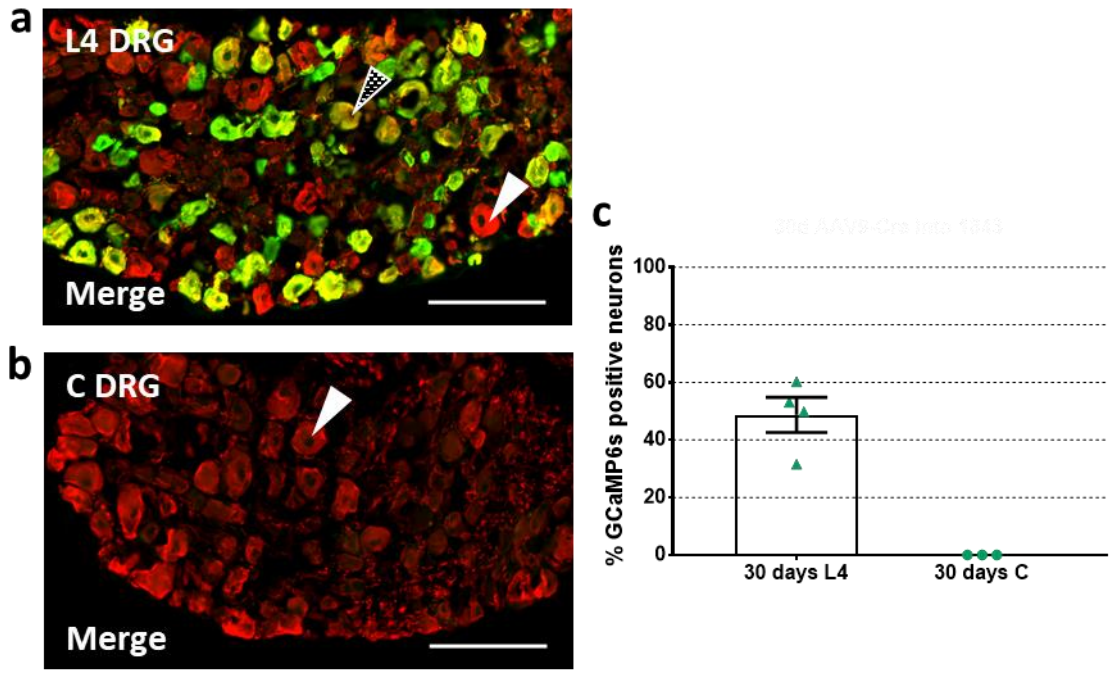

Figure 4.7 – Intrathecal delivery of AAV9-Cre into GCaMP6s-floxed-STOP-cassette mice results in GCaMP6s expression in DRG neurons after 30 days. *GCaMP6s-floxed-STOP-cassette mice were injected with 5 µl AAV9-Cre at 3.29x10^{13} gc/ml. Representative IHC images of* ***a)*** *lumbar 4 and* ***b)*** *cervical DRG sections. Sections were stained for β-III-Tubulin (red) and GFP (green). Example of transduced and non-transduced neurons are marked with black and white arrows respectively. Scale bar = 100 µm.* ***c)*** *Quantification of transduction efficiency for lumbar (48.7% ± 6.1%, n = 4) and cervical (0.0%, n = 3) DRGs.*

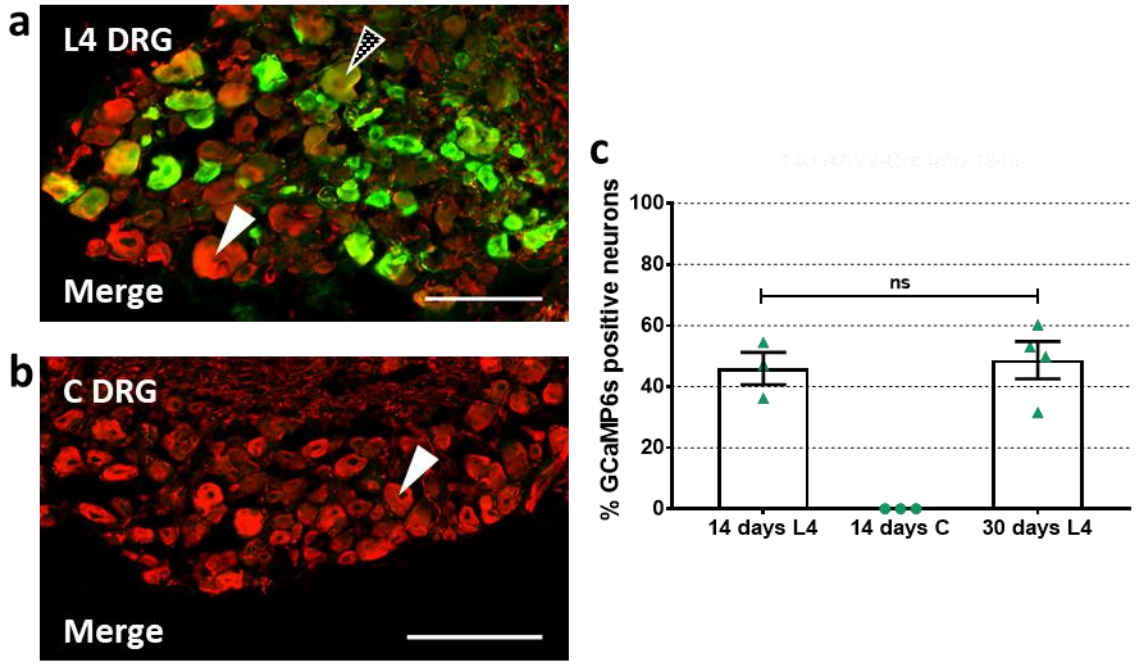

Figure 4.8 – Reducing the time after injection to 14 days does not change the transduction profile of AAV9-Cre in GCaMP6s-floxed-STOP-cassette mice. *GCaMP6s-floxed-STOP-cassette mice were injected with 5 µl AAV9-Cre at 3.29x10^{13} gc/ml. Representative IHC images of* ***a)*** *lumbar 4 and* ***b)*** *cervical DRG sections. Sections were stained for β-III-Tubulin (red) and GFP (green). Example of transduced and non-transduced neurons are marked with black and white arrows respectively. Scale bar = 100 µm.* ***c)*** *Quantification of transduction efficiency for lumbar 4 (45.95% ± 5.03%, n = 3), cervical (0.0% ± 0%, n = 3), as well as lumbar 4 DRG 30 days after AAV9-GCamP6s injection (48.7% ± 6.1%, n = 4). There was no significant difference in the percentage of transduced L4 DRG neurons between 14-day and 30-day after AAV9-GCaMP6s administration (Two-tailed t-test, p = 0.76, n = 3-4 animals).*

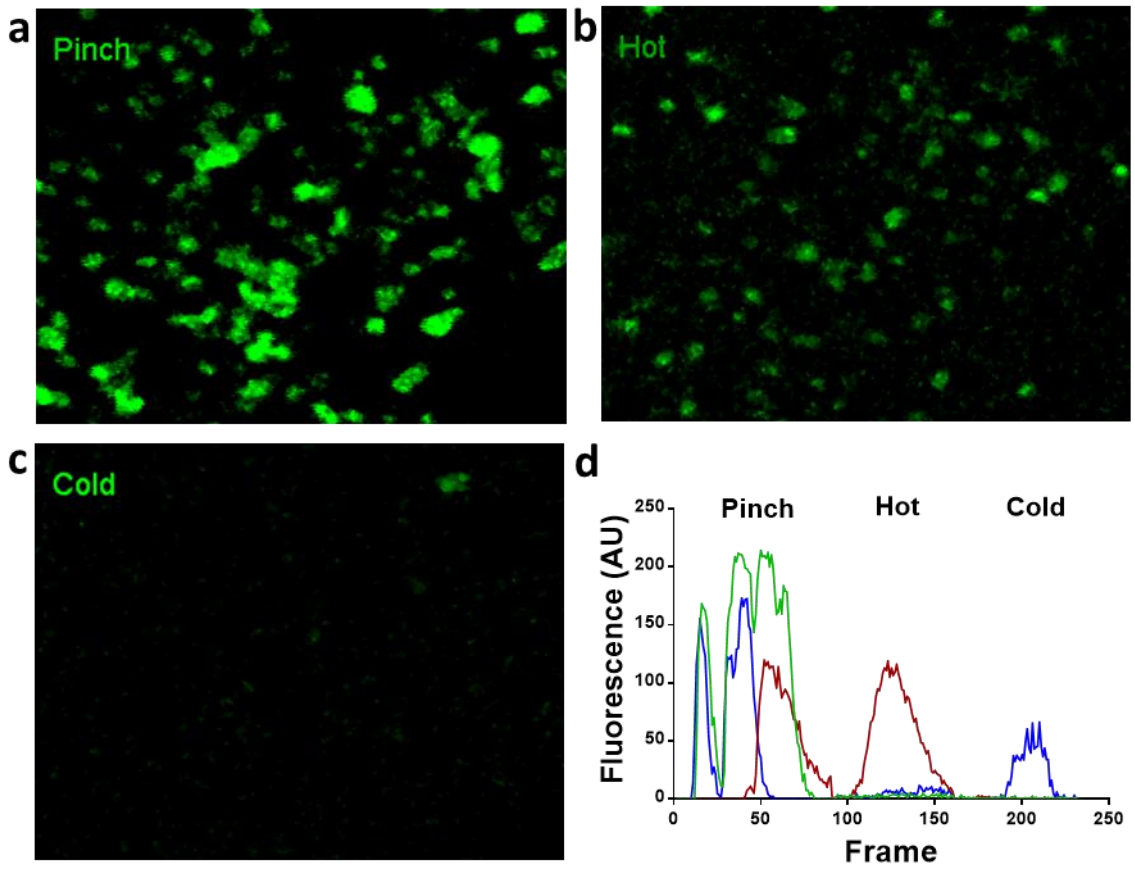

Figure 4.9 – Delivery of AAV9-Cre into homozygous GCaMP6s-floxed-STOP-cassette mice can be used for in vivo imaging 14 days after injection. *A homozygous GCaMP6s-floxed-STOP-cassette mouse was injected with 5 µl AAV9-Cre at 3.29x10^{13} gc/ml. Representative frames from an in vivo recording of the L4 DRG while the plantar surface of the ipsilateral hindpaw was being stimulated mechanically* ***a)*** *or* ***b, c)*** *thermally.* ***d)*** *Example traces of GCaMP6s signals of three neurons that responded to pinch only (green), pinch and hot stimulus (red) and pinch and cold (blue). Data provided by Dr Chisholm (unpublished).*

4.3.4 Intrathecal delivery of AAV9 can be used to express a functional engineered GluCl channel in L4 DRG neurons

Lastly, we explored the use of AAV vectors to deliver chemogenetic tools that can be activated by specific exogenous compounds and are capable of controlling neuronal activity. This work was done in collaboration with Dr Weir, and my contribution was intrathecal delivery of AAV9 vectors encoding the GluCl channel (see Weir et al. 2017 for the complete study). In this case we used intrathecal delivery of AAV9 to express an artificial GluCl channel in the L4 DRG neurons. This channel is activated by ivermectin (IVM), and upon activation facilitates an influx of chloride ions into the cytoplasm. In the DRG neurons, this leads to a large drop in membrane resistance that interferes with action potential generation and inhibits neuronal activity (Weir *et al.*, 2017). For a functional channel, both alpha and beta subunits must be present. Because of their size, they have to be delivered by two separate AAV9 vectors. We injected 8 µl of a mix of AAV9-GluClα and AAV9-GluClβ. Both GluCl channel subunits are expressed in 66.7% of L4 DRG neurons (**Fig. 4.10 a,b**). In cells expressing both subunits, when cultured, IVM treatment significantly increased membrane conductance, indicating that the GluCl channel is functional and responds to IVM. This effect is absent in vehicle-treated cells and in IVM-treated cells with only a beta-subunit (**Fig. 4.10, c**). To determine the effect of IVM treatment on the cell activity, current injections were used to determine the rheobase value of individual neurons. The cells were then classified based on their rheobase value. Values of < 3 SD above the mean of control (Naive β-only, mean = 160.1 ± 160.6 pA) were classified as excitable, 3-10 SD as partially silenced and > 10 SD as fully silenced (Weir *et al.*, 2017). Cells expressing both subunits of GluCl were readily silenced by IVM, while vehicle-treated or cells expressing one subunit only did not exhibit silencing (chi-squared test, $\chi^2 = 32.52$ with 6 degrees of freedom, n = 7-10 animals per group **Fig. 4.10 d**).

Importantly, the silencing that was seen *ex vivo* was also evident *in vivo*. IVM treatment increased the mechanical paw withdrawal threshold, as well as thermal threshold (**Fig. 4.11**).

This effect was not present in vehicle-treated animals or in those with only a single GluCl subunit (**Fig. 4.11**). These data suggest that viral delivery of chemogenetic transgenes can be used to study various aspects of DRG neurons, both in health and pathology, such as chronic pain (Weir *et al.*, 2017).

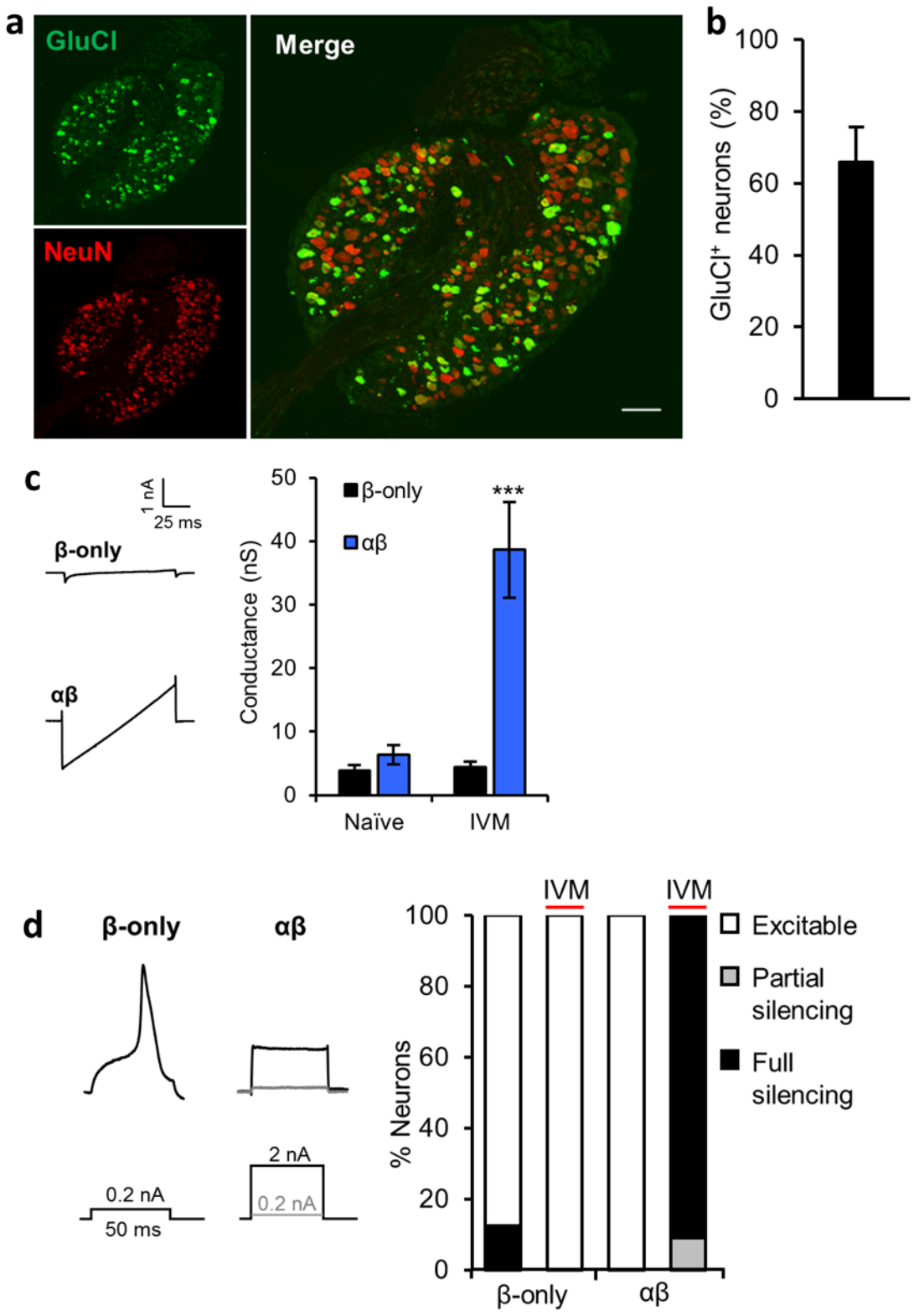

Figure 4.10 – Intrathecal delivery of AAV9-GluCl results in expression of a functional GluCl channel in sensory neurons after 30 days. a) *Representative IHC image of lumbar 4 DRG sections. Sections were stained for YFP (GluCl tag, green) and NeuN (red). Scale bar 100 µm.* ***b)*** *Quantification of the percentage of transduced neurons (66.7% ± 9.6%, n = 3).* ***c)*** *Ex vivo assessment of membrane conductance. Membrane voltage ramp from -90 to -40 mV caused a change in membrane conductance in ivermectin (IVM) treated animals with both subunits, but not in those with only β subunit or those treated with vehicle.* ***d)*** *Ex vivo recording of DRG*

neuronal membrane potential in response to depolarising current injection in animals injected with AAVs carrying only the β-subunit (left) or both subunits (right). Excitability status as defined by a rheobase value: <3 (excitable), 3–10 (partial silencing) or >10 (full silencing) standard deviations above the mean of control (Naive β-only, mean = 160.1 ± 160.6 pA). IVM treated animals with both GluCl subunits show silencing compared to vehicle-treated or single subunit groups (chi-squared test, χ^2 = 32.52 with 6 degrees of freedom, n = 7-10 animals per group). Figure adapted from (Weir *et al.*, 2017).

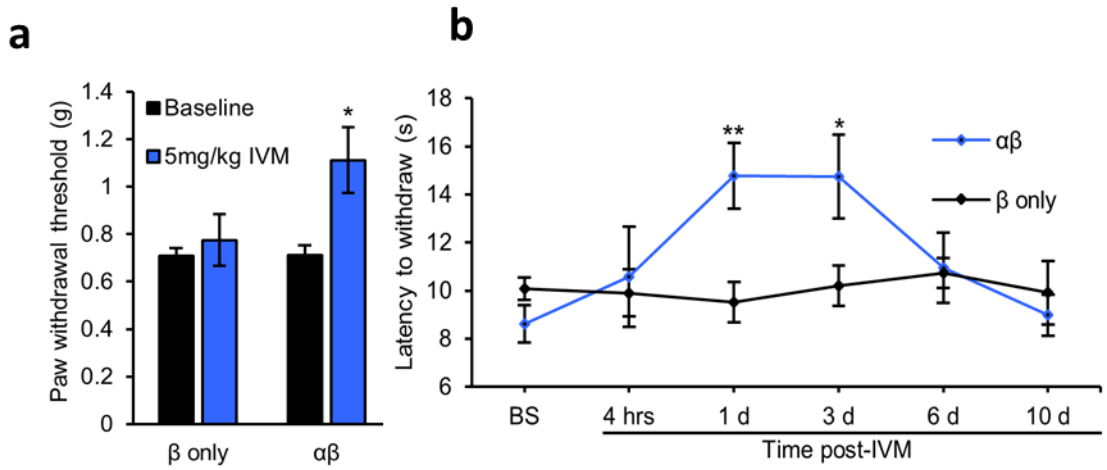

Figure 4.11 – GluCl activation alters mechanical and thermal pain thresholds. a) *Von-Frey test to assess mechanical pain threshold 30 days after AAV9-GluCl injection. Animals were given 5 mg/kg ivermectin (IVM) 24h prior to testing. IVM treatment increased mechanical threshold of mice with both subunits by 63.04% ± 20.86%, p=0.015, n = 13 αβ subunit and n = 14 β only animals.* ***b)*** *Thermal threshold assessment using Hargreves test at different times after IVM treatment (One-way ANOVA with Bonferroni test, p<0.05, n = 9 both subunits and 8 β-subunit only animals). Figure adapted from* (Weir *et al.*, 2017).

4.4 Discussion

There is a great variety of transgenes that can be packaged into AAV vectors, with functions ranging from control of gene expression to visualization of neuronal activity to control of cellular activity. The ability to transduce a large number of lumbar DRG neurons using the intrathecal cannula infusion technique developed in this project (see chapter 2), coupled with the various transgenes packaged into AAVs, opens up numerous avenues of research into understanding the organisation, physiology and pathology of DRG neurons, as well as their role in the pain pathway. The aim of this chapter was to investigate the functionality of a range of transgenes delivered using the intrathecal catheter delivery method.

4.4.1 Neuronal activity assessment with GECI

It is possible to monitor neuronal activity visually with the use of GECI. We found that intrathecal catheter delivery of AAV9-GCaMP6s results in transduction of a majority of L4 DRG neurons, and the number of transduced neurons was still high when post injection time period was reduced from 30 to 14 days. Similar to our results with AAV9-eGFP (see chapter 2.3), we observed no preference for a particular sub-population of DRG neurons. Most importantly, we have shown that GCaMP6s delivered via intrathecal infusion can be used to image activity in a large number of DRG neurons *in vivo,* and that this set up can be used to study responses of these neurons to electrical, thermal, mechanical and chemical stimuli (Chisholm *et al.*, 2018).

It is common to use two-photon microscopy to image neuronal activity *in vivo.* It has several advantages over confocal microscopy, including greater penetrance of tissue that allows imaging of deeper structures; low out-of-focus noise due to limiting the excitation to the point of intersection of the laser beams; little bleaching and tissue damage due to longer wavelengths of individual beams and lack of excitation in regions other than the intersection point (Denk and Svoboda, 1997; Helmchen and Denk, 2005; Girven and Sparta, 2017). Two-photon microscopy has been used to image neuronal activity in the brain and the spinal cord (Q. Chen *et al.*, 2012; T. W. Chen *et al.*, 2013; Peron *et al.*, 2015; Tang *et al.*, 2015; Howe and

Dombeck, 2016). However, it has several drawbacks that made us switch to single-photon confocal microscopy for GCaMP6s signal imaging in the DRGs. Two-photon microscopy is highly sensitive to tissue movement, so animal stabilisation is paramount. While the brain is easier to stabilise and make it largely unaffected by movement artefacts caused by animal respiration, this is a major problem in the spinal cord. In addition, aligning the DRG so that the whole structure is in one focal plane is problematic due to the convex surface of the DRG. Because of this, we opted for confocal microscopy with an open pinhole, which was not as affected by animal respiration and allowed for a greater number of DRG cells to be in focus. We observed no bleaching or phototoxicity across long imaging sessions (>2 hours) (Chisholm *et al.*, 2018). In addition, confocal microscopy is not as sensitive to ambient light fluctuations as the two-photon system is, which allows us to access the imaging chamber and the animal inside it. This can be used to apply different stimuli to the animal, such as air puffs, stroking and pinching, as well as thermal stimuli using a Peltier device. Imaging a large group of neurons responding to different stimuli can give us insight into the distribution of stimulus-specific neurons in the DRG (Chisholm *et al.*, 2018).

To characterise GCaMP6s performance in our system we used electrical stimulation of the ipsilateral sciatic nerve to drive neuronal activity in the L4 DRG, as electrical stimulation provides great control over the stimulus intensity and frequency. We found that GCaMP6s fluorescence was proportional to stimulus intensity and frequency. Greater fluorescence signal was observed during high frequency stimulation and more neurons were active as the stimulus frequency increased. We found that low intensity stimuli recruited primarily large-diameter neurons that correspond to A-fibres, while high intensity stimuli resulted in GCaMP6s fluorescence signal in both large and small-diameter nociceptive fibres. This is in accordance with DRG neuronal physiology, suggesting the observed GCaMP6s signal accurately reflects the neuronal activity patterns (Chisholm *et al.*, 2018). Additionally, we found that although GCaMP6s kinetics do not allow its fluorescence signal to accurately follow the intracellular calcium fluctuations during high-frequency stimulation, we observed that GCaMP6s

fluorescence exhibits summation, with greater fluorescence observed at higher frequencies. Therefore, GCaMP6s fluorescence can serve as an indicator of the action potential frequency. Interestingly, when we used natural stimuli instead of electrical stimulation to test neuronal responses we found evidence of neuronal polymodality, with same neurons responding to mechanical and thermal stimuli, which contrasted a recently published study by Emery et al. (Emery *et al.*, 2016; Chisholm *et al.*, 2018).

In vivo imaging of virally-delivered GCaMP6s in L4 DRG neurons makes it possible to study neuronal activity during pathology in great depth, as it allows us to apply various stimuli to the animal with pathology and record neuronal responses to these stimuli, to then be compared to results obtained in healthy controls. For instance, neuronal responses to both warming and cooling of the plantar surface of a hindpaw after UVB-induced inflammation are significantly higher than control group, which his consistent with electrophysiological findings (Bishop *et al.*, 2010). In addition, we found that the number of neurons responding to warming of the hindpaw following UVB-induced inflammation was greater than in control animals (Chisholm *et al.*, 2018). This example serves to illustrate that our *in vivo* imaging method of studying neuronal activity in the primary sensory neurons can be applied to answer a number of biological questions and study neuronal activity both in health and in a range of pathological conditions, such as neuropathic pain and chronic inflammation.

4.4.2 Control of gene expression with virally-delivered Cre recombinase

One of the widespread transgenic tools used to control gene expression is targeting of LoxP floxed genes with Cre recombinase. We show in this study that expression of Cre recombinase using intrathecal delivery of AAV vectors is a viable strategy for controlling gene expression in the majority of L4 DRG neurons. With a single injection of AAV9-Cre we managed to express Cre recombinase in DRG neurons at a sufficient level to enable expression of TdTomato reporter in over 70% of L4 DRG neurons. This number is higher compared to our results after transduction with AAV9-eGFP (61%, see chapter 2.3). This is likely due to the differences

between Cre-dependent expression of TdTomato and eGFP expression after AAV9-eGFP transduction. In case of AAV9-eGFP, transgene expression is tied to the genetic cargo of AAV9. The level of eGFP expression in a cell is proportional to the number of viral particles that transduced each individual cell, *e.g.* a cell with 10 times the virus particles will make 10 times the eGFP protein in a given time frame. For a cell to be detected with IHC, a certain threshold of eGFP expression must be reached, so cells that were transduced with few viral particles are not likely to be counted as positive, even though they were transduced. However, in TdTomato-floxed-STOP-cassette mice, Cre recombinase excises a single STOP cassette that in naïve animals prevents expression of TdTomato. Once the STOP signal is removed, the TdTomato transgene expression is driven by a strong innate promoter. Therefore, transduction with even a few AAV9-Cre particles can result in strong transgene expression.

In addition to regulating expression of fluorescent markers, in this study we also show that virally-delivered Cre recombinase can control expression of complex transgenes. In our study, we used AAV9-Cre to express GCaMP6s in a GCaMP6s-floxed-STOP-cassette mouse line. The number of cells expressing GCaMP6s was lower than that in the TdTomato experiment (48% vs 70%). The reason for the discrepancy in the number of transduced cells is unknown, and could be due to experimental variability. However, expression of GCaMP6s in the L4 DRGs was high enough to be used for *in vivo* calcium imaging. We show an *in vivo* recording of an L4 DRG that is responding to thermal stimuli applied to the hindpaw as a proof of concept. Further confirmation of successful transduction following intrathecal administration of AAV9-Cre could be achieved by analysing RNA composition using RT-PCR. Unfortunately, due to time constraints, we were unable to complete this experiment.

These data illustrate that the Cre recombinase delivered via intrathecal infusion of AAV9-Cre retains its functionality in DRG neurons and can be used in cases when transgenic Cre animal lines are unavailable or when temporal control over Cre expression is required. Additionally, it may be possible to restrict Cre expression by targeted peripheral injection, such as intraneural

(see chapter 2.3) or intramuscular injection (Anderson *et al.*, 2018), although the injection method has to be verified to avoid off-target transduction.

4.4.3 Neuronal activity control with GluCl transgene

Lastly, we used our intrathecal injection method to deliver chemogenetic tools to the DRG neurons and to investigate their effectiveness. Chemogenetic tools, such as DREADDs and GluCl channel, allow inhibition or excitation of cells by controlling ion flux across the cell membrane in response to binding of a specific ligand. However, most chemogenetic channels are large proteins, and the DNA encoding the full channel may be too long to fit in a single AAV vector. Here, we show that it is possible to express complete GluCl channel by intrathecal infusion of two AAV9 vectors, each carrying a GluCl subunit (Weir *et al.*, 2017). The majority of L4 DRG neurons in adult mice were transduced, an improvement compared to our earlier data (see chapter 2), which could be due to higher titre (2.4-1.5 x 10^{13} gc/ml vs 6.39 x 10^{12} gc/ml) as well as greater injection volume (8 µl vs 5 µl) .

To test whether GluCl was functional, membrane conductance of transduced neurons was assessed following treatment with ivermectin (IVM), the ligand for this modified GluCl channel. IVM-treated neurons with both GluCl subunits showed increased conductance, indicating that GluCl channel was functional and responded to IVM ligand. This increase in conductance was absent in non-transduced IVM-treated neurons and in transduced vehicle-treated neurons, suggesting that the GluCl channel is closed in the absence of IVM. Furthermore, we see that activated GluCl channel is capable of silencing transduced DRG neurons.

It is important to note that the silencing effect of GluCl activation in DRG neurons is different from that in CNS neurons. In the CNS, neurons maintain low intracellular chloride ion concentration. Opening of the GluCl channel allows an influx of chloride ions from the extracellular space, hyperpolarising the neurons (Slimko *et al.*, 2002; Lerchner *et al.*, 2007; Frazier, Cohen and Lester, 2013). DRG neurons, however, maintain high intracellular chloride ion concentration, so GluCl channel activation does not trigger an influx of chloride ions and

hyperpolarisation. The silencing that is evident in our study is likely due to a general increase in membrane conductance, however the precise mechanism of action is not clear (Weir *et al.*, 2017).

Administration of IVM to animals injected with AAV9-GluCl produced a profound increase in the mechanical and thermal sensory thresholds. This finding is important as it shows that transduction levels in DRG neurons after a single AAV infusion are sufficient to influence behaviour. This opens a wide range of possible applications for AAV-mediated delivery of other chemogenetic tools. For example, virally-administered DREADDs have been previously used to control neuronal activity in the brain, both to inhibit neuronal activity in nucleus accumbens neurons using the hM4Di DREADD (T. Zhang *et al.*, 2018), and to activate hypothalamic neurons using the hM3D (N. Zhang *et al.*, 2018). Intrathecal administration of AAV9 carrying these tools could make it possible to express them in a large number of DRG neurons, and to study their role in the pain circuit by influencing their activity both in health and in a range of pathological conditions, such as neuropathic pain (Weir *et al.*, 2017).

4.4.4 Conclusion

In this chapter we have shown that the intrathecal delivery of AAV vectors developed in chapter 2 can be used to express a number of functional transgenes in the L4 DRG neurons. This includes GECI such as GCaMP6s to study the neuronal activity patterns in the DRGs, Cre recombinase to allow control of the gene expression in floxed-STOP-cassette transgenic lines and chemogenetic tools, such as the GluCl channel, to control neuronal activity. Importantly, these examples show that the level of neuronal transduction after AAV9 delivery using this method is sufficient to be used for many applications in the study of pain and pain circuitry.

Chapter 5: Project conclusions and future directions

5.1 Project outcomes

Viral vectors are invaluable tools that can be used to study multiple aspects of the physiology of the nervous system in health and in pathological conditions. Further, they can be used as potential treatments for a multitude of nervous system disorders, including chronic pain (Glorioso, Mata and Fink, 2003; Mata, Hao and Fink, 2008; Srinivasan, Fink and Glorioso, 2008; Lentz, Gray and Samulski, 2012; Kantor *et al.*, 2014; Guedon *et al.*, 2015). In the case of pain research and therapy, primary afferent neurons in the dorsal root ganglia are of a particular interest as they play a critical role in nociception and physiological, as well as pathological, sensitization (Basbaum *et al.*, 2009; Ringkamp *et al.*, 2013; Liem *et al.*, 2016). Targeting these neurons with viral vectors is a very powerful experimental approach that can be used to express a wide array of transgenes for research and therapy (Lentz, Gray and Samulski, 2012; Guedon *et al.*, 2015; Liem *et al.*, 2016; Chen *et al.*, 2018). There are many types of viral vectors available, each with its own advantages, however AAV vectors are the most popular type used for transgene delivery in the nervous system (Lentz, Gray and Samulski, 2012; Kantor *et al.*, 2014). AAV vectors have been used to target DRG neurons, however variables such as delivery route and AAV serotype have been shown to greatly impact transduction levels in these neurons (see chapter 2.1).

The aim of this project was two-fold. The first aim was to characterise the transduction pattern of AAV9 vectors in adult mouse DRG neurons following intrathecal delivery, and to explore the impact of various experimental variables, such intrathecal delivery method, post injection time, viral titre, transgene and AAV serotype. This also included assessment of any unintended effects of IT delivery and AAV transduction, such as a change in nocifensive behaviour and the triggering of an immune response following transduction. Also, we aimed to restrict transgene expression to DRG neurons that send projections to distinct anatomical structures by the means of peripheral injections of AAV9. The second aim of this study was to explore the

applications for AAV transduction of DRG neurons following intrathecal delivery using several functional transgenes *in vitro* and *in vivo*, including GECI GCaMP6s for visualising neuronal activity, Cre recombinase for control of gene expression and mutated GluCl channel for neuronal activity modulation.

5.1.1 Characterisation of DRG transduction following *in vivo* delivery of AAV9

Initially, we used lumbar puncture to deliver AAV9 into the intrathecal space. We observed transduction in the majority of L4 and cervical DRGs after intrathecal injection of 5 µl of AAV9-eGFP. However, this method suffered from low reliability, as many injected animals showed very low or absent expression. This is likely due to the variability in uptake and administration volumes of AAV vector due to syringe dead space. Furthermore, it is possible that the lack of visual confirmation of needle placement meant that some injections were not intrathecal. The issues caused by the syringe dead space can be overcome by using specialised syringes with zero dead space, however this does not address the problem of visual confirmation of the needle placement. We designed a method of intrathecal delivery that eliminates dead space by using a thin polytetrafluoroethylene (PTFE) catheter connected to a syringe pump to deliver AAV intrathecally. By inserting the catheter into an opening in the dura it is possible to visually confirm intrathecal placement of the catheter. A similar AAV intrathecal delivery method has been used in rats (Xu *et al.*, 2012), however it involved catheter implantation for 72 hours, while our method only requires the catheter to be in the animal for 7 to 9 minutes. DRG transduction observed using this technique was as good as lumbar puncture delivery, however the reliability was much greater, with only few animals (8%) showing low transduction in their L4 DRGs. Importantly, the proportions of CGRP, IB4 and NF200-positive neurons both in transduced neuronal population and in all L4 DRG neurons were not significantly different, suggesting that our IT delivery does not target a particular DRG neuronal subtype. However, assessment of transduced neuronal sub-populations was performed only at L4 DGR level, and future experiments are needed to assess neuronal distribution at other DRG levels.

Although this technique is more reliable, it is also more invasive and more complex compared to lumbar puncture. The intrathecal space in the mice is extremely limited, and introduction of foreign objects such as a catheter may cause damage to the spinal cord and nerve roots (Fairbanks, 2003). Mechanical hyperalgesia has been reported following spinal cord injury (Brewer and Yezierski, 1998; Yezierski *et al.*, 1998). Therefore, we used the Von Frey test to assess mechanical sensitivity in animals following intrathecal saline administration using the catheter approach. We observed no significant change in mechanical sensitivity, suggesting that the catheter does not cause spinal cord damage. However, further confirmation with other behavioural tests, such as the Hargreaves test for thermal sensitivity (Hargreaves *et al.*, 1988) or the Basso, Beattie, Bresnahan (BBB) Locomotor Rating Scale for motor function is required (Basso, Beattie and Bresnahan, 1995; Ma *et al.*, 2001).

In addition to the delivery method, AAV9 transduction itself may cause behavioural alterations and a local immune response (Samaranch *et al.*, 2014). However, when we tested this we found no significant difference in the mechanical sensitivity or the immune cell composition of lumbar DRGs between saline and AAV9-eGFP injected mice. This suggests that AAV9 transduction following intrathecal delivery does not cause a local immune response and does not change the mechanical sensory phenotype. However, it is important to note that other assessments are required to fully explore the effect AAV9 transduction might have on the animal behaviour, as well as its immunogenicity.

As part of this project, we assessed the impact of several experimental factors, such as virus titre and post injection time, on DRG transduction efficiency following IT delivery of AAV9. Reducing the post injection time period from 30 days to 7 days resulted in comparable numbers of transduced neurons in the L4 DRG. Interestingly, our data for 14-day post injection time period show reduced transduction in the cervical DRGs compared to 30-day post injection. However, this difference is not likely to be due to the reduced time available for vector spread in the CSF, as the 7-day post injection time period results in cervical transduction comparable

to 30 days. It is rather caused by the methodological variability, and further experiments with 14 days post injection time periodare required to assess reproducibility of these results. Furthermore, we found that decreasing the virus titre had a tendency to reduce the number of transduced neurons in the L4 DRG, albeit this did not reach statistical significance. Further investigation with a larger experimental group is needed to determine the precise impact of viral titre on transduction in DRG neurons. Importantly, this trend was more pronounced in cervical ganglia, with a statistically significant reduction in transduction at lower titres. This could be explained by the progressive fall in the number of viral particles with increasing distance from the injection epicentre, with fewer viral particles spreading to the cervical level at lower titres.

We also assessed whether changing the AAV serotype or the packaged transgene has an impact on neuronal transduction. We found no significant difference in L4 DRG neuronal transduction between AAV9-eGFP and AAV9-mCherry, suggesting that the transgene itself does not impact transduction. However, when we examined IT injection AAV serotype 8 we observed a reduction in the percentage of transduced neurons in L4 DRG. This data is in agreement with the literature, where AAV transduction has been shown to be influenced by the serotype, and AAV9 has been shown to have superior transduction rates in DRG neurons compared to AAV8 (Vulchanova *et al.*, 2010; Snyder *et al.*, 2011; Schuster *et al.*, 2014).

In our attempt to target sensory neurons innervating distinct anatomical structures, we injected AAV9 into the sciatic nerve, the knee joint and the plantar surface of the hind paw. We observed that intra-sciatic injection produced moderate labelling in the ipsilateral L4 DRG, while no labelling was present in the contralateral L4 DRG. This suggests that intra-sciatic injections can be used to selectively deliver transgenes to a sub-population of sensory neurons on the ipsilateral side of the animal. However, in experiments with intraarticular and intraplanar injections we observed labelling on both ipsilateral and contralateral sides in L3 and L4 DRGs, respectively. This is likely due to the AAV9 leaking into the bloodstream. In the

future, it may be beneficial to assess whether changing the injection volume or the viral titre can restrict transduction only to the ipsilateral DRG neurons. In addition, future experiments investigating whether injections into other peripheral targets, such as tibial bone (Kushida *et al.*, 2001; Liu *et al.*, 2012), bladder wall (Fu *et al.*, 2011) and parts of the digestive system (Benskey *et al.*, 2015) could be used to specifically target primary afferent neurons that send projections to these structures.

Overall, we achieved the first aim of this project by characterising AAV9 transduction after intrathecal delivery. We set up a new intrathecal delivery method for AAV9 using a catheter that achieved high transduction in the L4 DRG neurons, and assessed the impact several experimental variables, such as titre and post injection time, have on the transduction. We also investigated the potential for peripheral administration of AAV9 into anatomically distinct structures as a way to target only sensory neurons that project to these structures.

5.1.2 Setting up an *in vitro* sensitisation model

The second aim of my project was to explore the applications of intrathecal delivery to express different transgenes that can be used to study several aspects of primary sensory neurons physiology. Before assessing whether AAV9-delivered transgenic tools could be used for *in vivo* experiments, such as *in vivo* calcium imaging, we first confirmed that GCaMP6s was functional *in vitro*, and tested whether it could be used to study acute sensitisation in DRG cultures. To do this, we set up a neuronal sensitisation model that uses electrical field stimulation as a trigger for neuronal activity. We opted to use electrical stimuli instead of the more commonly used chemical triggers like capsaicin, as electrical stimulation circumvents the caveat of neuronal tachyphylaxis, often observed with chemical stimuli (Koplas, Rosenberg and Oxford, 1997; Mohapatra and Nau, 2003). We observed that virally-delivered GCaMP6s could be used to image neuronal activity in dissociated adult mixed DRG cultures. GCaMP6s performance was comparable to that of a commonly used chemical calcium dye Fura-2 AM. Although GCaMP6s has been shown to have superior signal-to-noise ratio and brightness compared to synthetic

calcium dye Oregon Green Bapta-1-AM (T. W. Chen *et al.*, 2013), future experiments comparing various aspects of GCaMP6s and Fura-2 AM performance, such as deactivation kinetics, are needed to quantitatively compare these two dyes.

By comparing the trigger-elicited neuronal activity before and after addition of a potential sensitizer, we hoped to quantify the neuronal sensitisation. We analysed the difference in neuronal responses after application of several compounds that are known neuronal sensitizers, including PGE2 and bradykinin. Overall, we detected only mild sensitisation of neuronal responses that was mostly elicited by stronger stimuli and was only present after addition of PGE2 or inflammatory soup. The lack of potentiation of neuronal responses observed in this study compared to that reported in the literature could be attributed to the way these compounds elicit neuronal sensitisation. The sensitizers trigger intracellular signalling pathways that alter activity of several membrane proteins, such as TRPV1 (Lopshire and Nicol, 1997; Geppetti and Trevisani, 2004; Huang, Zhang and McNaughton, 2006). This causes stimulation with capsaicin, a TRPV1 activator, to produce greater neuronal responses. However, electrical stimulation may not elicit neuronal activity via the targets of these intracellular pathways, and therefore would not show an increased neuronal response. Alternatively, these sensitizers may exert their action on a particular subset of DRG neurons, such as small-diameter unmyelinated C-fibres that express $Na_v1.8$ (Gold *et al.*, 2002; Meves, 2006). In this study DRG cultures contained a mix of neurons from different sub-populations, so it is possible that an effect on a small proportion of the neurons in culture was diluted by the rest of the neurons.

In future experiments, it may be beneficial to explore other stimulation paradigms, possibly ones that deliver stronger stimuli, as most of the significant increases in neuronal responses in this study were found following the strongest trigger stimuli. Furthermore, prolonged application of the sensitizers may increase the sensitivity to electrical stimuli. Future experiments could also be carried out to explore the use of other sensitizer compounds, such

as cytokines and chemokines, to sensitize neurons to electrical stimuli (Dawes *et al.*, 2013). Lastly, although a large number of neurons was used to assess the effect of each sensitizer, the number of biological repeats used for cultures was low. Therefore, it is important to repeat these experiments with an increased number of animals, to control for animal differences.

Overall, we showed that virally-delivered GCaMP6s remains functional and can be used to visualise neuronal activity *in vitro*. We used GCaMP6s and Fura-2 AM to attempt to set up an *in vitro* sensitisation model, however we did not manage to elicit robust neuronal sensitisation. Further work is required to develop and optimise this model.

5.1.3 Confirmation of transgene functionality *in vivo*

Although we did not succeed in setting up an *in vitro* sensitisation model, our cell culture experiments showed that virally-delivered GCaMP6s is functional and can be used to image neuronal activity in DRG neurons. When AAV9-GCaMP6s was administered intrathecally using a catheter, we observed transduction in the majority of L4 DRG neurons following immunohistochemical assessment. My colleague Dr Chisholm designed and optimised an *in vivo* calcium imaging set up that could be used to image activity in L4 neurons of mice previously injected with AAV9-GCaMP6s. We observed a strong increase in GCaMP6s signal in L4 DRG neurons post-mortem, coinciding with the increase in intracellular calcium. This showed that virally-delivered GCaMP6s retains its functionality *in vivo* and can be used as a proxy for neuronal activity. Furthermore, we were able to use AAV9-delivered GCaMP6s to study neuronal responses to electrical stimulation of the sciatic nerve. We showed that GCaMP6s could report single action potentials at low frequencies of stimulation, and at higher frequencies the strength of GCaMP6s fluorescence was proportional to the stimulus frequency. In addition, we showed that it is possible to recruit only A-fibres or A- and C-fibres by varying the strength of the electrical stimuli. These experiments show that virally-delivered GCaMP6s can be used to study neuronal activity of DRG neurons *in vivo.* Although not shown here, the use of this technique has allowed us to study the responses of sensory neurons to natural

stimuli, such as heat, cooling, stroking and pinching in healthy mice and those with a plantar UV burn, as well as neuronal activity in animals that received an intraplantar injection of formalin (Chisholm *et al.*, 2018).

We also explored the use of virally-delivered Cre recombinase to modulate expression of genes in transgenic mouse lines. We found that intrathecal delivery of AAV9-Cre into TdTomato-floxed-STOP-cassette mice produced strong expression of TdTomato in a majority of L4 DRG neurons. Similar results were observed in GCaMP6s-floxed-STOP-cassette mice, although the percentage of transduced neurons was lower. This could be attributed to methodological variability. Repeating these experiments with an increased number of animals would help to establish whether the difference in transduction is due to differences between these two transgenic lines or the result of methodological variability. However, we have shown that despite reduced transduction, levels of Cre-dependent GCaMP6s expression were sufficient for the use in *in vivo* calcium imaging experiments.

Finally, through collaboration with Dr Weir at Oxford University, we explored the use of intrathecal AAV delivery for expression of chemogenetic tools. In these experiments, we used our IT delivery method to express an engineered glutamate-gated chloride channel GluCl in primary afferent neurons. We found that intrathecal catheter co-administration of two AAV9 vectors carrying α and β subunits of the GluCl, respectively, results in expression of a functional GluCl channel in the majority of the L4 DRG neurons. Furthermore, activation of GluCl by ivermectin fully silenced over 90% of the transduced neurons *in vitro*. Finally, administration of ivermectin to AAV9-GluCl injected animals resulted in changes in animal behaviour, increasing the mechanical and thermal threshold, assessed by Von Frey and Hargreaves tests, respectively. This suggests that the GluCl channel was functional *in vivo*, and that the number of transduced neurons was high enough to elicit a change in behaviour. Dr Weir and colleagues went on to show that in a model of neuropathic pain, activation of AAV9-delivered GluCl can alleviate injury-induced hypersensitivity (Weir *et al.*, 2017).

These experiments show that intrathecal delivery of AAV9 can be used to express a number of functional transgenes in DRG neurons that can be used to interrogate various aspects of the primary afferent neurons physiology in health and disease.

5.2 Future directions

The results in this project, and other studies, show that intrathecal administration of AAV9 results in potent transduction in DRG neurons. It is not known which part of the DRG neurons the AAV9 particles initially transduce. One possibility is that after intrathecal injection AAV9 particles transduce DRG neuronal projections in the posterior root, which are then retrogradely transported to the neuronal soma in the DRG. This could explain the superior transduction seen with AAV9 compared to other serotypes after intrathecal injection (Snyder *et al.*, 2011; Schuster *et al.*, 2014), as AAV9 exhibits strong retrograde transport (Castle, Gershenson, *et al.*, 2014; Castle, Perlson, *et al.*, 2014). Recently, a new designer AAV, rAAV2-retro, has been developed, and it has shown superior retrograde transport compared to all other commonly used AAV vectors, including AAV9 (Tervo *et al.*, 2016). Therefore, it could be beneficial to assess the DRG neuronal transduction efficiency of rAAV2-retro using intrathecal delivery, as the superior retrograde transport capabilities may result in a higher percentage of neurons transduced compared to 60% observed in this project with AAV9.

The majority of our experiments focused on transducing sensory neurons in the lumbar DRGs. However, there are many areas of research that focus on sensory and motor function at higher levels. For instance, in stroke research the forelimb pellet reaching and grip strength tests are common behavioural assessments of the pathology severity and is used to test the effects of various interventions (Kathe *et al.*, 2016). Another example is migraine research, where there is great interest in the trigeminal ganglia and the role the trigeminal sensory neurons play in the development of migraine (Edvinsson *et al.*, 2018; Messlinger, 2018). Therefore, a viral delivery technique that is capable of transducing sensory neurons in the higher ganglia would have many applications both within the pain research field and beyond. There are several

experimental approaches that may produce better labelling in the higher ganglia. First, we showed that delivering a high-titre AAV9 with a lumbar catheter results in transduction of around 60% DRG neurons in the cervical ganglia. Therefore, further experiments that focus on transduction in the cervical and trigeminal ganglia after intrathecal lumbar catheter delivery of a high-titre AAV9 may help us to determine factors that are important for high ganglia transduction. Second, changing the catheter orientation so that it points rostrally may boost the spread of the virus to the higher ganglia. However, it is likely that the spinal level and the technique of catheter will have to be altered to avoid damaging the spinal cord as the intrathecal space around the thoracic level is very restricted. Alternatively, switching to cisterna magna (CM) delivery of the AAV vectors could result in higher transduction in higher ganglia, as the injection epicentre would be much closer to the cervical and trigeminal ganglia. CM injections are often performed in larger laboratory animals such as rats, rabbits and primates (Kikkawa, Kurogi and Sasaki, 2014; Samaranch *et al.*, 2016; Hinderer *et al.*, 2017; Lee *et al.*, 2018). However, CM injections in mice are more difficult due to the small size of the injection target (Yili Chen *et al.*, 2013). There are several methods for CM injection in mice, from direct injection through the atlanto-occipital membrane using a standard Hamilton syringe (Fu *et al.*, 2003, 2007; Sinnett *et al.*, 2017), to the use of modified needles with stoppers to regulate penetration depth (Lee *et al.*, 2011, 2013), and the use of curved needles to allow easier access (Yili Chen *et al.*, 2013). All these methods may be applicable to AAV9 CM delivery, however loading of small volumes of viral suspension may be problematic as observed with lumbar puncture delivery in this project. Finally, a recently developed O'Buckley intrathecal delivery method relies on insertion of a thin catheter through the condylar canal in the mouse skull (Oladosu *et al.*, 2016). This method may be effective for the transduction of cervical and trigeminal ganglia, as it allows visual verification of the injection site and uses pre-loaded catheters instead of syringes, which makes it easier to observe correct loading and delivery volumes. Future experiments should focus on exploring the use of these methods to deliver AAV9 into the CM. This would include an assessment of transduction in the trigeminal,

cervical, thoracic and lumbar ganglia, a head-to-head comparison of these delivery methods, a characterisation of the transduction pattern and an assessment of the impact of viral titre and post injection time on the transduction efficiency.

Our results show that AAV9 does not target a specific sub-population of DRG sensory neurons. This feature is beneficial, as it reduces the population bias in the results. However, it can also cause a dilution effect if only a particular sub-population of the transduced neurons responds to a specific treatment. In that case, analysis of all transduced neurons together is likely to result in a statistically insignificant effect. Therefore, it may be beneficial to target viral transduction, or the expression of the transgene, to specific neuronal sub-populations. This could be achieved by using AAV serotypes that have a preference for a particular sub-group of sensory neurons, for instance AAV8 has been reported to preferentially target large-diameter neurons in the DRG (Vulchanova *et al.*, 2010; Jacques *et al.*, 2012). However, this approach may not produce the desired level of specificity, as other neuronal sub-types are also transduced. A better approach may be restricting transgene expression by using sub-population-specific promoters. For instance, *in vitro* transduction with an adenovirus that packages a lacZ reporter gene under the control of a CGRP promoter resulted in a 91% co-expression of the LacZ gene with the endogenous CGRP neurons (Durham *et al.*, 2004). Alternatively, it is possible to use Cre-dependent AAV vectors (Saunders and Sabatini, 2015; Haenraets *et al.*, 2018). For instance, reversing the transgene sequence and flanking it with LoxP sites in the expression plasmid will make the transgene expression impossible. However, when cells expressing the Cre recombinase are transduced, Cre will cause recombination and inversion of the transgene, making its expression possible (Saunders and Sabatini, 2015). These viral vectors can be used in conjunction with transgenic mouse lines that express a Cre recombinase in a particular subset of DRG neurons, for instance in the $Na_v1.8$-positive nociceptors (Stirling *et al.*, 2005), to restrict expression of the transgene to a particular sub-population of neurons.

We have shown that GCaMP6s delivered using IT injection of AAV9 is functional in animals and can be used for *in vitro* and *in vivo* calcium imaging. Using this technique, we have explored the responses of DRG neurons to different modalities of stimuli, and showed that there is a degree of polymodality in the L4 DRG neurons (Chisholm *et al.*, 2018). In the future, it would be beneficial to explore how the pattern and the magnitude of neuronal responses change in animal models of chronic pain, such as the chronic constriction injury model of neuropathic pain, or the intraplantar CFA injection model of chronic inflammatory pain, as there is evidence that the activity of DRG neurons as well as their modality is altered in chronic pain (Basbaum *et al.*, 2009; Gangadharan and Kuner, 2013). For instance, we found that relatively few primary afferent neurons responded to cold stimuli compared to the number of neurons responding to hot stimuli (Chisholm *et al.*, 2018). Neuropathic pain is known to induce cold hypersensitivity, and that effect is partially mediated by primary afferents (Allchorne, Broom and Woolf, 2005; Basbaum *et al.*, 2009; Draxler *et al.*, 2014). It would be interesting to investigate whether neuropathic pain results in an increased number of cold-responsive DRG neurons, as well as augmentation of the intensity of their responses to cold stimuli. In addition, central terminals of the DRG neurons also express the transgene after AAV9 transduction. Therefore, it is possible to image the activity in the central terminals of the primary afferents in animals after AAV9-GCaMP6s IT administration, which can be used to study the dorsal horn pain circuitry. Moreover, it may be possible to further interrogate the interactions between neurons in the spinal circuitry involved in nociception by using a second GECI of a different colour, such as red-shifted RCaMP or R-GECO (Zhao *et al.*, 2011; Akerboom *et al.*, 2013). These GECI use excitation and emission frequencies that are different from those of GCaMP6s, so their signal would not interfere with that of GCaMP6s, and therefore this allows expression of two GECI in the same animal. For example, by expressing the GCaMP6s in the sensory neuron terminals and the red-shifted GECI in the other parts of the nociceptive circuitry in the spinal cord, we may be able to image how these two parts interact. For instance, it is possible to transduce neurokinin-1 receptor positive projection neurons that receive input from the sensory neurons

and project from the dorsal horn to the higher centres by injecting AAV9 into the parabrachial nucleus (Cameron *et al.*, 2015). By expressing a red-shifted GECI in these neurons and a GCaMP6s in the primary afferents, it could be possible to image how activity in the afferent neurons influences that in the projection neurons. This could then be expanded to investigating the changes in signal processing in various chronic pain models, such as the chronic constriction injury neuropathic pain model, in the targeted area of the pain circuitry.

Transgenic mouse lines are being developed for targeted GCaMP6s expression, such as ones where GCaMP6s expression is under the control of Cre recombinase, which in turn is only expressed in primary afferent neurons by expressing it from the *Advillin* gene locus (Zurborg *et al.*, 2011). In this study we started breeding of GCaMP6s-floxed-STOP-cassette mice with an Advillin-Cre-ERT2 mice. By using a Cre fused to a mutated oestrogen receptor this allows temporal control over the GCaMP6s expression by activating the Cre with tamoxifen administration (Lau *et al.*, 2011). This way, we eliminate the need for the intrathecal injection of the AAV9-GCaMP6s to image activity in the sensory neurons. However, we were unable to breed a cohort of mice of sufficient size due to time constraints. In addition, viral delivery of GCaMP allows greater flexibility, for example for targeted administration to an anatomical subset of neurons, or for co-expression of several transgenes in the animal.

Viral vectors have been used extensively as a method for modulation of gene expression, for instance as delivery vehicles for Cre recombinase. Virally-delivered Cre has been used in pain research to study the effects of knockout of certain genes, for instance the $Na_v1.6$ knockout in neuropathic pain (Chen *et al.*, 2018), or the signal transducers and transcription activator 3 (STAT3) in both oxaliplatin-induced chronic pain and pain caused by lumbar disk herniation (Y. Y. Li *et al.*, 2017; Zhang *et al.*, 2017). The usefulness of the Cre-LoxP system for modulation of gene expression is limited by the availability of transgenic lines with LoxP site insertions at the relevant paint in the genome. It is also possible to interfere with the expression of genes at the RNA level by using miRNAs and shRNAs. Viral vectors have been used to deliver these tools in

a wide variety of fields (Herrera-Carrillo, Liu and Berkhout, 2017). In the field of pain research, AAV-administered shRNAs have been used to knock down many genes to study their roles in more detail, such as ion channels $Na_v1.3$ and $Ca_v2.2$, as well as TRPV1, in neuropathic pain (Samad *et al.*, 2013; Hirai *et al.*, 2014; Yang *et al.*, 2018). Therefore, it would be beneficial to explore the use of virally-delivered RNAi tools in conjunction with intrathecal administration of AAV9 carrier. If successful, this would be a powerful model for studying the importance of many genes in the DRGs, both in healthy animals and in pathological pain models.

Despite extensive use of RNAi approaches, it has some disadvantages. These tools act at the mRNA level, therefore they are not suitable for studying non-coding genome regions (Schmidt and Grimm, 2015). Furthermore, virally-delivered shRNA has been shown to cause cell damage and death (Grimm *et al.*, 2006; Grimm, 2011). Therefore, alternative methods of influencing gene expression may be necessary to overcome these limitations. One such tool is the CRIPSR/Cas9 system. Briefly, this system uses guide RNA (gRNA), comprised of CRISPR-associated RNA (crRNA) and *trans*-activating CRISPR RNA (tracrRNA), to target the Cas9 nuclease to specific sections of the host genome. Once in place,Cas9 nuclease can then create a double-strand break at the target site (Doudna and Charpentier, 2014; Hsu, Lander and Zhang, 2014; Sander and Joung, 2014). Both the Cas9 and the gRNA can be delivered in a single AAV vector (Senís *et al.*, 2014), and this delivery system has been successfully used in several studies. For instance, for deleting the mutant exons of the dystrophin gene to correct Duchenne muscular dystrophy (Tabebordbar *et al.*, 2016; Wang *et al.*, 2017). Therefore, the use of this technique to study the contribution of various gene to pain states is another avenue that is worth exploring in the future through viral delivery of CRISPR/Cas9 system to neurons in the pain circuit.

Another powerful experimental approach is using AAV vectors to deliver chemogenetic and optogenetic tools to modulate neuronal activity. Targeted expression of optogenetic tools that influence activity of neurons can be used to interrogate specific parts of the neuronal circuit

(Yamawaki *et al.*, 2016). This approach has been extensively used for interrogating neuronal circuitry in several research fields, including sleep (Fuller, Yamanaka and Lazarus, 2015), stress (Sparta *et al.*, 2013) and hearing (Shimano *et al.*, 2013). It has also been used in the pain field. For example, AAV vectors have been used to target expression of optogenetic tools to neurons in the anterior cingulate cortex, where inhibition of these neurons by the optogenetic tools delivered resulted in a reduction in nocifensive behaviour in animals with trigeminal neuralgia (Moon *et al.*, 2017). Another example is the attenuation of mechanical and thermal hypersensitivity in a mouse model of neuropathic pain by silencing primary sensory neurons after intrathecal AAV-mediated delivery of GluCl channel (Weir *et al.*, 2017). Furthermore, as with other transgenic tools, it is possible to restrict their expression to particular neuronal population by using cell-specific promoters, or Cre-dependent AAV vectors (Koh *et al.*, 2015). In the future, targeted expression of optogenetic and chemogenetic tools in the DRG neuronal sub-population will be of tremendous help in untangling their contributions to nociception.

Overall, viral vectors are a very useful tool in expressing a wide range of tools that can be used in research. Although most of these tools can be expressed in the animals by generating transgenic lines, viral vectors offer a much greater degree of flexibility. Different delivery routes, as well as viral serotypes and promoters can be used to select the cell type transduced by these vectors. In addition, levels of transgene expression that are useful for research are achieved in a very short period of time, often within a week (see chapter 2). Furthermore, it is possible to administer multiple vectors to express several products at the same time, as well as using multiple injections of the vectors to achieve expression in the intersection neurons that project to these areas.

Finally, AAV vectors are not only capable of delivering transgenic tools but can also be used to express pathology-correcting proteins. These are largely restricted to diseases that are caused by a mutation in a single gene, such as Duchenne muscular dystrophy that caused by a mutation in the gene that encodes dystrophin (Lai and Duan, 2012; Lostal *et al.*, 2014). These

diseases can be effectively countered by administration of the correct gene using AAV vectors, which often results in partial correction of the pathology (Passini *et al.*, 2005; Thöny, 2010; Elmallah *et al.*, 2014; Lostal *et al.*, 2014; Gray-Edwards *et al.*, 2015; Nichols *et al.*, 2015). Currently, there are 153 clinical trials that are testing the therapeutic potential of AAV vectors in humans for a wide range of diseases ((ClinicalTrials.gov), accessed 28/08/2018). Of these, 3 studies are using intrathecal delivery of AAV vectors, and all three of them are using AAV9 ((ClinicalTrials.gov) accessed 28/08/2018). There are, however, some drawbacks to using AAV vectors for therapy. The small size of the encoding region (~4.7 kb) means that some whole genes cannot be packaged in a single AAV vector, such as the dystrophin gene (Lostal *et al.*, 2014). This means that truncated gene sequences have to be used instead of full gene sequence, often resulting in an incomplete rescue (Lostal *et al.*, 2014). This in part can be circumvented by simultaneous administration of several AAV vectors each carrying a part of the full gene sequence (Lostal *et al.*, 2014). In addition, pre-existing AAV neutralizing antibodies (Nabs) in humans are known to significantly reduce transduction efficiency of AAV vectors (Lykken *et al.*, 2018). Interestingly, the prevalence of neutralizing antibodies in the population varies between serotype-specific Nabs, with anti-AAV2 and anti-AAV1 being most prevalent (72% and 67%, respectively), while anti-AAV9 Nabs were only detected in 47% of the population (Boutin *et al.*, 2010). This suggests that certain AAV serotypes may be more applicable to gene therapy in humans (Boutin *et al.*, 2010; Lykken *et al.*, 2018). Despite these drawbacks, AAVs are becoming the vector of choice for therapy, and progress is being made towards circumventing these problems (Deverman *et al.*, 2018; Lykken *et al.*, 2018).

5.3 Conclusion

AAV vectors are powerful tools that have a wide range of research and therapeutic applications. In this project, we investigated the use of AAV9 for transduction of sensory neurons and explored functionality of AAV9-delivered transgenic tool in several experimental settings. We developed a new intrathecal delivery method for AAV9 that resulted in

transduction of the majority of lumbar and cervical DRG neurons. We characterised the impact various experimental factors such as viral titre and post injection time have on the transduction efficiency. Furthermore, we assessed the feasibility of peripheral delivery of AAV9 into distinct anatomical structures in order to target specific populations of DRG neurons. Finally, we explored the use of AAV9 for delivery of several transgenic tools, including GCaMP6s for neuronal activity imaging *in vitro* and *in vivo*, Cre recombinase for control of gene expression and GluCl for modulation of neuronal activity. Future experiments will be aimed at exploring alternative intrathecal administration routes, restriction of expression to sub-populations of DRG neurons and further exploration of the use of AAV9-delivered transgenic tools in the pain research. Beyond that, our work may also be able to inform a number of other scientific fields, such as proprioception and ageing, to continue the advancement of science.

Bibliography

Adler, E. *et al.* (1991) 'Alien Intracellular Calcium Chelators Attenuate Release at the Squid Giant Synapse', *The Journal of Neuroscience*. Society for Neuroscience, 11(6), pp. 1496–1507. doi: 10.1523/JNEUROSCI.11-06-01496.1991.

Adrover, M. F. *et al.* (2003) 'Hippocampal infection with HSV-1-derived vectors expressing an NMDAR1 antisense modifies behavior', *Genes, Brain and Behavior*, 2(2), pp. 103–113. doi: 10.1034/j.1601-183X.2003.00015.x.

Ahlgren, S. C., Wang, J. F. and Levine, J. D. (1996) 'C-fiber mechanical stimulus-response functions are different in inflammatory versus neuropathic hyperalgesia in the rat', *Neuroscience*. Pergamon, 76(1), pp. 285–290. doi: 10.1016/S0306-4522(96)00290-4.

Ahrens, M. B. *et al.* (2013) 'Whole-brain functional imaging at cellular resolution using light-sheet microscopy', *Nature Methods*. Nature Publishing Group, 10(5), pp. 413–420. doi: 10.1038/nmeth.2434.

Akache, B. *et al.* (2006) 'The 37/67-Kilodalton Laminin Receptor Is a Receptor for Adeno-Associated Virus Serotypes 8, 2, 3, and 9', *Journal of Virology*, 80(19), pp. 9831–9836. doi: 10.1128/JVI.00878-06.

Akerboom, J. *et al.* (2012) 'Optimization of a GCaMP Calcium Indicator for Neural Activity Imaging', *Journal of Neuroscience*, 32(40), pp. 13819–13840. doi: 10.1523/JNEUROSCI.2601-12.2012.

Akerboom, J. *et al.* (2013) 'Genetically encoded calcium indicators for multi-color neural activity imaging and combination with optogenetics', *Frontiers in Molecular Neuroscience*, 6(March), p. 2. doi: 10.3389/fnmol.2013.00002.

Alexander, G. M. *et al.* (2009) 'Remote Control of Neuronal Activity in Transgenic Mice Expressing Evolved G Protein-Coupled Receptors', *Neuron*. Elsevier, 63(1), pp. 27–39. doi:

10.1016/j.neuron.2009.06.014.

Allchorne, A. J., Broom, D. C. and Woolf, C. J. (2005) 'Detection of cold pain, cold allodynia and cold hyperalgesia in freely behaving rats', *Molecular Pain*. SAGE Publications, 1, p. 36. doi: 10.1186/1744-8069-1-36.

Alonso, M. T., Manjarrés, I. M. and García-Sancho, J. (2009) 'Modulation of calcium signalling by intracellular organelles seen with targeted aequorins', in *Acta Physiologica*, pp. 37–49. doi: 10.1111/j.1748-1716.2008.01920.x.

Alviña, K., Ellis-Davies, G. and Khodakhah, K. (2009) 'T-type calcium channels mediate rebound firing in intact deep cerebellar neurons', *Neuroscience*. Pergamon, 158(2), pp. 635–641. doi: 10.1016/j.neuroscience.2008.09.052.

Anderson, H. E. *et al.* (2018) 'Imaging of electrical activity in small diameter fibers of the murine peripheral nerve with virally-delivered GCaMP6f', *Scientific Reports*. Springer US, 8(1), pp. 2–10. doi: 10.1038/s41598-018-21528-1.

Anderson, M., Zheng, Q. and Dong, X. (2018) 'Investigation of Pain Mechanisms by Calcium Imaging Approaches', *Neuroscience Bulletin*. Springer Singapore, 34(1), pp. 194–199. doi: 10.1007/s12264-017-0139-9.

Andrade-Moraes, C. H. *et al.* (2013) 'Cell number changes in Alzheimer's disease relate to dementia, not to plaques and tangles.', *Brain : a journal of neurology*. Oxford University Press, 136(Pt 12), pp. 3738–3752. doi: 10.1093/brain/awt273.

Andrew, D. and Greenspan, J. D. (1999) 'Mechanical and Heat Sensitization of Cutaneous Nociceptors After Peripheral Inflammation in The Rat', *Journal of Neurophysiology*. American Physiological SocietyBethesda, MD, 82(5), pp. 2649–2656. doi: 10.1152/jn.1999.82.5.2649.

Anstötz, M., Lee, S. K. and Maccaferri, G. (2018) 'Expression of TRPV1 channels by Cajal-Retzius cells and layer-specific modulation of synaptic transmission by capsaicin in the mouse hippocampus', *The Journal of Physiology*. Wiley/Blackwell (10.1111). doi: 10.1113/JP275685.

Apkarian, A. V. *et al.* (2005) 'Human brain mechanisms of pain perception and regulation in health and disease', *European Journal of Pain*. Wiley-Blackwell, 9(4), pp. 463–484. doi: 10.1016/j.ejpain.2004.11.001.

Apolonia, L. *et al.* (2007) 'Stable gene transfer to muscle using non-integrating lentiviral vectors', *Molecular Therapy*, 15(11), pp. 1947–1954. doi: 10.1038/sj.mt.6300281.

Aponte-Ubillus, J. J. *et al.* (2018) 'Molecular design for recombinant adeno-associated virus (rAAV) vector production', *Applied Microbiology and Biotechnology*. Applied Microbiology and Biotechnology, 102(3), pp. 1045–1054. doi: 10.1007/s00253-017-8670-1.

Argoff, C. E. *et al.* (2004) 'Effectiveness of the lidocaine patch 5% on pain qualities in three chronic pain states: assessment with the Neuropathic Pain Scale', *Current Medical Research and Opinion*, 20(sup2), pp. S21–S28. doi: 10.1185/030079904X12960.

Aschauer, D. F., Kreuz, S. and Rumpel, S. (2013) 'Analysis of Transduction Efficiency, Tropism and Axonal Transport of AAV Serotypes 1, 2, 5, 6, 8 and 9 in the Mouse Brain', *PLoS ONE*, 8(9), pp. 1–16. doi: 10.1371/journal.pone.0076310.

Atchison, R. W., Casto, B. C. and Hammon, W. M. (1965) 'Adenovirus-associated defective virus particle.', *Science (New York, N.Y.)*, 149(3685), pp. 754–6. doi: 10.1126/science.149.3685.754.

Ayers, J. I. *et al.* (2015) 'Widespread and efficient transduction of spinal cord and brain following neonatal AAV injection and potential disease modifying effect in ALS mice', *Molecular Therapy*, 23(1), pp. 53–62. doi: 10.1038/mt.2014.180.

Badura, A. *et al.* (2014) 'Fast calcium sensor proteins for monitoring neural activity', *Neurophotonics*, 1(2), p. 025008. doi: 10.1117/1.NPh.1.2.025008.

Bailey, R. M. *et al.* (2018) 'Development of Intrathecal AAV9 Gene Therapy for Giant Axonal Neuropathy', *Molecular Therapy - Methods and Clinical Development*. American Society of Gene & Cell Therapy, 9, pp. 160–171. doi: 10.1016/j.omtm.2018.02.005.

Baird, G. S., Zacharias, D. A. and Tsien, R. Y. (1999) 'Circular permutation and receptor insertion within green fluorescent proteins', *Proceedings of the National Academy of Sciences*, 96(20), pp. 11241–11246. doi: 10.1073/pnas.96.20.11241.

Bakayan, A. *et al.* (2011) 'Red fluorescent protein-aequorin fusions as improved bioluminescent Ca2+ reporters in single cells and mice', *PLoS ONE*. Public Library of Science, 6(5), p. e19520. doi: 10.1371/journal.pone.0019520.

Baliki, M. N. and Apkarian, A. V. (2015) 'Nociception, Pain, Negative Moods, and Behavior Selection', *Neuron*. NIH Public Access, 87(3), pp. 474–491. doi: 10.1016/j.neuron.2015.06.005.

Bandell, M. *et al.* (2004) 'Noxious cold ion channel TRPA1 is activated by pungent compounds and bradykinin', *Neuron*, 41(6), pp. 849–857. doi: 10.1016/S0896-6273(04)00150-3.

Banik, R. K. *et al.* (2001) 'B2 Receptor–Mediated Enhanced Bradykinin Sensitivity of Rat Cutaneous C-Fiber Nociceptors During Persistent Inflammation', *Journal of Neurophysiology*, 86(6), pp. 2727–2735. doi: 10.1152/jn.2001.86.6.2727.

Barabas, M. E., Kossyreva, E. A. and Stucky, C. L. (2012) 'TRPA1 Is Functionally Expressed Primarily by IB4-Binding, Non-Peptidergic Mouse and Rat Sensory Neurons', *PLoS ONE*. Public Library of Science, 7(10), p. e47988. doi: 10.1371/journal.pone.0047988.

Barreto-Chang, O. L. and Dolmetsch, R. E. (2009) 'Calcium Imaging of Cortical Neurons using Fura-2 AM', *Journal of Visualized Experiments*. MyJoVE Corporation, (23). doi: 10.3791/1067.

von Bartheld, C. S., Bahney, J. and Herculano-Houzel, S. (2016) 'The search for true numbers of neurons and glial cells in the human brain: A review of 150 years of cell counting', *Journal of Comparative Neurology*. NIH Public Access, pp. 3865–3895. doi: 10.1002/cne.24040.

Basbaum, A. I. *et al.* (2009) 'Cellular and Molecular Mechanisms of Pain', *Cell*, 139(2), pp. 267–284. doi: 10.1016/j.cell.2009.09.028.

Basbaum, A. I. and Bráz, J. M. (2010) 'Transgenic Mouse Models for the Tracing of "Pain"

Pathways', in Kruger, L. and Light, A. (eds) *Translational Pain Research: From Mouse to Man*. CRC Press/Taylor & Francis. Available at: http://www.ncbi.nlm.nih.gov/pubmed/21882471 (Accessed: 9 August 2018).

Basbaum, A. I. and Jessell, T. M. (2000) 'The perception of pain', in Kandel, E. R., Schwartz, J. H., and Jessell, T. M. (eds) *Principles of Neural Science*. 4th editio. Elsevier.

Basso, D. M., Beattie, M. S. and Bresnahan, J. C. (1995) 'A Sensitive and Reliable Locomotor Rating Scale for Open Field Testing in Rats', *Journal of Neurotrauma*, 12(1), pp. 1–21. doi: 10.1089/neu.1995.12.1.

Baubet, V. *et al.* (2000) 'Chimeric green fluorescent protein-aequorin as bioluminescent Ca2+ reporters at the single-cell level.', *Proceedings of the National Academy of Sciences of the United States of America*. National Academy of Sciences, 97(13), pp. 7260–5. Available at: http://www.ncbi.nlm.nih.gov/pubmed/10860991 (Accessed: 19 July 2018).

Bayer, M. *et al.* (2008) 'A large U3 deletion causes increased in vivo expression from a nonintegrating lentiviral vector', *Molecular Therapy*, 16(12), pp. 1968–1976. doi: 10.1038/mt.2008.199.

Bell, C. L. *et al.* (2011) 'The AAV9 receptor and its modification to improve in vivo lung gene transfer in mice', *Journal of Clinical Investigation*, 121(6), pp. 2427–2435. doi: 10.1172/JCI57367.

Bell, D. C. and Dallas, M. L. (2018) 'Using automated patch clamp electrophysiology platforms in pain-related ion channel research: insights from industry and academia', *British Journal of Pharmacology*, pp. 2312–2321. doi: 10.1111/bph.13916.

Benkhelifa-Ziyyat, S. *et al.* (2013) 'Intramuscular scAAV9-SMN injection mediates widespread gene delivery to the spinal cord and decreases disease severity in SMA mice', *Molecular Therapy*. Elsevier, 21(2), pp. 282–290. doi: 10.1038/mt.2012.261.

Bennett, D. L. H. and Woods, C. G. (2014) 'Painful and painless channelopathies', *The Lancet*

Neurology. Elsevier, pp. 587–599. doi: 10.1016/S1474-4422(14)70024-9.

Benskey, M. J. *et al.* (2015) 'Targeted gene delivery to the enteric nervous system using AAV: A comparison across serotypes and capsid mutants', *Molecular Therapy*, 23(3), pp. 488–500. doi: 10.1038/mt.2015.7.

Berridge, M. J., Bootman, M. D. and Roderick, H. L. (2003) 'Calcium signalling: dynamics, homeostasis and remodelling', *Nature Reviews Molecular Cell Biology*. Nature Publishing Group, 4(7), pp. 517–529. doi: 10.1038/nrm1155.

Berridge, M. J., Lipp, P. and Bootman, M. D. (2000) 'The versatility and universality of calcium signalling', *Nature Reviews Molecular Cell Biology*. Nature Publishing Group, pp. 11–21. doi: 10.1038/35036035.

Bessis, N., GarciaCozar, F. J. and Boissier, M. C. (2004) 'Immune responses to gene therapy vectors: Influence on vector function and effector mechanisms', *Gene Therapy*. Nature Publishing Group, pp. S10–S17. doi: 10.1038/sj.gt.3302364.

Bey, K. *et al.* (2017) 'Efficient CNS targeting in adult mice by intrathecal infusion of single-stranded AAV9-GFP for gene therapy of neurological disorders', *Gene Therapy*. Nature Publishing Group, 24(5), pp. 325–332. doi: 10.1038/gt.2017.18.

Bhave, G. *et al.* (2003) 'Protein kinase C phosphorylation sensitizes but does not activate the capsaicin receptor transient receptor potential vanilloid 1 (TRPV1)', *Proceedings of the National Academy of Sciences*. National Academy of Sciences, 100(21), pp. 12480–12485. doi: 10.1073/pnas.2032100100.

Bischof, D. and Cornetta, K. (2010) 'Flexibility in cell targeting by pseudotyping lentiviral vectors.', *Methods in molecular biology (Clifton, N.J.)*. Humana Press, Totowa, NJ, 614, pp. 53–68. doi: 10.1007/978-1-60761-533-0_3.

Bishop, T. *et al.* (2010) 'Ultraviolet-B-induced mechanical hyperalgesia: A role for peripheral sensitisation', *Pain*. No longer published by Elsevier, 150(1), pp. 141–152. doi:

10.1016/j.pain.2010.04.018.

Bleakman, D., Brorson, J. R. and Miller, R. J. (1990) 'The effect of capsaicin on voltage-gated calcium currents and calcium signals in cultured dorsal root ganglion cells.', *British journal of pharmacology*. Wiley/Blackwell (10.1111), 101(2), pp. 423–31. doi: 10.1111/j.1476-5381.1990.tb12725.x.

Bloodgood, B. L. and Sabatini, B. L. (2007) 'Nonlinear Regulation of Unitary Synaptic Signals by CaV2.3 Voltage-Sensitive Calcium Channels Located in Dendritic Spines', *Neuron*. Elsevier, 53(2), pp. 249–260. doi: 10.1016/j.neuron.2006.12.017.

Bloodgood, B. L. and Sabatini, B. L. (2009) *NMDA Receptor-Mediated Calcium Transients in Dendritic Spines*, *Biology of the NMDA Receptor*. CRC Press/Taylor & Francis. Available at: http://www.ncbi.nlm.nih.gov/pubmed/21204410 (Accessed: 31 August 2018).

Bolsover, S. R. and Spector, I. (1986) 'Measurements of calcium transients in the soma, neurite, and growth cone of single cultured neurons.', *The Journal of neuroscience : the official journal of the Society for Neuroscience*, 6(7), pp. 1934–40. Available at: http://www.ncbi.nlm.nih.gov/pubmed/3734868 (Accessed: 31 August 2018).

Bonin, R. P., Bories, C. and De Koninck, Y. (2014) 'A Simplified Up-Down Method (SUDO) for Measuring Mechanical Nociception in Rodents Using von Frey Filaments', *Molecular Pain*, 10, pp. 1744-8069-10–26. doi: 10.1186/1744-8069-10-26.

Bonnington, J. K. and McNaughton, P. A. (2003) 'Signalling pathways involved in the sensitisation of mouse nociceptive neurones by nerve growth factor', *Journal of Physiology*, 551(2), pp. 433–446. doi: 10.1113/jphysiol.2003.039990.

Boudreau, R. L., Martins, I. and Davidson, B. L. (2009) 'Artificial MicroRNAs as siRNA shuttles: Improved safety as compared to shRNAs in vitro and In vivo', *Molecular Therapy*. Elsevier, 17(1), pp. 169–175. doi: 10.1038/mt.2008.231.

Boutin, S. *et al.* (2010) 'Prevalence of Serum IgG and Neutralizing Factors Against Adeno-

Associated Virus (AAV) Types 1, 2, 5, 6, 8, and 9 in the Healthy Population: Implications for Gene Therapy Using AAV Vectors', *Human Gene Therapy*. Mary Ann Liebert, Inc. 140 Huguenot Street, 3rd Floor New Rochelle, NY 10801 USA, 21(6), pp. 704–712. doi: 10.1089/hum.2009.182.

Bowles, D. E. *et al.* (2012) 'Phase 1 gene therapy for duchenne muscular dystrophy using a translational optimized AAV vector', *Molecular Therapy*, 20(2), pp. 443–455. doi: 10.1038/mt.2011.237.

Boyden, E. S. *et al.* (2005) 'Millisecond-timescale, genetically targeted optical control of neural activity', *Nature Neuroscience*. Nature Publishing Group, 8(9), pp. 1263–1268. doi: 10.1038/nn1525.

Boyle, K. A. *et al.* (2017) 'A quantitative study of neurochemically defined populations of inhibitory interneurons in the superficial dorsal horn of the mouse spinal cord', *Neuroscience*. Pergamon, 363, pp. 120–133. doi: 10.1016/j.neuroscience.2017.08.044.

Braz, J. *et al.* (2001) 'Therapeutic efficacy in experimental polyarthritis of viral-driven enkephalin overproduction in sensory neurons.', *The Journal of neuroscience : the official journal of the Society for Neuroscience*, 21(20), pp. 7881–7888. doi: 21/20/7881 [pii].

Braz, J. M., Rico, B. and Basbaum, A. I. (2002) 'Transneuronal tracing of diverse CNS circuits by Cre-mediated induction of wheat germ agglutinin in transgenic mice', *Proceedings of the National Academy of Sciences*, 99(23), pp. 15148–15153. doi: 10.1073/pnas.222546999.

Breivik, H. *et al.* (2006) 'Survey of chronic pain in Europe: Prevalence, impact on daily life, and treatment', *European Journal of Pain*, 10(4), pp. 287–333. doi: 10.1016/j.ejpain.2005.06.009.

Brendel, A. *et al.* (2014) 'Downregulation of PMCA2 increases the vulnerability of midbrain neurons to mitochondrial complex I inhibition', *NeuroToxicology*. Elsevier, 40, pp. 43–51. doi: 10.1016/j.neuro.2013.11.003.

Brewer, K. L. and Yezierski, R. P. (1998) 'Effects of adrenal medullary transplants on pain-

related behaviors following excitotoxic spinal cord injury', *Brain Research*, 798(1–2), pp. 83–92. doi: 10.1016/S0006-8993(98)00398-9.

Brini, M. (2008) 'Calcium-sensitive photoproteins', *Methods*. Academic Press, 46(3), pp. 160–166. doi: 10.1016/j.ymeth.2008.09.011.

Brini, M. *et al.* (2014) 'Neuronal calcium signaling: Function and dysfunction', *Cellular and Molecular Life Sciences*. Springer Basel, pp. 2787–2814. doi: 10.1007/s00018-013-1550-7.

Brooks, A. I. *et al.* (2000) 'Enhanced learning in mice parallels vector-mediated nerve growth factor expression in hippocampus.', *Human gene therapy*, 11(17), pp. 2341–52. doi: 10.1089/104303400750038453.

Brooks, S. P. and Dunnett, S. B. (2009) 'Tests to assess motor phenotype in mice: a user's guide', *Nature Reviews Neuroscience*. Nature Publishing Group, 10(7), pp. 519–529. doi: 10.1038/nrn2652.

Broussard, G. J., Liang, R. and Tian, L. (2014) 'Monitoring activity in neural circuits with genetically encoded indicators', *Frontiers in Molecular Neuroscience*. Frontiers Media SA, 7(December), p. 97. doi: 10.3389/fnmol.2014.00097.

Brumovsky, P. R. (2016) 'Dorsal root ganglion neurons and tyrosine hydroxylase - An intriguing association with implications for sensation and pain', *Pain*. NIH Public Access, pp. 314–320. doi: 10.1097/j.pain.0000000000000381.

Brumovsky, P., Villar, M. J. and Hökfelt, T. (2006) 'Tyrosine hydroxylase is expressed in a subpopulation of small dorsal root ganglion neurons in the adult mouse', *Experimental Neurology*, 200(1), pp. 153–165. doi: 10.1016/j.expneurol.2006.01.023.

Bucurenciu, I. *et al.* (2008) 'Nanodomain Coupling between Ca2+Channels and Ca2+Sensors Promotes Fast and Efficient Transmitter Release at a Cortical GABAergic Synapse', *Neuron*. Elsevier, 57(4), pp. 536–545. doi: 10.1016/j.neuron.2007.12.026.

Burger, C. *et al.* (2004) 'Recombinant AAV viral vectors pseudotyped with viral capsids from serotypes 1, 2, and 5 display differential efficiency and cell tropism after delivery to different regions of the central nervous system', *Molecular Therapy*. Elsevier, 10(2), pp. 302–317. doi: 10.1016/j.ymthe.2004.05.024.

Calvo-Rodríguez, M., Villalobos, C. and Nuñez, L. (2015) 'Fluorescence and Bioluminescence Imaging of Subcellular Ca2+ in Aged Hippocampal Neurons', *Journal of Visualized Experiments*. MyJoVE Corporation, (106). doi: 10.3791/53330.

Cameron, D. *et al.* (2015) 'The organisation of spinoparabrachial neurons in the mouse.', *Pain*. Wolters Kluwer Health, 156(10), pp. 2061–71. doi: 10.1097/j.pain.0000000000000270.

Cameron, M. *et al.* (2016) 'Calcium imaging of am dyes following prolonged incubation in acute neuronal tissue', *PLoS ONE*. Public Library of Science, 11(5), p. e0155468. doi: 10.1371/journal.pone.0155468.

Campos, S. K. and Barry, M. A. (2008) 'Current advances and future challenges in adenoviral vector biology and targeting', *Curr. Gene Ther.* NIH Public Access, 7(3), pp. 189–204. doi: 10.1016/j.bbi.2008.05.010.

Cardoso, F. C. and Lewis, R. J. (2017) 'Sodium channels and pain: From toxins to therapies', *British Journal of Pharmacology*. Wiley/Blackwell (10.1111), 175(12), pp. 2138–2157. doi: 10.1111/bph.13962.

Carter, M. and Shieh, J. (2015) 'Electrophysiology', in Carter, M. and Shieh, J. (eds) *Guide to Research Techniques in Neuroscience*. 2nd edn. Academic Press, pp. 89–115. doi: 10.1016/B978-0-12-800511-8.00004-6.

Castle, M. J., Gershenson, Z. T., *et al.* (2014) 'Adeno-Associated Virus Serotypes 1, 8, and 9 Share Conserved Mechanisms for Anterograde and Retrograde Axonal Transport', *Human Gene Therapy*, 25(8), pp. 705–720. doi: 10.1089/hum.2013.189.

Castle, M. J., Perlson, E., *et al.* (2014) 'Long-distance axonal transport of AAV9 is driven by

dynein and kinesin-2 and is trafficked in a highly motile Rab7-positive compartment', *Molecular Therapy*, 22(3), pp. 554–566. doi: 10.1038/mt.2013.237.

Caterina, M. J. *et al.* (1997) 'The capsaicin receptor: A heat-activated ion channel in the pain pathway', *Nature*. Nature Publishing Group, 389(6653), pp. 816–824. doi: 10.1038/39807.

Caterina, M. J. *et al.* (2000) 'Impaired nociception and pain sensation in mice lacking the capsaicin receptor', *Science*, 288(5464), pp. 306–313. doi: 10.1126/science.288.5464.306.

Caterina, M. J., Gold, M. S. and Meyer, R. A. (2005) 'Molecular biology of nociceptors', in Hunt, S. and Koltzenburg, M. (eds) *Ther neurobiology of pain*. Oxford University Press, pp. 1–33.

Caterina, M. J. and Julius, D. (2001) 'The Vanilloid Receptor: A Molecular Gateway to the Pain Pathway', *Annual Review of Neuroscience*. Annual Reviews 4139 El Camino Way, P.O. Box 10139, Palo Alto, CA 94303-0139, USA, 24(1), pp. 487–517. doi: 10.1146/annurev.neuro.24.1.487.

Catterall, W. A. (2000) 'Structure and Regulation of Voltage-Gated Ca 2+ Channels', *Annual Review of Cell and Developmental Biology*, 16(1), pp. 521–555. doi: 10.1146/annurev.cellbio.16.1.521.

Catterall, W. A. (2011) 'Voltage-gated calcium channels', *Cold Spring Harbor Perspectives in Biology*. Cold Spring Harbor Laboratory Press, 3(8), pp. 1–23. doi: 10.1101/cshperspect.a003947.

Cearley, C. N. and Wolfe, J. H. (2006) 'Transduction characteristics of adeno-associated virus vectors expressing cap serotypes 7, 8, 9, and Rh10 in the mouse brain', *Molecular Therapy*, 13(3), pp. 528–537. doi: 10.1016/j.ymthe.2005.11.015.

Cearley, C. N. and Wolfe, J. H. (2007) 'A Single Injection of an Adeno-Associated Virus Vector into Nuclei with Divergent Connections Results in Widespread Vector Distribution in the Brain and Global Correction of a Neurogenetic Disease', *Journal of Neuroscience*, 27(37), pp. 9928–9940. doi: 10.1523/JNEUROSCI.2185-07.2007.

Cesare, P. and McNaughton, P. (1996) 'A novel heat-activated current in nociceptive neurons and its sensitization by bradykinin.', *Proceedings of the National Academy of Sciences of the United States of America*, 93(26), pp. 15435–9. doi: 10.1073/pnas.93.26.15435.

Chakrabarty, P. *et al.* (2013) 'Capsid Serotype and Timing of Injection Determines AAV Transduction in the Neonatal Mice Brain', *PLoS ONE*. Public Library of Science, 8(6), p. e67680. doi: 10.1371/journal.pone.0067680.

Chandrasekar, A. *et al.* (2018) 'Parvalbumin Interneurons Shape Neuronal Vulnerability in Blunt TBI', *Cerebral Cortex*. doi: 10.1093/cercor/bhy139.

Chang, H. M. *et al.* (1989) 'Sufentanil, morphine, met-enkephalin, and κ-agonist (U-50,488H) inhibit substance P release from primary sensory neurons: A model for presynaptic spinal opioid actions', *Anesthesiology*. NIH Public Access, 70(4), pp. 672–677. doi: 10.1097/00000542-198904000-00022.

Chaplan, S. R. *et al.* (1994) 'Quantitative assessment of tactile allodynia in the rat paw', *Journal of Neuroscience Methods*. Elsevier, 53(1), pp. 55–63. doi: 10.1016/0165-0270(94)90144-9.

Chattopadhyay, M. *et al.* (2005) 'Long-term neuroprotection achieved with latency-associated promoter-driven herpes simplex virus gene transfer to the peripheral nervous system', *Molecular Therapy*, 12(2), pp. 307–313. doi: 10.1016/j.ymthe.2005.04.009.

Chen, J. *et al.* (2017) 'Deletion of TRPC6 attenuates NMDA receptor-mediated Ca2+entry and Ca2+-induced neurotoxicity following cerebral ischemia and oxygen-glucose deprivation', *Frontiers in Neuroscience*. Frontiers Media SA, 11(MAR), p. 138. doi: 10.3389/fnins.2017.00138.

Chen, L. *et al.* (2018) 'Conditional knockout of NaV1.6 in adult mice ameliorates neuropathic pain', *Scientific Reports*. Nature Publishing Group, 8(1), p. 3845. doi: 10.1038/s41598-018-22216-w.

Chen, Q. *et al.* (2012) 'Imaging Neural Activity Using Thy1-GCaMP Transgenic Mice', *Neuron*. Elsevier, 76(2), pp. 297–308. doi: 10.1016/j.neuron.2012.07.011.

Chen, T. W. *et al.* (2013) 'Ultrasensitive fluorescent proteins for imaging neuronal activity', *Nature*. Nature Publishing Group, 499(7458), pp. 295–300. doi: 10.1038/nature12354.

Chen, Y. *et al.* (2013) 'Novel modified method for injection into the cerebrospinal fluid via the cerebellomedullary cistern in mice', *Acta Neurobiologiae Experimentalis*, 73(2), pp. 304–311. Available at: http://www.ncbi.nlm.nih.gov/pubmed/23823990 (Accessed: 24 August 2018).

Chen, Y. *et al.* (2013) 'Structural insight into enhanced calcium indicator GCaMP3 and GCaMPJ to promote further improvement', *Protein and Cell*, 4(4), pp. 299–309. doi: 10.1007/s13238-013-2103-4.

Chen, Y. H. *et al.* (2012) 'Sialic acid deposition impairs the utility of AAV9, but not peptide-modified AAVs for brain gene therapy in a mouse model of lysosomal storage disease', *Molecular Therapy*. Nature Publishing Group, 20(7), pp. 1393–1399. doi: 10.1038/mt.2012.100.

Chew, W. L. *et al.* (2016) 'A multifunctional AAV-CRISPR-Cas9 and its host response', *Nature Methods*, 13(10), pp. 868–874. doi: 10.1038/nmeth.3993.

Chiesa, A. *et al.* (2001) 'Recombinant aequorin and green fluorescent protein as valuable tools in the study of cell signalling', *Biochemical Journal*. Portland Press Ltd, 355(Pt 1), pp. 1–12. doi: 10.1042/0264-6021:3550001.

Chisholm, K. I. *et al.* (2018) 'Large Scale in Vivo Recording of Sensory Neuron Activity with GCaMP6', *eNeuro*, 5(1), p. ENEURO.0417-17.2018. doi: 10.1523/ENEURO.0417-17.2018.

Chiu, C. Q. *et al.* (2013) 'Compartmentalization of GABAergic inhibition by dendritic spines', *Science*. NIH Public Access, 340(6133), pp. 759–762. doi: 10.1126/science.1234274.

Chow, B. Y. *et al.* (2010) 'High-performance genetically targetable optical neural silencing by light-driven proton pumps', *Nature*. Nature Publishing Group, 463(7277), pp. 98–102. doi: 10.1038/nature08652.

Chuang, H. H. *et al.* (2001) 'Bradykinin and nerve growth factor release the capsaicin receptor

from PtdIns(4,5)P2-mediated inhibition', *Nature*. Nature Publishing Group, 411(6840), pp. 957–962. doi: 10.1038/35082088.

Ciesielska, A. *et al.* (2013) 'Cerebral infusion of AAV9 vector-encoding non-self proteins can elicit cell-mediated immune responses', *Molecular Therapy*. Nature Publishing Group, 21(1), pp. 158–166. doi: 10.1038/mt.2012.167.

Clapham, D. E. (2007) 'Calcium Signaling', *Cell*. Cell Press, pp. 1047–1058. doi: 10.1016/j.cell.2007.11.028.

Clarke, J. N. *et al.* (2011) 'Non-peptidergic small diameter primary afferents expressing VGluT2 project to lamina I of mouse spinal dorsal horn', *Molecular Pain*, 7, pp. 1744-8069-7–95. doi: 10.1186/1744-8069-7-95.

ClinicalTrials.gov (no date a) *Search of: (AAV OR scAAV) AND intrathecal - List Results - ClinicalTrials.gov*.

ClinicalTrials.gov (no date b) *Search of: (AAV OR scAAV) NOT ANCA - List Results - ClinicalTrials.gov*. Available at: https://clinicaltrials.gov/ct2/results?term=%28AAV+OR+scAAV%29+NOT+ANCA (Accessed: 28 August 2018).

Cobos, E. J. *et al.* (2018) 'Mechanistic Differences in Neuropathic Pain Modalities Revealed by Correlating Behavior with Global Expression Profiling.', *Cell reports*. NIH Public Access, 22(5), pp. 1301–1312. doi: 10.1016/j.celrep.2018.01.006.

Coffin, J. M., Hughes, S. H. and Varmus, H. E. (1997) 'The Interactions of Retroviruses and their Hosts', *Retroviruses*. doi: NBK19465 [bookaccession].

Colella, P., Ronzitti, G. and Mingozzi, F. (2018) 'Emerging Issues in AAV-Mediated In Vivo Gene Therapy', *Molecular Therapy - Methods and Clinical Development*. Elsevier Ltd., 8(March), pp. 87–104. doi: 10.1016/j.omtm.2017.11.007.

Coste, B. *et al.* (2010) 'Piezo1 and Piezo2 are essential components of distinct mechanically activated cation channels', *Science*. NIH Public Access, 330(6000), pp. 55–60. doi: 10.1126/science.1193270.

Coutinho, V. and Knöpfel, T. (2002) 'Metabotropic Glutamate Receptors: Electrical and Chemical Signaling Properties', *The Neuroscientist*, 8(6), pp. 551–561. doi: 10.1177/1073858402238514.

Cronin, J., Zhang, X.-Y. and Reiser, J. (2005) 'Altering the Tropism of Lentiviral Vectors through Pseudotyping', *Current Gene Therapy*, 5(4), pp. 387–398. doi: 10.2174/1566523054546224.

Crow, M. *et al.* (2015) 'HDAC4 is required for inflammation-associated thermal hypersensitivity', *FASEB Journal*, 29(8), pp. 3370–3378. doi: 10.1096/fj.14-264440.

Cully, D. F. *et al.* (1994) 'Cloning of an avermectin-sensitive glutamate-gated chloride channel from Caenorhabditis elegans', *Nature*. Nature Publishing Group, 371(6499), pp. 707–711. doi: 10.1038/371707a0.

D'Acunzo, P. *et al.* (2014) 'A conditional transgenic reporter of presynaptic terminals reveals novel features of the mouse corticospinal tract', *Frontiers in Neuroanatomy*. Frontiers Media SA, 7, p. 50. doi: 10.3389/fnana.2013.00050.

Dana, H. *et al.* (2014) 'Thy1-GCaMP6 transgenic mice for neuronal population imaging in vivo', *PLoS ONE*. Edited by B. Arenkiel. Public Library of Science, 9(9), p. e108697. doi: 10.1371/journal.pone.0108697.

Daou, I. *et al.* (2013) 'Remote Optogenetic Activation and Sensitization of Pain Pathways in Freely Moving Mice', *Journal of Neuroscience*. Society for Neuroscience, 33(47), pp. 18631–18640. doi: 10.1523/JNEUROSCI.2424-13.2013.

Dashkoff, J. *et al.* (2016) 'Tailored transgene expression to specific cell types in the central nervous system after peripheral injection with AAV9', *Molecular Therapy - Methods and Clinical Development*, 3(October), p. 16081. doi: 10.1038/mtm.2016.81.

Davidson, B. L. (2000) 'Recombinant adeno-associated virus type 2, 4, and 5 vectors: Transduction of variant cell types and regions in the mammalian central nervous system', *Proceedings of the National Academy of Sciences*. National Academy of Sciences, 97(7), pp. 3428–3432. doi: 10.1073/pnas.050581197.

Davis, J. B. *et al.* (2000) 'Vanilloid receptor-1 is essential for inflammatory thermal hyperalgesia', *Nature*. Nature Publishing Group, 405(6783), pp. 183–187. doi: 10.1038/35012076.

Davis, K. D., Meyer, R. A. and Campbell, J. N. (1993) 'Chemosensitivity and sensitization of nociceptive afferents that innervate the hairy skin of monkey.', *Journal of Neurophysiology*. American Physiological Society Bethesda, MD, 69(4), pp. 1071–1081. doi: 10.1152/jn.1993.69.4.1071.

Dawes, J. M. *et al.* (2013) 'Inflammatory Mediators and Modulators of Pain', in McMahon, S. B. et al. (eds) *Wall & Melzack's Textbook of Pain*. 6th edn. Elsevier.

Denk, F. *et al.* (2015) 'Tamoxifen induces cellular stress in the nervous system by inhibiting cholesterol synthesis', *Acta neuropathologica communications*, 3(1), p. 74. doi: 10.1186/s40478-015-0255-6.

Denk, W. and Svoboda, K. (1997) 'Photon upmanship: Why multiphoton imaging is more than a gimmick', *Neuron*. Elsevier, 18(3), pp. 351–357. doi: 10.1016/S0896-6273(00)81237-4.

Derow, A. *et al.* (2007) 'Prostaglandin E2 and I2 facilitate noxious heat-induced spike discharge but not iCGRP release from rat cutaneous nociceptors', *Life Sciences*. Pergamon, 81(25–26), pp. 1685–1693. doi: 10.1016/j.lfs.2007.10.001.

Deverman, B. E. *et al.* (2018) 'Gene therapy for neurological disorders: progress and prospects', *Nature Reviews Drug Discovery*. Nature Publishing Group. doi: 10.1038/nrd.2018.110.

Devor, M. (2013) 'Neuropathic Pain: Pathophysiological Response of Nerves to Injury', in McMahon, S. B. et al. (eds) *Wall & Melzack's Textbook of Pain*. 6th edn. Elsevier.

Dib-Hajj, S. D. *et al.* (2005) 'Gain-of-function mutation in Nav1.7 in familial erythromelalgia induces bursting of sensory neurons', *Brain*, 128(8), pp. 1847–1854. doi: 10.1093/brain/awh514.

Ding, Y. Q. *et al.* (1995) 'Spinoparabrachial tract neurons showing substance P receptor-like immunoreactivity in the lumbar spinal cord of the rat', *Brain Research*, 674(2), pp. 336–340. doi: 10.1016/0006-8993(95)00022-I.

Dirren, E. *et al.* (2014) 'Intracerebroventricular Injection of Adeno-Associated Virus 6 and 9 Vectors for Cell Type–Specific Transgene Expression in the Spinal Cord', *Human Gene Therapy*, 25(2), pp. 109–120. doi: 10.1089/hum.2013.021.

Djouhri, L. *et al.* (2015) 'Persistent hindlimb inflammation induces changes in activation properties of hyperpolarization-activated current (Ih) in rat C-fiber nociceptors in vivo', *Neuroscience*. Pergamon, 301, pp. 121–133. doi: 10.1016/j.neuroscience.2015.05.074.

Djouhri, L. (2016) 'L5 spinal nerve axotomy induces sensitization of cutaneous L4 Aβ-nociceptive dorsal root ganglion neurons in the rat in vivo', *Neuroscience Letters*, 624, pp. 72–77. doi: 10.1016/j.neulet.2016.05.008.

Dombeck, D. A. *et al.* (2010) 'Functional imaging of hippocampal place cells at cellular resolution during virtual navigation', *Nature Neuroscience*, 13(11), pp. 1433–1440. doi: 10.1038/nn.2648.

Ver Donck, A. *et al.* (2014) 'Intrathecal Drug Administration in Chronic Pain Syndromes', *Pain Practice*, 14(5), pp. 461–476. doi: 10.1111/papr.12111.

Dong, J.-Y., Fan, P.-D. and Frizzell, R. A. (1996) 'Quantitative Analysis of the Packaging Capacity of Recombinant Adeno-Associated Virus', *Human Gene Therapy*, 7(17), pp. 2101–2112. doi: 10.1089/hum.1996.7.17-2101.

Donsante, A. *et al.* (2016) 'Intracerebroventricular delivery of self-complementary adeno-associated virus serotype 9 to the adult rat brain', *Gene Therapy*. Nature Publishing Group,

23(5), pp. 401–407. doi: 10.1038/gt.2016.6.

Doudna, J. A. and Charpentier, E. (2014) 'The new frontier of genome engineering with CRISPR-Cas9', *Science*, pp. 1258096–1258096. doi: 10.1126/science.1258096.

Draxler, P. *et al.* (2014) 'VGluT3+ Primary Afferents Play Distinct Roles in Mechanical and Cold Hypersensitivity Depending on Pain Etiology', *Journal of Neuroscience*. Society for Neuroscience, 34(36), pp. 12015–12028. doi: 10.1523/JNEUROSCI.2157-14.2014.

Duan, D. *et al.* (1998) 'Circular intermediates of recombinant adeno-associated virus have defined structural characteristics responsible for long-term episomal persistence in muscle tissue.', *Journal of virology*, 72(11), pp. 8568–77. Available at: http://www.ncbi.nlm.nih.gov/pubmed/9765395 (Accessed: 15 August 2018).

Duflo, F., Zhang, Y. and Eisenach, J. C. (2004) 'Electrical field stimulation to study inhibitory mechanisms in individual sensory neurons in culture', *Anesthesiology*. [American Society of Anesthesiologists, etc.], pp. 740–743. Available at: http://anesthesiology.pubs.asahq.org/article.aspx?articleid=1943398 (Accessed: 26 July 2018).

Le Duigou, C. *et al.* (2018) 'Imaging pathological activities of human brain tissue in organotypic culture', *Journal of Neuroscience Methods*. Elsevier, 298, pp. 33–44. doi: 10.1016/j.jneumeth.2018.02.001.

Dull, T. *et al.* (1998) 'A third-generation lentivirus vector with a conditional packaging system.', *Journal of virology*, 72(11), pp. 8463–71. doi: 98440501.

Dupont, G. and Combettes, L. (2016) 'Fine tuning of cytosolic Ca (2+) oscillations.', *F1000Research*. Faculty of 1000 Ltd, 5. doi: 10.12688/f1000research.8438.1.

Duque, S. *et al.* (2009) 'Intravenous administration of self-complementary AAV9 enables transgene delivery to adult motor neurons', *Molecular Therapy*. Nature Publishing Group, 17(7), pp. 1187–1196. doi: 10.1038/mt.2009.71.

Durham, P. L. *et al.* (2004) 'Neuronal expression and regulation of CGRP promoter activity following viral gene transfer into cultured trigeminal ganglia neurons', *Brain Research*, 997(1), pp. 103–110. doi: 10.1016/j.brainres.2003.11.005.

Van Duyne, G. D. (2015) 'Cre Recombinase', *Microbiology Spectrum*. American Society of Microbiology, 3(1), pp. 119–138. doi: 10.1128/microbiolspec.MDNA3-0014-2014.

Edvinsson, L. *et al.* (2018) 'CGRP as the target of new migraine therapies - Successful translation from bench to clinic', *Nature Reviews Neurology*. Nature Publishing Group, pp. 338–350. doi: 10.1038/s41582-018-0003-1.

Eisenach, J. C., Zhang, Y. and Duflo, F. (2005) 'α2-adrenoceptors inhibit the intracellular Ca2+ response to electrical stimulation in normal and injured sensory neurons, with increased inhibition of calcitonin gene-related peptide expressing neurons after injury', *Neuroscience*. Pergamon, 131(1), pp. 189–197. doi: 10.1016/j.neuroscience.2004.10.017.

Elmallah, M. K. *et al.* (2014) 'Sustained correction of motoneuron histopathology following intramuscular delivery of AAV in pompe mice', *Molecular Therapy*. American Society of Gene & Cell Therapy, 22(4), pp. 702–712. doi: 10.1038/mt.2013.282.

Emery, E. C. *et al.* (2016) 'In vivo characterization of distinct modality-specific subsets of somatosensory neurons using GCaMP', *Science Advances*, 2(11), pp. e1600990–e1600990. doi: 10.1126/sciadv.1600990.

Engelhardt, B. and Liebner, S. (2014) 'Novel insights into the development and maintenance of the blood-brain barrier', *Cell and Tissue Research*. Springer, 355(3), pp. 687–699. doi: 10.1007/s00441-014-1811-2.

England, S., Bevan, S. and Docherty, R. J. (1996) 'PGE2 modulates the tetrodotoxin-resistant sodium current in neonatal rat dorsal root ganglion neurones via the cyclic AMP-protein kinase A cascade.', *The Journal of physiology*. Wiley-Blackwell, 495(2), pp. 429–440. doi: 10.1113/jphysiol.1996.sp021604.

Epstein, A. L. (2005) 'HSV-1-based amplicon vectors: Design and applications', *Gene Therapy*, 12(S1), pp. S154–S158. doi: 10.1038/sj.gt.3302617.

Epstein, A. L. (2009) 'HSV-1-derived amplicon vectors: Recent technological improvements and remaining difficulties - A Review', *Memorias do Instituto Oswaldo Cruz*. Fundação Oswaldo Cruz, pp. 399–410. doi: 10.1590/S0074-02762009000300002.

Escors, D. and Breckpot, K. (2010) 'Lentiviral vectors in gene therapy: Their current status and future potential', *Archivum Immunologiae et Therapiae Experimentalis*. Europe PMC Funders, pp. 107–119. doi: 10.1007/s00005-010-0063-4.

Eun, S.-Y. Y. *et al.* (2001) 'Effects of capsaicin on Ca2+release from the intracellular Ca2+stores in the dorsal root ganglion cells of adult rats', *Biochemical and Biophysical Research Communications*. Academic Press, 285(5), pp. 1114–1120. doi: 10.1006/bbrc.2001.5272.

Fairbanks, C. A. (2003) 'Spinal delivery of analgesics in experimental models of pain and analgesia', *Advanced Drug Delivery Reviews*, 55(8), pp. 1007–1041. doi: 10.1016/S0169-409X(03)00101-7.

Feil, R. *et al.* (1996) 'Ligand-activated site-specific recombination in mice.', *Proceedings of the National Academy of Sciences*. National Academy of Sciences, 93(20), pp. 10887–10890. doi: 10.1073/pnas.93.20.10887.

Feil, R. *et al.* (1997) 'Regulation of Cre recombinase activity by mutated estrogen receptor ligand-binding domains', *Biochemical and Biophysical Research Communications*. Academic Press, 237(3), pp. 752–757. doi: 10.1006/bbrc.1997.7124.

Feil, S., Valtcheva, N. and Feil, R. (2009) 'Inducible cre mice', *Methods in Molecular Biology*. Humana Press, 530, pp. 343–363. doi: 10.1007/978-1-59745-471-1_18.

Ferreira, J., Da Silva, G. L. and Calixto, J. B. (2004) 'Contribution of vanilloid receptors to the overt nociception induced by B 2 kinin receptor activation in mice', *British Journal of Pharmacology*, 141(5), pp. 787–794. doi: 10.1038/sj.bjp.0705546.

Fire, A. *et al.* (1998) 'Potent and specific genetic interference by double-stranded RNA in caenorhabditis elegans', *Nature*. Nature Publishing Group, 391(6669), pp. 806–811. doi: 10.1038/35888.

Fischer, G. *et al.* (2011) 'Direct injection into the dorsal root ganglion: Technical, behavioral, and histological observations', *Journal of Neuroscience Methods*. Elsevier B.V., 199(1), pp. 43–55. doi: 10.1016/j.jneumeth.2011.04.021.

Fischer, G. *et al.* (2014) 'Sustained relief of neuropathic pain by AAV-targeted expression of CBD3 peptide in rat dorsal root ganglion', *Gene Therapy*, 21(1), pp. 44–51. doi: 10.1038/gt.2013.56.

Fischer, T. Z. and Waxman, S. G. (2010) 'Familial pain syndromes from mutations of the Nav1.7 sodium channel', *Annals of the New York Academy of Sciences*. Wiley/Blackwell (10.1111), pp. 196–207. doi: 10.1111/j.1749-6632.2009.05110.x.

Fitzgerald, E. M. *et al.* (1999) 'cAMP-dependent phosphorylation of the tetrodotoxin-resistant voltage-dependent sodium channel SNS', *Journal of Physiology*. Wiley-Blackwell, 516(2), pp. 433–446. doi: 10.1111/j.1469-7793.1999.0433v.x.

Fleischer, E., Handwerker, H. O. and Joukhadar, S. (1983) 'Unmyelinated nociceptive units in two skin areas of the rat', *Brain Research*. Elsevier, 267(1), pp. 81–92. doi: 10.1016/0006-8993(83)91041-7.

Fletcher, M. L. *et al.* (2009) 'Optical Imaging of Postsynaptic Odor Representation in the Glomerular Layer of the Mouse Olfactory Bulb', *Journal of Neurophysiology*, 102(2), pp. 817–830. doi: 10.1152/jn.00020.2009.

Foley, C. P. *et al.* (2014) 'Intra-arterial delivery of AAV vectors to the mouse brain after mannitol mediated blood brain barrier disruption', *Journal of Controlled Release*, 196, pp. 71–78. doi: 10.1016/j.jconrel.2014.09.018.

Fornasari, D. (2012) 'Pain mechanisms in patients with chronic pain', *Clinical Drug Investigation*.

Springer International Publishing, pp. 45–52. doi: 10.2165/11630070-000000000-00000.

Foust, K. D. *et al.* (2009) 'Intravascular AAV9 preferentially targets neonatal neurons and adult astrocytes', *Nature Biotechnology*, 27(1), pp. 59–65. doi: 10.1038/nbt.1515.

Foust, K. D. *et al.* (2010) 'Rescue of the spinal muscular atrophy phenotype in a mouse model by early postnatal delivery of SMN', *Nature Biotechnology*. Nature Publishing Group, 28(3), pp. 271–274. doi: 10.1038/nbt.1610.

Frazier, S. J., Cohen, B. N. and Lester, H. A. (2013) 'An engineered glutamate-gated chloride (GLUCL) channel for sensitive, consistent neuronal silencing by ivermectin', *Journal of Biological Chemistry*. American Society for Biochemistry and Molecular Biology, 288(29), pp. 21029–21042. doi: 10.1074/jbc.M112.423921.

Frings, S. (2012) 'Primary processes in sensory cells: Current advances', *Advances in Experimental Medicine and Biology*. Springer, New York, NY, 739, pp. 32–58. doi: 10.1007/978-1-4614-1704-0_3.

Fu, C. L. *et al.* (2011) 'Mouse bladder wall injection', *J Vis Exp*, (53), p. e2523. doi: 10.3791/2523.

Fu, H. *et al.* (2003) 'Self-complementary adeno-associated virus serotype 2 vector: Global distribution and broad dispersion of AAV-mediated transgene expression in mouse brain', *Molecular Therapy*. Elsevier, 8(6), pp. 911–917. doi: 10.1016/j.ymthe.2003.08.021.

Fu, H. *et al.* (2007) 'Significantly increased lifespan and improved behavioral performances by rAAV gene delivery in adult mucopolysaccharidosis IIIB mice', *Gene Therapy*. Nature Publishing Group, 14(14), pp. 1065–1077. doi: 10.1038/sj.gt.3302961.

Fuller, P. M., Yamanaka, A. and Lazarus, M. (2015) 'How genetically engineered systems are helping to define, and in some cases redefine, the neurobiological basis of sleep and wake', *Temperature*, 2(3), pp. 406–417. doi: 10.1080/23328940.2015.1075095.

Galoyan, S. M., Petruska, J. C. and Mendell, L. M. (2003) 'Mechanisms of sensitization of the response of single dorsal root ganglion cells from adult rat to noxious heat', *European Journal of Neuroscience*. Wiley/Blackwell (10.1111), 18(3), pp. 535–541. doi: 10.1046/j.1460-9568.2003.02775.x.

Gammaitoni, A. R., Alvarez, N. A. and Galer, B. S. (2003) 'Safety and tolerability of the lidocaine patch 5%, a targeted peripheral analgesic: A review of the literature', *Journal of Clinical Pharmacology*. Wiley-Blackwell, pp. 111–117. doi: 10.1177/0091270002239817.

Gangadharan, V. and Kuner, R. (2013) 'Pain hypersensitivity mechanisms at a glance', *Disease Models & Mechanisms*. Company of Biologists, 6(4), pp. 889–895. doi: 10.1242/dmm.011502.

Garland, E. L. (2014) 'Treating chronic pain: The need for non-opioid options', *Expert Review of Clinical Pharmacology*. Taylor & Francis, pp. 545–550. doi: 10.1586/17512433.2014.928587.

Gavériaux-Ruff, C. and Kieffer, B. L. (2007) 'Conditional gene targeting in the mouse nervous system: Insights into brain function and diseases', *Pharmacology and Therapeutics*. Pergamon, pp. 619–634. doi: 10.1016/j.pharmthera.2006.12.003.

Ge, F. *et al.* (2017) 'Glutamatergic projections from the entorhinal cortex to dorsal dentate gyrus mediate context-induced reinstatement of heroin seeking', *Neuropsychopharmacology*. Nature Publishing Group, 42(9), pp. 1860–1870. doi: 10.1038/npp.2017.14.

Gee, M. D. *et al.* (1999) 'The relationship between axonal spike shape and functional modality in cutaneous C-fibres in the pig and rat', *Neuroscience*. Pergamon, 90(2), pp. 509–518. doi: 10.1016/S0306-4522(98)00454-0.

Geppetti, P. and Trevisani, M. (2004) 'Activation and sensitisation of the vanilloid receptor: Role in gastrointestinal inflammation and function', *British Journal of Pharmacology*. Wiley-Blackwell, pp. 1313–1320. doi: 10.1038/sj.bjp.0705768.

Gierut, J. J., Jacks, T. E. and Haigis, K. M. (2014) 'In vivo delivery of lenti-cre or adeno-cre into mice using intranasal instillation', *Cold Spring Harbor Protocols*, 2014(3), pp. 307–309. doi:

10.1101/pdb.prot073445.

Girven, K. S. and Sparta, D. R. (2017) 'Probing Deep Brain Circuitry: New Advances in in Vivo Calcium Measurement Strategies', *ACS Chemical Neuroscience*. American Chemical Society, 8(2), pp. 243–251. doi: 10.1021/acschemneuro.6b00307.

Glascock, J. J. *et al.* (2012) 'Decreasing Disease Severity in Symptomatic, *Smn* $^{-/-}$; *SMN2* $^{+/+}$, Spinal Muscular Atrophy Mice Following scAAV9-SMN Delivery', *Human Gene Therapy*. Mary Ann Liebert, Inc., 23(3), pp. 330–335. doi: 10.1089/hum.2011.166.

Glorioso, J. C., Mata, M. and Fink, D. J. (2003) 'Therapeutic gene transfer to the nervous system using viral vectors', *Journal of NeuroVirology*, pp. 165–172. doi: 10.1080/13550280390193984.

Gold, M. S. *et al.* (1996) 'Hyperalgesic agents increase a tetrodotoxin-resistant Na+ current in nociceptors.', *Proceedings of the National Academy of Sciences of the United States of America*. National Academy of Sciences, 93(3), pp. 1108–12. doi: 10.1073/pnas.93.3.1108.

Gold, M. S. *et al.* (2002) 'Prostaglandin E2 Modulates TTX-R I Na in Rat Colonic Sensory Neurons', *J Neurophysiol Journal of Neurophysiology at Penn State Univ on February*, 88(23), pp. 1512–1522. doi: 10.1152/jn.2002.88.3.1512.

Gold, M. S. (2013) 'Molecular Biology of Sensory Transduction', in McMahon, S. B. et al. (eds) *Wall & Melzack's Textbook of Pain*. 6th edn. Elsevier.

Gold, M. S., Levine, J. D. and Correa, A. M. (1998) 'Modulation of TTX-R INa by PKC and PKA and their role in PGE2-induced sensitization of rat sensory neurons in vitro.', *The Journal of Neuroscience*. Society for Neuroscience, 18(24), pp. 10345–10355. doi: 10.1523/JNEUROSCI.18-24-10345.1998.

Goldberg, Y. P. *et al.* (2007) 'Loss-of-function mutations in the Nav1.7 gene underlie congenital indifference to pain in multiple human populations', *Clinical Genetics*, 71(4), pp. 311–319. doi: 10.1111/j.1399-0004.2007.00790.x.

Gompf, H. S. *et al.* (2015) 'Targeted genetic manipulations of neuronal subtypes using promoter-specific combinatorial AAVs in wild-type animals', *Frontiers in Behavioral Neuroscience*, 9(July), p. 152. doi: 10.3389/fnbeh.2015.00152.

Goss, J. R. *et al.* (2001) 'Antinociceptive effect of a genomic herpes simplex virus-based vector expressing human proenkephalin in rat dorsal root ganglion', *Gene Therapy*, 8(7), pp. 551–556. doi: 10.1038/sj.gt.3301430.

Goss, J. R. *et al.* (2002) 'Herpes simplex-mediated gene transfer of nerve growth factor protects against peripheral neuropathy in streptozotocin-induced diabetes in the mouse', *Diabetes*, 51(7), pp. 2227–2232. doi: 10.2337/diabetes.51.7.2227.

Graham, F. L. *et al.* (1977) 'Characteristics of a human cell line transformed by DNA from human adenovirus type 5', *Journal of General Virology*, 36(1), pp. 59–72. doi: 10.1099/0022-1317-36-1-59.

Gray-Edwards, H. L. *et al.* (2015) 'Mucopolysaccharidosis-like phenotype in feline Sandhoff disease and partial correction after AAV gene therapy', *Molecular Genetics and Metabolism*. Academic Press, 116(1–2), pp. 80–87. doi: 10.1016/j.ymgme.2015.05.003.

Gray, S. J. *et al.* (2010) 'Directed evolution of a novel adeno-associated virus (AAV) vector that crosses the seizure-compromised blood-brain barrier (BBB)', *Molecular Therapy*, 18(3), pp. 570–578. doi: 10.1038/mt.2009.292.

Gray, S. J., Foti, S. B., *et al.* (2011) 'Optimizing Promoters for Recombinant Adeno-Associated Virus-Mediated Gene Expression in the Peripheral and Central Nervous System Using Self-Complementary Vectors', *Human Gene Therapy*, 22(9), pp. 1143–1153. doi: 10.1089/hum.2010.245.

Gray, S. J., Matagne, V., *et al.* (2011) 'Preclinical differences of intravascular aav9 delivery to neurons and glia: A comparative study of adult mice and nonhuman primates', *Molecular Therapy*. Nature Publishing Group, 19(6), pp. 1058–1069. doi: 10.1038/mt.2011.72.

Gray, S. J. (2013) ‘Gene therapy and neurodevelopmental disorders’, *Neuropharmacology*, pp. 136–142. doi: 10.1016/j.neuropharm.2012.06.024.

Gray, S. J., Woodard, K. T. and Samulski, R. J. (2010) ‘Viral vectors and delivery strategies for CNS gene therapy’, *Therapeutic Delivery*. NIH Public Access, 1(4), pp. 517–534. doi: 10.4155/tde.10.50.

Grienberger, C. and Konnerth, A. (2012) ‘Imaging Calcium in Neurons’, *Neuron*. Elsevier, 73(5), pp. 862–885. doi: 10.1016/j.neuron.2012.02.011.

Grimm, D. *et al.* (2006) ‘Fatality in mice due to oversaturation of cellular microRNA/short hairpin RNA pathways’, *Nature*, 441(7092), pp. 537–541. doi: 10.1038/nature04791.

Grimm, D. (2011) ‘The dose can make the poison: Lessons learned from adverse in vivo toxicities caused by RNAi overexpression’, *Silence*, p. 8. doi: 10.1186/1758-907X-2-8.

Grynkiewicz, G., Poenie, M. and Tsien, R. Y. (1985) ‘A new generation of Ca2+ indicators with greatly improved fluorescence properties.’, *The Journal of biological chemistry*, 260(6), pp. 3440–50. Available at: http://www.ncbi.nlm.nih.gov/pubmed/3838314 (Accessed: 19 July 2018).

Gu, Q., Kwong, K. and Lee, L.-Y. (2003) ‘Ca 2+ Transient Evoked by Chemical Stimulation Is Enhanced by PGE $_2$ in Vagal Sensory Neurons: Role of cAMP/PKA Signaling Pathway’, *Journal of Neurophysiology*. American Physiological SocietyBethesda, MD, 89(4), pp. 1985–1993. doi: 10.1152/jn.00748.2002.

Guedon, J.-M. G. *et al.* (2015) ‘Current Gene Therapy using Viral Vectors for Chronic Pain’, *Molecular Pain*. SAGE Publications, 11, pp. s12990-015-0018. doi: 10.1186/s12990-015-0018-1.

Gunter, T. E. and Pfeiffer, D. R. (1990) ‘Mechanisms by which mitochondria transport calcium.’, *The American journal of physiology*. American Physiological Society Bethesda, MD , 258(5 Pt 1), pp. C755-86. doi: 10.1152/ajpcell.1990.258.5.C755.

Guo, A. *et al.* (1999) 'Immunocytochemical localization of the vanilloid receptor 1 (VR1), relationship to neuropeptides, the P2X3 purinoceptor and IB4 binding sites', *European Journal of Neuroscience*, 11(3), pp. 946–958. doi: 10.1046/j.1460-9568.1999.00503.x.

Guo, Y. *et al.* (2016) 'A Single Injection of Recombinant Adeno-Associated Virus into the Lumbar Cistern Delivers Transgene Expression Throughout the Whole Spinal Cord', *Molecular Neurobiology*. Molecular Neurobiology, 53(5), pp. 3235–3248. doi: 10.1007/s12035-015-9223-1.

Gutierrez-Mecinas, M. *et al.* (2018) 'Substance P-expressing excitatory interneurons in the mouse superficial dorsal horn provide a propriospinal input to the lateral spinal nucleus', *Brain Structure and Function*. Springer Berlin Heidelberg, 223(5), pp. 2377–2392. doi: 10.1007/s00429-018-1629-x.

Haenraets, K. *et al.* (2017) 'Spinal nociceptive circuit analysis with recombinant adeno-associated viruses: the impact of serotypes and promoters', *Journal of Neurochemistry*. Wiley/Blackwell (10.1111), 142(5), pp. 721–733. doi: 10.1111/jnc.14124.

Haenraets, K. *et al.* (2018) 'Adeno-associated Virus Mediated Transgene Expression in Genetically Defined Neurons of the Spinal Cord', *Journal of Visualized Experiments*, (April), pp. 1–9. doi: 10.3791/57382.

Hamatani, T. *et al.* (2004) 'Dynamics of global gene expression changes during mouse preimplantation development', *Developmental Cell*. Cell Press, 6(1), pp. 117–131. doi: 10.1016/S1534-5807(03)00373-3.

Hammer, P. *et al.* (2010) 'mRNA-seq with agnostic splice site discovery for nervous system transcriptomics tested in chronic pain', *Genome Research*, 20(6), pp. 847–860. doi: 10.1101/gr.101204.109.

Hammond, S. L. *et al.* (2017) 'Cellular selectivity of AAV serotypes for gene delivery in neurons and astrocytes by neonatal intracerebroventricular injection', *PLoS ONE*. Edited by J. Qiu,

12(12), p. e0188830. doi: 10.1371/journal.pone.0188830.

Hargreaves, K. *et al.* (1988) 'A new and sensitive method for measuring thermal nociception in cutaneous hyperalgesia', *Pain*. No longer published by Elsevier, 32(1), pp. 77–88. doi: 10.1016/0304-3959(88)90026-7.

Harvey, C. D., Coen, P. and Tank, D. W. (2012) 'Choice-specific sequences in parietal cortex during a virtual-navigation decision task', *Nature*, 484(7392), pp. 62–68. doi: 10.1038/nature10918.

Haurigot, V. *et al.* (2013) 'Whole body correction of mucopolysaccharidosis IIIA by intracerebrospinal fluid gene therapy', *Journal of Clinical Investigation*. American Society for Clinical Investigation, 123(8), pp. 3254–3271. doi: 10.1172/JCI66778.

Hayek, S. M. and Hanes, M. C. (2014) 'Intrathecal therapy for chronic pain: Current trends and future needs', *Current Pain and Headache Reports*, p. 388. doi: 10.1007/s11916-013-0388-x.

Van Hecke, O., Torrance, N. and Smith, B. H. (2013) 'Chronic pain epidemiology and its clinical relevance', *British Journal of Anaesthesia*. Elsevier, pp. 13–18. doi: 10.1093/bja/aet123.

Helmchen, F., Borst, J. G. G. and Sakmann, B. (1997) 'Calcium dynamics associated with a single action potential in a CNS presynaptic terminal', *Biophysical Journal*, 72(3), pp. 1458–1471. doi: 10.1016/S0006-3495(97)78792-7.

Helmchen, F. and Denk, W. (2005) 'Deep tissue two-photon microscopy', *Nature Methods*, 2(12), pp. 932–940. doi: 10.1038/nmeth818.

Herrera-Carrillo, E., Liu, Y. P. and Berkhout, B. (2017) 'Improving miRNA delivery by optimizing miRNA expression cassettes in viral vectors', *Human Gene Therapy Methods*. Mary Ann Liebert, Inc., 28(4), p. hgtb.2017.036. doi: 10.1089/hgtb.2017.036.

Heyman, I. and Rang, H. P. (1985) 'Depolarizing responses to capsaicin in a subpopulation of rat dorsal root ganglion cells', *Neuroscience Letters*. Elsevier, 56(1), pp. 69–75. doi:

10.1016/0304-3940(85)90442-2.

Hinderer, C. *et al.* (2017) 'Evaluation of intrathecal routes of administration for adeno-associated virus vectors in large animals', *Human Gene Therapy*, 29(1), p. hum.2017.026. doi: 10.1089/hum.2017.026.

Hinderer, C. *et al.* (2018) 'Severe toxicity in nonhuman primates and piglets following high-dose intravenous administration of an AAV vector expressing human SMN', *Human Gene Therapy*, X(X), p. hum.2018.015. doi: 10.1089/hum.2018.015.

Hirai, T. *et al.* (2012) 'Intrathecal shRNA-AAV9 Inhibits Target Protein Expression in the Spinal Cord and Dorsal Root Ganglia of Adult Mice', *Human Gene Therapy Methods*, 23(2), pp. 119–127. doi: 10.1089/hgtb.2012.035.

Hirai, T. *et al.* (2014) 'Intrathecal AAV serotype 9-mediated delivery of shRNA against TRPV1 attenuates thermal hyperalgesia in a mouse model of peripheral nerve injury', *Molecular Therapy*. The American Society of Gene & Cell Therapy, 22(2), pp. 409–419. doi: 10.1038/mt.2013.247.

Hoess, R. H., Wierzbicki, A. and Abremski, K. (1986) 'The role of the loxP spacer region in P1 site-specific recombination.', *Nucleic acids research*. Oxford University Press, 14(5), pp. 2287–300. doi: 10.1093/nar/gkn942.

Hoess, R. H., Ziese, M. and Sternberg, N. (1982) 'P1 site-specific recombination: nucleotide sequence of the recombining sites.', *Proceedings of the National Academy of Sciences*. National Academy of Sciences, 79(11), pp. 3398–3402. doi: 10.1073/pnas.79.11.3398.

Holle, D., Obermann, M. and Katsarava, Z. (2009) 'The electrophysiology of cluster headache', *Current Pain and Headache Reports*, pp. 155–159. doi: 10.1007/s11916-009-0026-9.

Holz, G. G., Dunlap, K. and Kream, R. M. (1988) 'Characterization of the electrically evoked release of substance P from dorsal root ganglion neurons: methods and dihydropyridine sensitivity.', *The Journal of neuroscience : the official journal of the Society for Neuroscience*.

NIH Public Access, 8(2), pp. 463–471. Available at: http://www.ncbi.nlm.nih.gov/pubmed/2448433 (Accessed: 26 July 2018).

Homs, J. *et al.* (2014) 'Intrathecal administration of IGF-I by AAVrh10 improves sensory and motor deficits in a mouse model of diabetic neuropathy', *Molecular Therapy - Methods & Clinical Development*. American Society of Gene & Cell Therapy, 1(November 2013), p. 7. doi: 10.1038/mtm.2013.7.

Honan, S. A. and McNaughton, P. A. (2007) 'Sensitisation of TRPV1 in rat sensory neurones by activation of SNSRs', *Neuroscience Letters*. Elsevier, 422(1), pp. 1–6. doi: 10.1016/j.neulet.2007.04.083.

Hong, C. S. *et al.* (2006) 'Herpes simplex virus RNAi and neprilysin gene transfer vectors reduce accumulation of Alzheimer's disease-related amyloid-β peptide in vivo', *Gene Therapy*, 13(14), pp. 1068–1079. doi: 10.1038/sj.gt.3302719.

Hordeaux, J. *et al.* (2015) 'Efficient central nervous system AAVrh10-mediated intrathecal gene transfer in adult and neonate rats', *Gene Therapy*. Nature Publishing Group, 22(4), pp. 316–324. doi: 10.1038/gt.2014.121.

Hoschouer, E. L., Basso, D. M. and Jakeman, L. B. (2010) 'Aberrant sensory responses are dependent on lesion severity after spinal cord contusion injury in mice', *Pain*. International Association for the Study of Pain, 148(2), pp. 328–342. doi: 10.1016/j.pain.2009.11.023.

Howe, M. W. and Dombeck, D. A. (2016) 'Rapid signalling in distinct dopaminergic axons during locomotion and reward', *Nature*. NIH Public Access, 535(7613), pp. 505–510. doi: 10.1038/nature18942.

Howorth, P. W. *et al.* (2009) 'Retrograde Viral Vector-Mediated Inhibition of Pontospinal Noradrenergic Neurons Causes Hyperalgesia in Rats', *Journal of Neuroscience*, 29(41), pp. 12855–12864. doi: 10.1523/JNEUROSCI.1699-09.2009.

Hsu, P. D., Lander, E. S. and Zhang, F. (2014) 'Development and applications of CRISPR-Cas9 for

genome engineering', *Cell*. NIH Public Access, 157(6), pp. 1262–1278. doi: 10.1016/j.cell.2014.05.010.

Hu, H. J. *et al.* (2018) 'Intrathecal Injection of scAAV9–hIGF1 Prolongs the Survival of ALS Model Mice by Inhibiting the NF-kB Pathway', *Neuroscience*, 381(February), pp. 1–10. doi: 10.1016/j.neuroscience.2018.02.004.

Huang, J., Zhang, X. and McNaughton, P. (2006) 'Inflammatory Pain: The Cellular Basis of Heat Hyperalgesia', *Current Neuropharmacology*. Bentham Science Publishers, 4(3), pp. 197–206. doi: 10.2174/157015906778019554.

Huber, D. *et al.* (2012) 'Multiple dynamic representations in the motor cortex during sensorimotor learning', *Nature*, 484(7395), pp. 473–478. doi: 10.1038/nature11039.

Hwang, S. J. and Valtschanoff, J. G. (2003) 'Vanilloid receptor VR1-positive afferents are distributed differently at different levels of the rat lumbar spinal cord', *Neuroscience Letters*. Elsevier, 349(1), pp. 41–44. doi: 10.1016/S0304-3940(03)00750-X.

Hylden, J. L. K. and Wilcox, G. L. (1980) 'Intrathecal morphine in mice: A new technique', *European Journal of Pharmacology*, 67(2–3), pp. 313–316. doi: 10.1016/0014-2999(80)90515-4.

IASP Task Force on Taxonomy (1994) *Classification of Chronic Pain*, *IASP Press*. Edited by H. Merskey and N. Bogduk. Seattle: IASP press. doi: 10.1002/ana.20394.

Indra, A. K. *et al.* (1999) 'Temporally-controlled site-specific mutagenesis in the basal layer of the epidermis: Comparison of the recombinase activity of the tamoxifen-inducible Cre-ER(T) and Cre-ER(T2) recombinases', *Nucleic Acids Research*. Oxford University Press, 27(22), pp. 4324–4327. doi: 10.1093/nar/27.22.4324.

Ivanavicius, S. P. *et al.* (2004) 'Isolectin B4 binding neurons are not present in the rat knee joint', *Neuroscience*, 128(3), pp. 555–560. doi: 10.1016/j.neuroscience.2004.06.047.

Ivanova, E., Hwang, G. S. and Pan, Z. H. (2010) 'Characterization of transgenic mouse lines

expressing Cre recombinase in the retina', *Neuroscience*, 165(1), pp. 233–243. doi: 10.1016/j.neuroscience.2009.10.021.

Iwamoto, N. *et al.* (2009) 'Global diffuse distribution in the brain and efficient gene delivery to the dorsal root ganglia by intrathecal injection of adeno-associated viral vector serotype 1', *The Journal of Gene Medicine*, 11(6), pp. 498–505. doi: 10.1002/jgm.1325.

Jackson, K. L. *et al.* (2016) 'Better Targeting, Better Efficiency for Wide-Scale Neuronal Transduction with the Synapsin Promoter and AAV-PHP.B', *Frontiers in Molecular Neuroscience*, 9(November), pp. 1–11. doi: 10.3389/fnmol.2016.00116.

Jacques, S. J. *et al.* (2012) 'AAV8 gfp preferentially targets large diameter dorsal root ganglion neurones after both intra-dorsal root ganglion and intrathecal injection', *Molecular and Cellular Neuroscience*. Elsevier Inc., 49(4), pp. 464–474. doi: 10.1016/j.mcn.2012.03.002.

Jakobsson, J. and Lundberg, C. (2006) 'Lentiviral vectors for use in the central nervous system', *Molecular Therapy*. Cell Press, pp. 484–493. doi: 10.1016/j.ymthe.2005.11.012.

Jares-Erijman, E. A. and Jovin, T. M. (2003) 'FRET imaging', *Nature Biotechnology*. Nature Publishing Group, pp. 1387–1395. doi: 10.1038/nbt896.

Ji, R. R. *et al.* (2002) 'p38 MAPK activation by NGF in primary sensory neurons after inflammation increases TRPV1 levels and maintains heat hyperalgesia', *Neuron*. Elsevier, 36(1), pp. 57–68. doi: 10.1016/S0896-6273(02)00908-X.

von Jonquieres, G. *et al.* (2016) 'Recombinant Human Myelin-Associated Glycoprotein Promoter Drives Selective AAV-Mediated Transgene Expression in Oligodendrocytes', *Frontiers in Molecular Neuroscience*. Frontiers, 9, p. 13. doi: 10.3389/fnmol.2016.00013.

Jordt, S. E. *et al.* (2004) 'Mustard oils and cannabinoids excite sensory nerve fibres through the TRP channel ANKTM1', *Nature*. Nature Publishing Group, 427(6971), pp. 260–265. doi: 10.1038/nature02282.

Ju, G., Han, Z. and Fan, L. (1989) 'Fluorogold as a retrograde tracer used in combination with immunohistochemistry', *Journal of Neuroscience Methods*. Elsevier, 29(1), pp. 69–72. doi: 10.1016/0165-0270(89)90109-X.

Kaludov, N. *et al.* (2001) 'Adeno-associated virus serotype 4 (AAV4) and AAV5 both require sialic acid binding for hemagglutination and efficient transduction but differ in sialic acid linkage specificity.', *Journal of Virology*. American Society for Microbiology, 75(15), pp. 6884–93. doi: 10.1128/JVI.75.15.6884-6893.2001.

Kano, M. *et al.* (1994) 'Bradykinin-responsive cells of dorsal root ganglia in culture: Cell size, firing, cytosolic calcium, and substance P', *Cellular and Molecular Neurobiology*, 14(1), pp. 49–57. doi: 10.1007/BF02088588.

Kantor, B. *et al.* (2009) 'Epigenetic activation of unintegrated HIV-1 genomes by gut-associated short chain fatty acids and its implications for HIV infection', *Proceedings of the National Academy of Sciences*, 106(44), pp. 18786–18791. doi: 10.1073/pnas.0905859106.

Kantor, B. *et al.* (2014) 'Methods for gene transfer to the central nervous system', *Advances in Genetics*. NIH Public Access, 87, pp. 125–197. doi: 10.1016/B978-0-12-800149-3.00003-2.

Kaplitt, M. G. *et al.* (1994) 'Long-term gene expression and phenotypic correction using adeno-associated virus vectors in the mammalian brain', *Nature Genetics*. Nature Publishing Group, 8(2), pp. 148–154. doi: 10.1038/ng1094-148.

Kaplitt, M. G. and Makimura, H. (1997) 'Defective viral vectors as agents for gene transfer in the nervous system', *Journal of Neuroscience Methods*, pp. 125–132. doi: 10.1016/S0165-0270(96)00132-X.

Karashima, Y. *et al.* (2007) 'Bimodal Action of Menthol on the Transient Receptor Potential Channel TRPA1', *Journal of Neuroscience*. Society for Neuroscience, 27(37), pp. 9874–9884. doi: 10.1523/JNEUROSCI.2221-07.2007.

Karashima, Y. *et al.* (2009) 'TRPA1 acts as a cold sensor in vitro and in vivo', *Proceedings of the*

National Academy of Sciences. National Academy of Sciences, 106(4), pp. 1273–1278. doi: 10.1073/pnas.0808487106.

Kathe, C. *et al.* (2016) 'Intramuscular neurotrophin-3 normalizes low threshold spinal reflexes, reduces spasms and improves mobility after bilateral corticospinal tract injury in rats', *eLife*. eLife Sciences Publications, Ltd, 5(OCTOBER2016). doi: 10.7554/eLife.18146.

Kelleher, J. H., Tewari, D. and McMahon, S. B. (2017) 'Neurotrophic factors and their inhibitors in chronic pain treatment', *Neurobiology of Disease*. Academic Press, pp. 127–138. doi: 10.1016/j.nbd.2016.03.025.

Khan, A. A. *et al.* (1992) 'The effects of bradykinin and sequence-related analogs on the response properties of cutaneous nociceptors in monkeys', *Somatosensory & Motor Research*, 9(2), pp. 97–106. doi: 10.3109/08990229209144765.

Kikkawa, Y., Kurogi, R. and Sasaki, T. (2014) 'The Single and Double Blood Injection Rabbit Subarachnoid Hemorrhage Model', *Translational Stroke Research*, pp. 88–97. doi: 10.1007/s12975-014-0375-5.

Kim, J.-Y. *et al.* (2014) 'Intracerebroventricular Viral Injection of the Neonatal Mouse Brain for Persistent and Widespread Neuronal Transduction', *Journal of Visualized Experiments*. MyJoVE Corporation, (91), p. 51863. doi: 10.3791/51863.

Kim, Y. S. *et al.* (2014) 'Central terminal sensitization of TRPV1 by descending serotonergic facilitation modulates chronic pain', *Neuron*. Elsevier Inc., 81(4), pp. 873–887. doi: 10.1016/j.neuron.2013.12.011.

Kim, Y. S. *et al.* (2016) 'Coupled Activation of Primary Sensory Neurons Contributes to Chronic Pain', *Neuron*. Elsevier Inc., 91(5), pp. 1085–1096. doi: 10.1016/j.neuron.2016.07.044.

Kip, S. N. and Strehler, E. E. (2007) 'Rapid downregulation of NCX and PMCA in hippocampal neurons following H2O2oxidative stress', in *Annals of the New York Academy of Sciences*. NIH Public Access, pp. 436–439. doi: 10.1196/annals.1387.005.

Klein, R. L. *et al.* (2008) 'AAV8, 9, Rh10, Rh43 vector gene transfer in the rat brain: Effects of serotype, promoter and purification method', *Molecular Therapy*, 16(1), pp. 89–96. doi: 10.1038/sj.mt.6300331.

Köbbert, C. *et al.* (2000) 'Current concepts in neuroanatomical tracing', *Progress in Neurobiology*. Pergamon, pp. 327–351. doi: 10.1016/S0301-0082(00)00019-8.

Koda, H. and Mizumura, K. (2002) 'Sensitization to mechanical stimulation by inflammatory mediators and by mild burn in canine visceral nociceptors in vitro.', *Journal of Neurophysiology*, 87(4), pp. 2043–51. doi: 10.1152/jn.00593.2001.

Koeberl, D. D. *et al.* (2008) 'AAV vector-mediated reversal of hypoglycemia in canine and murine glycogen storage disease type Ia', *Molecular Therapy*. Cell Press, 16(4), pp. 665–672. doi: 10.1038/mt.2008.15.

Koerber, H. R., Druzinsky, R. E. and Mendell, L. M. (1988) 'Properties of somata of spinal dorsal root ganglion cells differ according to peripheral receptor innervated.', *Journal of neurophysiology*. American Physiological Society Bethesda, MD, 60(5), pp. 1584–1596. doi: 10.1152/jn.1988.60.5.1584.

Koh, K. *et al.* (2015) 'Possible involvement of activated locus coeruleus-noradrenergic neurons in pain-related sleep disorders', *Neuroscience Letters*. Elsevier, pp. 200–206. doi: 10.1016/j.neulet.2014.12.002.

Koltzenburg, M., Stucky, C. L. and Lewin, G. R. (1997) 'Receptive properties of mouse sensory neurons innervating hairy skin.', *Journal of Neurophysiology*. American Physiological SocietyBethesda, MD, 78(4), pp. 1841–1850. doi: 10.1152/jn.1997.78.4.1841.

Komiyama, T. *et al.* (2010) 'Learning-related fine-scale specificity imaged in motor cortex circuits of behaving mice', *Nature*. Nature Publishing Group, 464(7292), pp. 1182–1186. doi: 10.1038/nature08897.

Koopmeiners, A. S. *et al.* (2013) 'Effect of electrical field stimulation on dorsal root ganglion

neuronal function', *Neuromodulation*. Wiley/Blackwell (10.1111), 16(4), pp. 304–311. doi: 10.1111/ner.12028.

Koplas, P. A., Rosenberg, R. L. and Oxford, G. S. (1997) 'The role of calcium in the desensitization of capsaicin responses in rat dorsal root ganglion neurons.', *The Journal of neuroscience : the official journal of the Society for Neuroscience*. Society for Neuroscience, 17(10), pp. 3525–3537. doi: 10.1523/JNEUROSCI.17-10-03525.1997.

Korkotian, E. and Segal, M. (1998) 'Fast confocal imaging of calcium released from stores in dendritic spines', *European Journal of Neuroscience*. Wiley/Blackwell (10.1111), 10(6), pp. 2076–2084. doi: 10.1046/j.1460-9568.1998.00219.x.

Kovalchuk, Y. *et al.* (2000) 'NMDA receptor-mediated subthreshold Ca(2+) signals in spines of hippocampal neurons.', *The Journal of neuroscience : the official journal of the Society for Neuroscience*. Society for Neuroscience, 20(5), pp. 1791–1799. doi: 10.1523/JNEUROSCI.20-05-01791.2000.

Kress, M. *et al.* (1992) 'Responsiveness and functional attributes of electrically localized terminals of cutaneous C-fibers in vivo and in vitro.', *Journal of neurophysiology*. American Physiological Society Bethesda, MD, 68(2), pp. 581–595. doi: 10.1152/jn.1992.68.2.581.

Krisky, D. M. *et al.* (1998) 'Development of herpes simplex virus replication-defective multigene vectors for combination gene therapy applications', *Gene Therapy*, 5(11), pp. 1517–1530. doi: 10.1038/sj.gt.3300755.

Kucyi, A. and Davis, K. D. (2017) 'The Neural Code for Pain: From Single-Cell Electrophysiology to the Dynamic Pain Connectome', *Neuroscientist*. SAGE PublicationsSage CA: Los Angeles, CA, pp. 397–414. doi: 10.1177/1073858416667716.

Kuniyoshi, K. *et al.* (2007) 'Characteristics of sensory DRG neurons innervating the wrist joint in rats', *European Journal of Pain*, 11(3), pp. 323–328. doi: 10.1016/j.ejpain.2006.05.003.

Kurnellas, M. P., Donahue, K. C. and Elkabes, S. (2007) 'Mechanisms of neuronal damage in

multiple sclerosis and its animal models: role of calcium pumps and exchangers', *Biochemical Society transactions*. NIH Public Access, 35(Pt 5), pp. 923–6. doi: 10.1042/BST0350923.

Kushida, T. *et al.* (2001) 'Intra-bone marrow injection of allogeneic bone marrow cells: A powerful new strategy for treatment of intractable autoimmune diseases in MRL/lpr mice', *Blood*, 97(10), pp. 3292–3299. doi: 10.1182/blood.V97.10.3292.

Kyrozis, A. *et al.* (1995) 'Calcium entry through a subpopulation of AMPA receptors desensitized neighbouring NMDA receptors in rat dorsal horn neurons.', *The Journal of Physiology*. Wiley-Blackwell, 485(2), pp. 373–381. doi: 10.1113/jphysiol.1995.sp020736.

Lachmann, R. H. (2004) 'Herpes simplex virus-based vectors', *International Journal of Experimental Pathology*. Wiley-Blackwell, pp. 177–190. doi: 10.1111/j.0959-9673.2004.00383.x.

Lai, Y. and Duan, D. (2012) 'Progress in gene therapy of dystrophic heart disease', *Gene Therapy*. NIH Public Access, pp. 678–685. doi: 10.1038/gt.2012.10.

Lang, E. *et al.* (1990) 'Chemosensitivity of fine afferents from rat skin in vitro', *Journal of Neurophysiology*, 63(4), pp. 887–901. doi: 10.1152/jn.1990.63.4.887.

Lau, J. *et al.* (2011) 'Temporal control of gene deletion in sensory ganglia using a tamoxifen-inducible Advillin-Cre-ERT2 recombinase mouse', *Molecular Pain*, 7, pp. 1744-8069-7–100. doi: 10.1186/1744-8069-7-100.

Lecoq, J. *et al.* (2014) 'Visualizing mammalian brain area interactions by dual-axis two-photon calcium imaging', *Nature Neuroscience*. NIH Public Access, 17(12), pp. 1825–1829. doi: 10.1038/nn.3867.

Lee, I. O. *et al.* (2011) 'Pharmacology of intracisternal or intrathecal glycine, muscimol, and baclofen in strychnine-induced thermal hyperalgesia of mice', *Journal of Korean Medical Science*. Korean Academy of Medical Sciences, 26(10), pp. 1371–1377. doi: 10.3346/jkms.2011.26.10.1371.

Lee, I. O. *et al.* (2013) 'Evaluation of a novel mouse model of intracisternal strychnine-induced trigeminal allodynia', *Canadian Journal of Anesthesia*. Springer US, 60(8), pp. 780–786. doi: 10.1007/s12630-013-9975-x.

Lee, K.-H. *et al.* (2018) 'In Vivo Spinal Distribution of Cy5.5 Fluorescent Dye after Injection via the Lateral Ventricle and Cisterna Magna in Rat Model.', *Journal of Korean Neurosurgical Society*. The Korean Neurosurgical Society, 61(4), pp. 434–440. doi: 10.3340/jkns.2017.0252.

Lee, P. R. *et al.* (2005) 'Gene expression in the conversion of early-phase to late-phase long-term potentiation', in *Annals of the New York Academy of Sciences*. Wiley/Blackwell (10.1111), pp. 259–271. doi: 10.1196/annals.1342.023.

Lehrman, S. (1999) 'Virus treatment questioned after gene therapy death.', *Nature*, 401(6753), pp. 517–518. doi: 10.1038/43977.

Leite-Almeida, H., Valle-Fernandes, A. and Almeida, A. (2006) 'Brain projections from the medullary dorsal reticular nucleus: An anterograde and retrograde tracing study in the rat', *Neuroscience*. Pergamon, 140(2), pp. 577–595. doi: 10.1016/j.neuroscience.2006.02.022.

Lelic, D. (2014) 'Electrophysiology as a tool to unravel the origin of pancreatic pain', *World Journal of Gastrointestinal Pathophysiology*, 5(1), p. 33. doi: 10.4291/wjgp.v5.i1.33.

Lennertz, R. C. *et al.* (2012) 'TRPA1 mediates mechanical sensitization in nociceptors during inflammation.', *PloS one*. Public Library of Science, 7(8), p. e43597. doi: 10.1371/journal.pone.0043597.

Lentz, T. B., Gray, S. J. and Samulski, R. J. (2012) 'Viral vectors for gene delivery to the central nervous system', *Neurobiology of Disease*. Elsevier Inc., 48(2), pp. 179–188. doi: 10.1016/j.nbd.2011.09.014.

Lerchner, W. *et al.* (2007) 'Reversible Silencing of Neuronal Excitability in Behaving Mice by a Genetically Targeted, Ivermectin-Gated Cl-Channel', *Neuron*. Elsevier, 54(1), pp. 35–49. doi: 10.1016/j.neuron.2007.02.030.

Lewandoski, M. (2001) 'Conditional control of gene expression in the mouse', *Nature Reviews Genetics*. Nature Publishing Group, pp. 743–755. doi: 10.1038/35093537.

Lewin, G. R. and McMahon, S. B. (1991) 'Physiological properties of primary sensory neurons appropriately and inappropriately innervating skin in the adult rat.', *Journal of neurophysiology*. American Physiological Society Bethesda, MD, 66(4), pp. 1205–17. doi: 10.1152/jn.1991.66.4.1205.

Li, B. *et al.* (2015) 'A novel analgesic approach to optogenetically and specifically inhibit pain transmission using TRPV1 promoter', *Brain Research*. Elsevier, 1609(1), pp. 12–20. doi: 10.1016/j.brainres.2015.03.008.

Li, D. *et al.* (2017) 'Slow intrathecal injection of rAAVrh10 enhances its transduction of spinal cord and therapeutic efficacy in a mutant SOD1 model of ALS', *Neuroscience*. IBRO, 365, pp. 192–205. doi: 10.1016/j.neuroscience.2017.10.001.

Li, P., Slimko, E. M. and Lester, H. A. (2002) 'Selective elimination of glutamate activation and introduction of fluorescent proteins into a Caenorhabditis elegans chloride channel', *FEBS Letters*. No longer published by Elsevier, 528(1–3), pp. 77–82. doi: 10.1016/S0014-5793(02)03245-3.

Li, Y. Y. *et al.* (2017) 'Activation of STAT3-mediated CXCL12 up-regulation in the dorsal root ganglion contributes to oxaliplatin-induced chronic pain', *Molecular Pain*, 13(600), pp. 1–11. doi: 10.1177/1744806917747425.

Liang, Y. F., Haake, B. and Reeh, P. W. (2004) 'Sustained sensitization and recruitment of rat cutaneous nociceptors by bradykinin and a novel theory of its excitatory action', *Journal of Physiology*. Wiley/Blackwell (10.1111), 532(1), pp. 229–239. doi: 10.1111/j.1469-7793.2001.0229g.x.

Liem, L. *et al.* (2016) 'The dorsal root ganglion as a therapeutic target for chronic pain', *Regional Anesthesia and Pain Medicine*, pp. 511–519. doi: 10.1097/AAP.0000000000000408.

Lin, M. *et al.* (2014) 'Thermal Pain in Teeth: Electrophysiology Governed by Thermomechanics', *Applied Mechanics Reviews*, 66(3), p. 031001. doi: 10.1115/1.4026912.

Lin, M. Z. and Schnitzer, M. J. (2016) 'Genetically encoded indicators of neuronal activity', *Nature Neuroscience*. NIH Public Access, pp. 1142–1153. doi: 10.1038/nn.4359.

Lingueglia, E. (2007) 'Acid-sensing ion channels in sensory perception', *Journal of Biological Chemistry*. American Society for Biochemistry and Molecular Biology, pp. 17325–17329. doi: 10.1074/jbc.R700011200.

Linhart, O., Obreja, O. and Kress, M. (2003) 'The inflammatory mediators serotonin, prostaglandin e2and bradykinin evoke calcium influx in rat sensory neurons', *Neuroscience*. Pergamon, 118(1), pp. 69–74. doi: 10.1016/S0306-4522(02)00960-0.

Liu, B. *et al.* (2010) 'The acute nociceptive signals induced by bradykinin in rat sensory neurons are mediated by inhibition of M-type K+ channels and activation of Ca2+-activated Cl- channels', *Journal of Clinical Investigation*, 120(4), pp. 1240–1252. doi: 10.1172/JCI41084.

Liu, D. L. *et al.* (2015) 'Upregulation of Ih expressed in IB4-negative Aδ nociceptive DRG neurons contributes to mechanical hypersensitivity associated with cervical radiculopathic pain', *Scientific Reports*. Nature Publishing Group, 5, p. 16713. doi: 10.1038/srep16713.

Liu, H. Y. *et al.* (2012) 'The effect of diminished osteogenic signals on reduced osteoporosis recovery in aged mice and the potential therapeutic use of adipose-derived stem cells', *Biomaterials*. Elsevier, 33(26), pp. 6105–6112. doi: 10.1016/j.biomaterials.2012.05.024.

Lolignier, S., Eijkelkamp, N. and Wood, J. N. (2014) 'Mechanical allodynia', *Pflugers Archiv European Journal of Physiology*. Springer, pp. 133–139. doi: 10.1007/s00424-014-1532-0.

Lopes, D. M. *et al.* (2017) 'Sex differences in peripheral not central immune responses to pain-inducing injury', *Scientific Reports*. Nature Publishing Group, 7(1), p. 16460. doi: 10.1038/s41598-017-16664-z.

Lopshire, J. C. and Nicol, G. D. (1997) 'Activation and recovery of the PGE2-mediated sensitization of the capsaicin response in rat sensory neurons.', *Journal of neurophysiology*. American Physiological SocietyBethesda, MD, 78(6), pp. 3154–3164. doi: 10.1152/jn.1997.78.6.3154.

Lopshire, J. C. and Nicol, G. D. (1998) 'The cAMP transduction cascade mediates the prostaglandin E2 enhancement of the capsaicin-elicited current in rat sensory neurons: whole-cell and single-channel studies.', *The Journal of neuroscience : the official journal of the Society for Neuroscience*. Society for Neuroscience, 18(16), pp. 6081–92. doi: 10.1523/JNEUROSCI.18-16-06081.1998.

Lostal, W. *et al.* (2014) 'Full-Length Dystrophin Reconstitution with Adeno-Associated Viral Vectors', *Human Gene Therapy*. Mary Ann Liebert, Inc., 25(6), pp. 552–562. doi: 10.1089/hum.2013.210.

Löw, K., Aebischer, P. and Schneider, B. L. (2013) 'Direct and Retrograde Transduction of Nigral Neurons with AAV6, 8, and 9 and Intraneuronal Persistence of Viral Particles', *Human Gene Therapy*. Mary Ann Liebert, Inc., 24(6), pp. 613–629. doi: 10.1089/hum.2012.174.

Lu, S. G. and Gold, M. S. (2008) 'Inflammation-induced increase in evoked calcium transients in subpopulations of rat dorsal root ganglion neurons', *Neuroscience*. NIH Public Access, 153(1), pp. 279–288. doi: 10.1016/j.neuroscience.2008.02.006.

Lukashchuk, V. *et al.* (2016) 'AAV9-mediated central nervous system–targeted gene delivery via cisterna magna route in mice', *Molecular Therapy - Methods and Clinical Development*. Elsevier, 3(July 2015), p. 15055. doi: 10.1038/mtm.2015.55.

Lütcke, H. *et al.* (2010) 'Optical recording of neuronal activity with a genetically-encoded calcium indicator in anesthetized and freely moving mice.', *Frontiers in neural circuits*. Frontiers Media SA, 4, p. 9. doi: 10.3389/fncir.2010.00009.

Lykken, E. A. *et al.* (2018) 'Recent progress and considerations for AAV gene therapies

targeting the central nervous system', *Journal of Neurodevelopmental Disorders*. BioMed Central, p. 16. doi: 10.1186/s11689-018-9234-0.

Lyons, M. R. and West, A. E. (2011) 'Mechanisms of specificity in neuronal activity-regulated gene transcription', *Progress in Neurobiology*. Pergamon, pp. 259–295. doi: 10.1016/j.pneurobio.2011.05.003.

Ma, C., Greenquist, K. W. and Lamotte, R. H. (2006) 'Inflammatory mediators enhance the excitability of chronically compressed dorsal root ganglion neurons.', *Journal of neurophysiology*. American Physiological Society, 95(4), pp. 2098–2107. doi: 10.1152/jn.00748.2005.

Ma, C. and LaMotte, R. H. (2007) 'Multiple Sites for Generation of Ectopic Spontaneous Activity in Neurons of the Chronically Compressed Dorsal Root Ganglion', *Journal of Neuroscience*. NIH Public Access, 27(51), pp. 14059–14068. doi: 10.1523/JNEUROSCI.3699-07.2007.

Ma, M. *et al.* (2001) 'Behavioral and histological outcomes following graded spinal cord contusion injury in the C57Bl/6 mouse', *Experimental Neurology*, 169(2), pp. 239–254. doi: 10.1006/exnr.2001.7679.

Ma, W. *et al.* (2005) 'Medium and large injured dorsal root ganglion cells increase TRPV-1, accompanied by increased α2C-adrenoceptor co-expression and functional inhibition by clonidine', *Pain*, 113(3), pp. 386–394. doi: 10.1016/j.pain.2004.11.018.

Madisen, L. *et al.* (2010) 'A robust and high-throughput Cre reporting and characterization system for the whole mouse brain', *Nature Neuroscience*. NIH Public Access, 13(1), pp. 133–140. doi: 10.1038/nn.2467.

Magnus, C. J. *et al.* (2011) 'Chemical and genetic engineering of selective ion channel-ligand interactions', *Science*. Howard Hughes Medical Institute, 333(6047), pp. 1292–1296. doi: 10.1126/science.1206606.

Maheshri, N. *et al.* (2006) 'Directed evolution of adeno-associated virus yields enhanced gene

delivery vectors', *Nature Biotechnology*, 24(2), pp. 198–204. doi: 10.1038/nbt1182.

Majdzadeh, N. *et al.* (2008) 'HDAC4 inhibits cell-cycle progression and protects neurons from cell death', *Developmental Neurobiology*, 68(8), pp. 1076–1092. doi: 10.1002/dneu.20637.

Malin, S. A. *et al.* (2008) 'Thermal nociception and TRPV1 function are attenuated in mice lacking the nucleotide receptor P2Y2', *Pain*. NIH Public Access, 138(3), pp. 484–496. doi: 10.1016/j.pain.2008.01.026.

Malinow, R. *et al.* (1994) 'Visualizing hippocampal synaptic function by optical detection of Ca2+ entry through the N-methyl-D-aspartate channel.', *Proceedings of the National Academy of Sciences of the United States of America*. National Academy of Sciences, 91(17), pp. 8170–4. doi: 10.1073/pnas.91.17.8170.

Mammucari, C. *et al.* (2018) 'Mitochondrial calcium uptake in organ physiology: from molecular mechanism to animal models', *Pflügers Archiv - European Journal of Physiology*. Springer Berlin Heidelberg, 470(8), pp. 1165–1179. doi: 10.1007/s00424-018-2123-2.

Man, H. Y. (2011) 'GluA2-lacking, calcium-permeable AMPA receptors - inducers of plasticity?', *Current Opinion in Neurobiology*. NIH Public Access, pp. 291–298. doi: 10.1016/j.conb.2011.01.001.

Mank, M. *et al.* (2006) 'A FRET-Based Calcium Biosensor with Fast Signal Kinetics and High Fluorescence Change', *Biophysical Journal*, 90(5), pp. 1790–1796. doi: 10.1529/biophysj.105.073536.

Mank, M. *et al.* (2008) 'A genetically encoded calcium indicator for chronic in vivo two-photon imaging', *Nature Methods*. Nature Publishing Group, 5(9), pp. 805–811. doi: 10.1038/nmeth.1243.

Marconi, P. *et al.* (2009) 'HSV as a vector in vaccine development and gene therapy', *Advances in Experimental Medicine and Biology*, 655, pp. 118–144. doi: 10.1007/978-1-4419-1132-2_10.

Marsh, S. J. *et al.* (1987) 'The mechanism of action of capsaicin on sensory C-type neurons and their axons in vitro', *Neuroscience*. Pergamon, 23(1), pp. 275–289. doi: 10.1016/0306-4522(87)90289-2.

Marshall, M. S. *et al.* (2018) 'Long-Term Improvement of Neurological Signs and Metabolic Dysfunction in a Mouse Model of Krabbe's Disease after Global Gene Therapy', *Molecular Therapy*, 26(3), pp. 874–889. doi: 10.1016/j.ymthe.2018.01.009.

Martin, H. A. *et al.* (1987) 'Leukotriene and prostaglandin sensitization of cutaneous high-threshold C- and A-delta mechanonociceptors in the hairy skin of rat hindlimbs', *Neuroscience*. Pergamon, 22(2), pp. 651–659. doi: 10.1016/0306-4522(87)90360-5.

Martino, S. *et al.* (2005) 'A direct gene transfer strategy via brain internal capsule reverses the biochemical defect in Tay-Sachs disease', *Human Molecular Genetics*, 14(15), pp. 2113–2123. doi: 10.1093/hmg/ddi216.

Mason, A., Larkman, A. and Eldridge, J. L. (1988) 'A method for intracellular injection of horseradish peroxidase by pressure', *Journal of Neuroscience Methods*. Elsevier, 22(3), pp. 181–187. doi: 10.1016/0165-0270(88)90038-6.

Mason, M. R. J. *et al.* (2010) 'Comparison of AAV serotypes for gene delivery to dorsal root ganglion neurons', *Molecular Therapy*. Nature Publishing Group, 18(4), pp. 715–724. doi: 10.1038/mt.2010.19.

Mata, M., Hao, S. and Fink, D. J. (2008) 'Applications of gene therapy to the treatment of chronic pain.', *Current gene therapy*, 8(1), pp. 42–48. doi: 10.2174/156652308783688527.

Mauleon, G. *et al.* (2013) 'Enhanced loading of Fura-2/AM calcium indicator dye in adult rodent brain slices via a microfluidic oxygenator', *Journal of Neuroscience Methods*. NIH Public Access, 216(2), pp. 110–117. doi: 10.1016/j.jneumeth.2013.04.007.

Maurer, K. *et al.* (2014) 'Acetylsalicylic acid enhances tachyphylaxis of repetitive capsaicin responses in TRPV1-GFP expressing HEK293 cells', *Neuroscience Letters*. Elsevier, 563, pp. 101–

106. doi: 10.1016/j.neulet.2014.01.050.

Mays, L. E. *et al.* (2009) 'Adeno-Associated Virus Capsid Structure Drives CD4-Dependent CD8 $^{+}$ T Cell Response to Vector Encoded Proteins', *The Journal of Immunology*, 182(10), pp. 6051–6060. doi: 10.4049/jimmunol.0803965.

McCarty, D. M. *et al.* (2009) 'Mannitol-facilitated CNS entry of rAAV2 vector significantly delayed the neurological disease progression in MPS IIIB mice', *Gene Therapy*. Nature Publishing Group, 16(11), pp. 1340–1352. doi: 10.1038/gt.2009.85.

McCarty, D. M., Monahan, P. E. and Samulski, R. J. (2001) 'Self-complementary recombinant adeno-associated virus (scAAV) vectors promote efficient transduction independently of DNA synthesis', *Gene Therapy*, 8(16), pp. 1248–1254. doi: 10.1038/sj.gt.3301514.

McConnell, M. J. and Imperiale, M. J. (2004) 'Biology of Adenovirus and Its Use as a Vector for Gene Therapy', *Human Gene Therapy*, 15(11), pp. 1022–1033. doi: 10.1089/hum.2004.15.1022.

McMahon, S. B., Cafferty, W. B. J. and Marchand, F. (2005) 'Immune and glial cell factors as pain mediators and modulators', *Experimental Neurology*. Academic Press, pp. 444–462. doi: 10.1016/j.expneurol.2004.11.001.

McNamara, C. R. *et al.* (2007) 'TRPA1 mediates formalin-induced pain', *Proceedings of the National Academy of Sciences*, 104(33), pp. 13525–13530. doi: 10.1073/pnas.0705924104.

Messlinger, K. (2018) 'The big CGRP flood - sources, sinks and signalling sites in the trigeminovascular system', *Journal of Headache and Pain*, p. 22. doi: 10.1186/s10194-018-0848-0.

Meves, H. (2006) 'The action of prostaglandins on ion channels.', *Current neuropharmacology*. Bentham Science Publishers, 4(1), pp. 41–57. doi: 10.2174/157015906775203048.

Meyer, R. A. and Campbell, J. N. (1981) 'Myelinated nociceptive afferents account for the hyperalgesia that follows a burn to the hand', *Science*. American Association for the

Advancement of Science, 213(4515), pp. 1527–1529. doi: 10.1126/science.7280675.

Mittmann, W. *et al.* (2011) 'Two-photon calcium imaging of evoked activity from L5 somatosensory neurons in vivo', *Nature Neuroscience*. Nature Publishing Group, 14(8), pp. 1089–1093. doi: 10.1038/nn.2879.

Miyanohara, A. *et al.* (2016) 'Potent spinal parenchymal AAV9-mediated gene delivery by subpial injection in adult rats and pigs', *Molecular Therapy - Methods and Clinical Development*. American Society of Gene & Cell Therapy, 3(April), p. 16046. doi: 10.1038/mtm.2016.46.

Miyawaki, A. *et al.* (1997) 'Fluorescent indicators for Ca2+based on green fluorescent proteins and calmodulin', *Nature*. Nature Publishing Group, 388(6645), pp. 882–887. doi: 10.1038/42264.

Miyawaki, A. (2011) 'Development of Probes for Cellular Functions Using Fluorescent Proteins and Fluorescence Resonance Energy Transfer', *Annual Review of Biochemistry*. Annual Reviews, 80(1), pp. 357–373. doi: 10.1146/annurev-biochem-072909-094736.

Mizumura, K. *et al.* (2009) 'Excitation and sensitization of nociceptors by bradykinin: What do we know?', *Experimental Brain Research*. Springer-Verlag, pp. 53–65. doi: 10.1007/s00221-009-1814-5.

Mizumura, K., Koda, H. and Kumazawa, T. (1997) 'Evidence that protein kinase C activation is involved in the excitatory and facilitatory effects of bradykinin on canine visceral nociceptors in vitro', *Neuroscience Letters*, 237(1), pp. 29–32. doi: 10.1016/S0304-3940(97)00793-3.

Mogil, J. S., Max, M. B. and Belfer, I. (2013) 'Genetics of Pain', in McMahon, S. B. et al. (eds) *Wall & Melzack's Textbook of Pain*. 6th edn. Elsevier.

Mohapatra, D. P. and Nau, C. (2003) 'Desensitization of Capsaicin-activated Currents in the Vanilloid Receptor TRPV1 Is Decreased by the Cyclic AMP-dependent Protein Kinase Pathway', *Journal of Biological Chemistry*. American Society for Biochemistry and Molecular Biology, 278(50), pp. 50080–50090. doi: 10.1074/jbc.M306619200.

Mohapatra, D. P. and Nau, C. (2005) 'Regulation of Ca2+-dependent desensitization in the vanilloid receptor TRPV1 by calcineurin and cAMP-dependent protein kinase', *Journal of Biological Chemistry*. American Society for Biochemistry and Molecular Biology, 280(14), pp. 13424–13432. doi: 10.1074/jbc.M410917200.

Molineux, M. L. *et al.* (2006) 'Specific T-type calcium channel isoforms are associated with distinct burst phenotypes in deep cerebellar nuclear neurons', *Proceedings of the National Academy of Sciences*. National Academy of Sciences, 103(14), pp. 5555–5560. doi: 10.1073/pnas.0601261103.

Momin, A. *et al.* (2008) 'Role of the hyperpolarization-activated current Ih in somatosensory neurons', *Journal of Physiology*, 586(24), pp. 5911–5929. doi: 10.1113/jphysiol.2008.163154.

Momin, A. and McNaughton, P. A. (2009) 'Regulation of firing frequency in nociceptive neurons by pro-inflammatory mediators', *Experimental Brain Research*. Springer-Verlag, pp. 45–52. doi: 10.1007/s00221-009-1744-2.

Montero, M. *et al.* (1995) 'Monitoring dynamic changes in free Ca2+ concentration in the endoplasmic reticulum of intact cells', *Embo J*, 14(22), pp. 5467–5475. Available at: http://www.ncbi.nlm.nih.gov/pubmed/8521803 (Accessed: 19 July 2018).

Montgomery, K. L. *et al.* (2015) 'Wirelessly powered, fully internal optogenetics for brain, spinal and peripheral circuits in mice', *Nature Methods*. Nature Publishing Group, 12(10), pp. 969–974. doi: 10.1038/nmeth.3536.

Moon, H. C. *et al.* (2017) 'Optical inactivation of the anterior cingulate cortex modulate descending pain pathway in a rat model of trigeminal neuropathic pain created via chronic constriction injury of the infraorbital nerve', *Journal of Pain Research*, 10, pp. 2355–2364. doi: 10.2147/JPR.S138626.

Moriyama, T. *et al.* (2005) 'Sensitization of TRPVI by EP1 and IP reveals peripheral nociceptive mechanism of prostaglandins', *Molecular Pain*. SAGE Publications, 1, pp. 1744-8069-1–3. doi:

10.1186/1744-8069-1-3.

Mosconi, T., Snider, W. D. and Jacquin, M. F. (2001) 'Neurotrophin receptor expression in retrogradely labeled trigeminal nociceptors - Comparisons with spinal nociceptors', *Somatosensory and Motor Research*, 18(4), pp. 312–321. doi: 10.1080/01421590120089695.

Murlidharan, G., Samulski, R. J. and Asokan, A. (2014) 'Biology of adeno-associated viral vectors in the central nervous system', *Frontiers in Molecular Neuroscience*. Frontiers, 7(September), pp. 1–9. doi: 10.3389/fnmol.2014.00076.

Muruve, D. A. (2004) 'The Innate Immune Response to Adenovirus Vectors', *Human Gene Therapy*. Mary Ann Liebert, Inc. 2 Madison Avenue Larchmont, NY 10538 USA, 15(12), pp. 1157–1166. doi: 10.1089/hum.2004.15.1157.

Nakai, J., Ohkura, M. and Imoto, K. (2001) 'A high signal-to-noise ca2+ probe composed of a single green fluorescent protein', *Nature Biotechnology*, 19(2), pp. 137–141. doi: 10.1038/84397.

Naldini, L., Blomer, U., *et al.* (1996) 'Efficient transfer, integration, and sustained long-term expression of the transgene in adult rat brains injected with a lentiviral vector.', *Proceedings of the National Academy of Sciences*. National Academy of Sciences, 93(21), pp. 11382–11388. doi: 10.1073/pnas.93.21.11382.

Naldini, L., Blömer, U., *et al.* (1996) 'In vivo gene delivery and stable transduction of nondividing cells by a lentiviral vector', *Science*, 272(5259), pp. 263–267. doi: 10.1126/science.272.5259.263.

Nassini, R. *et al.* (2014) 'The TRPA1 channel in inflammatory and Neuropathic pain and migraine', *Reviews of Physiology, Biochemistry and Pharmacology*. Springer, Cham, 167, pp. 1–44. doi: 10.1007/112_2014_18.

Nedivi, E. *et al.* (1993) 'Numerous candidate plasticity-related genes revealed by differential cDNA cloning', *Nature*. Nature Publishing Group, 363(6431), pp. 718–722. doi:

10.1038/363718a0.

Nees, T. A. *et al.* (2016) 'Early-onset treadmill training reduces mechanical allodynia and modulates calcitonin gene-related peptide fiber density in lamina III/IV in a mouse model of spinal cord contusion injury', *Pain*, 157(3), pp. 687–697. doi: 10.1097/j.pain.0000000000000422.

Neher, E. and Sakaba, T. (2008) 'Multiple Roles of Calcium Ions in the Regulation of Neurotransmitter Release', *Neuron*. Elsevier, pp. 861–872. doi: 10.1016/j.neuron.2008.08.019.

Nichols, T. C. *et al.* (2015) 'Translational Data from Adeno-Associated Virus-Mediated Gene Therapy of Hemophilia B in Dogs', *Human Gene Therapy Clinical Development*. Mary Ann Liebert, Inc., 26(1), pp. 5–14. doi: 10.1089/humc.2014.153.

Nicolson, T. A. *et al.* (2007) 'Prostaglandin E2sensitizes primary sensory neurons to histamine', *Neuroscience*, 150(1), pp. 22–30. doi: 10.1016/j.neuroscience.2007.09.003.

Niswender, C. M. and Conn, P. J. (2010) 'Metabotropic Glutamate Receptors: Physiology, Pharmacology, and Disease', *Annual Review of Pharmacology and Toxicology*. Annual Reviews, 50(1), pp. 295–322. doi: 10.1146/annurev.pharmtox.011008.145533.

O'Connor, D. H. *et al.* (2010) 'Neural activity in barrel cortex underlying vibrissa-based object localization in mice', *Neuron*. Cell Press, 67(6), pp. 1048–1061. doi: 10.1016/j.neuron.2010.08.026.

Obata, K. *et al.* (2005) 'TRPA1 induced in sensory neurons contributes to cold hyperalgesia after inflammation and nerve injury', *Journal of Clinical Investigation*, 115(9), pp. 2393–2401. doi: 10.1172/JCI25437.

Oh, M. S. *et al.* (2009) 'Expression of transgenes in midbrain dopamine neurons using the tyrosine hydroxylase promoter', *Gene Therapy*. Nature Publishing Group, 16(3), pp. 437–440. doi: 10.1038/gt.2008.148.

Ohkura, M. *et al.* (2005) 'Genetically encoded bright Ca2+ probe applicable for dynamic Ca2+ imaging of dendritic spines', *Analytical Chemistry*. American Chemical Society, 77(18), pp. 5861–5869. doi: 10.1021/ac0506837.

Ohmiya, Y. and Hirano, T. (1996) 'Shining the light: The mechanism of the bioluminescence reaction of calcium-binding photoproteins', *Chemistry and Biology*. Cell Press, pp. 337–347. doi: 10.1016/S1074-5521(96)90116-7.

Ohta, T. *et al.* (2006) 'Potentiation of transient receptor potential V1 functions by the activation of metabotropic 5-HT receptors in rat primary sensory neurons', *Journal of Physiology*, 576(3), pp. 809–822. doi: 10.1113/jphysiol.2006.112250.

Oladosu, F. A. *et al.* (2016) 'Novel intrathecal and subcutaneous catheter delivery systems in the mouse', *Journal of Neuroscience Methods*, 264, pp. 119–128. doi: 10.1016/j.jneumeth.2016.03.006.

Olson, W. *et al.* (2017) 'Sparse genetic tracing reveals regionally specific functional organization of mammalian nociceptors', *eLife*. eLife Sciences Publications, Ltd, 6. doi: 10.7554/eLife.29507.

Ozbay, B. N. *et al.* (2018) 'Three dimensional two-photon brain imaging in freely moving mice using a miniature fiber coupled microscope with active axial-scanning', *Scientific Reports*. Nature Publishing Group, 8(1), p. 8108. doi: 10.1038/s41598-018-26326-3.

Palmer, A. E. *et al.* (2011) 'Design and application of genetically encoded biosensors', *Trends in Biotechnology*. NIH Public Access, pp. 144–152. doi: 10.1016/j.tibtech.2010.12.004.

Palmer, D. J. and Ng, P. (2005) 'Helper-Dependent Adenoviral Vectors for Gene Therapy', *Human gene therapy*, 16(January), pp. 1–16. doi: 10.1089/hum.2005.16.1.

Pan, G. Y., Liu, X. D. and Liu, G. Q. (2000) 'Intracarotid infusion of hypertonic mannitol changes permeability of blood-brain barrier to methotrexate in rats.', *Acta pharmacologica Sinica*, 21(7), pp. 613–616. Available at: http://www.ncbi.nlm.nih.gov/pubmed/11360668 (Accessed: 1

August 2018).

Paredes, R. M. *et al.* (2008) 'Chemical calcium indicators', *Methods*. Academic Press, 46(3), pp. 143–151. doi: 10.1016/j.ymeth.2008.09.025.

Parr-Brownlie, L. C. *et al.* (2015) 'Lentiviral vectors as tools to understand central nervous system biology in mammalian model organisms', *Frontiers in Molecular Neuroscience*. Frontiers Media SA, 8, p. 14. doi: 10.3389/fnmol.2015.00014.

Passini, M. A. *et al.* (2005) 'AAV vector-mediated correction of brain pathology in a mouse model of Niemann-Pick A disease', *Molecular Therapy*. Cell Press, 11(5), pp. 754–762. doi: 10.1016/j.ymthe.2005.01.011.

Passini, M. A. and Wolfe, J. H. (2001) 'Widespread gene delivery and structure-specific patterns of expression in the brain after intraventricular injections of neonatal mice with an adeno-associated virus vector.', *Journal of virology*. American Society for Microbiology (ASM), 75(24), pp. 12382–92. doi: 10.1128/JVI.75.24.12382-12392.2001.

Penaud-Budloo, M. *et al.* (2018) 'Pharmacology of Recombinant Adeno-associated Virus Production', *Molecular Therapy - Methods and Clinical Development*. American Society of Gene & Cell Therapy, pp. 166–180. doi: 10.1016/j.omtm.2018.01.002.

Pérez Koldenkova, V. and Nagai, T. (2013) 'Genetically encoded Ca2+indicators: Properties and evaluation', *Biochimica et Biophysica Acta - Molecular Cell Research*. Elsevier, 1833(7), pp. 1787–1797. doi: 10.1016/j.bbamcr.2013.01.011.

Peron, S. P. *et al.* (2015) 'A Cellular Resolution Map of Barrel Cortex Activity during Tactile Behavior', *Neuron*. Elsevier Inc., 86(3), pp. 783–799. doi: 10.1016/j.neuron.2015.03.027.

Persson, A. K. *et al.* (2009) 'Correlational analysis for identifying genes whose regulation contributes to chronic neuropathic pain', *Molecular Pain*, 5, pp. 1744-8069-5–7. doi: 10.1186/1744-8069-5-7.

Petho, G. and Reeh, P. W. (2012) 'Sensory and Signaling Mechanisms of Bradykinin, Eicosanoids, Platelet-Activating Factor, and Nitric Oxide in Peripheral Nociceptors', *Physiological Reviews*. American Physiological Society Bethesda, MD, 92(4), pp. 1699–1775. doi: 10.1152/physrev.00048.2010.

Pezet, S. and McMahon, S. B. (2006) 'NEUROTROPHINS: Mediators and Modulators of Pain', *Annual Review of Neuroscience*. Annual Reviews, 29(1), pp. 507–538. doi: 10.1146/annurev.neuro.29.051605.112929.

Pillay, S. *et al.* (2016) 'An essential receptor for adeno-associated virus infection', *Nature*. Nature Publishing Group, 530(7588), pp. 108–112. doi: 10.1038/nature16465.

Piper, A. S. and Docherty, R. J. (2000) 'One-way cross-desensitization between P2X purinoceptors and vanilloid receptors in adult rat dorsal root ganglion neurones', *Journal of Physiology*. Wiley-Blackwell, 523(3), pp. 685–696. doi: 10.1111/j.1469-7793.2000.t01-1-00685.x.

Pitchford, S. and Levine, J. D. (1991) 'Prostaglandins sensitize nociceptors in cell culture', *Neuroscience Letters*, 132(1), pp. 105–108. doi: 10.1016/0304-3940(91)90444-X.

Pleticha, J. *et al.* (2014) 'Intraneural convection enhanced delivery of AAVrh20 for targeting primary sensory neurons', *Molecular and Cellular Neuroscience*. Academic Press, 60, pp. 72–80. doi: 10.1016/j.mcn.2014.04.004.

Post, D. E. *et al.* (2004) 'Replicative oncolytic herpes simplex viruses in combination cancer therapies.', *Current gene therapy*, 4(1), pp. 41–51. doi: 10.2174/1566523044577988.

Purves, D. *et al.* (2018) *Neuroscience*. 5th edn. Available at: https://global.oup.com/ukhe/product/neuroscience-9781605357416?q=purves&lang=en&cc=us (Accessed: 6 August 2018).

Rabinowitz, J. E. *et al.* (2002) 'Cross-packaging of a single adeno-associated virus (AAV) type 2 vector genome into multiple AAV serotypes enables transduction with broad specificity.',

Journal of virology, 76(2), pp. 791–801. doi: 10.1128/JVI.76.2.791-801.2002.

Rahim, A. A. *et al.* (2009) 'Efficient gene delivery to the adult and fetal CNS using pseudotyped non-integrating lentiviral vectors', *Gene Therapy*. Nature Publishing Group, 16(4), pp. 509–520. doi: 10.1038/gt.2008.186.

Rajapakse, D., Liossi, C. and Howard, R. F. (2014) 'Presentation and management of chronic pain', *Archives of Disease in Childhood*, pp. 474–480. doi: 10.1136/archdischild-2013-304207.

Reeh, P. W. (1986) 'Sensory receptors in mammalian skin in an in vitro preparation', *Neuroscience Letters*. Elsevier, 66(2), pp. 141–146. doi: 10.1016/0304-3940(86)90180-1.

Reichling, D. B. and MacDermott, A. B. (1996) 'NMDA receptor-mediated calcium entry in the absence of AMPA receptor activation in rat dorsal horn neurons', *Neuroscience Letters*, 204(1–2), pp. 17–20. doi: 0304-3940(96)12305-3 [pii].

Reik, W. (2007) 'Stability and flexibility of epigenetic gene regulation in mammalian development', *Nature*, pp. 425–432. doi: 10.1038/nature05918.

Rein, M. L. and Deussing, J. M. (2012) 'The optogenetic (r)evolution', *Molecular Genetics and Genomics*. Springer-Verlag, pp. 95–109. doi: 10.1007/s00438-011-0663-7.

Reiser, J. *et al.* (1996) 'Transduction of nondividing cells using pseudotyped defective high-titer HIV type 1 particles.', *Proceedings of the National Academy of Sciences of the United States of America*, 93(26), pp. 15266–71. doi: 10.1073/pnas.93.26.15266.

Ridgway, E. B. and Ashley, C. C. (1967) 'Calcium transients in single muscle fibers', *Biochemical and Biophysical Research Communications*. Academic Press, 29(2), pp. 229–234. doi: 10.1016/0006-291X(67)90592-X.

Ringkamp, M. *et al.* (2013) 'Peripheral Mechanisms of Cutaneous Nociception', in McMahon, S. B. et al. (eds) *Wall & Melzack's Textbook of Pain*. 6th edn. Elsevier.

Ritter, A. M. and Mendell, L. M. (1992) 'Somal membrane properties of physiologically

identified sensory neurons in the rat: effects of nerve growth factor.', *Journal of neurophysiology*. American Physiological Society Bethesda, MD, 68(6), p. 41. doi: 10.1152/jn.1992.68.6.2033.

Roome, C. J., Knöpfel, T. and Empson, R. M. (2013) 'Functional contributions of the plasma membrane calcium ATPase and the sodium-calcium exchanger at mouse parallel fibre to Purkinje neuron synapses', *Pflugers Archiv European Journal of Physiology*, 465(2), pp. 319–331. doi: 10.1007/s00424-012-1172-1.

Rose, C. R. and Konnerth, A. (2001) 'Stores not just for storage: Intracellular calcium release and synaptic plasticity', *Neuron*. Elsevier, pp. 519–522. doi: 10.1016/S0896-6273(01)00402-0.

Roth, B. L. (2016) 'DREADDs for Neuroscientists', *Neuron*. Elsevier, 89(4), pp. 683–694. doi: 10.1016/j.neuron.2016.01.040.

Rubaiy, H. N. (2017) 'A short guide to electrophysiology and ion channels', *Journal of Pharmacy and Pharmaceutical Sciences*, 20(1), pp. 48–67. doi: 10.18433/J32P6R.

Rueden, C. T. *et al.* (2017) 'ImageJ2: ImageJ for the next generation of scientific image data', *BMC Bioinformatics*, 18(1), p. 529. doi: 10.1186/s12859-017-1934-z.

Sadakane, O. *et al.* (2015) 'Long-Term Two-Photon Calcium Imaging of Neuronal Populations with Subcellular Resolution in Adult Non-human Primates', *Cell Reports*. Cell Press, 13(9), pp. 1989–1999. doi: 10.1016/j.celrep.2015.10.050.

Sakka, L., Coll, G. and Chazal, J. (2011) 'Anatomy and physiology of cerebrospinal fluid', *European Annals of Otorhinolaryngology, Head and Neck Diseases*. Elsevier Masson, pp. 309–316. doi: 10.1016/j.anorl.2011.03.002.

Salo, P. T. and Tatton, W. G. (1993) 'Age-related loss of knee joint afferents in mice', *Journal of Neuroscience Research*, 35(6), pp. 664–677. doi: 10.1002/jnr.490350609.

Salzer, I. *et al.* (2016) 'Control of sensory neuron excitability by serotonin involves 5HT2C

receptors and Ca2+-activated chloride channels', *Neuropharmacology*. Pergamon, 110, pp. 277–286. doi: 10.1016/j.neuropharm.2016.08.006.

Samad, O. A. *et al.* (2013) 'Virus-mediated shRNA knockdown of Na v 1.3 in rat dorsal root ganglion attenuates nerve injury-induced neuropathic pain', *Molecular Therapy*, 21(1), pp. 49–56. doi: 10.1038/mt.2012.169.

Samaniego, L. A., Neiderhiser, L. and DeLuca, N. A. (1998) 'Persistence and expression of the herpes simplex virus genome in the absence of immediate-early proteins.', *Journal of virology*, 72(4), pp. 3307–20. Available at: http://www.ncbi.nlm.nih.gov/pubmed/9525658 (Accessed: 14 August 2018).

Samaranch, L. *et al.* (2014) 'AAV9-mediated expression of a non-self protein in nonhuman primate central nervous system triggers widespread neuroinflammation driven by antigen-presenting cell transduction', *Molecular Therapy*, 22(2), pp. 329–337. doi: 10.1038/mt.2013.266.

Samaranch, L. *et al.* (2016) 'Cerebellomedullary Cistern Delivery for AAV-Based Gene Therapy: A Technical Note for Nonhuman Primates', *Human Gene Therapy Methods*. Mary Ann Liebert, Inc., 27(1), pp. 13–16. doi: 10.1089/hgtb.2015.129.

Samulski, R. J. *et al.* (1991) 'Targeted integration of adeno-associated virus (AAV) into human chromosome 19.', *The EMBO journal*, 10(12), pp. 3941–50. doi: 10.1523/JNEUROSCI.4323-08.2008.

Sander, J. D. and Joung, J. K. (2014) 'CRISPR-Cas systems for editing, regulating and targeting genomes', *Nature Biotechnology*. NIH Public Access, pp. 347–350. doi: 10.1038/nbt.2842.

Sands, M. S. (2011) 'AAV-mediated liver-directed gene therapy', *Methods in Molecular Biology*. NIH Public Access, 807, pp. 141–157. doi: 10.1007/978-1-61779-370-7_6.

Sato, A. *et al.* (2008) 'Gene expression profiles of necrosis and apoptosis induced by 5-fluoro-2'-deoxyuridine', *Genomics*. Academic Press, 92(1), pp. 9–17. doi:

10.1016/j.ygeno.2008.02.002.

Sato, M. *et al.* (2015) 'Generation and imaging of transgenic mice that express G-CaMP7 under a tetracycline response element', *PLoS ONE*, 10(5), pp. 1–13. doi: 10.1371/journal.pone.0125354.

Sauer, B. (1998) 'Inducible gene targeting in mice using the Cre/lox system', *Methods: A Companion to Methods in Enzymology*. Academic Press, 14(4), pp. 381–392. doi: 10.1006/meth.1998.0593.

Saunders, A. and Sabatini, B. L. (2015) 'Cre activated and inactivated recombinant adeno-associated viral vectors for neuronal anatomical tracing or activity manipulation', *Current Protocols in Neuroscience*. NIH Public Access, 2015, p. 1.24.1-1.24.15. doi: 10.1002/0471142301.ns0124s72.

Schaffer, D. V and Maheshri, N. (2004) 'Directed evolution of AAV mutants for enhanced gene delivery.', *Conference proceedings : ... Annual International Conference of the IEEE Engineering in Medicine and Biology Society. IEEE Engineering in Medicine and Biology Society. Conference*. IEEE, 5, pp. 3520–3523. doi: 10.1109/IEMBS.2004.1403990.

Schaible, H. G. (2006) 'Peripheral and Central Mechanisms of Pain Generation', in Stein, C. (ed.) *Analgesia*. Berlin, Heidelberg: Springer Berlin Heidelberg, pp. 3–28. doi: 10.1007/978-3-540-33823-9_1.

Schaible, H. G. (2012) 'Mechanisms of chronic pain in osteoarthritis', *Current Rheumatology Reports*. Current Science Inc., pp. 549–556. doi: 10.1007/s11926-012-0279-x.

Schindelin, J. *et al.* (2012) 'Fiji: An open-source platform for biological-image analysis', *Nature Methods*. Nature Publishing Group, pp. 676–682. doi: 10.1038/nmeth.2019.

Schlegel, R. *et al.* (1983) 'Inhibition of VSV binding and infectivity by phosphatidylserine: Is phosphatidylserine a VSV-binding site?', *Cell*, 32(2), pp. 639–646. doi: 10.1016/0092-8674(83)90483-X.

Schmidt, F. and Grimm, D. (2015) 'CRISPR genome engineering and viral gene delivery: A case of mutual attraction', *Biotechnology Journal*. Wiley-Blackwell, pp. 258–272. doi: 10.1002/biot.201400529.

Schmidt, R. *et al.* (1995) 'Novel classes of responsive and unresponsive C nociceptors in human skin.', *The Journal of neuroscience : the official journal of the Society for Neuroscience*. Society for Neuroscience, 15(1 Pt 1), pp. 333–41. doi: 10.1523/JNEUROSCI.15-01-00333.1995.

Schon, K., Parker, A. and Woods, C. G. (2018) *Congenital Insensitivity to Pain Overview*, *GeneReviews®*. Available at: http://www.ncbi.nlm.nih.gov/pubmed/29419974 (Accessed: 6 August 2018).

Schuster, D. J. *et al.* (2014) 'Biodistribution of adeno-associated virus serotype 9 (AAV9) vector after intrathecal and intravenous delivery in mouse', *Frontiers in Neuroanatomy*, 8(June), p. 42. doi: 10.3389/fnana.2014.00042.

Sekiguchi, K. J. *et al.* (2016) 'Imaging large-scale cellular activity in spinal cord of freely behaving mice', *Nature Communications*. Nature Publishing Group, 7, p. 11450. doi: 10.1038/ncomms11450.

Sengupta, R. *et al.* (2017) 'Viral Cre-LoxP tools aid genome engineering in mammalian cells', *Journal of Biological Engineering*, 11(1), p. 45. doi: 10.1186/s13036-017-0087-y.

Senís, E. *et al.* (2014) 'CRISPR/Cas9-mediated genome engineering: An adeno-associated viral (AAV) vector toolbox', *Biotechnology Journal*, 9(11), pp. 1402–1412. doi: 10.1002/biot.201400046.

Sharon, D. and Kamen, A. (2018) 'Advancements in the design and scalable production of viral gene transfer vectors', *Biotechnology and Bioengineering*. Wiley-Blackwell, 115(1), pp. 25–40. doi: 10.1002/bit.26461.

Shen, S. *et al.* (2011) 'Terminal n-linked galactose is the primary receptor for adeno-associated virus', *Journal of Biological Chemistry*, 286(15), pp. 13532–13540. doi:

10.1074/jbc.M110.210922.

Shi, J.-Y. *et al.* (2011) 'Glial Cell Line–Derived Neurotrophic Factor Gene Transfer Exerts Protective Effect on Axons in Sciatic Nerve Following Constriction-Induced Peripheral Nerve Injury', *Human Gene Therapy*, 22(6), pp. 721–731. doi: 10.1089/hum.2010.036.

Shimano, T. *et al.* (2013) 'Assessment of the AAV-mediated expression of channelrhodopsin-2 and halorhodopsin in brainstem neurons mediating auditory signaling', *Brain Research*. NIH Public Access, 1511, pp. 138–152. doi: 10.1016/j.brainres.2012.10.030.

Shimomura, O., Kishi, Y. and Inouye, S. (1993) 'The relative rate of aequorin regeneration from apoaequorin and coelenterazine analogues.', *The Biochemical journal*. Portland Press Ltd, 296 (Pt 3)(Pt 3), pp. 549–51. Available at: http://www.ncbi.nlm.nih.gov/pubmed/8280050 (Accessed: 19 July 2018).

Shinomura, O., Johnson, F. H. and Saiga, Y. (1962) 'Extraction, purification and properties of aequorin, a bioluminescent', *Journal of cellular and comparative physiology*. Wiley-Blackwell, 59(3), pp. 223–239. doi: 10.1002/jcp.1030590302.

Shu, X. and Mendell, L. M. (2001) 'Acute sensitization by NGF of the response of small-diameter sensory neurons to capsaicin', *J Neurophysiol*, 86(6), pp. 2931–2938. doi: 10.1152/jn.2001.86.6.2931.

Siegel, F. and Lohmann, C. (2013) 'Probing synaptic function in dendrites with calcium imaging', *Experimental Neurology*, pp. 27–32. doi: 10.1016/j.expneurol.2012.02.007.

Silasi, G. *et al.* (2016) 'Intact skull chronic windows for mesoscopic wide-field imaging in awake mice', *Journal of Neuroscience Methods*. PMC Canada manuscript submission, 267, pp. 141–149. doi: 10.1016/j.jneumeth.2016.04.012.

Simms, B. A. and Zamponi, G. W. (2014) 'Neuronal voltage-gated calcium channels: Structure, function, and dysfunction', *Neuron*. Elsevier, 82(1), pp. 24–45. doi: 10.1016/j.neuron.2014.03.016.

Simons, T. J. B. (1988) 'Calcium and neuronal function', *Neurosurgical Review*. Springer-Verlag, pp. 119–129. doi: 10.1007/BF01794675.

Sinnett, S. E. *et al.* (2017) 'Improved MECP2 Gene Therapy Extends the Survival of MeCP2-Null Mice without Apparent Toxicity after Intracisternal Delivery', *Molecular Therapy - Methods and Clinical Development*. Elsevier, 5, pp. 106–115. doi: 10.1016/j.omtm.2017.04.006.

Slimko, E. M. *et al.* (2002) 'Selective electrical silencing of mammalian neurons in vitro by the use of invertebrate ligand-gated chloride channels.', *The Journal of neuroscience : the official journal of the Society for Neuroscience*. Society for Neuroscience, 22(17), pp. 7373–7379. doi: 20026775.

Slugg, R. M., Meyer, R. A. and Campbell, J. N. (2000) 'Response of cutaneous A- and C-fiber nociceptors in the monkey to controlled-force stimuli.', *Journal of neurophysiology*. American Physiological SocietyBethesda, MD, 83(4), pp. 2179–2191. doi: 10.1152/jn.2000.83.4.2179.

Smetters, D., Majewska, A. and Yuste, R. (1999) 'Detecting action potentials in neuronal populations with calcium imaging', *Methods: A Companion to Methods in Enzymology*. Academic Press, 18(2), pp. 215–221. doi: 10.1006/meth.1999.0774.

Smith, C. J. *et al.* (2013) 'Sensory neuron fates are distinguished by a transcriptional switch that regulates dendrite branch stabilization', *Neuron*. Elsevier, 79(2), pp. 266–280. doi: 10.1016/j.neuron.2013.05.009.

Smith, J. A. M., Davis, C. L. and Burgess, G. M. (2000) 'Prostaglandin E2-induced sensitization of bradykinin-evoked responses in rat dorsal root ganglion neurons is mediated by cAMP-dependent protein kinase A', *European Journal of Neuroscience*. Wiley/Blackwell (10.1111), 12(9), pp. 3250–3258. doi: 10.1046/j.1460-9568.2000.00218.x.

Smith, T. *et al.* (2015) 'Increased expression of HCN2 channel protein in L4 dorsal root ganglion neurons following axotomy of L5- and inflammation of L4-spinal nerves in rats', *Neuroscience*. Pergamon, 295, pp. 90–102. doi: 10.1016/j.neuroscience.2015.03.041.

Snyder, B. R. *et al.* (2011) 'Comparison of Adeno-Associated Viral Vector Serotypes for Spinal Cord and Motor Neuron Gene Delivery', *Human Gene Therapy*, 22(9), pp. 1129–1135. doi: 10.1089/hum.2011.008.

Sohya, K. *et al.* (2007) 'GABAergic Neurons Are Less Selective to Stimulus Orientation than Excitatory Neurons in Layer II/III of Visual Cortex, as Revealed by In Vivo Functional Ca2+ Imaging in Transgenic Mice', *Journal of Neuroscience*. Society for Neuroscience, 27(8), pp. 2145–2149. doi: 10.1523/JNEUROSCI.4641-06.2007.

Spaete, R. R. and Frenkel, N. (1982) 'The herpes simplex virus amplicon: A new eucaryotic defective-virus cloning-amplifying vector', *Cell*, 30(1), pp. 295–304. doi: 10.1016/0092-8674(82)90035-6.

Spampanato, C. *et al.* (2011) 'Efficacy of a combined intracerebral and systemic gene delivery approach for the treatment of a severe lysosomal storage disorder', *Molecular Therapy*. Elsevier, 19(5), pp. 860–869. doi: 10.1038/mt.2010.299.

Sparta, D. R. *et al.* (2013) 'Optogenetic strategies to investigate neural circuitry engaged by stress', *Behavioural Brain Research*. Elsevier B.V., 255, pp. 19–25. doi: 10.1016/j.bbr.2013.05.007.

Spencer, N. J. *et al.* (2018) 'Identifying unique subtypes of spinal afferent nerve endings within the urinary bladder of mice', *Journal of Comparative Neurology*. Wiley-Blackwell, 526(4), pp. 707–720. doi: 10.1002/cne.24362.

Srinivasan, R. *et al.* (2016) 'New Transgenic Mouse Lines for Selectively Targeting Astrocytes and Studying Calcium Signals in Astrocyte Processes In Situ and In Vivo', *Neuron*. Elsevier, 92(6), pp. 1181–1195. doi: 10.1016/j.neuron.2016.11.030.

Srinivasan, R., Fink, D. J. and Glorioso, J. C. (2008) 'HSV vectors for gene therapy of chronic pain', *Current Opinion in Molecular Therapeutics*, 10(5), pp. 449–455. Available at: http://www.ncbi.nlm.nih.gov/pubmed/18830920 (Accessed: 20 August 2018).

Srivastava, A. (2016) ‘In vivo tissue-tropism of adeno-associated viral vectors’, *Current Opinion in Virology*. Elsevier, 21, pp. 75–80. doi: 10.1016/j.coviro.2016.08.003.

Stanley, E. F. (1993) ‘Single calcium channels and acetylcholine release at a presynaptic nerve terminal’, *Neuron*. Elsevier, 11(6), pp. 1007–1011. doi: 10.1016/0896-6273(93)90214-C.

Sternson, S. M. and Roth, B. L. (2014) ‘Chemogenetic Tools to Interrogate Brain Functions’, *Annual Review of Neuroscience*. Annual Reviews, 37(1), pp. 387–407. doi: 10.1146/annurev-neuro-071013-014048.

Sterratt, D. C. *et al.* (2012) ‘Spine calcium transients induced by synaptically-evoked action potentials can predict synapse location and establish synaptic democracy’, *PLoS Computational Biology*. Edited by O. Sporns. Public Library of Science, 8(6), p. e1002545. doi: 10.1371/journal.pcbi.1002545.

Stirling, L. C. *et al.* (2005) ‘Nociceptor-specific gene deletion using heterozygous NaV1.8-Cre recombinase mice’, *Pain*. No longer published by Elsevier, 113(1–2), pp. 27–36. doi: 10.1016/j.pain.2004.08.015.

Story, G. M. *et al.* (2003) ‘ANKTM1, a TRP-like channel expressed in nociceptive neurons, is activated by cold temperatures’, *Cell*. Elsevier, 112(6), pp. 819–829. doi: 10.1016/S0092-8674(03)00158-2.

Stosiek, C. *et al.* (2003) ‘In vivo two-photon calcium imaging of neuronal networks’, *Proceedings of the National Academy of Sciences*. National Academy of Sciences, 100(12), pp. 7319–7324. doi: 10.1073/pnas.1232232100.

Südhof, T. C. (2004) ‘The synaptic vesicle cycle’, *Annu. Rev. Neurosci*, 27(1), pp. 509–47. doi: 10.1146/annurev.neuro.26.041002.131412.

Sugiura, T. *et al.* (2014) ‘Bradykinin Lowers the Threshold Temperature for Heat Activation of Vanilloid Receptor 1 Bradykinin Lowers the Threshold Temperature for Heat Activation of Vanilloid Receptor 1’, *Journal of Neurophysiology*. American Physiological SocietyBethesda, MD,

88(1), pp. 544–548. doi: 10.1152/jn.2002.88.1.544.

Sun, J. *et al.* (2018) 'Increased Na $_v$ 1.7 expression in the dorsal root ganglion contributes to pain hypersensitivity after plantar incision in rats', *Molecular Pain*. SAGE PublicationsSage CA: Los Angeles, CA, 14, p. 174480691878232. doi: 10.1177/1744806918782323.

Szallasi, A. and Blumberg, P. M. (1999) 'Vanilloid (Capsaicin) receptors and mechanisms.', *Pharmacological reviews*, 51(2), pp. 159–212. Available at: http://www.ncbi.nlm.nih.gov/pubmed/10353985 (Accessed: 25 July 2018).

Tabebordbar, M. *et al.* (2016) 'In vivo gene editing in dystrophic mouse muscle and muscle stem cells', *Science*. American Association for the Advancement of Science, 351(6271), pp. 407–411. doi: 10.1126/science.aad5177.

Taguchi, T. *et al.* (2007) 'Neuroanatomical pathway of nociception originating in a low back muscle (multifidus) in the rat', *Neuroscience Letters*, 427(1), pp. 22–27. doi: 10.1016/j.neulet.2007.08.021.

Tallini, Y. N. *et al.* (2006) 'Imaging cellular signals in the heart in vivo: Cardiac expression of the high-signal Ca2+ indicator GCaMP2', *Proceedings of the National Academy of Sciences*, 103(12), pp. 4753–4758. doi: 10.1073/pnas.0509378103.

Tang, H. Bin *et al.* (2004) 'Sensitization of vanilloid receptor 1 induced by bradykinin via the activation of second messenger signaling cascades in rat primary afferent neurons', *European Journal of Pharmacology*, 498(1–3), pp. 37–43. doi: 10.1016/j.ejphar.2004.07.076.

Tang, P. *et al.* (2015) 'In vivo two-photon imaging of axonal dieback, blood flow, and calcium influx with methylprednisolone therapy after spinal cord injury', *Scientific Reports*, 5(1), p. 9691. doi: 10.1038/srep09691.

Taymans, J.-M. *et al.* (2007) 'Comparative Analysis of Adeno-Associated Viral Vector Serotypes 1, 2, 5, 7, And 8 in Mouse Brain', *Human Gene Therapy*, 18(3), pp. 195–206. doi: 10.1089/hum.2006.178.

Tervo, D. G. R. *et al.* (2016) 'A Designer AAV Variant Permits Efficient Retrograde Access to Projection Neurons', *Neuron*, 92(2), pp. 372–382. doi: 10.1016/j.neuron.2016.09.021.

Thakur, M. *et al.* (2014) 'Defining the nociceptor transcriptome', *Frontiers in Molecular Neuroscience*, 7(November), pp. 1–11. doi: 10.3389/fnmol.2014.00087.

Thayer, S. A., Perney, T. M. and Miller, R. J. (1988) 'Regulation of calcium homeostasis in sensory neurons by bradykinin.', *The Journal of neuroscience : the official journal of the Society for Neuroscience*, 8(11), pp. 4089–97. Available at: http://www.ncbi.nlm.nih.gov/pubmed/3183714 (Accessed: 19 July 2018).

Themis, M. *et al.* (2005) 'Oncogenesis following delivery of a nonprimate lentiviral gene therapy vector to fetal and neonatal mice', *Molecular Therapy*, 12(4), pp. 763–771. doi: 10.1016/j.ymthe.2005.07.358.

Thestrup, T. *et al.* (2014) 'Optimized ratiometric calcium sensors for functional in vivo imaging of neurons and T lymphocytes', *Nature Methods*, 11(2), pp. 175–182. doi: 10.1038/nmeth.2773.

Thöny, B. (2010) 'Long-term correction of murine phenylketonuria by viral gene transfer: Liver versus muscle', *Journal of Inherited Metabolic Disease*. Springer Netherlands, pp. 677–680. doi: 10.1007/s10545-010-9044-3.

Tian, L. *et al.* (2009) 'Imaging neural activity in worms, flies and mice with improved GCaMP calcium indicators', *Nature Methods*. Nature Publishing Group, 6(12), pp. 875–881. doi: 10.1038/nmeth.1398.

Tian, L. *et al.* (2012) *Neural activity imaging with genetically encoded calcium indicators*. 1st edn, *Progress in Brain Research*. 1st edn. Elsevier B.V. doi: 10.1016/B978-0-444-59426-6.00005-7.

Tian, L., Hires, A. and Looger, L. L. (2012) 'Imaging neuronal activity with genetically encoded calcium indicators', *Cold Spring Harbor Protocols*. Cold Spring Harbor Laboratory Press, 7(6), pp.

647–656. doi: 10.1101/pdb.top069609.

Todd, A. J. *et al.* (2002) 'Projection neurons in lamina I of rat spinal cord with the neurokinin 1 receptor are selectively innervated by substance p-containing afferents and respond to noxious stimulation.', *The Journal of neuroscience : the official journal of the Society for Neuroscience*, 22(10), pp. 4103–4113. doi: 20026261.

Todd, A. J. (2010) 'Neuronal circuitry for pain processing in the dorsal horn', *Nature Reviews Neuroscience*, 11(12), pp. 823–836. doi: 10.1038/nrn2947.

Todd, A. J. and Koerber, H. R. (2013) 'Neuroanatomical Substrates of Spinal Nociception', in McMahon, S. B. et al. (eds) *Wall & Melzack's Textbook of Pain*. 6th edn. Elsevier.

Todo, T. (2008) 'Oncolytic virus therapy using genetically engineered herpes simplex viruses', *Front Biosci*, 13(3), pp. 2060–2064. doi: 2823 [pii].

Tominaga, M. *et al.* (1998) 'The cloned capsaicin receptor integrates multiple pain-producing stimuli', *Neuron*. Elsevier, 21(3), pp. 531–543. doi: 10.1016/S0896-6273(00)80564-4.

Tonini, R. *et al.* (2013) 'Small-conductance Ca 2+ -activated K + channels modulate action potential-induced Ca 2+ transients in hippocampal neurons', *Journal of Neurophysiology*. American Physiological Society, 109(6), pp. 1514–1524. doi: 10.1152/jn.00346.2012.

Towne, C. *et al.* (2008) 'Systemic AAV6 delivery mediating RNA interference against SOD1: Neuromuscular transduction does not alter disease progression in fALS mice', *Molecular Therapy*, 16(6), pp. 1018–1025. doi: 10.1038/mt.2008.73.

Towne, C. *et al.* (2009) 'Recombinant adeno-associated virus serotype 6 (rAAV2/6)-mediated gene transfer to nociceptive neurons through different routes of delivery', *Molecular Pain*, 5, pp. 1–17. doi: 10.1186/1744-8069-5-52.

Towne, C. *et al.* (2013) 'Optogenetic Control of Targeted Peripheral Axons in Freely Moving Animals', *PLoS ONE*. Edited by E. J. Kremer. Public Library of Science, 8(8), p. e72691. doi:

10.1371/journal.pone.0072691.

Traub, R. J. and Mendell, L. M. (1988) 'The spinal projection of individual identified A-delta- and C-fibers.', *Journal of neurophysiology*, 59(1), pp. 41–55. doi: 10.1152/jn.1988.59.1.41.

Treede, R.-D. D. *et al.* (2015) 'A classification of chronic pain for ICD-11', *Pain*. Wolters Kluwer Health, 156(6), p. 1. doi: 10.1097/j.pain.0000000000000160.

Treede, R. D. *et al.* (1998) 'Myelinated mechanically insensitive afferents from monkey hairy skin: heat-response properties', *J.Neurophysiol.* American Physiological SocietyBethesda, MD, 80(0022–3077 (Print)), pp. 1082–1093. doi: 10.1152/jn.1998.80.3.1082.

Tsantoulas, C. *et al.* (2013) 'Probing Functional Properties of Nociceptive Axons Using a Microfluidic Culture System', *PLoS ONE*. Edited by Y. Yang. Public Library of Science, 8(11), p. e80722. doi: 10.1371/journal.pone.0080722.

Tsien, R. Y. (1981) 'A non-disruptive technique for loading calcium buffers and indicators into cells', *Nature*, 290(5806), pp. 527–528. doi: 10.1038/290527a0.

Tsien, R. Y., Rink, T. J. and Poenie, M. (1985) 'Measurement of cytosolic free Ca2+in individual small cells using fluorescence microscopy with dual excitation wavelengths', *Cell Calcium*. Churchill Livingstone, 6(1–2), pp. 145–157. doi: 10.1016/0143-4160(85)90041-7.

Urnov, F. D. *et al.* (2010) 'Genome editing with engineered zinc finger nucleases', *Nature Reviews Genetics*. Nature Publishing Group, pp. 636–646. doi: 10.1038/nrg2842.

Usoskin, D. *et al.* (2015) 'Unbiased classification of sensory neuron types by large-scale single-cell RNA sequencing', *Nature Neuroscience*. Nature Publishing Group, 18(1), pp. 145–153. doi: 10.1038/nn.3881.

Valenti, O., Jeffrey Conn, P. and Marino, M. J. (2002) 'Distinct physiological roles of the Gq-coupled metabotropic glutamate receptors co-expressed in the same neuronal populations', *Journal of Cellular Physiology*. Wiley-Blackwell, pp. 125–137. doi: 10.1002/jcp.10081.

Vega, R. B. *et al.* (2004) 'Histone deacetylase 4 controls chondrocyte hypertrophy during skeletogenesis', *Cell*, 119(4), pp. 555–566. doi: 10.1016/j.cell.2004.10.024.

Vellani, V. *et al.* (2001) 'Protein kinase C activation potentiates gating of the vanilloid receptor VR1 by capsaicin, protons, heat and anandamide', *Journal of Physiology*. Wiley-Blackwell, 534(3), pp. 813–825. doi: 10.1111/j.1469-7793.2001.00813.x.

Vellani, V. (2006) 'Sensitization of Transient Receptor Potential Vanilloid 1 by the Prokineticin Receptor Agonist Bv8', *Journal of Neuroscience*. Society for Neuroscience, 26(19), pp. 5109–5116. doi: 10.1523/JNEUROSCI.3870-05.2006.

Vellani, V., Zachrisson, O. and McNaughton, P. A. (2004) 'Functional bradykinin B1 receptors are expressed in nociceptive neurones and are upregulated by the neurotrophin GDNF.', *The Journal of physiology*. Wiley-Blackwell, 560(Pt 2), pp. 391–401. doi: 10.1113/jphysiol.2004.067462.

Venkatachalam, V. *et al.* (2016) 'Pan-neuronal imaging in roaming Caenorhabditis elegans', *Proceedings of the National Academy of Sciences*, 113(8), pp. E1082–E1088. doi: 10.1073/pnas.1507109113.

Vercelli, A. *et al.* (2000) 'Recent techniques for tracing pathways in the central nervous system of developing and adult mammals', *Brain Research Bulletin*. Elsevier, pp. 11–28. doi: 10.1016/S0361-9230(99)00229-4.

Verkhratsky, A. (2004) 'Endoplasmic reticulum calcium signaling in nerve cells.', *Biological research*, 37(4), pp. 693–9. Available at: http://www.ncbi.nlm.nih.gov/pubmed/15709699 (Accessed: 19 July 2018).

Verkhratsky, A. J. and Petersen, O. H. (1998) 'Neuronal calcium stores', *Cell Calcium*, pp. 333–343. doi: 10.1016/S0143-4160(98)90057-4.

Vertes, R. P. and Stackman, R. W. (2011) *Electrophysiological recording techniques*. Humana Press.

Vincent, M., Gao, G. and Jacobson, L. (2014) 'Comparison of the efficacy of five adeno-associated virus vectors for transducing dorsal raphé nucleus cells in the mouse', *Journal of Neuroscience Methods*, 235, pp. 189–192. doi: 10.1016/j.jneumeth.2014.07.005.

Vulchanova, L. *et al.* (2010) 'Differential adeno-associated virus mediated gene transfer to sensory neurons following intrathecal delivery by direct lumbar puncture', *Molecular Pain*. SAGE Publications, 6, p. 31. doi: 10.1186/1744-8069-6-31.

VulchanovaDaniel, L. (2012) 'Open Access Differential adeno-associated virus mediated gene transfer to sensory neurons following intrathecal delivery by direct lumbar puncture', *Molecular pain*, 8(31), pp. 1–10. Available at: http://www.biomedcentral.com/content/pdf/1744-8069-6-31.pdf (Accessed: 5 December 2014).

Vyklický, L. *et al.* (1998) 'Inflammatory mediators at acidic pH activate capsaicin receptors in cultured sensory neurons from newborn rats.', *Journal of neurophysiology*. American Physiological SocietyBethesda, MD, 79(2), pp. 670–6. doi: 10.1152/jn.1998.79.2.670.

Walker, M. W. *et al.* (1988) 'Neuropeptide Y modulates neurotransmitter release and Ca2+ currents in rat sensory neurons', *J Neurosci*, 8(7), pp. 2438–2446. Available at: http://www.ncbi.nlm.nih.gov/pubmed/2907913 (Accessed: 19 July 2018).

Wang, D. B. *et al.* (2010) 'Expansive gene transfer in the rat CNS rapidly produces amyotrophic lateral sclerosis relevant sequelae when TDP-43 is overexpressed', *Molecular Therapy*. Elsevier, 18(12), pp. 2064–2074. doi: 10.1038/mt.2010.191.

Wang, H. and Peng, R. Y. (2016) 'Basic roles of key molecules connected with NMDAR signaling pathway on regulating learning and memory and synaptic plasticity', *Military Medical Research*. BioMed Central, 3(1), p. 26. doi: 10.1186/s40779-016-0095-0.

Wang, J. W. *et al.* (2003) 'Two-photon calcium imaging reveals an odor-evoked map of activity in the fly brain', *Cell*, 112(2), pp. 271–282. doi: 10.1016/S0092-8674(03)00004-7.

Wang, J. Z. *et al.* (2017) 'The AAV-mediated and RNA-guided CRISPR/Cas9 system for gene therapy of DMD and BMD', *Brain and Development*. Elsevier, pp. 547–556. doi: 10.1016/j.braindev.2017.03.024.

Wang, P. *et al.* (2015) 'Antinociceptive effect of intrathecal amiloride on neuropathic pain in rats', *Neuroscience Letters*, 604, pp. 24–29. doi: 10.1016/j.neulet.2015.07.028.

Wang, S. *et al.* (2008) 'Phospholipase C and protein kinase A mediate bradykinin sensitization of TRPA1: A molecular mechanism of inflammatory pain', *Brain*, 131(5), pp. 1241–1251. doi: 10.1093/brain/awn060.

Weinkauf, B. *et al.* (2013) 'Modality-Specific Nociceptor Sensitization Following UV-B Irradiation of Human Skin', *The Journal of Pain*. Elsevier, 14(7), pp. 739–746. doi: 10.1016/j.jpain.2013.02.007.

Weir, G. A. *et al.* (2017) 'Using an engineered glutamate-gated chloride channel to silence sensory neurons and treat neuropathic pain at the source', *Brain*, 140(10), pp. 2570–2585. doi: 10.1093/brain/awx201.

Weng, X. *et al.* (2012) 'Chronic inflammatory pain is associated with increased excitability and hyperpolarization-activated current (Ih) in C- but not Aδ-nociceptors', *Pain*, 153(4), pp. 900–914. doi: 10.1016/j.pain.2012.01.019.

Werth, J. L. and Thayer, S. A. (1994) 'Mitochondria buffer physiological calcium loads in cultured rat dorsal root ganglion neurons.', *The Journal of neuroscience : the official journal of the Society for Neuroscience*. Society for Neuroscience, 14(1), pp. 348–56. doi: 10.1523/JNEUROSCI.14-01-00348.1994.

West, S. J. J. *et al.* (2015) 'Circuitry and plasticity of the dorsal horn - Toward a better understanding of neuropathic pain', *Neuroscience*. IBRO, 300, pp. 254–275. doi: 10.1016/j.neuroscience.2015.05.020.

Wickenden, A. D. (2014) 'Overview of electrophysiological techniques', *Current Protocols in*

Pharmacology. Wiley-Blackwell, 11(SUPPL.64), p. 11.1.1-11.1.17. doi: 10.1002/0471141755.ph1101s64.

Wiegert, J. S. *et al.* (2017) 'Silencing Neurons: Tools, Applications, and Experimental Constraints', *Neuron*. Cell Press, 95(3), pp. 504–529. doi: 10.1016/j.neuron.2017.06.050.

Woodbury, C. J. *et al.* (2004) 'Nociceptors Lacking TRPV1 and TRPV2 Have Normal Heat Responses', *Journal of Neuroscience*, 24(28), pp. 6410–6415. doi: 10.1523/JNEUROSCI.1421-04.2004.

Woodward, J. J. and Pava, M. (2012) 'Ethanol Inhibition of Up-States in Prefrontal Cortical Neurons Expressing the Genetically Encoded Calcium Indicator GCaMP3', *Alcoholism: Clinical and Experimental Research*, 36(5), pp. 780–787. doi: 10.1111/j.1530-0277.2011.01674.x.

Woolf, C. J. (2004) 'Pain: Moving from Symptom Control toward Mechanism-Specific Pharmacologic Management', *Annals of Internal Medicine*, pp. 441–451. doi: 10.7326/0003-4819-140-8-200404200-00010.

Wooten, M. *et al.* (2014) 'Three functionally distinct classes of C-fibre nociceptors in primates', *Nature Communications*. NIH Public Access, 5, p. 4122. doi: 10.1038/ncomms5122.

Wu, N. *et al.* (1996) 'Prolonged gene expression and cell survival after infection by a herpes simplex virus mutant defective in the immediate-early genes encoding ICP4, ICP27, and ICP22', *Journal of Virology*, 70(9), pp. 6358–6369. Available at: http://www.ncbi.nlm.nih.gov/pubmed/8709264 (Accessed: 14 August 2018).

Wu, Z. *et al.* (2006) ' 2,3 and 2,6 N-Linked Sialic Acids Facilitate Efficient Binding and Transduction by Adeno-Associated Virus Types 1 and 6', *Journal of Virology*. American Society for Microbiology, 80(18), pp. 9093–9103. doi: 10.1128/JVI.00895-06.

Wu, Z., Asokan, A. and Samulski, R. J. (2006) 'Adeno-associated Virus Serotypes: Vector Toolkit for Human Gene Therapy', *Molecular Therapy*, pp. 316–327. doi: 10.1016/j.ymthe.2006.05.009.

Xiao, X. *et al.* (1997) 'A novel 165-base-pair terminal repeat sequence is the sole cis requirement for the adeno-associated virus life cycle.', *Journal of virology*, 71(2), pp. 941–8. Available at: http://www.pubmedcentral.nih.gov/articlerender.fcgi?artid=191142&tool=pmcentrez&rendertype=abstract (Accessed: 15 August 2018).

Xiao, X., Li, J. and Samulski, R. J. (1998) 'Production of high-titer recombinant adeno-associated virus vectors in the absence of helper adenovirus.', *Journal of virology*, 72(3), pp. 2224–32. doi: 10.1073/pnas.1201800109.

Xie, W., Strong, J. A. and Zhang, J. M. (2010) 'Increased excitability and spontaneous activity of rat sensory neurons following in vitro stimulation of sympathetic fiber sprouts in the isolated dorsal root ganglion', *Pain*. NIH Public Access, 151(2), pp. 447–459. doi: 10.1016/j.pain.2010.08.006.

Xie, Y., Wang, J. and Bonin, R. P. (2018) 'Optogenetic exploration and modulation of pain processing', *Experimental Neurology*. Academic Press, 306(April), pp. 117–121. doi: 10.1016/j.expneurol.2018.05.003.

Xu, J. *et al.* (2005) 'A combination of mutations enhances the neurotropism of AAV-2', *Virology*, 341(2), pp. 203–214. doi: 10.1016/j.virol.2005.06.051.

Xu, Q. *et al.* (2012) 'In vivo gene knockdown in rat dorsal root ganglia mediated by self-complementary adeno-associated virus serotype 5 following intrathecal delivery', *PLoS ONE*, 7(3). doi: 10.1371/journal.pone.0032581.

Yamawaki, N. *et al.* (2016) 'Combining optogenetics and electrophysiology to analyze projection neuron circuits', *Cold Spring Harbor Protocols*. NIH Public Access, 2016(10), pp. 840–847. doi: 10.1101/pdb.prot090084.

Yang, B. *et al.* (2014) 'Global CNS transduction of adult mice by intravenously delivered rAAVrh.8 and rAAVrh.10 and nonhuman primates by rAAVrh.10', *Molecular Therapy*. Elsevier,

22(7), pp. 1299–1309. doi: 10.1038/mt.2014.68.

Yang, C. *et al.* (2013) 'Pre-immunization with an Intramuscular Injection of AAV9-Human Erythropoietin Vectors Reduces the Vector-Mediated Transduction following Re-Administration in Rat Brain', *PLoS ONE*. Edited by J. A. Chiorini. Public Library of Science, 8(5), p. e63876. doi: 10.1371/journal.pone.0063876.

Yang, C. *et al.* (2016) 'Sequential Adeno-Associated Viral Vector Serotype 9–Green Fluorescent Protein Gene Transfer Causes Massive Inflammation and Intense Immune Response in Rat Striatum', *Human Gene Therapy*, 27(7), pp. 528–543. doi: 10.1089/hum.2015.083.

Yang, F. C. *et al.* (2013) 'Genetic control of the segregation of pain-related sensory neurons innervating the cutaneous versus deep tissues', *Cell Reports*. NIH Public Access, 5(5), pp. 1353–1364. doi: 10.1016/j.celrep.2013.11.005.

Yang, J. *et al.* (2018) 'Upregulation of N-type calcium channels in the soma of uninjured dorsal root ganglion neurons contributes to neuropathic pain by increasing neuronal excitability following peripheral nerve injury', *Brain, Behavior, and Immunity*. Academic Press, 71, pp. 52–65. doi: 10.1016/j.bbi.2018.04.016.

Yang, P. *et al.* (2015) 'Sensorimotor Cortex Injection of Adeno-Associated Viral Vector Mediates Knockout of PTEN in Neurons of the Brain and Spinal Cord of Mice', *Journal of Molecular Neuroscience*. Springer US, 57(4), pp. 470–476. doi: 10.1007/s12031-015-0610-x.

Yang, Y. *et al.* (2004) 'Mutations in SCN9A, encoding a sodium channel alpha subunit, in patients with primary erythermalgia.', *Journal of medical genetics*. BMJ Publishing Group, 41(3), pp. 171–4. doi: 10.1136/JMG.2003.012153.

Yezierski, R. P. *et al.* (1998) 'Excitotoxic spinal cord injury: Behavioral and morphological characteristics of a central pain model', *Pain*, 75(1), pp. 141–155. doi: 10.1016/S0304-3959(97)00216-9.

Yoshida, E. *et al.* (2018) 'In vivo wide-field calcium imaging of mouse thalamocortical synapses

with an 8 K ultra-high-definition camera', *Scientific Reports*. Nature Publishing Group, 8(1), p. 8324. doi: 10.1038/s41598-018-26566-3.

Yoshihara, Y. *et al.* (1999) 'A genetic approach to visualization neurotechnique of multisynaptic neural pathways using plant lectin transgene', *Neuron*, 22(1), pp. 33–41. doi: 10.1016/S0896-6273(00)80676-5.

Yu, H., Fischer, G. and Hogan, Q. H. (2016) 'AAV-Mediated Gene Transfer to Dorsal Root Ganglion.', *Methods in molecular biology (Clifton, N.J.)*. NIH Public Access, 1382, pp. 251–61. doi: 10.1007/978-1-4939-3271-9_18.

Yu, L. *et al.* (2008) 'The role of TRPV1 in different subtypes of dorsal root ganglion neurons in rat chronic inflammatory nociception induced by complete Freund's adjuvant', *Molecular Pain*. SAGE Publications, 4, p. 61. doi: 10.1186/1744-8069-4-61.

Yu, S.-J. *et al.* (2016) 'Methamphetamine induces a rapid increase of intracellular Ca^{++} levels in neurons overexpressing GCaMP5', *Addiction Biology*. Wiley/Blackwell (10.1111), 21(2), pp. 255–266. doi: 10.1111/adb.12193.

Yu, S. J. *et al.* (2013) 'Local administration of AAV-BDNF to subventricular zone induces functional recovery in stroke rats', *PLoS ONE*. Edited by C. V Borlongan, 8(12), p. e81750. doi: 10.1371/journal.pone.0081750.

Yuste, R. and Denk, W. (1995) 'Dendritic spines as basic functional units of neuronal integration', *Nature*. Nature Publishing Group, pp. 682–684. doi: 10.1038/375682a0.

Zaiss, A.-K. *et al.* (2002) 'Differential activation of innate immune responses by adenovirus and adeno-associated virus vectors.', *Journal of virology*, 76(9), pp. 4580–90. Available at: http://www.ncbi.nlm.nih.gov/pubmed/11932423 (Accessed: 15 August 2018).

Zariwala, H. A. *et al.* (2012) 'A Cre-Dependent GCaMP3 Reporter Mouse for Neuronal Imaging In Vivo', *Journal of Neuroscience*. NIH Public Access, 32(9), pp. 3131–3141. doi: 10.1523/JNEUROSCI.4469-11.2012.

Zhang, H. *et al.* (2011) 'Several rAAV vectors efficiently cross the blood-brain barrier and transduce neurons and astrocytes in the neonatal mouse central nervous system', *Molecular Therapy*. Nature Publishing Group, 19(8), pp. 1440–1448. doi: 10.1038/mt.2011.98.

Zhang, N. *et al.* (2018) 'Activation of Dorsomedial Hypothalamic Neurons Promotes Physical Activity and Decreases Food Intake and Body Weight in Zucker Fatty Rats', *Frontiers in Molecular Neuroscience*. Frontiers, 11, p. 179. doi: 10.3389/fnmol.2018.00179.

Zhang, T. *et al.* (2018) 'Activation of GABAergic Neurons in the Nucleus Accumbens Mediates the Expression of Cocaine-Associated Memory', *Biological and Pharmaceutical Bulletin*. The Pharmaceutical Society of Japan, 41(7), pp. 1084–1088. doi: 10.1248/bpb.b18-00221.

Zhang, X.-S. *et al.* (2017) 'Activation of the RAGE/STAT3 Pathway in the Dorsal Root Ganglion Contributes to the Persistent Pain Hypersensitivity Induced by Lumbar Disc Herniation.', *Pain physician*, 20(5), pp. 419–427. Available at: http://www.ncbi.nlm.nih.gov/pubmed/28727705.

Zhang, X., Huang, J. and McNaughton, P. A. (2005) 'NGF rapidly increases membrane expression of TRPV1 heat-gated ion channels', *EMBO Journal*. European Molecular Biology Organization, 24(24), pp. 4211–4223. doi: 10.1038/sj.emboj.7600893.

Zhang, X., Li, L. and McNaughton, P. A. (2008) 'Proinflammatory Mediators Modulate the Heat-Activated Ion Channel TRPV1 via the Scaffolding Protein AKAP79/150', *Neuron*, 59(3), pp. 450–461. doi: 10.1016/j.neuron.2008.05.015.

Zhao, F.-Y. *et al.* (2014) 'In Vivo Electrophysiological Recording Techniques for the Study of Neuropathic Pain in Rodent Models', in *Current Protocols in Pharmacology*. Hoboken, NJ, USA: John Wiley & Sons, Inc., p. 11.15.1-11.15.26. doi: 10.1002/0471141755.ph1115s66.

Zhao, Y. *et al.* (2011) 'An expanded palette of genetically encoded Ca2+ indicators', *Science*, 333(6051), pp. 1888–1891. doi: 10.1126/science.1208592.

Zheng, C.-X. *et al.* (2018) 'Lentiviral Vectors and Adeno-Associated Virus Vectors: Useful Tools for Gene Transfer in Pain Research', *The Anatomical Record*. Wiley-Blackwell, 836(March 2017),

pp. 825–836. doi: 10.1002/ar.23723.

Zhou, X. X., Pan, M. and Lin, M. Z. (2015) 'Investigating neuronal function with optically controllable proteins', *Frontiers in Molecular Neuroscience*. Frontiers Media SA, 8, p. 37. doi: 10.3389/fnmol.2015.00037.

Zincarelli, C. *et al.* (2008) 'Analysis of AAV serotypes 1-9 mediated gene expression and tropism in mice after systemic injection', *Molecular Therapy*. The American Society of Gene Therapy, 16(6), pp. 1073–1080. doi: 10.1038/mt.2008.76.

Zirpel, L., Lachica, E. A. and Rubel, E. W. (1995) 'Activation of a metabotropic glutamate receptor increases intracellular calcium concentrations in neurons of the avian cochlear nucleus.', *The Journal of neuroscience : the official journal of the Society for Neuroscience*, 15(1 Pt 1), pp. 214–222. Available at: http://www.ncbi.nlm.nih.gov/pubmed/7823131 (Accessed: 1 September 2018).

Ziv, Y. *et al.* (2013) 'Long-term dynamics of CA1 hippocampal place codes', *Nature Neuroscience*. NIH Public Access, 16(3), pp. 264–266. doi: 10.1038/nn.3329.

Zufferey, R. *et al.* (1997) 'Multiply attenuated lentiviral vector achieves efficient gene delivery in vivo', *Nature Biotechnology*, 15(9), pp. 871–875. doi: 10.1038/nbt0997-871.

Zurborg, S. *et al.* (2011) 'Generation and characterization of an Advillin-Cre driver mouse line', *Molecular Pain*. SAGE Publications, 7, p. 66. doi: 10.1186/1744-8069-7-66.